VOLUME 39 SECOND SERIES NUMBER 6

THE PHYSICAL REVIEW

A JOURNAL OF EXPERIMENTAL AND THEORETICAL PHYSICS

CONDUCTED BY

THE AMERICAN PHYSICAL SOCIETY

BOARD OF EDITORS

Managing Editor, JOHN T. TATE, University of Minnesota, Minneapolis
Assistant Editor, J. W. BUCHTA, University of Minnesota, Minneapolis
K. F. HERZFELD, A. W. HULL, F. W. LOOMIS, A. J. DEMPSTER, DAVID M. DENNISON, J. C. SLATER, R. C. GIBBS, E. O. LAWRENCE, J. H. VAN VLECK

MARCH 15, 1932

Ionization by Penetrating Radiation as a Function of Pressure and Temperature — A. H. COMPTON, R. D. BENNETT AND J. C. STEARNS 873
Cosmic-Ray Particles — GORDON L. LOCHER 883
X-ray Reflection from Inhomogeneously Strained Quartz — CHARLES S. BARRETT AND CARL E. HOWE 889
Zeeman Effect of the K II Spectrum — ALBERT E. WHITFORD 896
Photoionization Probabilities of Atomic Potassium — MELBA PHILLIPS 905
Approximate Calculation of the Lower Energy Levels of the Carbon Atom — NIEL FREEBORN BEARDSLEY 913
Emission and Absorption Spectra of BaF — F. A. JENKINS AND A. HARVEY 922
Absorption Spectrum of Cyanogen Gas in the Ultraviolet — SHO-CHOW WOO AND RICHARD M. BADGER 932
Parallel Type Absorption Bands of Ammonia — DAVID M. DENNISON AND J. D. HARDY 938
Line Reflection Spectra of Solids — FRANK H. SPEDDING AND RICHARD S. BEAR 948
Temperature Shift of the Transmission Band of Silver — J. V. PENNINGTON 953
Absorption by Formaldehyde Vapor in the Infrared — JOHN R. PATTY AND HARALD H. NIELSEN 957
Surface-Electrons — J. E. NYROP 967
Tables of the Ionization in the Upper Atmosphere — E. O. HULBURT 977
Vapor Pressure Constant of Ammonia, the Entropy of Crystalline Ammonia, and the Reaction $N_2+3H_2 \rightleftarrows 2NH_3$ — T. E. STERNE 993
Some Thermal Properties of Tantalum — C. L. UTTERBACK AND L. A. SANDERMAN 1008
Letters to the Editor — 1012

Accurate Determination of Excitation Energy by Electron Impact — L. C. VAN ATTA 1012
Evaporation of Platinum in Vacuum from a Tungsten Filament — JOHN STRONG 1012
Far Ultraviolet Eigenfrequencies of the Alkali Halides — ALBERT SMITH 1013
Determination of Small Quantities of Radon and Thoron — ROBLEY D. EVANS 1014
Velocity of Sound in a Fermi-Dirac or Einstein-Bose Ideal Gas — G. E. UHLENBECK AND E. A. UEHLING 1014
Excited Electronic States of Li_2 — WENDELL H. FURRY 1015
Relative Abundance of the Isotopes of Lead in Uranium Bearing Minerals — J. L. ROSE AND L. P. GRANATH 1017
Thermomagnetic e.m.f.'s in Transversely and Longitudinally Magnetized Wires — ROLAND SCHAFFERT 1017
Solid Solutions of Lead and Tin in Bismuth — ERIC R. JETTE AND FRANK FOOTE 1018
Infrared and Raman Spectra of CS_2 — S. BHAGAVANTAM 1020
Constitution of Tellurium — K. T. BAINBRIDGE 1021

Book Reviews — 1022
Index to Volume 39 — 1026
Current Literature of Physics

PUBLISHED BY THE AMERICAN PHYSICAL SOCIETY
EDITORIAL OFFICE: MINNEAPOLIS, MINN.

THE AMERICAN PHYSICAL SOCIETY

OFFICERS OF THE SOCIETY

President:	W. F. G. SWANN	Bartol Research Foundation, Philadelphia, Pa.
Vice-President:	PAUL D. FOOTE	The Gulf Companies, Pittsburgh, Pa.
Secretary:	W. L. SEVERINGHAUS	Columbia University, New York City
Treasurer:	G. B. PEGRAM	Columbia University, New York City
Editor:	JOHN T. TATE	University of Minnesota, Minneapolis, Minn.
Local Secretary for the Pacific Coast:	L. B. LOEB	University of California, Berkeley, Calif.

THE PHYSICAL REVIEW

Published by the American Physical Society. Executive office: University of Minnesota, Minneapolis, Minn. Four volumes annually, six issues per volume.

First series. From July 1, 1893, to January 1, 1913, the REVIEW was conducted by Edward L. Nichols, Ernest Merritt and Frederick Bedell, with the financial support of Cornell University. The first four volumes were issued annually; subsequent volumes, semi-annually; thirty-five volumes in all.

Second series. On January 1, 1913, the REVIEW was transferred to the American Physical Society as announced on the first page of the new series which was then begun. Since then it has been conducted by a Board of Editors elected by the Society. Volumes 1-38 are semi-annual, beginning in January and July of each year from 1913 to 1931. Volumes 1-33 contain six issues each. Volumes 34-38 twelve issues. Beginning with Volume 39 there will be four volumes per year of six issues each.

Contributors are referred to page 2 of the advertisements for further information.

Annual subscription, throughout the Postal Union, $12.00 in advance.

General index, 1893-1920, $4.00 in advance.

Back Volumes, Volumes 1-38, $9.00 per volume; Volume 39, $4.50; Back Numbers, $1.50 per copy for issues prior to July 1, 1929 (Vols. 1-33), $.75 per copy for issues subsequent thereto. Postage is free if remittance accompanies order; otherwise postage is extra. No bound volumes can be supplied. The REVIEW offers to purchase a limited number of First Series, Vol. 1, No. 1 (at $2.00 each); Second Series, Vol. 7, No. 1, January 1916; Vol. 7, No. 2, February 1916; Vol. 7, No. 4, April 1916; and Vol. 7, No. 5, May 1916 (at $2.00 each).

Advertisements. Rates will be supplied by the Editor on request. Copy for each number must be received at Minneapolis two weeks prior to the dates of issue; old copy is used until new copy is received. Send electrotypes direct to printers, George Banta Publishing Co., Menasha, Wis.

Discount of ten percent is allowed to members of the American Physical Society on purchase of back numbers.

Changes of Address and Complaints of failure to receive the REVIEW, in the case of members of the Physical Society, should be addressed to the Treasurer; in the case of other subscribers, to the Editor. New copies can be sent free in response to complaints of non-delivery only if notice of non-delivery is received within three months of date of issue.

Editorial Correspondence should be addressed to the PHYSICAL REVIEW, University of Minnesota, Minneapolis, Minn.

Entered at the post office at Menasha, Wis., as second class matter.
Acceptance for mailing at special rate of postage provided for in section 1103, Act of October 3, 1917, authorised September 6, 1926.

TEMPERATURE-CONTROL UNITS

PIEZO-ELECTRIC quartz crystals used to stabilize the frequency of vacuum-tube oscillators must be operated at constant temperature, if a high degree of frequency stability is to be expected from the system. To meet the needs of this service General Radio supplies temperature-control boxes which hold temperature constant to within $\pm 0.1^\circ$ Centigrade for room temperature variations of $\pm 20^\circ$ Centigrade.

These boxes require no circulating air or water bath. The sensitive element is an adjustable mercury type thermostat which actuates a relay. The whole system is compact and rugged and is intended to operate without adjustments. The temperature-control space is approximately 4 x 4 x 4 inches.

Boxes of this type are adaptable for other temperature-control purposes. Your inquiries are invited.

TYPE 547-A Temperature-Control Box :: Price $150.00

GENERAL RADIO COMPANY

CAMBRIDGE A, ∴ MASSACHUSETTS

PHYSICAL REVIEW

PREPARATION OF PRELIMINARY ABSTRACTS

An article will not be accepted for publication in THE PHYSICAL REVIEW unless the manuscript is accompanied by an adequate abstract for publication at the beginning of the article. This abstract is intended to aid the reader by furnishing an index and a brief summary of the contents of the article. Besides serving these purposes it should also be suitable for reproduction in abstract journals so as to make it unnecessary for the editors of these journals to have another abstract prepared.

As *an index* it should be complete; all the subjects, major and minor, concerning which new information is presented, should each be given, with sufficient precision so that any reader can tell from the abstract whether the article contains anything of interest to him. The subject indexes of abstract journals are fundamental in reference work. These indexes are prepared exclusively from the abstracts and whatever is omitted from the abstracts cannot be included in the index and may thus be lost. The writer of an abstract should therefore feel himself under an important obligation to his scientific colleagues to make sure that the abstract is accurate and complete, at least as an index.

As *a summary* the abstract should give briefly the conclusions of the article, important advances in experimental technique and theory, and all numerical results of general interest that may be conveniently given including all that might belong in a handbook and table of contents. It should give all the information that readers who are not specialists in the particular field involved might desire to know about the article thus saving them the time and trouble in referring to the article itself. Experience has shown that in general the length of the abstract should be from four to eight percent of the length of the article.

THE PHYSICAL REVIEW, 1923-1925, contains many examples of adequate abstracts. Most of these contain paragraph titles and subtitles which indicate the subjects concerning which new information is given and it is required that authors include such subtitles when all the information contained in the article does not refer to the subject indicated by the title of the article. Such subtitles may be frequently avoided by rewording the title so as to make it more precise.

Second Series *March 15, 1932* *Vol. 39, No. 6*

THE
PHYSICAL REVIEW

IONIZATION BY PENETRATING RADIATION AS A FUNCTION OF PRESSURE AND TEMPERATURE

By A. H. Compton, R. D. Bennett and J. C. Stearns
University of Chicago, Massachusetts Institute of Technology, and University of Denver

(Received February 10, 1932)

Abstract

To account for the experimental fact that the ionization of a gas exposed to γ-rays or cosmic rays is not proportional to the pressure, but approaches a limiting value for pressures of about 140 atmospheres, the hypothesis is suggested that at these high pressures the initially formed ions may remain so close together that they frequently reunite under their mutual electrostatic attractions. The probability is calculated for the ions to become separated by diffusion, and formulas are thus obtained for the saturation ionization current as a function of pressure. The most satisfactory formula is based upon an arbitrary but reasonable assumption regarding the ranges of the secondary electrons ejected by ionizing beta particles. Knowing the variation of ionization with pressure, this diffusion theory predicts a definite variation of ionization with temperature. Such a temperature variation is experimentally discovered and is in good accord with the theoretical prediction. The temperature coefficient is negligible for pressures less than 10 atmospheres, but at pressures over 100 atmospheres the ionization approaches proportionality to the absolute temperature.

IT HAS been shown by Swann[1] and his students[2] that the ionization in an ionization chamber, due to either gamma rays or cosmic rays, is not proportional to the pressure, but approaches a maximum value for pressures of about 140 atmospheres. Miss Downey[3] proposed the explanation that the ions are formed by high speed beta particles ejected from the walls of the ionization chamber, and that these beta particles are completely absorbed by the gas in the chamber if the pressure is sufficiently high. Broxon, in his 1931 paper, was able to show that this hypothesis leads to an exponential formula for the relation between pressure and ionization which agrees well with his experimental measurements. Yet there has seemed to be no explanation on this hypothesis for such facts as the following: 1. The variation of ionization with pressure when gamma rays are used is approximately the same

[1] W. F. G. Swann, J. Frank. Inst. **209**, 151 (1930).

[2] K. M. Downey, Phys. Rev. **20**, 186 (1922); H. F. Fruth, Phys. Rev. **22**, 109 (1923); J. W. Broxon, Phys. Rev. **27**, 542 (1926); **37**, 1320, (1931).

[3] Reference 2.

as when cosmic rays are used,[4] whereas on the average the beta rays ejected by gamma rays have a much shorter range than those associated with cosmic rays. 2. The ionization-pressure relation is nearly independent of the diameter of the chamber,[5] contrary to expectation. 3. In pure nitrogen the ionization is more nearly proportional to the pressure than in air.[6]

An alternative explanation of the phenomenon is that a kind of recombination may occur at high pressures, due to the fact that the electron ejected from a molecule by the ionizing beta ray may lose its initial energy through molecular collisions before it has moved far enough from the parent positive ion to escape from the effect of its electrostatic attraction.[7] In accord with the ideas underlying Thomson's theory of recombination[8] we may suppose that if the initial energy of the electron carries it beyond a critical distance, molecular diffusion will probably carry it away, and a permanent ion will be formed. If i_1 is the ionization per unit pressure when all ions remain permanent, p is the pressure, and P is the probability that an ion will remain permanent, the measured ionization may be written as

$$i = i_1 pP. \tag{1}$$

The probability P will approach unity for low pressures. It will also have a greater value at high temperatures than at low temperatures, since diffusion will be more rapid. Experiments described below show that the ionization at high temperatures is indeed greater than at low temperatures, as this statement would imply. The hypothesis of the absorption of the beta rays from the walls does not account for such a temperature variation. Moreover, the difficulties enumerated above in connection with the beta ray absorption hypothesis disappear, as we shall see, when the phenomenon is considered as one of recombination. It remains to develop a quantitative theory of ionization as a function of pressure and temperature, and to compare its predictions with experiment.

Theory of Ionization as a Function of Pressure

Let us suppose that when a beta particle passing through gas ionizes an atom, the ejected electron moves a distance r before it loses its initial energy and comes to thermal equilibrium with the surrounding molecules. The average energy spent by the beta particle in producing an ion pair is found to be 25 or 30 electron volts, so that the energy with which the electron escapes is usually much greater than the equilibrium thermal energy. Since most of the electron collisions are elastic, or nearly so, we may expect the distance r to be much larger than a molecular mean free path. As a result of molecular diffu-

[4] H. F. Fruth, reference 2, supported by later measurements.

[5] J. W. Broxon, reference 2 (1926).

[6] H. F. Fruth, reference 2.

[7] This explanation has been proposed independently by R. A. Millikan and I. S. Bowen, Nature **128,** 582 (Oct. 3, 1931) and A. H. Compton, R. D. Bennett and J. C. Stearns, Phys. Rev. **38,** 1865 (Oct. 15, 1931).

[8] J. J. Thomson, Phil. Mag. **47,** 337 (1924).

sion the positive and negative ions will now tend to move farther apart, while their mutual electrostatic attraction will tend to draw them together.[9]

To calculate the rate at which diffusion separates the ions, let us suppose that when the ejected electron comes to thermal equilibrium it forms a negative molecular ion of the same mass as the parent positive ion. If we assume the electron to remain free, the final result is unaltered. Let λ be the mean free path of either ion, and r their initial distance apart. After one free motion, the probable distance of the second ion from the initial position of the first is

$$r + \delta_2 r = (r^2 + \lambda^2)^{1/2}.$$

Similarly, the probable distance of the first ion from the initial position of the second is

$$r + \delta_1 r = (r^2 + \lambda^2)^{1/2}.$$

Thus, after one mean free time τ, the probable separation of the ions is to a close approximation, since $\lambda^2 \ll r^2$,

$$r + \delta_1 + \delta_2 r = r(1 + \lambda^2/r^2).$$

Thus,

$$\delta r = \delta_1 r + \delta_2 r = \lambda^2/r.$$

The probable rate at which the ions separate by diffusion is accordingly,

$$\frac{dr}{dt} = \frac{\delta r}{\tau} = \frac{\lambda^2}{\tau r}. \tag{2}$$

The rate of approach due to electrostatic attraction may be calculated as follows. The average distance of approach of each ion toward the other during the molecular free time interval τ is $\frac{1}{2}a\tau^2$, whence during this interval r will have changed by

$$\delta r = -2 \cdot \frac{1}{2} \frac{e^2/r^2}{m} \tau^2,$$

and the rate of approach is given by

$$\frac{dr}{dt} = \frac{\delta r}{\tau} = -\frac{e^2\tau}{mr^2}. \tag{4}$$

The condition that the ion pair shall remain permanent is thus that

$$\frac{\lambda^2}{\tau r} > \frac{e^2\tau}{mr^2},$$

or that

$$r > r_0,$$

[9] Cf. E. B. Loeb and L. C. Marshall, J. Franklin Inst. **208**, 371 (1929), who have considered a very similar problem.

where

$$r_0 \equiv \frac{\tau^2 e^2}{m\lambda^2} \cdot \tag{5}$$

Writing $\tau = \lambda/v$, where v is given by the relation

$$\tfrac{1}{2}mv^2 = \frac{3}{2}kT,$$

we have[10]

$$r_0 = e^2/3kT. \tag{6}$$

At 20°C, using the usual values of e and k, r_0 becomes 1.88×10^{-6} cm. At this distance the field due to an electron is about 4×10^4 volts per cm, which means that ordinary electric fields will not appreciably affect the permanence of these ions.

If we are to determine the probability that the ion will remain permanent, we must now calculate the probability that the electron comes to equilibrium at a distance greater than r_0 from its parent ion. This would be possible if we knew the function $F(r)dr$ representing the probability that the electron will stop between r and $r+dr$. Unfortunately the form of this function is not known.

Let us first suppose that the distribution of distances is similar to that which applies to the diffusion of a gas molecule. If R is the probable (root mean square) distance to which the electron goes, the probability that it will stop in the range dr is then,

$$F(r)dr = \frac{4r^2}{\alpha^3(\pi)^{1/2}} e^{-r^2/\alpha^2} dr, \tag{7}$$

where

$$\alpha^2 = \tfrac{2}{3}R^2. \tag{8}$$

The probability of going beyond r_0 is then

$$\begin{aligned} P &= \frac{4}{\alpha^3(\pi)^{1/2}} \int_{r_0}^{\infty} r^2 e^{-r^2/\alpha^2} dr \\ &= \frac{2}{(\pi)^{1/2}} \frac{r_0}{\alpha} e^{-r_0^2/\alpha^2} + \frac{2}{(\pi)^{1/2}} \int_{r_0/\alpha}^{\infty} e^{-x^2} dx. \end{aligned} \tag{9}$$

This is also the probability of permanence of the ion pair. By Eq. (1), the saturation ionization current is however $i = i_1\, p\, P$. P may be expressed as a function of the pressure if we note that α varies as $1/p$. We may thus write

$$z \equiv r_0/\alpha = cp \tag{10}$$

where c is a constant of proportionality. Then

[10] Loeb and Marshall (reference 9) find $r_0 = e^2/6kT$. Their calculation is however for the case where λ is large compared with r_0, whereas in the present case λ is small compared with r.

$$i = i_1 pP = \frac{i}{c} \cdot zP$$
$$= C\left\{z^2 e^{-z^2} + z\int_z^\infty e^{-z^2} dz\right\}, \tag{11}$$

where C is a new proportionality constant.

In the broken curve of Fig. 1, Eq. (11), with suitably chosen constants C and $c = z/p$, is compared with a typical set of Broxon's data[11] for the ionization by cosmic rays in air for various pressures. The evident differences between the theoretical curve and the experimental data indicate that our assumed function $F(r)$, as given by Eq. (7), does not allow as wide a range of r values as actually occur. Experiments, such as cloud expansion photographs, indicate that the electrons ejected by a fast beta ray frequently have

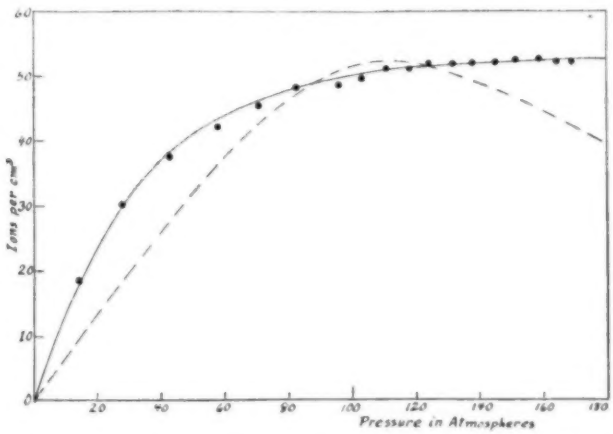

Fig. 1. Ionization as function of pressure. Data, Broxon. Broken line, Eq. 11. Solid line, Eq. 14.

ranges comparable with a millimeter at atmospheric pressure. According to Eq. (9), however, using the value of α which works best in comparing Eq. (11) with experiment, the probability that the electron should have a range greater than 0.1 mm at atmospheric pressure is only about 10^{-400}. If an arbitrary function $F(r)$ is chosen which will give a theoretical relation between i and p in accord with the experiments, the chance of observing an electron with a large range is found to be much greater.

A suitable function is found to be,

$$F(r)dr = \frac{ar}{(a^2 + r^2)^{3/2}}\, dr, \tag{12}$$

where a is an arbitrary constant. Writing

$$P = a\int_{r_0}^\infty \frac{rdr}{(a^2 + r^2)^{3/2}},$$

[11] J. W. Broxon, Phys. Rev. **37**, 1325 (1931), Curve II, Fig. 5.

we find on integration,

$$P = \left(1 + \frac{r_0^2}{a^2}\right)^{-1/2}. \tag{13}$$

The constant a may be interpreted as an average range of the electron, which will vary inversely as the pressure. Since r_0 is a constant at a particular temperature, we may write

$$r_0/a = hp,$$

where h is a new constant of proportionality, and we get for the ionization current,

$$i = i_1 p(1 + h^2 p^2)^{-1/2}. \tag{14}$$

To fit Broxon's data of Fig. 1 we choose $i_1 = 1.3$ and $h = 0.0241$, which gives the solid curve of this figure. It will be seen that the agreement is satisfactory.

The derivation of a suitable formula, such as Eq. (14), to represent the relation between ionization and pressure is thus to a large extent arbitrary, since we have no independent knowledge of the range distribution of the ejected electrons. It is however possible thus to formulate a satisfactory relation between the ionization and the temperature.

Theory of Ionization as a Function of Temperature

In the last section we have considered the temperature as constant. Let us now remove this restriction, and consider the ionization current as a function of the density of the gas ρ and the absolute temperature T. From Eqs. (9) and (13) it becomes evident that the probability that an ion pair will remain permanent is a function of r_0/a, where a is an average range of the ejected electron and r_0 is the critical distance for forming a permanent ion pair. We note that

$$a = b/\rho, \tag{15}$$

where ρ is the density of the gas, and the proportionality constant b is presumably independent of temperature and density, From Eqs. (6) and (15) we then have,

$$\frac{r_0}{a} = A\frac{\rho}{T} \tag{16}$$

where $A = e^2/3kb$ is also independent of temperature and density. Thus the probability of permanence is

$$P = f_1\left(\frac{r_0}{a}\right) = f_2\left(\frac{\rho}{T}\right). \tag{17}$$

If I is the number of initial ions produced for unit density of the gas, for density ρ the initial ionization is $I\rho$, and the ionization current is

$$i = I\rho f_2(\rho/T). \tag{18}$$

Thus

$$i/I\rho = f_2(\rho/T). \tag{19}$$

If ρ is expressed in units of ρ_1 = density of the gas at $T = 293°$ and $p = 1$ atmosphere, then ρ is numerically equal to the pressure as observed under ordinary conditions. Then,

$$f_2(\rho/T) = f_2(p/T) = i/Ip, \tag{20}$$

where p is the pressure at 293°K. Using experimental data such as those of Broxon, the form of the function f_2 may be determined from Eq. (20), and by substitution in Eq. (18) the variation of i with T may be calculated.

In view of the satisfactory agreement of Eq. (14) with experiment, as shown in Fig. 1, we may use the value of P given by Eq. (13). Combining this with Eq. (16) we have

$$f_2\left(\frac{\rho}{T}\right) = \left(1 + A^2\frac{\rho^2}{T^2}\right)^{-1/2},$$

and

$$i = I\rho\left(1 + A^2\frac{\rho^2}{T^2}\right)^{-1/2}. \tag{21}$$

The temperature coefficient of the ionization is then

$$\beta = \frac{di}{idT} = \frac{A^2\rho^2}{T^3}\Big/\left(1 + \frac{A^2\rho^2}{T^2}\right). \tag{22}$$

If we express ρ in terms of ρ_1 as described above, then $\rho = p$, and $A = e^2/3kb$, whereby comparison with Eq. (14) et seq., $b = r_0/c$. With Broxon's data for air,

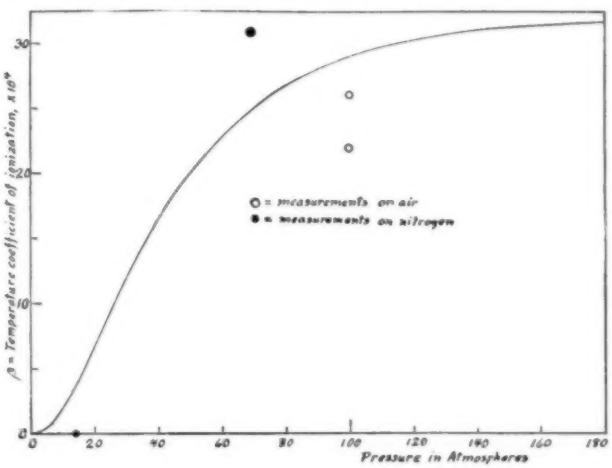

Fig. 2. Temperature coefficient of ionization of air as function of pressure. Data for nitrogen are plotted on same scale by multiplying pressure by A_{N_2}/A_{air}. Curve represents predicted values.

$c = 0.0241$, whence $b = 7.8 \times 10^{-5}$, and A for air becomes 7.1. For air at 293°K, the values of the temperature coefficient β for different pressures as calculated from Eq. (22) by using this value of A are shown in Fig. 2. At pressures

of the order of 1 atmosphere the temperature coefficient is negligible—6×10^{-6} per degree at 1 atmosphere. At high pressures, however, the coefficient approaches the value 1/293, i.e., the ionization becomes proportional to the absolute temperature.

Experimental Tests

We have already shown in the solid curve of Fig. 1 that it is possible to present this recombination theory of the variation of ionization with pressure such a form that it agrees acceptably with the experiments. This is however no distinctive test of the recombination theory, since Broxon has developed a formula on the hypothesis of the absorption of beta rays which is likewise in good agreement with his experiments.

An experiment to measure the temperature coefficient of the ionization affords however a crucial test of the two theories; for the present theory gives a definite prediction of the magnitude of this coefficient, whereas on the beta ray absorption theory there is no reason to suppose that the ionization should depend upon the temperature.

In looking for a possible temperature coefficient, we used a spherical steel ionization chamber of 10 cm internal diameter, which had been built for another purpose. The ionization, due to the gamma rays from a milligram of radium at about 1 meter distance and filtered through a centimeter of lead, was measured by a Lindemann electrometer, operating at about 50 scale divisions per volt. The chamber was immersed in a water bath, which could be cooled with ice or heated by a flame. The measurements consisted merely in recording the temperature and timing the motion of the electrometer needle over 10 divisions. It was necessary to allow ample time, at least 10 minutes, for the temperature and the large ions in the chamber to come to equilibrium.

Two series of readings on air at 100 atmospheres pressure, taken between 0° and 30°C and between 0° and 37°C, showed greater ionization at the higher temperature by 7.8 percent and 8.3 percent respectively. The corresponding values of $\beta=\delta i/\delta T$ are 0.0026 and 0.0022 per degree. For nitrogen at 100 atmospheres between 0° and 31°, which theoretically should have nearly the same temperature coefficient, the increase was 9.5 percent, whence $\beta=0.0031$. The average of these values is $\beta=0.0026\pm0.0002$, which is in good accord with the value 0.0029 predicted for air at this pressure by Eq. (22).

Only one set of temperature readings was made at a lower pressure. This was for nitrogen at 20 atmospheres. The observed effect was 0.0000 ± 0.0003, whereas the predicted value of β for nitrogen at this pressure is 0.0004.

Thus the ionization in a pressure chamber is found to increase with the temperature, and this increase is at approximately the rate predicted by the recombination theory.

Relative Ionization by Gamma Rays and Cosmic Rays

If the ionization is due to beta rays ejected from the walls, which are absorbed by the gas in the ionization chamber, the variation of the ionization with pressure should differ with different sources of radiation. For the speed of

both photoelectrons and recoil electrons is a function of the frequency of the radiation. If the cosmic rays are photons of very high energy, the range of the excited beta rays should be much greater than of those excited by gamma rays, and the ionization by gamma rays should reach its maximum value at lower pressure. On the recombination theory, however, since the speed at which a beta particle ejects electrons from the molecules which it traverses varies very little with the speed of the beta ray, there should be little if any difference between the pressure-ionization curves obtained with cosmic rays and gamma rays.

To test this point, a cylindrical ionization chamber of 14.8 cm internal diameter and 46 cm length, having steel walls 1.2 cm thick, was used. With this chamber measurements were made of the ratio of the ionization due to cosmic rays to that due to cosmic rays plus gamma rays from a radium standard, using pressures up to 50 atmospheres. The average results of the readings taken on Mt. Evans and at Denver are given in Table I. A different

TABLE I. $i_c/i_{c+\gamma}$ *as function of pressure.*

Pressure, atmospheres	10	20	30	40	50
$i_c/i_{c+\gamma}$ elev. 12,700 ft.	0.230	0.230	0.231	0.228	0.231
$i_c/i_{c+\gamma}$ elev. 5,300 ft.	0.490	0.492	0.490	0.492	0.491

radium standard was used at the two locations. The variations in these readings taken for different pressures are not larger than are to be expected from the probable error.

The beta rays ejected from the steel walls by the action of the gamma rays should be almost completely absorbed by 10 cm of air at some 30 atmospheres, so if this absorption were the cause of the limited ionization current, the differences between $i_c/i_{c+\gamma}$ over the range of pressures here used should have been very marked. The results are however in complete accord with the recombination theory.

ANOMALOUS EFFECTS WITH NITROGEN

In comparing the ionization due to cosmic rays in various gases under pressure, Fruth[12] noted that the ionization in nitrogen remained more nearly proportional to the pressure than that in oxygen or air. Thus, though at atmospheric pressure the ionization in nitrogen is less than in oxygen, at high pressures it becomes considerably greater. This result has been qualitatively confirmed by Broxon, though the differences between nitrogen and air which he observed were not as great as those found by Fruth. Our measurements with gamma rays confirm those of Broxon with cosmic rays. We found the ionization in commercial nitrogen at 100 atmospheres to be 25 percent greater than for air, whereas Broxon found 28 percent.

In terms of the limited range of the beta rays from the walls, this phenomenon seems to have no explanation.[13] On the recombination theory, the lower

[12] H. F. Fruth, reference 2.

[13] Cf., however, J. W. Broxon, Phys. Rev. **38**, 1704 (1931).

probability of recombination in nitrogen implied by this phenomenon indicates that the electrons ejected by the fast beta rays have a greater range in nitrogen than in air. This is what might well be expected from Loeb's observation[14] that an electron will make 10^3 times as many molecular collisions in pure nitrogen as in air before attaching itself to form a negative molecular ion. The fact that slight impurities greatly reduce this ratio may perhaps account for the different results with nitrogen obtained by Fruth and Broxon.

Conclusion

It would seem that the existence of a temperature coefficient of ionization of the predicted magnitude is definite evidence that the recombination-diffusion hypothesis is fundamentally sound.

We cannot place any more confidence in the formula (Eq. (14)) for the ionization as a function of pressure than is justified by its agreement with experiment, since the function (12) describing the ranges of the electron ions is entirely empirical. Yet the predicted variation with temperature as given by Eq. (19) is a necessary consequence of the hypothesis, and the formula (22) for the temperature coefficient of ionization should be considerably more precise than are our present experiments.

It is not improbable that this variation of ionization with temperature may have caused apparent diurnal variations in measurements of the intensity of cosmic rays, especially when the ionization chamber has been placed out of doors.

We wish to thank Messrs. P. Barth, C. Hedberg and W. Overbeck, the University of Denver, and Messrs. V. J. Andrew, J. A. Longman and L. N. Ridenour of the University of Chicago for their help in taking the readings. We are indebted also to Mr. J. W. Ailinger, Superintendent of the Department of Mountain Parks, and to Mr. Donald Keim of the Chamber of Commerce, of the city of Denver, for facilitating our work on Mt. Evans, and to the Rumford Committee for a grant for the purchase of part of the equipment.

[14] Cf. K. T. Compton and I. Langmuir, Rev. Mod. Phys. **2**, 193 (1930).

COSMIC-RAY PARTICLES

By Gordon L. Locher
The Rice Institute

(Received January 28, 1932)

Abstract

Specific Ionization. In a previous experiment, a number of thin straight tracks formed in a Wilson cloud-apparatus were identified as cosmic-ray particle tracks, by means of a Geiger-counter. The specific ionization along these has now been determined and is found not to exceed 36 ion-pairs per cm, in air at 1 atmosphere. This is less than one third the ionization calculated by Kolhörster and Tuwim, whose value is believed to be erroneous, at least for individual tracks, for reasons set forth in this paper.

"Group Phenomenon". On 148 stereopictures of tracks attributed to cosmic-ray particles, 20 groups of 2 or more such tracks were found. The tracks of a group usually converge to a point near at hand, which suggests that they have a common source. Each group is believed to be made by secondary electrons ejected by one photon. Possible explanations of the origin of the groups have been considered; the one that seems most favorable supposes that a cosmic-ray photon may interact with an atomic nucleus and eject one or more fast β-particles from it; the convergent groups are, then, formed when 2 or more particles are ejected from one nucleus. The production of groups may affect the interpretation of various ionization and Geiger-counter experiments with cosmic-rays. Some energy calculations have been made on the basis of the measured specific ionization of the cosmic-ray particles; for example, a minimum of 5×10^8 e-volts energy are required to send an electron through the earth's atmosphere. An ionization experiment is proposed, by which it should be possible to tell whether or not cosmic-rays produce groups of tracks by nuclear disruption.

The Specific Ionization

THE specific ionization of cosmic-ray particles may be calculated by determining the rate of their influx with a Geiger-Müller counter of known dimensions and getting the corresponding ionization produced in an ionization chamber whose dimensions are also known, or more directly, by counting the number of ions in a Wilson cloud-chamber along tracks that are identified to be due to these particles.

Using the former method, Kolhörster and Tuwim[1] have recently calculated that the average specific ionization is 135 ion-pairs per cm ± 10 percent, in air at normal pressure, or about the same as that of β-particles of velocity 0.6 C. In order for β-particles of cosmic origin to have the necessary penetration and still produce the observed ionization, they calculated that the energy must be $E>2\times10^9$ electron-volts. On the other hand, an ordinary β-particle of velocity 0.6 C has only 127,000 volts energy, so it is very hard to reconcile the high energy of a cosmic-ray corpuscle with its high rate of ionization, since the ionization of a β-particle is thought to approach a minimum of about 40 ion-pairs per cm as the velocity approaches that of light. Assum-

[1] W. Kolhörster and L. Tuwim, Zeits. f. Physik **73**, 130 (1931).

ing that 135 ion-pairs per cm is correct, 2×10^9 volts is of the right order to allow the cosmic-rays to penetrate the whole atmosphere and still have enough energy to eject 2×10^8-volt electrons, independently of whether the cosmic-rays, themselves, are photons or swift β-particles.

The present paper proposes, first, that the specific ionization along *individual* cosmic-ray particle tracks is very much less than 135 per cm, and, second, that the particles arrive in *groups*, which may explain the high average ionization got by Kolhörster and Tuwim.

In a recent experiment,[2] L. M. Mott-Smith and the writer obtained ion-tracks in a Wilson cloud-apparatus simultaneously with discharges of a Geiger-Müller counter arranged above the chamber. Then, from stereoscopic reconstruction of the tracks formed under such conditions, it was found that they were usually in line with the counting-tube. The evident conclusion was that a cosmic-ray particle had, in each case, set off the counter discharge and proceeded through the chamber, making the observed ion-track.

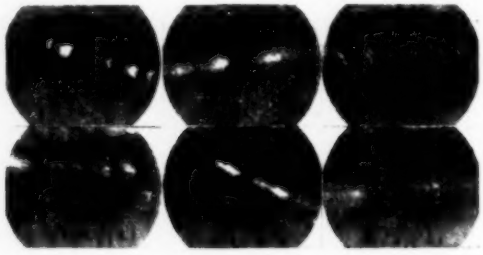

Fig. 1. Cosmic-ray particle tracks in air at 68 cm pressure. Magnification $\times4.03$.

All of the good pictures of tracks that were identified in that way have been photographed again under a low-power microscope, in order to count the ions, with results such as are shown in Fig. 1. This could only be done with the denser tracks, for some were so faint, either due to their small ionization or to weak illumination, that it was previously found necessary to mark the positions of their images by scratching fine lines on the negatives before using them in the stereo-reconstruction outfit. For this reason, also because of the evident difficulty of resolving individual droplets in the tracks, it is only possible to fix an approximate upper limit to the ionization along them. In all cases a liberal allowance was made for the bunching of ions, which results in a diminution of the number of drops. The specific ionization thus determined does not exceed 32 ion-pairs per cm, in water-saturated air at 68 cm pressure, or $32\times76/68=36$ pairs per cm at normal pressure. This is less than one third of the value calculated by Kolhörster and Tuwim, but is in agreement with the 40 pairs per cm estimated by Skobelzyn[3] for similar tracks that he found to be undeflected by a magnetic field of 1500 gauss.

The problem is, then, to explain the discrepancy between the values obtained on Kolhörster and Tuwim's calculation and the cloud-chamber deter-

[2] L. M. Mott-Smith and G. L. Locher, Phys. Rev. **38**, 1399 (1931).
[3] D. Skobelzyn, Zeits. f. Physik **54**, 686 (1929).

minations, since it seems especially desirable that the specific ionization should be known with some certainty, because of its bearing on the interpretation of ionization experiments and for determining the energy (so perhaps deducing the origin) of cosmic-rays.

Very heavy tracks were produced in the cloud-chamber by α-particles and x-ray photoelectrons, under conditions exactly similar to those existing during the formation of the cosmic-ray particle tracks. This leads to the belief that every ion-pair in these relatively thin tracks was the nucleus of a droplet, since there was always an abundance of super-saturated water vapor available for condensation. The present count is based on the assumption that every drop represents an ion-pair, and that every ion-pair gave a drop, the separation of the ions of any pair being too small to be detected by the means used, at 68 cm pressure.* Concerning the electrical method, it seems quite certain that not every cosmic-ray particle passing through a counter will give an impulse in it, especially because of the "group phenomenon" described in the next section, and if the number counted is less than the number penetrating the tube, the specific ionization calculated on this basis will be too large. On the other hand, there is a possibility that some of the ions in the cloud-tracks recombine before condensation can occur on them, resulting in an apparent reduction of the specific ionization; but the same argument would apply even more strongly to recombination in the ionization chambers, because of their higher pressure, thus emphasizing the present disagreement, instead of removing it.

The "Group Phenomenon"

By the "group phenomenon" is meant the practically simultaneous arrival of two or more penetrating particles, in a given small region, more often than can be explained by accidental coincidence. It was first noticed by Auger and Skobelzyn,[4] who found, on 27 cloud-pictures of tracks that were undeflected

Series Number	Pictures with thin, straight tracks	Groups of these tracks
1	74	13
2	11	1
3	63	6
Totals:	148	20

"Track-pictures" showing groups: 20/148 = 13.5 percent (If the count is not restricted to thin straight tracks, the ratio becomes: 33/177 = 18.6 percent).

by a field of 1500 gauss, 4 cases in which there were groups of these tracks. It was thought that the particles were recoil electrons due, in each case, to repeated Compton scattering of one of the hardest components of "ultra-gamma" radiation. They calculated that such electrons would have sufficient

* Another effect might tend to reduce the number of drops photographed: one drop may screen off the light from another, while the picture is being taken. But the sparseness of the ionization in these thin tracks makes it unlikely that this is important, even with the worst orientation of the track with respect to the line of illumination.

[4] P. Auger and D. Skobelzyn, Comptes Rendues **189**, 55 (1929).

penetrating power to follow the quantum through the chamber, making a group of tracks.

The 1770 pairs of pictures collected in the present experiment[2] show the results, (see table on preceding page) with regard to groups.

A significant observation was made: *the tracks of a group usually converge to a point near at hand.* Fig. 2, *a*, *b*, *d*, and *f*, shows some groups of this type. The agreement of the 13.5 percent of groups with Auger and Skobelzyn's $4/27 = 14.8$ percent may be accidental, but the high percentage (especially of 3), and the convergence of the tracks, is believed to be important. In one case, there were 5 straight tracks on one picture, 3 of which converged at the wall of the chamber; in 5 cases there were groups of 3 tracks, while the other 14 were pairs. One member of one group was aligned with the counting-tube above the chamber; also, a discharge of the counter was recorded simultaneously

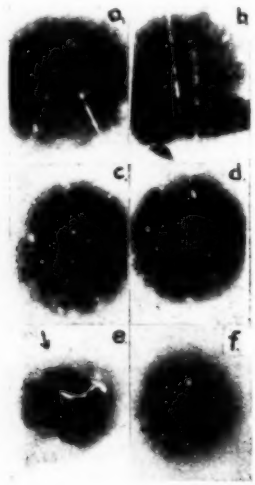

Fig. 2. *a*, *b*, *d*, and *f*, groups of tracks emanating from a common point; *c*, a bent track; *e*, track with a 22,000-volt branch. Magnification ×1.21.

with the formation of the track, indicating that the particle had passed through it, hence was of the type previously discussed. Examination of the tracks of the groups with a microscope shows that the specific ionization along them is about the same as for tracks identified by means of the counter, so the velocities of the particles must exceed 0.9 C.

The convergence of the tracks shows that the particles could not have been liberated at great distances from the apparatus, and indicates that they were produced by one cause and are not merely due to chance arrival of several particles at nearly the same time (within 0.06 sec.). In view of the existence of these groups, as well as their convergence, it is difficult to support the view of Bothe and Kolhörster, that cosmic-rays are only swift β-particles coming from inter-stellar space; it is more probable that the observed particles are secondary electrons ejected from atoms near at hand, by high energy photons. These electrons may come either from inside or outside the nuclei of the atoms, since the cosmic-ray energies so greatly exceed those of

γ-rays. If the tracks of each group converge to a point, approximately, it is difficult to explain them as being made by recoil electrons due to Compton scattering, because of the low probability of getting more than one scattering within so small a thickness of matter as the wall of the cloud-chamber (5mm of glass). The same difficulty would apply to the ejection of electrons from the nuclei, unless more than one electron is ejected when a cosmic-ray photon collides with a nucleus. It may be, however, that the constituents of the nucleus are so closely packed as to allow a considerable probability of the simultaneous ejection of two or more particles, due to a collision of this type; or the ejection of even one such electron may destroy the equilibrium of the nucleus and cause it to eject additional corpuscles, within a very short time. These processes would constitute atomic disintegration, brought about by cosmic rays, instead of beginning spontaneously as in ordinary radioactivity.

Clearly, a group of particles passing simultaneously through a Geiger-counter, or any arrangement of counters, will cause only a single impulse; hence the number of impulses recorded will be less than the number of particles passing through. This will affect ionization determinations, and perhaps other measurements, involving the use of counters. For example, Kolhörster and Tuwim's value of the specific ionization of cosmic-ray particles is about 3.7 times as great as the author's. To explain the discrepancy on the basis of this effect alone, it would only be necessary to assume that Tuwim's counter gave, on the average, one impulse for every 3 or 4 electrons traversing an equivalent volume of Kolhörster's ionization chamber. It will be further noticed that the divergence of the tracks of the groups increases the effective size of any counting-tube or other device arranged to intercept them.

Another point to consider is the effect of the secondary electrons liberated from the walls of an ionization chamber, on the ionization measured therein. In this connection, suppose a beam of very penetrating rays produces secondary electrons as it passes through successive layers of matter of different densities, but undergoes little total absorption. A simple calculation shows that the number of secondary electrons in any cross-section of the beam is constant, hence independent of the density of the material traversed, even at a boundary, provided that the number ejected per cm varies directly with the density of the material, and the length of track varies inversely with the density. These conditions are approximately satisfied by γ-rays, and may even apply to cosmic-rays, if these latter only eject recoil electrons from outside the nucleus and *single* electrons from inside. But if there is a finite probability that more than one electron will be ejected from a nucleus by a single photon, this probability must be a function of the atomic number of the element under bombardment, so that the mass law will not hold. For example, the number of cosmic-ray particles crossing a section would be the same for gaseous oxygen as for liquid oxygen, but the number would be different for oxygen and iron, on this supposition, because the nuclei are different. To test this experimentally, one could compare the cosmic-ray ionization in a series of ionization chambers that have the same dimensions and gas content, but have walls of metals of different atomic numbers (with the same mass per

unit area). This might well be done by comparing the ionization in pairs of the chambers, using a differential method. (Evidently Geiger-counters could not be used, because the effect investigated is due to simultaneous groups of particles.) The ionization produced in the same chambers by radioactive γ-rays could be used as a check, in case the experiment gave positive results; this should be the same in all the chambers. The author believes that this experiment would lead to positive results, because of the groups of tracks observed in cloud-chambers. The absorption anomalies found by Geiger, Steinke, and others[5] are also thought to be connected with the group phenomenon.

Some Energy Considerations

Some simple deductions about the order of magnitude of the energy of cosmic rays have been made from the value of the specific ionization. These calculations are mostly speculative, because of the uncertainty of the hypotheses on which they are based, but they may be of interest.

A β-particle of energy $E > 7 \times 10^8$ volts, and specific ionization 36, could pass through the atmosphere and still have residual energy $> 2 \times 10^8$ volts, which is sufficient to allow it to penetrate about 40 cm of lead. (A specific ionization of 135 in air would require $E > 2 \times 10^9$ volts.)

The path of an electron of 2×10^8 volts energy is $\geqq 3500$ meters in air at normal pressure; this corresponds to about 4.6 meters in water, or 42 cm in lead. If a photon of 2×10^9 volts energy produces, on the average, one 2×20^8 volt electron at every 950 meters of its path through the atmosphere, then any cross-section of the photon's path should have 3.7 electrons in it, if they are ejected in the forward direction. This would account for the high value of the specific ionization calculated by Kolhörster and Tuwim. Such photons would undergo about 10 scatterings in traversing the atmosphere, so that homogeneous incident radiation would be degraded into a spectrum with energy between 2×10^9 and zero, at the earth's surface. This is suggested as a possible process, rather than a probable one. Elaboration and test of a good theory of nuclear absorption seems especially desirable.

Fig. 2, *c*, and *e*, shows two interesting tracks, probably of recoil electrons from radioactive γ-rays, that were found among the pictures collected in this work. A sharp bend in the first (43° deflection) indicates close approach of the particle to a nucleus. In the case of the track shown in *e*, a 22,000 -volt branch was produced, causing a deflection of only 5.7° in the path of the β-particle. Assuming that both were electrons, and that momentum was conserved at the impact, the velocity of the impinging one was 0.92 C (energy 7.8×10^5 volts). Evidently an electron of 10^8 volts energy would undergo no appreciable deflection in producing a similar branch.

The author is indebted to the National Research Council for a grant which met part of the expense of the experimental work herein described.

Professor H. A. Wilson has very kindly criticized this paper and has suggested part of the ideas and calculations incorporated in it, for which the author wishes to express his appreciation.

[5] Discussion of Ultra-Penetrating Rays, Proc. Roy. Soc. **A132**, 331 (1931).

X-RAY REFLECTION FROM INHOMOGENEOUSLY STRAINED QUARTZ

CHARLES S. BARRETT AND CARL E. HOWE
NAVAL RESEARCH LABORATORY, BELLEVUE, ANACOSTIA, D. C.*

(Received February 8, 1932)

ABSTRACT

Laue spots from quartz crystals undergoing piezo-electric vibrations are found to have a fine structure. The nature of this structure is such as to indicate that the increase of reflecting power of a given crystallographic plane varies greatly from point to point in the crystal, while at a given point in the crystal the reflecting power of different planes is increased in different amounts with a resultant intensity distribution unlike that obtained from a rough-ground surface of the crystal. It is proposed that these effects are due to the existence of strain gradients in the crystal, distributed at random in the rough-ground surface but in definite directions in the case of a vibrating crystal. This view is substantiated by some static tests on inhomogeneously strained crystals. Some specimens of quartz with imperfect interior regions are found to have random strain gradients. The effect on reflected intensity may be accounted for on the basis of a reduction of extinction. The phenomenon is used in the study of modes of vibration of quartz plates.

IT IS well known that the ability of a crystal to reflect x-rays is influenced by the degree of perfection of the crystal. This is explained by assuming the presence of an extinction of the x-ray beam superimposed upon the ordinary absorption of the beam.[1] Extinction is of two types, primary and secondary. Considering a crystal to be a mosaic of perfect crystallites, the relation of each type to the structure of the crystal lattice may be stated thus: primary extinction arises within the perfect crystallites and is reduced by a reduction of the size of these (provided they are not already smaller than about 10^{-4} cm); secondary extinction depends upon the parallelism of the blocks and is reduced when this is reduced.

Many investigators[2,3,4,5,6,7] have noted that grinding or polishing the surfaces of various crystals greatly increases their reflecting power as would be expected if this treatment reduced perfection and consequently extinction in the crystal.

Fox and Carr,[8] looking for a change in the sharpness of Laue reflections

* Published with the permission of the Navy Department.

[1] cf. C. G. Darwin, Phil. Mag. **43,** 800 (1922); W. L. Bragg, C. G. Darwin, R. W. James, Phil. Mag. **1,** 897 (1926).

[2] A. H. Compton, Phys. Rev. **10,** 95 (1917).

[3] W. L. Bragg, R. W. James, and C. H. Bosanquet, Phil. Mag. **41,** 309 (1921); **42,** 1 (1921).

[4] R. G. Dickenson and E. A. Goodhue, J. Am. Chem. Soc. **43,** 2045 (1921).

[5] B. Davis and W. M. Stempel, Phys. Rev. **17,** 608 (1921); **19,** 504 (1922).

[6] E. Wagner and H. Kurlenkampff, Ann. d. Physik **68,** 369 (1922)

[7] Y Sakisaka, Jap. Jour. Phys. **4,** 171 (1927); Proc. Phys.-Math. Soc. of Japan, Ser. III, **12,** 189 (1930).

[8] G. W. Fox and P. H. Carr, Phys. Rev. **37,** 1622 (1931).

from a quartz plate put into piezoelectric oscillation, found instead a large change in intensity of the Laue spots. Langer[9] suggested that the phenomenon could be explained by a tilting of the mosaic blocks during oscillation of the crystal—a theory based on the reduction of secondary extinction as a result of the tilting. Explanations were independently advanced by Nishikawa, Sakisaka, and Sumoto,[10] and by Barrett[11] on the basis of a reduction of extinction due to inhomogeneous strains in the crystal, and Laue photographs were published showing that the interior of the crystal becomes highly reflecting during oscillation[12] in the same way that the surfaces become highly reflecting when ground. That static inhomogeneous strains within the elastic limit could thus affect the reflecting power of quartz and certain other crystals was demonstrated by Nishikawa, Sakisaka and Sumoto,[13] who also showed that homogeneous strains had little or no effect.

The failure of Fox and Cork[14] to observe changes in intensity of oscillating quartz using reflection from the surface of a quartz plate in a Bragg spectrometer was probably due to the existence of an imperfect surface layer which was the seat of practically all the reflected energy in their experiment, a layer in which extinction had already been reduced to a minimum by the preparation of their crystal.[15]

Experimental Method and Results

When the Laue method is used with a sufficiently well-defined primary beam, the Laue spots are elongated images of the slit, each portion of the spot being formed by rays reflected from a corresponding region within the crystal. Contrary to results of previous observers who did not attend carefully to the parallelism of the beam, the spots from a vibrating quartz crystal are not uniformly dark, but generally display a fine structure. Laue photographs of the same part of a crystal in both vibrating and rest conditions showed that this fine structure is not similar to that produced by permanent flaws in the crystal which sometimes become evident by this method. Nor is it caused by the ground or polished surface of the crystals: the different type of structure seen in the spots from non-oscillating ground or polished crystals as well as the added length of exposure time necessary to form a pattern of non-oscillating crystals proves this. Peculiarities of x-ray focal spot or slits could not have caused the fine structure, nor could the presence of characteristic radiation in the primary beam. The origin of the fine structure was

[9] R. M. Langer, Phys. Rev. **38,** 573 (1931).

[10] S. Nishikawa, Y. Sakisaka, and I. Sumoto, Phys. Rev. **38,** 1078 (1931).

[11] C. S. Barrett, Phys. Rev. **38,** 832 (1931).

[12] Here, and wherever hereafter the term "oscillating" occurs in this paper, the reader will understand that the word "vibrating" is intended. The former term is so completely established in electrical usage that it is adopted in this paper, even at the risk of confusion with its ordinary implication to those familiar with x-ray spectrographs.

[13] S. Nishikawa, Y. Sakisaka and I. Sumoto, Phys. Rev. **38,** 1078 (1931); Y. Sakisaka and I. Sumoto, Proc. Phys.-Math. Soc. of Japan, Ser. III, **13,** 211 (1931).

[14] G. W. Fox and J. M. Cork, Phys. Rev. **38,** 1420 (1931).

[15] C. S. Barrett and C. E. Howe, Phys. Rev. **38,** 2290 (1931).

found to shift with the crystal when the crystal was shifted and to disappear when the crystal ceased vibrating. There appears no room for doubt that the fine structure represents a variation of reflecting power from point to point in the crystal resulting from the processes of vibration.

To facilitate the investigation, pin-hole slit systems were constructed whereby several beams from a single x-ray tube could be made to strike adjacent portions of the same crystal and produce simultaneously several Laue patterns on the same film. With a suitable distance from crystal to film each pattern could be obtained free from confusion with the others.

Another device to aid in the rapid production of suitable Laue patterns brought into use the focussing property of rays reflected through a crystal plate, illustrated in Fig. 1. A narrow diverging beam from a point source penetrates a crystal standing perpendicular to the beam at a distance from the source. In passing through the crystal these diverging rays are reflected from atomic planes throughout their path in the crystal. Those reflected from the front of the crystal will be brought to a focus at a certain point in space, those from the back of the crystal will focus at another point, and similar focussing

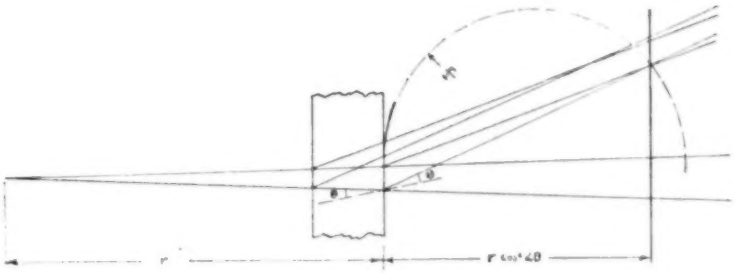

Fig. 1.

will occur for reflections originating at any given depth in the crystal. The layer at a distance r from the source will reflect rays to a focus on a sphere of radius $r/2$ tangent to this layer. From Fig. 1 it will be seen that a photographic plate at the distance $r \cos^2 2\theta$ from this layer will receive the focussed rays reflected from crystallographic planes inclined $\theta°$ to the beam. If $r \cos^2 2\theta$ is large compared with the cross-section of the beam and the thickness of the crystal, the film will be approximately in focus for all layers of the crystal and for a considerable range of θ. The radial distribution of intensity in the Laue spot will then represent the distribution of reflecting power in the different layers of the crystal, as it does in the simple case of a narrow bundle of parallel rays. A point source of x-rays not being available, rays were used leaving a flat target at an angle of 4°, which gave effectively a line source. With the target face horizontal, satisfactory focussing occurred for reflections occurring in or near a vertical plane. Other reflections lacked detail and were disregarded. It was necessary, of course, to limit the cross-section of the primary beam until no important loss of detail in the spots resulted from either the averaging over the crystal surface or the cross fire in the horizontal direction.

Fig. 2 shows a portion of a Laue pattern from an x-cut (0° or Curie cut)[16] quartz crystal of dimensions $l_x = 4.0$ mm, $l_y = 20.78$ mm, $l_z = 26.40$ mm, where l_x and l_z are measured parallel to the electric and optic axes respectively, and l_y perpendicular to both these. The crystal was cut and polished with an accuracy of about 45′ with respect to the optic axis and 15′ with respect to the electric axis. It was oscillating piezoelectrically at a calculated frequency of about 715 kilocycles (the so-called x-oscillation).[17] The spots in this pattern are grouped by threes corresponding to the three pin-hole slits (each $0.02'' \times 0.02'' \times 1\frac{3}{4}''$) diverging from a common point at the focal spot of the tube with an angular separation of 1° between adjacent slits. The portion of the pattern reproduced is one in which focussing is satisfactory—space prohibits printing the whole pattern on a scale sufficiently large to show the fine structure of the spots.

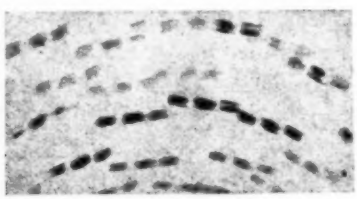

Fig. 2. Laue spots from an x-oscillating x-cut quartz plate.

It will be seen at once from Fig. 2 that the reflecting power of the interior of the oscillating crystal is not uniform. Since the fine structure of the spots differs among the three spots of a triplet it follows that a given crystallographic plane varies in reflecting power from point to point inside the crystal. Furthermore, corresponding members of triplets (for example, the middle spots) differ in structure showing that at certain points in the crystal the reflecting power of some planes is increased much more than that of others.

Similar Laue patterns with multiple slits of 3, 4 and 5 holes were taken of four different x-oscillating x-cut crystals in all, yet less than 10 percent of the stronger spots showed a uniform darkening and in general there was no similarity between the fine structure of any but adjacent spots.

An attempt was made to trace the reflecting power distribution throughout the interior of the x-cut crystal described above, by making a series of 96 Laue patterns with the primary beam penetrating the crystal at 96 different places. This crystal was mounted between x-face electrodes in the holder shown in Fig. 3. A bakelite framework fastened to a mechanical stage from a microscope supported the crystal and permitted it to be shifted parallel to itself at will. Two pieces of thin aluminum sheet served as electrodes, one moving with the crystal and the other fixed to the heavy brass plate of the

[16] For the method used in the preparation of crystals at the Naval Research Laboratory and the associated nomenclature, cf. Proc. Inst. Radio Eng. **18,** 2128 (1930).

[17] The circuit used was of the type used by Fox and Carr (reference 8), the plate voltage 420, the R. F. tank-circuit current 900 m.a., the rays were from a molybdenum x-ray tube at 30000 volts a.c.

holder. A hole in the brass plate allowed the passage of the direct and reflected rays.

With the crystal, triple slits, and circuit constants mentioned above, enough exposures were made to examine about half the volume of the crystal, the beam in each case entering the crystal approximately parallel to the

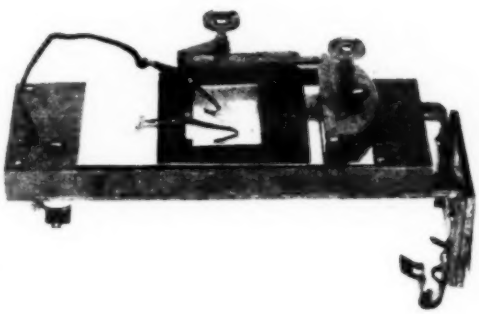

Fig. 3. Crystal holder.

x-axis. Prints were made of each film and the spots formed by reflection from the same strongly reflecting plane were cut out of each print. These individual spots, each representing the reflecting power of the same plane along a line through the crystal parallel to the x-axis, were assembled in correct relative positions on a plot (Fig. 4). The rectangle in Fig. 4 represents on an

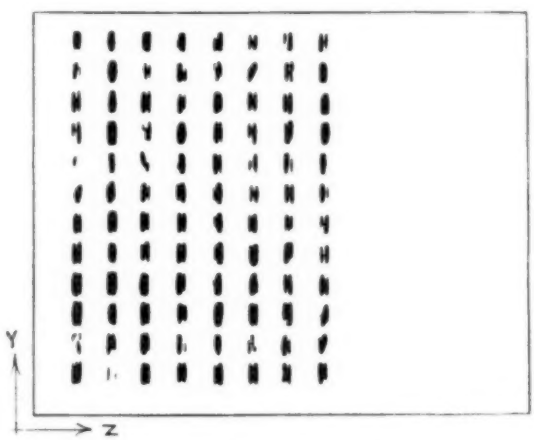

Fig. 4. Plot of reflecting power in an x-oscillating x-cut quartz crystal.

enlarged scale the surface of the crystal normal to the x-axis and containing the Y and Z axes as indicated. The left edge of each spot exhibits the reflecting power for the given plane at the front face of the crystal, the right edge does the same for the back surface and intermediate points for corresponding interior points in the crystal.

The complex distribution of the reflecting power in this vibrating crystal is at once obvious from the plot. The photographs were not taken closely enough together to enable one to trace continuously, from one spot to its neighbors, the streaks of high and low intensity. Regardless of how the reflecting power is related to the mechanical distortions, Fig. 4 testifies to an exceedingly complex mode of vibration. We were not surprised to find evidence of the same complexity by dusting lycopodium powder on the edges and surface of the crystal while oscillating: no simple or completely reproducible powder pattern resulted on any face. The nodes and loops were apparently even less regularly distributed than the complicated ones recently recorded by Wright and Stuart[18] by lycopodium powder methods. These observations confirm their conclusion that the frequency of a mode of this nature cannot be a simple function of Young's modulus in the direction of the thickness and the thickness dimension. The crystal fractured while the powder patterns were being investigated.

Fig. 5. Laue spots from an oscillating *y*-cut quartz crystal.

Laue patterns of oscillating *y*-cut (30°) crystals appear, in general, to be much simpler. A majority of the spots from four different specimens was merely simple doublets. A portion of one pattern containing only doublets is reproduced in Fig. 5. (This crystal had the dimensions $l_x = 28$ mm, $l_y = 4$ mm, $l_z = 26$ mm, and was oscillating at a calculated frequency of about 560 kilocycles.) The exposures to produce patterns from oscillating crystals were so much shorter than those required for non-oscillating crystals that no registration of the non-oscillating pattern could have occurred in Fig. 5. The doublets there are, therefore, not due to reflection from the ground surfaces. In fact, their appearance is quite different from non-oscillating crystal patterns taken with the same apparatus: Fig. 5 shows the intensely reflecting region to extend to a depth of over a millimeter beneath each face, while the effect of grinding extends down only about 1/10 mm below the surface.[19]

It can be said that in general the enhancement of the reflecting power of

[18] R. B. Wright and D. M. Stuart, Bur. of Standards, Jour. of Research **7**, 519 (1931).

[19] Null results were obtained with the so-called *y*-oscillation of an *x*-cut crystal ($l_x = 6.8$, $l_y = 20.2$, $l_z = 25.7$, 131 kilocycles calculated frequency) which showed a simple lycopodium powder pattern. The spots were of the same type and approximate intensity whether the crystal was oscillating or not. Several positions on the crystal were investigated, and the primary beam was tried at 30° to the *x*-axis as well as parallel to it, each case with the same result. It may be that the amplitude of the oscillations was insufficient (R. F. tank-circuit current 60 m.a., plate voltage 400) or that the very simplicity of the mode of vibration is to account for this.

various planes is essentially different when it results from grinding than from piezoelectric vibrations. If this were not so every spot in Fig. 3 would be identical in structure, as is always the case with a non-oscillating crystal with ground surfaces[20] and as is the case with some specimens of quartz having internal flaws or imperfect regions which came under our observation. The reduction of extinction in oscillating crystals is not the isotropic phenomenon that it appears to be in the ground surface of a crystal or in imperfect crystals. An interpretation in terms of the inhomogeneous strains that must be the cause of reduced extinction is that imperfection of the type produced by grinding results from a random orientation of strain gradients, while imperfection produced by vibration results from non-random direction of strain gradients.

Quantitative intensity measurements are not available to show whether or not this accurately describes the situation, but the following qualitative experiment is evidence for it. Laue photographs were taken of a quartz crys-

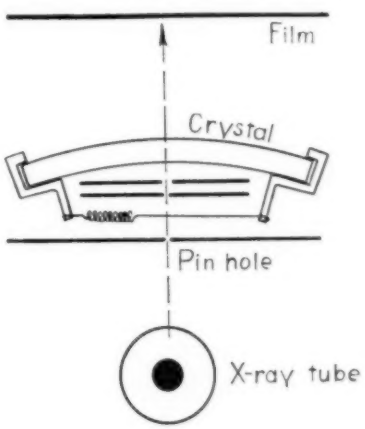

Fig. 6. Apparatus for diffraction from an inhomogeneously strained crystal.

tal with ground surfaces subjected to inhomogeneous static strain as shown in Fig. 6. Forces were applied to bend the quartz bar into a cylinder with the optic axis vertical, parallel to the axis of the cylinder, (perpendicular to the paper in Fig. 6) and the primary beam was directed radially. Under these conditions spots on the Laue pattern above and below the central spot remained doublets resembling those in the unstrained crystal, but spots to the right and left of the central spot increased in intensity and became uniformly darkened. These observations were confirmed with quartz slabs of differing dimensions, and with the plane of the x-ray tube target rotated 90° from the position indicated in Fig. 6 (this in order to eliminate confusion due to the shape of the focal spot).

Along the path of the beam in the interior of the quartz, this inhomogeneous strain should produce a maximum *variation* in atomic plane spacing and orientation for those reflecting planes standing approximately parallel

[20] cf. C. S. Barrett, reference 11, Fig. 1; Y. Sakisaka and I. Sumoto, reference 13, Fig. 1.

to the axis of bending and a minimum variation of interplanar spacing for those approximately perpendicular thereto. Extinction, dependent upon the variation, along the path of the ray, of interplanar spacing and angle of incidence of rays upon the planes, should accordingly be reduced for the planes approximately axial and practically unaltered for the others. The observed intensities were in agreement with this view.

Discussion

It cannot be doubted that the warping of quartz during vibration reduces extinction and causes increased reflection, but whether it is primary or secondary extinction that is involved is not so definite.

Suppose, in the first place, that *secondary* extinction is important for unstrained quartz. Could vibrations reduce this appreciably? The angular width of a monochromatic beam reflected from unstrained quartz was determined by Sakisaka[7] to be 45″ (width at half maximum intensity); estimating the variation in tilt of planes in a vibrating crystal from measurements of surface motion by Osterberg,[21] we find a distribution of the same order of magnitude. It appears, then, that secondary extinction would be reduced if present, for it would be unaltered only if the reflected line were much wider than the superimposed broadening due to the vibrations. The uneven distribution of extinction among the different reflecting planes, as reported in this paper,might be explained on the basis of secondary extinction simply by postulating a suitable distribution function for the orientation or for the interplanar distance of the reflecting planes along the path of the primary beam. This distribution function would be dependent upon the direction and magnitude of the strain gradients in the crystal.

It is by no means certain that the above supposition is correct; Sakisaka[7] in fact, concluded that only *primary* extinction was important in quartz. His conclusion was based on ionization measurements of reflected intensities, and was confirmed by his observations of the shape of the reflected line and the thickness of the reflecting layer of quartz as a function of the coarseness of grinding. He visualized quartz as a mozaic of rather large perfect crystallites in which primary extinction was large, with a scattering from parallelism between different crystallites sufficient to make secondary extinction negligible. More recently in a note by Nishikawa, Sakisaka and Sumoto[13] the statement is made that both primary and secondary extinction is large in quartz. No reason is given for this departure from the conclusions of the earlier experimental data; it does not appear to be justified.

To explain the present results on the basis of primary extinction requires simply that the distorting effect of strains extend into the perfect regions that are the seat of primary extinction. Whether the crystal is a mosaic of blocks with abrupt transitions between them, or a continuous but slightly warped lattice, it would be expected that stresses would reduce primary extinction. To deny this possibility would be equivalent to postulating that the crystal is a mosaic of blocks so loosely welded together that the perfection of the

[21] H. Osterberg, Proc. Nat. Acad. Sci. **15**, 802 (1929).

lattice of each block is unaffected by shifting or tilting the neighboring blocks, which seems unlikely. With the size of the perfect regions as the determining factor for primary extinction, it becomes necessary to postulate a temporary reduction in size under stress, followed by a return to normal with the removal of stress. A reduction in effective size of the perfect part of the lattice need not require a fracture or a permanent deformation; it should only be necessary to introduce strains great enough to destroy coherence in the diffraction from different portions of the normally perfect crystalline unit. If the applied stresses deform the individual perfect blocks of the lattice so that their effective size is larger in one direction than in another, they might produce the anisotropic character of the reflecting power reported in this paper.

The points to be emphasized are that inhomgeneous strains may deform a crystal, normally of high perfection, in such a way that certain lattice planes lose their near perfect spacing and parallelism, while others do not. On the other hand homogeneous strains do not destroy the perfection of any lattice planes. X-ray reflections are influenced by this perfection of planes (and not by the perfection of atomic distribution on a plane) and thus contain evidence of the condition of inhomogeneous strain in the lattice.

This x-ray method of observing distortions in materials contrasts sharply with the photo-elastic method; here the strain gradient at a point is measured, while photo-elastically one observes the strain itself but is unable to observe it as a function of depth below the surface. The numerous methods that have been used to observe modes of vibration in quartz resonators and oscillators —air currents, powder patterns, observation of surface motion, crossed Nicol prisms, air ionization patterns—all yield data of different type than this.

The authors are indebted to the personnel of the Radio Division of this Laboratory for its assistance and interest in this work.

THE ZEEMAN EFFECT OF THE K II SPECTRUM

By Albert E. Whitford
Department of Physics, University of Wisconsin

(Received February 3, 1932)

Abstract

The Zeeman effect of the $3p^54s \leftarrow 3p^54p$ and $3p^54p \leftarrow 3p^55s$ transitions of the K II spectrum has been investigated in an effort to throw light on the failure of the $3p^54s$ configuration to obey Houston's multiplet relations and of the $^3P_2 - {}^3P_0$ interval to follow the regular doublet law. The magnetically resolved lines from a Back vacuum arc were photographed in the 3rd order of a 21 ft grating in a Rowland mounting with a dispersion of 0.89A/mm. A special type of potassium press was developed for extruding potassium metal into the arc as needed. Analysis of the results shows that the classification of de Bruin and Bowen is correct. The g-sum for $J=1$ in. the $3p^54s$ configuration is 2.57 ± 0.02 instead of the theoretical value of 2.50. This breakdown of the sum rule is to be expected if the anomalous intervals in this configuration are caused by perturbations due to the overlapping terms of the $3p^53d$ configuration. Incomplete knowledge of the $3d$ levels prevents testing the constancy of the combined g-sums. The $3p^55s$ and $3p^54p$ configurations obey the g-sum rule satisfactorily.

I. Introduction

THE analysis of the K II spectrum was first given by de Bruin,[1] who was later able[2] to correlate many of the terms with the terms of A I as analyzed by Meissner.[3] Bowen[4] extended the correlation and located the ground term from the resonance lines in the extreme ultraviolet. He also classified the Ca III spectrum in the same iso-electronic sequence. While seeking to extend this sequence the author noticed an exception to the regular doublet law for the $^3P_2 - {}^3P_0$ interval of the $3p^54s$ configuration in K II. The screening constants calculated from the equation

$$\Delta\nu = \frac{R\alpha^2(Z-\sigma)^4}{n^3l(l+1)}$$

are given in Table I. The usual smooth gradual decrease of σ in an isoelectronic progression is here seen to be broken at K II.

Table I.

Spectrum	Z	Interval	σ
A I	18	$3p^54s\,{}^3P$	7.307
K II	19	$3p^54s\,{}^3P$	6.487
		$3p^55s\,{}^3P$	7.115
Ca III	20	$3p^54s\,{}^3P$	7.015

[1] T. L. de Bruin, Zeits. f. Physik **38**, 94 (1926).

[2] T. L. de Bruin, Dissertation Amsterdam (1927); Arch. Neérlandaises des Sciences **11**, 70 (1928).

[3] K. W. Meissner, Zeits. f. Physik **39**, 172 (1926); **40**, 839 (1927).

[4] I. S. Bowen, Phys. Rev. **31**, 497 (1928).

Laporte and Inglis[5] pointed out the failure of the four terms (^1P, ^3P) of this configuration to follow Houston's multiplet relations and suggested that possibly there was an error in the classification. They found that the $3p^5 5s$ configuration obeyed Houston's equations well.

It is noteworthy that, as shown in Table I, the triplet width in the $3p^5 5s$ configuration is just right to give a reasonable screening number for K II (the screening of a $5s$ electron should differ only very slightly from that of a $4s$ electron). Also, this triplet width agrees very closely, as it should, with the doublet width of the ground term of the K III spectrum as determined by Bowen.[4] Furthermore, if a plot of the $3p^5 4p$ terms relative to their centroid is made for the A I, K II, Ca III isoelectronic sequence,[6] the points for K II fall very nearly on straight lines between A I and Ca III.

It is thus apparent that the classification of the $5s$ and $4p$ terms in K II is very probably correct, making it less likely that the $4s$ terms are not right. A more probable explanation of the above mentioned anomalies seemed to be that the overlapping of the $3p^5 3d$ terms with the $4s$ terms causes as interaction between the two configurations. In such a case the usual regularities would no longer be expected to hold. A similar case has been found in Rb II by Laporte, Miller, and Sawyer,[7] and other examples of the same general phenomenon are continually being reported in the literature.

In view of the wide application of the almost universal regularities here violated, it was considered worthwhile to undertake a Zeeman effect study of the K II spectrum to throw more light on the anomalies. De Bruin[2] attempted to confirm his analysis by Zeeman effect photographs, but was not able to obtain any completely resolved patterns, so that g-values could not be determined. The triplet and quartet blends of 8 intense lines were shown to be of the right general type, however.

II. Experimental Details

The magnetic field was produced by a water cooled Weiss type electromagnet very generously loaned for this investigation by the Ryerson Physical Laboratory of the University of Chicago. The pole separation was 4.6 mm and the pole tip diameter 10 mm. With a current of 12 amperes through the coils, a magnetic field of about 32,500 gauss was obtained. This was determined separately for each exposure by using the Zn lines 4680, 4722, 4810 as standards.

The light source was a Back interrupted vacuum arc.[8] Considerable difficulty was experienced in exciting the potassium spectrum with sufficient intensity between the magnet poles over long enough periods of time. Finally a special potassium press was developed for extruding potassium metal into the arc as needed. Fig. 1 shows the construction. The whole arrangement

[5] O. Laporte and D. R. Inglis, Phys. Rev. **35,** 1337 (1930).

[6] For examples of this see, for example J. E. Mack, O. Laporte and R. J. Lang, Phys. Rev. **31,** 748 (1928).

[7] O. Laporte, G. R. Miller and R. B. Sawyer, Phys. Rev. **38,** 843 (1931).

[8] E. Back, Handbuch der Experimentalphysik XXII, 59. Akad. Verlagsgesellschaft, Leipzig, (1929).

was mounted on a flanged plug which fitted into one of the 1 inch holes around the rim of the cast bronze ring which formed the walls of the "Back box". A 6.3 mm plunger in a brass cylinder actuated by a screw forces potassium into a 1 mm hole in the center of a copper blade 2 mm thick which fits up against one pole piece, but is insulated from it with a strip of mica. On the axis of the pole piece a 0.5 mm hole is drilled in the copper blade parallel to the lines of force, through which the potassium is extruded. A fine copper tube carries cooling water around the edge of the copper blade to keep the potassium from melting. Without this the rate of flow became quite uncontrollable as soon as the potassium melted just back of the hole.

The other electrode was a thin strip of molybdenum. This was caused to oscillate about 10 times per second along the lines of force by a eccentric

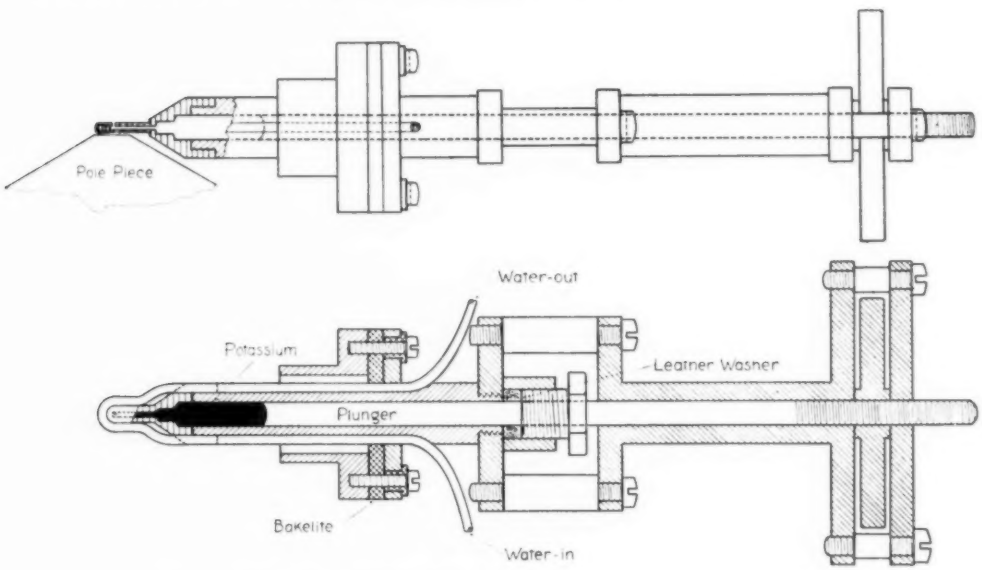

Fig. 1. Potassium press for extruding potassium metal into the arc.

mounted on the shaft of a small motor. The arc was operated from a 116 volt d.c. circuit with rheostats and an inductance in series and drew an average current of 1.8 amperes.

The magnetically resolved spectrum lines were photographed on Eastman 40 plates in the 3rd order of a 21 ft Rowland concave grating in a Rowland mounting. The grating was 5.6 inches wide and was ruled with 15,000 lines per inch. The alignment of the grating and slit and the focus were carefully adjusted by trial exposures of the hyperfine structure of the Hg 4358 line. The slit width used for the Zeeman pictures was 0.018 mm. The temperature of the grating room was held constant to within 0.03°C by a thermostat arrangement.

The region from 3400A to 5200A was covered on 5 plates, with a dispersion of 0.89A/mm. The exposure time varied from 24 hours to 42 hours. The parallel and perpendicular polarizations were not separated. This would have

necessitated doubling the already tedious exposures. Usually there is no doubt as to the identity of the parallel components because of their greater intensity. In certain cases where the two polarizations overlap there is a reduction in the amount of information derivable from a single pattern, in that only one of the g-values involved in the transition can be determined.

It was found that Zeeman components lying closer than about 0.07A (0.3 Lorentz unit) to each other were not resolved. This is somewhat greater than the line width usually obtained from the type of source used, but it is believed that the diffuseness is due to the inherent natural breadth of the potassium lines, rather than to imperfect experimental conditions, because Cd and Mo patterns on the same plates were very sharp, coming fully up to the results expected from the grating and plate used.

The measurement of the separation of the components was carried out on traces made with a Kipp and Zonen type *A* recording microphotometer giving a magnification of 50 times. Six records taken at different points vertically along a spectrum line were averaged. A millimeter scale was printed on the sensitive paper immediately after the trace of the photographic plate had been exposed. This insured that any changes in length during development or thereafter would be immaterial, as well as greatly facilitating the measurement.

III. Results

A sufficient number of completely resolved patterns was obtained to fix the g-values of the $4s$ terms and most of the $4p$ terms. Shenstone and Blair[9] have calculated the distance of the "center of intensity" from the position of the undisplaced line for unresolved triplet and quartet blends and shown how, when one of the g-values involved in a transition is known, this can be used to find the other g-value. Their method was applied to the unresolved potassium patterns and the remaining g-values thereby determined. The best success was obtained with the σ-components of quartet patterns ($\Delta J=0$), where the

Table II.

Wave-length	Classification	Type	Calculated	Observed	Remarks
5005.60	$4s_5-4p_{10}$	*C*	(0.52), 1.47, 1.99	0.53, 1.48, 2.01	
4943.24	$4s_2-4p_8$	*B*	(0), 1.18	0, 1.18	*bf*
4829.23	$4s_5-4p_{10}$	*A*	(*0*), (0.49), *1.01*, 1.50, 1.99	*0*, 0.49, *1.01*, 1.50, 1.99	
4659.38	$3d_3-4p_9$	*A*	(0), 1.10	0, 1.08	*bf*
4608.45	$4s_2-4p_6$	*B*	(0), 1.27	0, 1.32	*b*
4595.65	$3d_3-4p_8$	*C*	(0.35), (*0.70*), 0.80, *1.15*, *1.50*, 1.85	0.37, *0.74*, 1.14, 1.51, 1.88	
4466.65	$4s_3-4p_7$	*D*	(0), 0.69	0, 0.69	
4388.16	$4s_2-4p_4$	*C*	(0.16), 1.02	0, 1.06	*bp*
4340.03	$3d_5-4p_7$	*C*	(0.76), 0.69, 1.45	0.75, 1.46	*d*
4309.10	$4s_2-4p_3$	*B*	(0), 1.42	0, 1.50	*b*
4288.70	$4s_2-4p_5$	*D*	(0), 1.10	0, 1.12	*c*
4263.40	$4s_4-4p_8$	*A*	(*0*), (0.32), *0.83*, 1.15, 1.47	*0*, 0.31, *0.82*, 1.13, 1.43	
4225.67	$3d_5-4p_6$	*A*	(0), 1.09	0, 1.09	*b*

[9] A. G. Shenstone and H. A. Blair, Phil. Mag. **8**, 765 (1929).

TABLE II (*Continued*)

Wave-length	Classification	Type	Calculated	Observed	Remarks
4222.97	$4s_2-4p_2$	*C*	(0.29), 1.24	0.29, 1.24	*b*
4186.24	$4s_5-4p_9$	*A*	(0), 1.10	0, 1.09	*b*
4149.19	$4s_3-4p_4$	*D*	(0), 0.94	0, 0.94	*c*
4134.72	$4s_5-4p_8$	*C*	(0.35), (*0.70*), 0.80, *1.15*, *1.50*, 1.85	*0.74*, 1.16, 1.50, 1.84	
4114.99	$4s_4-4p_7$	*C*	(0.78), 0.69, 1.47	0.75, 1.46	*d*
4093.69	$4p_6-5s_5$	*C*	(0.52), 1.35	0.54, 1.35	*b*
4065.23	$4p_2-5s_3$	*D*	(0), 1.39	0, 1.39	
4042.59	$3d_3-4p_3$	*C*	(0.34), 1.40	0.35, 1.39	*b*
4039.69	$3d_5-4p_4$	*C*	(0.51), 0.94, 1.45	0.51, 0.94, 1.45	
4024.88	$4p_6-5s_4$	*A*	(0), 1.20	0, 1.22	*b*
4017.52	$4p_2-5s_2$	*C*	(0.12), 1.33	0, 1.33	*bp*
4012.10	$4s_4-4p_6$	*A*	(0), 1.08	0, 1.08	*b*
4001.24	$4s_3-4p_2$	*D*	(0), 1.39	0, 1.39	
3995.10	$4s_5-4p_7$	*B*	(*0*), (0.81), 0.69, 1.50, *2.31*	*0*, *0.81*, 1.51, *2.32*	*c*
3991.80	$4p_7-5s_5$	*B*	(*0*), (0.81), 0.69, 1.50, *2.31*	0, 0.78, 2.3	*f*
3972.58	$3d_5-4p_3$	*A*	(0), 1.24	0, 1.25	*b*
3966.72	$3d_3-4p_2$	*B*	(0), 1.56	0, 1.58	*b*
3959.84	$4p_5-5s_3$	*D*	(0), 1.27	0, 1.27	*f*
3955.21	$3d_5-4p_5$	*D*	(0), 1.45	0, 1.45	
3942.53	$4p_3-5s_2$	*B*	(0), 1.38	0, 1.43	*b*
3926.36	$4p_7-5s_4$	*C*	(0.54), 0.69, 1.23	0.59, 1.23	*d*
3923.00	$4p_4-5s_3$	*D*	(0), 0.94	0, 0.94	
3899.28	$3d_5-4p_2$	*C*	(0.06), 1.42	0, 1.41	*bpf*
3897.92	$4s_5-4p_6$	*C*	(0.52), 1.35	0.55, 1.35	*b*
3878.62	$4p_4-5s_2$	*C*	(0.33), 1.11	0.32, 1.11	*bf*
3873.74	$3d_6-4p_4$	*D*	(0), 0.94	0,0.94	
3861.41	$4p_8-5s_5$	*C*	(0.35), (*0.70*), 0.80, *1.15*, *1.50*, 1.85	0.35, *0.74*, 1.15, 1.50, 1.85	
3817.50	$4p_9-5s_5$	*A*	(0), 1.10	0, 1.10	*b*
3800.14	$4p_8-5s_4$	*A*	(0), 1.11	0, 1.07	*b*
3783.19	$4s_4-4p_3$	*A*	(0), 1.23	0, 1.21	*b*
3767.36	$4s_4-4p_5$	*D*	(0), 1.47	0, 1.48	
3739.13	$4s_5-4p_4$	*B*	(0), (0.56), 0.94, 1.50, *2.06*	*0*, 0.57, 1.50, *2.07*	
3721.34	$4p_6-5s_3$	*A*	(0), 1.18	0, 1.22	*b*
3716.60	$4s_4-4p_2$	*C*	(0.08), 1.43	0, 1.45	*bp*
3681.54	$4s_5-4p_2$	*C*	(0.34), 1.41	0.34, 1.41	*b*
3676.05	$4p_7-5s_3$	*D*	(0), 0.69	0, 0.68	
3618.49	$4s_5-4p_2$	*B*	(0). 1.56	0, 1.57	*b*
3530.75	$4s_2-4p_1$	*D*	(0), 1.10	0, 1.09	
3404.24	$4p_{10}-5s_5$	*A*	(*0*), (0.49), *1.01*, 1.50, 1.99	*0*, 0.48, *1.01*, 1.49	*f*

b = unresolved triplet or quartet blend. Here calculated means distance to center of intensity by Shenstone and Blair formula.
c = impurity line obscures part of pattern. Low accuracy.
d = σ and π components overlap.
f = faint line, difficult to measure. Low accuracy.
p = positive and negative π components blended together, making apparent triplet.

Notes. Calculated and observed columns give distance of component from field-free line in Lorentz units. ( ) means polarized $\parallel$ to field. Observed lines are not so marked because the two polarizations were not separated experimentally. Italic type means most intense component in group.

Types *A*, *B*, *C*, *D* are the same as in Back's Ne paper, reference 10, or as his "Grundtypen" I, II, III, IV respectively, in reference 8.

intensity is symmetrical about a point displaced a distance $(g_1+g_2)/2$ from the field-free line, measure in Lorentz units.

In the case of triplet blends the method is somewhat less reliable. The

laws of blackening of the photographic plate, and all the uncertainties of the photographic process make the location of the "center of intensity" very doubtful. Measurements were actually made to the peak of the microphotometer curve. With infinitely narrow microphotometer slits, this would be the point of maximum blackness, which would not be the center of intensity. However, the effect of finite slit width (plate grain necessitated fairly wide slits) is to push the peak toward the direction of smaller density gradient, a direction opposite to the previous error. A survey of all the results on triplet blends show that usually the first mentioned error predominates, indicating that the peak of the microphotometer curve is not the center of intensity, although it is the only practical point to select for measuring.

The observed Zeeman patterns and those calculated from the g-values selected as the most probable are shown in Table II. In the case of unresolved patterns the position of the center of intensity calculated from Shenstone and Blair's formulas is shown in the theoretical column. The notation use is the same as that used by Meissner for A I, except for prefixing the principal quantum number of the excited electron to a term in place of his series number. It is taken from Paschen's classic analysis of Ne I and is in general use for rare

TABLE III. *g-values of K II terms.*

Config.	Term		$J=0$	$J=1$	$J=2$	$J=3$
				g-values		
$3p^5 4s$	$4s_5$				1.50	
	$4s_4$			1.47		
	$4s_3$		0/0			
	$4s_2$			1.10		
		Sum	0/0	2.57	1.50	
		Theory	0/0	2.50	1.50	
$3p^5 5s$	$5s_5$				1.50	
	$5s_4$			1.23		
	$5s_3$		0/0			
	$5s_2$			1.27		
		Sum	0/0	2.50	1.50	
		Theory	0/0	2.50	1.50	
$3p^5 4f$	$4p_{10}$			1.99		
	$4p_9$					1.30*
	$4p_8$				1.15	
	$4p_7$			0.69		
	$4p_6$				1.21*	
	$4p_4$			0.94		
	$4p_3$				1.31*	
	$4p_5$		0/0			
	$4p_2$			1.39		
	$4p_1$		0/0			
		Sum	0/0	5.01	3.67	1.30
		Theory	0/0	5.00	3.67	1.33
$3p^5 3d$	$3d_6$		0/0			
	$3d_5$			1.45		
	$3d_3$				1.50	

* Determined entirely from blends.

gas type spectra. The correlation with de Bruin's empirical notation is given by Bowen.[4]

The g-values and the g-sums are summarized in Table III. The average probable error in a single g-value is about 0.01.

IV. Discussion

The complete agreement of the observed patterns with the types expected confirms the existing analysis of the spectrum due to de Bruin and Bowen. Furthermore, the g-values for the $4p$ terms follow closely those found by Back[10] for Ne I, the only other spectrum of this type for which a complete Zeeman study has been made. His values for the g-values of the terms in the same order as they occur here are: 1.984, 1.329, 1.137, 0.6695, 1.229, 0.999, 1.301, 0/0, 1.340, 0/0. This is further confirmation.

The g-sum for $J=1$ in the $4s$ configuration comes out definitely too large, having a value 2.57 ± 0.02 instead of the usual 2.50. If the anomalies in the $4s$ configuration are due, as was discussed above, to interaction with the $3d$ configuration, the g-sums of the two configurations would be shared and the sum of the g's of all the terms having a given value of J in *both* configurations would be invariant. It is not possible to test this out as only 5 of the 12 $3d$ terms are known, some of the others being so situated that transitions with the $4p$ configuration would lie in the infrared.

The breakdown of the g-sum rule for the $4s$ configuration, however, is just what would be expected if there were a perturbing influence due to the $3d$ configuration and is to be regarded as a confirmation of this explanation of the irregularities. It would not have been surprising if the g-value of the term $4s_5(^3P_2)$ had departed from the value of 1.50 fixed by the sum rule. The probable reason for its being unaffected is that it is farther removed from the $3d$ term which would be likely to perturb it.

The $3p^5 4p \leftarrow 3p^5\,5s$ transitions were of course weaker and many did not appear at all; a few fell outside the region photographed. Consequently it was not possible to determine the g-values of the $5s$ terms with as great accuracy as the others. The perfect agreement of the observed and theoretical g-sum for $J=1$ is probably fortuitous. The g-values for these two terms calculated from Houston's formula come out 1.25 for each. The difference between observed and calculated is possibly within the range of experimental error.

The difference between the observed value 1.30 and the theoretical value 1.33 for the g-sum of the term for which $J=3$ in the $4p$ configuration is undoubtedly due to the fact that it was determined entirely from two very broad triplet blends, where Shenstone and Blair's method is least reliable. The g-sums for $J=2$ and $J=1$ in the $4p$ configuration are in very satisfactory agreement with the sum rule.

It is a pleasure to acknowledge the author's indebtedness to Drs. J. E. Mack and C. E. Mendenhall for their helpful interest in this work. He also wishes to thank Mr. R. O. Anderson for assistance in making the microphotometer records.

[10] E. Back, Ann. d. Physik **76**, 317 (1925).

PHOTOIONIZATION PROBABILITIES OF ATOMIC POTASSIUM

By Melba Phillips
Department of Physics, University of California

(Received February 5, 1932)

Abstract

Calculations of the absorption probabilities in the continuous spectrum of the potassium atom were made to investigate the possibility that the second maximum in the experimental photoionization curve is of atomic origin. The model for the K atom is a single normal state valence electron moving in a non-Coulomb central force field. Two fields were used. The first was determined to satisfy the quantum conditions on the radial phase integrals for the x-ray and optical levels. This field is in error in the region of the deeper shells, and was replaced by Hartree's self-consistent field for the K atom, corrected for polarization of the core to give the observed term values for the normal state and 3_2 orbits as eigenvalues of the wave equation. The wave functions were obtained by numerical integration, and the matrix integrals for transition probabilities determined graphically. The resulting probability curve was found to decrease steadily from the series limit, with no hint of the experimental maximum. It further appears that no reasonable changes in the field will produce such a variation. The magnitude of the absorption coefficient at the series limit is about 2×10^{-20} by our calculations, and

$$-df/d\epsilon = 1/3\ \nu/R\ [I]^2,$$

where I is the matrix integral, is 0.0024, much smaller than for lighter hydrogen-like atoms. From the percentage association of the vapor and $-df/d\epsilon$ for the atom it is estimated that the second maximum could be attributed to molecules if $-df/d\epsilon$ per valence electron at the molecular threshold were about 2. This value seems very large, but not impossibly so.

THE photoionization per unit light intensity in potassium vapor as a function of the frequency of incident radiation shows two maxima,[1] one at the series limit, 2856A, and another at 2340A. The number of molecules present in the K vapor under the conditions of the observations was not very large, and it has seemed probable that the observed absorption was due to atomic K. If this were so the course of the absorption coefficient for the K atom would be very different from that of hydrogen or any other alkali atom, for except in the case of K the absorption falls off rapidly and steadily from the limit. It seemed of interest to determine whether this anomalous behavior could be understood theoretically. We have therefore calculated the absorption coefficient quantum mechanically, taking as a model for the K atom a single valence electron moving in a suitably chosen non-Coulomb field. Calculations similar in some respects to ours have been made earlier for other alkali atoms. Thus Hargreaves[2] determined relative intensities in the continuous spectrum of lithium, using the central field of Hartree, with numerical and graphical integration. During the progress of this work calculations by Trumpy[3] for lithium and sodium have appeared.

[1] Lawrence and Edlefsen, Phys. Rev. **34**, 1056 (1929).
[2] Hargreaves, Cambr. Phil. Soc. **XXV**, 75 (1929).
[3] Trumpy, Zeits. f Physik **71**, 720 (1931).

We have used two methods to determine the field in which the valence electron of our atom moves, in both of which the core electrons are taken into account only by the addition of their field to the field of the nucleus. One is

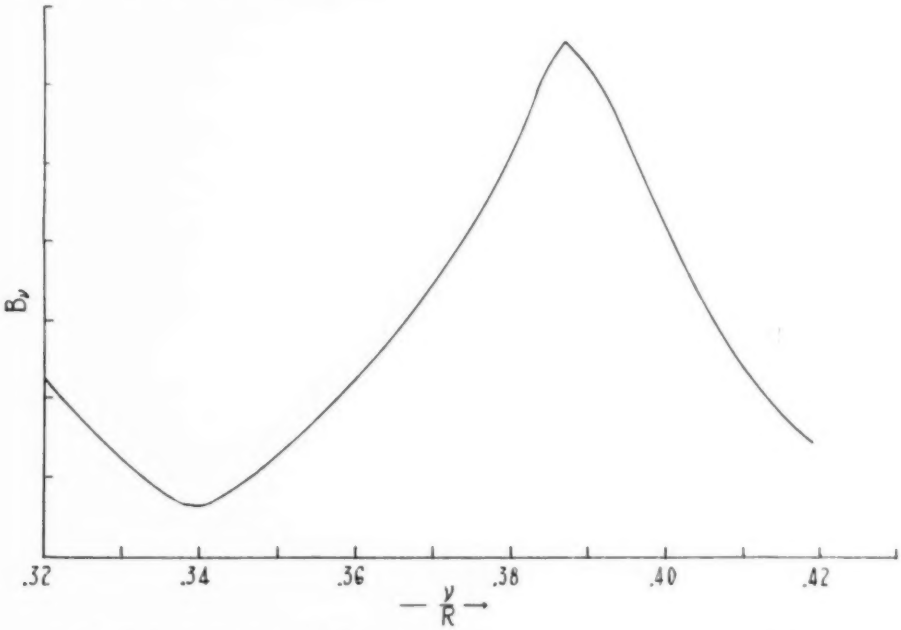

Fig. 1. Relative ionization probability, B_ν, of potassium vapor as a function of the frequency as obtained by Lawrence and Edlefsen. 0.32 is the term value for the normal state, and thus the, frequency of the series limit in units of R.

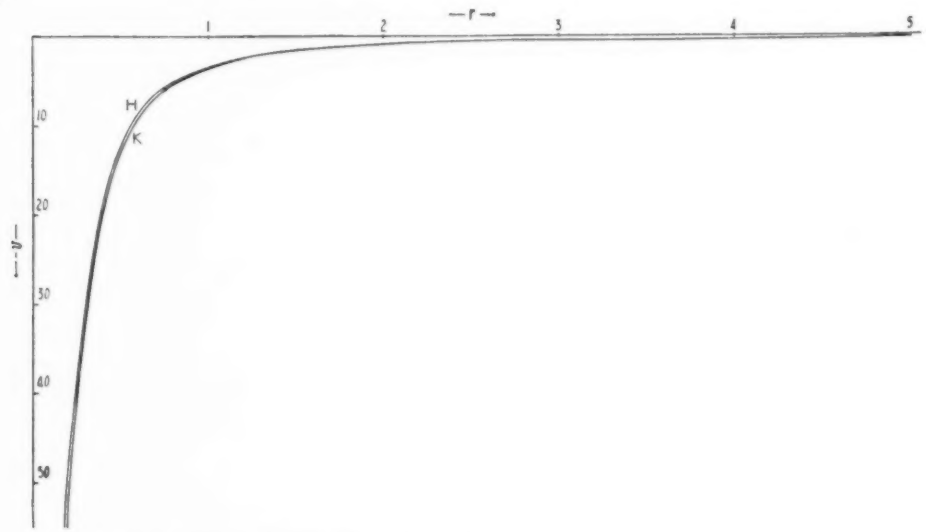

Fig. 2. Fields representing the K ion. Curve K was obtained by the phase integral method. Curve H is the Hartree self-consistent field, corrected for polarization of the core. r is in units of a_0.

substantially that applied by Zwaan[4] to the computation of the line intensities of Ca^+. In this method the field is so chosen that the radial phase integrals have the proper half integral values when the corresponding experimental term values are given to the energy. In the second method we started with the self-consistent field for the K ion; for this we are greatly indebted to Dr. Hartree, who communicated his values to us. This field we adjusted to give the correct term values for the normal state and the 3_3 orbit, by a theoretically derived correction for the polarization of the core. We shall discuss these two methods in order, and shall return later to a consideration of the possible error in our determination of the field, and its effect upon the absorption coefficient. The two fields differ appreciably, but they give approximately the same absorption curve; in both cases the absorption decreases steadily from the limit, and thus fails to agree with the experimental results.

It is convenient to work with "atomic units", which are defined:

Unit of length, $a_0 = h^2/4\pi^2 me^2$, radius of the first Bohr orbit of hydrogen.

Unit of energy, $E_0 = e^2/2a_0$, equal to the ionization potential of the H atom with a fixed nucleus. This is one half the unit adopted by Hartree.[5]

Unit of time, $1/4\pi cR$.

Then $-E = \epsilon E_0$, $V(r) = v(r)E_0$, and r is expressed in terms of a_0.

For the first method we proceed as follows: The Kramers phase integral with these units is

$$n - 1 - \tfrac{1}{2} = \frac{1}{\pi}\int_{r_{\max}}^{r_{\max}} \frac{1}{r}(-\epsilon r^2 - (l - \tfrac{1}{2})^2 - r^2 v(r))^{1/2} dr.$$

The field is determined graphically, using in this expression the empirical values of ϵ for each level in turn, with the proper quantum numbers. Values for the x-ray terms were obtained from Siegbahn's tables, or from the Moseley diagrams. Fine structure differences were neglected and a mean value taken for multiplet terms. Data for the optical levels were those given by Paschen and Goetze. For each orbit $\epsilon r^2 + (1+\frac{1}{2})^2$ is a parabola, and an initial vr^2 curve is assumed, to be varied until the integral, evaluated by means of a planimeter, is as nearly $(n-1-\frac{1}{2})$ in every case as possible. In thus attempting to satisfy simultaneously the quantum conditions for all the terms it is assumed that the field is the same no matter from which shell an electron is missing. The error introduced by this assumption could amount to almost a whole unit of charge for the inner shells, since the charge density of the valence electron near the nucleus is small compared with one belonging to the K or L group. When the curve of calculated intensities failed to reveal the experimental maximum the Kramers field was abandoned in favor to the self-consistent field of Hartree; for small radii, however, it serves as a lower limit to variations possible in the field, as will be explained later.

In the self-consistent field the actual field of every electron is represented by the field of its mean charge distribution. Such a field does not take into

[4] Zwaan, Doctor's Dissertation, Utrecht, 1929.

[5] Hartree, Cambr. Phil. Soc. Proc. **XXIV**, 19 (1928).

account the polarization of the core by the valence electron, and in the case of K the ionic field given by Hartree fails entirely to give the observed term value for the normal state. For large radii we may introduce a polarization correction by subtracting from the potential $\alpha e^2/r^4$, where α is the polarizability of the core, 0.8×10^{-24} for K. This correction was made directly for $r>3a_0$; in the region $r<0.8a_0$ the Hartree curve was left unchanged; in the intermediate range $0.8a_0<r<3a_0$ the Hartree curve was so lowered that it joins the other portions smoothly, and that it gives, on numerical integration of the wave equation, the experimental term value for the normal state and very nearly that for the 3_3 orbit.

The radial factor of the wave function satisfies the equation:

$$\chi'' + \frac{2}{r}\chi' + \left(v - \epsilon - \frac{l(l+1)}{r^2}\right)\chi = 0.$$

If we write $P=r\chi$, the equation for P is

$$P'' + (v - \epsilon - l(l+1)/r^2)P = 0.$$

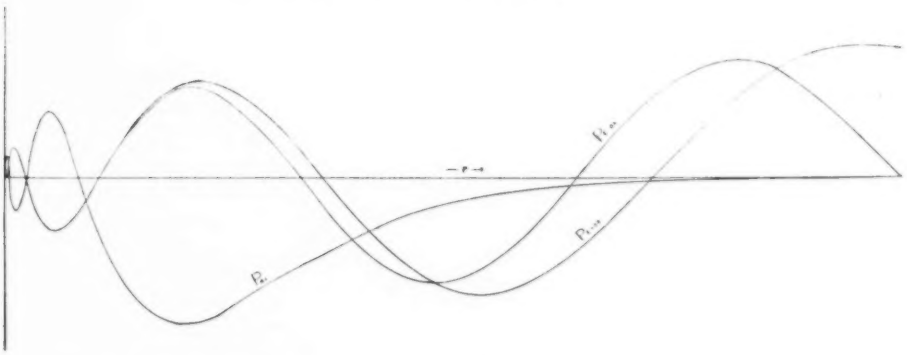

Fig. 3. Wave functions for the normal state, 4_1, and two points in the continuum: $\epsilon=0$, $\epsilon=-0.06$. The range of r in the diagram is 21 a_0.

The observed term value for the normal state (4_1 orbit) is 0.32, and $l=0$. The general method for determining wave functions was numerical integration,[6] starting from a series solution of the equation with $v=38/r$ very near $r=0$, but approximations suggested by Kramers[7] served for comparison and checking; at large r the analytic solution for a Coulomb field was used, being fitted on smoothly to the curve at a point beyond which it was justified. The maxima and nodes of the normal state wave function are almost independent of reasonable changes of the field, $(0.8a_0<r<3a_0)$, but the term value determines the point of inflection, so that the requirement that the function approach zero asymptotically for a given eigen energy gives a sensitive check on the field. Such a field is not unique, but, starting with Hartree's determination and keeping the condition on the phase integrals satisfied, a polarization correction is fairly well defined.

[6] See reference 5.

[7] See reference 4.

For transitions to the continuous spectrum of energy values we must have $l=1$, to satisfy the selection rule. The wave equation becomes

$$P'' + (v - \epsilon - 2/r^2)P = 0$$

where $-\epsilon$ is now positive. The wave function is oscillatory, and the solutions of the asymptotic form, $P''-\epsilon P=0$, are circular functions. The solution is chosen which is zero at $r=0$, and behaves there as r^{l+1}. The wave functions are found by numerical integration throughout the region in which there is a contribution to the matrix integrals.

The normal state function is normalized in the usual fashion, by determining graphically $\int_0^\infty P^2 dr$, but normalization in the continuous case is more troublesome. Hargreaves shows that the normalized solution is

$$\frac{1}{\pi^{1/2}\epsilon^{1/4}} \frac{aL + bM}{(a^2 + b^2)^{1/2}}$$

with

$$L = \frac{\alpha G - \beta H}{2}, \qquad M = \frac{\alpha H + \beta G}{2}.$$

Here

$$\alpha + i\beta = \epsilon\Gamma(2 + \epsilon^{1/2})\exp(-i\epsilon^{1/2}\pi/2)$$

and G and H are power series solutions of the equation $P''+(2/r-\epsilon-2/r^2)=0$.

$$G = \sigma^2(a_0 + a_1\sigma + a_2\sigma^2 + a_3\sigma^3 + \cdots)$$

$$H = \frac{1}{\sigma}(b_0 + b_1\sigma + b_2\sigma^2 + b_1\sigma^3 + \cdots) + \alpha G(\sigma)\log\sigma$$

with $\sigma = 2r$.

In practice G, H, G', H', were evaluated[8] for the point nearest the origin at which the field may be assumed Coulomb, α and β calculated, and thus L, M, L', M', determined. These were fitted onto the values of P and P' obtained by numerical integration at that radius by means of determining a and b in

$$\frac{1}{\pi^{1/2}\epsilon^{1/4}} \frac{aL + bM}{(a^2 + b^2)^{1/2}}.$$

It is obvious that this method fails for $\epsilon=0$. The normalized solution[9] for this case is

$$(1/2)^{1/2} \frac{aG_1 + bH_1}{(a^2 + b^2)^{1/2}}.$$

$$G_1 = \sigma^{1/2}J_3(2\sigma^{1/2})$$

$$H_1 = \sigma^{1/2}Y_3(2\sigma^{1/2})$$

[8] I wish to thank Mr. R. Edwin Worley for his assistance in the computation of these series.

[9] Hartree, Cambr. Phil. Soc. Proc. **XXIV**, 430 (1928).

J is the ordinary Bessel function and Y is Neumann's Bessel function of the second kind:

$$J_3(2\sigma^{1/2}) = \sum_{n=0}^{\infty} \frac{(-1)^n}{n!(n+3)!}\sigma^{3+2n/2}$$

$$Y_3(2\sigma^{1/2}) = \frac{2}{\pi} J_3(2\sigma^{1/2}) \log \sigma^{1/2} - \frac{1}{\pi} \sum_{n=0}^{\infty}(-1)^n \frac{\psi(n)+\psi(3+n)}{n!(3+n)!}\sigma^{(3+2n)/2}$$

$$- \frac{1}{\pi} \sum_{n=0}^{2} \frac{(2-n)!}{n!}\sigma^{(2n-3)/2}$$

where $\psi(n) = -0.0557216 + 1 + \frac{1}{2} + \cdots + 1/n$.

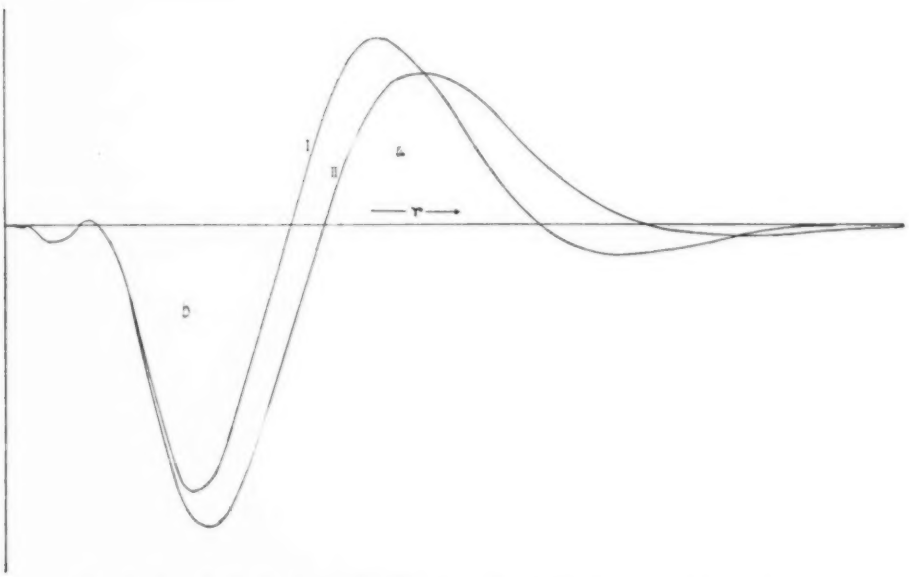

Fig. 4. Plot of $rP_{4_1}P_{-\epsilon}dr$ as a function of r. Curve I is for $\epsilon = -0.06$, and curve II for $\epsilon = 0$. Again the range of r is $21a_0$.

A value of r may be chosen for which $2\sigma^{1/2}$ is an integer, and values of J and Y obtained from tables of Bessel functions. J' and Y' are determined by their relations to the functions of adjacent order.

The absorption coefficient[10] is given by

$$\sigma = \frac{8\pi^3 e^2 \nu}{3hc} \frac{\left[\int_0^\infty rP_{4_1}P_{-\epsilon}dr\right]^2}{\left[\int_0^\infty P_{4_1}{}^2 dr\right]^2} = \frac{8\pi^3 e^2 \nu}{3hc}(I)^2$$

where $P_{-\epsilon}$ is normalized as above. The coefficient was computed for four values of ϵ: $\epsilon = 0$, the series limit, $\epsilon = -0.02$, corresponding to the minimum

[10] See reference 2.

of the experimental curve, $\epsilon = -0.06$, its maximum, and $\epsilon - 0.10$. The resulting curve of probabilities falls off monatonically from the series limit, as shown by Fig. 5, somewhat faster than the λ^3 law, and exhibits no suggestion of the experimental peak. Calculations made earlier with the Kramers field gave a curve of much the same form. The absolute value of the atomic absorption cross-section at the series limit is about 2.2×10^{-20}, while Mohler[11] gives 1×10^{-19} from estimations on Ditchburn's experiments, and 8×10^{-19} as that for sodium. The values of $-df/d\epsilon = \nu(I)^2/3R$ at the series limits for the hydrogen-like atoms are:

H (Sugiura)[12]	0.8
Li (Trumpy)	0.46
Na (Trumpy)	0.038
K	0.0024.

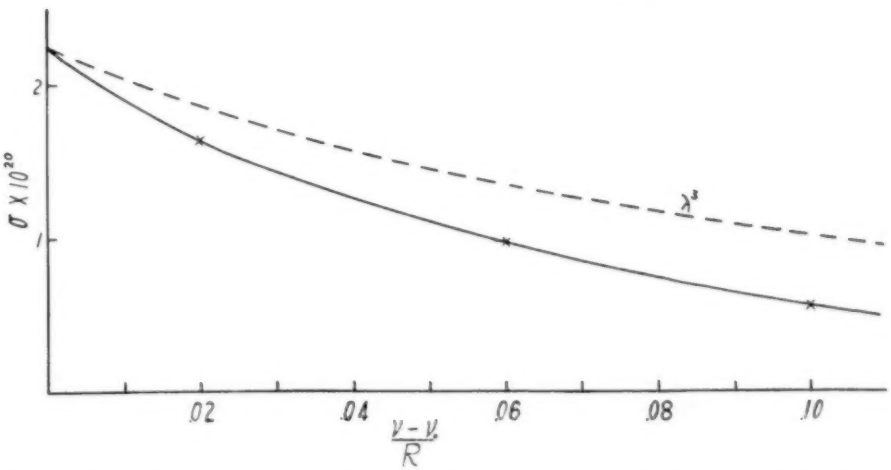

Fig. 5. Absorption coefficient as a function of frequency. The initial point and the three crosses represent calculated points, and the dotted curve shows the λ^3 law.

We now examine the field of the atom to find whether any possible changes will give the anomalous intensity maximum. It may again be divided into three parts. For $r > 5a_0$ it is fixed, being, except for $\alpha e^2/r^4$, very nearly Coulomb. For $r < a_0/2$ Hartree's field should be a good approximation, and any polarization effect would not bring it lower than the Kramers field, which, as we saw, also gave a decreasing curve of intensities. In the range $a_0/2 < r < 5a_0$ the field is not precisely determinate, but we have examined the effect of changes in this region in some detail. In the first place the nodes of the wave functions in the continuum (see Fig. 3) will for any field move in with an increase of energy. From the plot of the matrix integrals (Fig. 4) we see that the two regions a and b nearly cancel each other; for our field b is the larger. In order that an increase in energy should increase the absorption coefficient it would therefore be necessary: (1) that a be larger than b for small energies;

[11] Mohler, Phys. Rev. Suppl. **1**, 219 (1929).
[12] Sugiura, Jour. de Phys. **VIII**, 113 (1927).

or, (2) that the absolute magnitude of the normalized wave functions for the continuum should increase rapidly with the energy. We have convinced ourselves that no change which leaves correct the term value of the normal state can give a field satisfying condition (1); that is to say, it is impossible to change the field in the region $a_0/2 < r < 5a_0$ in such a way that the nodes are moved out appreciably and that the point of inflection of the normal state wave function remains in place. As to (2) we may say that for both the fields for which we have made calculations the magnitude of the continuous wave function decreases markedly and uniformly with increasing energy; we see no reason why an electron of energy 0.04, say, should spend a relatively very much larger time in the atom than one of energy 0.02. The analysis involved in the normalization of the continuous wave functions is, however, highly complicated, and we have not been able to exclude with complete rigor the occurrence of such anomalous behavior as suggested in (2).

We have seen that the absorption coefficient falls monatonically from the limit, and that its magnitude there is approximately 2×10^{-20}. It also appears that no reasonable changes in the atomic field will yield such a variation of the coefficient with the frequency as is shown in the experimental curve. It has been suggested by some authors that the second maximum is due to molecular ionization. According to calculations by Loomis and Nusbaum[13] of the percentage of association from the spectroscopically determined heat of dissociation, the ratio of molecules to atoms at 210°C, the temperature at which Lawrence and Edlefsen worked, is 2:1000. Their maximum could then be explained as a molecular phenomenon if $df/d\epsilon$ for the molecules at the threshold is approximately 2, as compared to the atomic $df/d\epsilon$ of 0.0024. This value, while not impossible, seems unreasonably large. Experiments are in progress in this laboratory to determine the velocities of the emitted electrons, and to find whether there is any dependence of the relative heights of the maxima on temperature, which should furnish a conclusive answer to the question.

The writer wishes to thank Professor H. A. Kramers for suggestions at the beginning of work on this problem, and to express appreciation of the advice and encouragement of Professor J. R. Oppenheimer, under whose supervision the investigation was carried out.

[13] Loomis and Nusbaum, Phys. Rev. **39**, 89 (1932).

AN APPROXIMATE CALCULATION OF THE LOWER ENERGY LEVELS OF THE CARBON ATOM

By Niel Freeborn Beardsley
Ryerson Physical Laboratory, University of Chicago

(Received January 27, 1932)

Abstract

Slater's theory of the complex atom as modified and extended by Zener and Eckart is applied to the $2p^2$ and $2p^3$ configurations of the carbon atom. The energy levels resulting from these configurations are computed. Some of the computed energy differences agree roughly with the experimental values, others indicate either that the method is not applicable or that the experimental data are not reliable. The $2p^3$, ^5S level is found to lie nearest to the normal $2p^2$, ^3P level. Of the levels for which experimental data are lacking or doubtful, the $2p^3$, ^1D is computed to lie 12.9 volts above the normal, the $2p^3$, ^3S, 13.7 volts and the $2p^3$, ^1P, 14.7 volts above the normal.

SINCE the completely rigorous solution of the complete wave equation for the more complex atoms seems to be impossible, many attempts at approximate solutions have been made. This paper is an application of certain of these approximate methods to the calculation of the lower energy levels of the carbon atom. Two principles must be considered in any such method. First, only those levels exist which are characteristic numbers of Schrödinger's equation for the atom. Second, only those levels exist which are associated with characteristic functions that are antisymmetric in the electrons. The electron spin is introduced from the beginning in connection with the second of these principles but is neglected with respect to the first. In determining approximate functions, it is assumed that each electron moves in a Coulomb field of force but that electrons with different total or different azimuthal quantum numbers move in fields of slightly different strengths. The best values for these fields, that is the best effective nuclear charges, are determined.

Following Slater,[1] the wave function for a single electron, that is, a solution of Schrödinger's equation for a single particle in a central field, may be written as $u(n_i/x_i)$ where n_i stands for the four quantum numbers: n_i, l_i, m_{s_i}, m_{l_i} and x_i stands for the four coordinates, three of position and one of spin. It is known that a product of N of these functions approximately satisfies the wave equation governing N electrons but is not antisymmetric. A linear combination of these solutions is also an approximate solution and that one which is antisymmetric may be written as a determinant:

$$\psi = \begin{vmatrix} u(n_1/x_1) & u(n_1/x_2) & \cdots & u(n_1/x_N) \\ \cdot & \cdot & \cdots & \cdot \\ u(n_N/x_1) & u(n_N/x_2) & \cdots & u(n_N/x_N) \end{vmatrix}. \qquad (1)$$

[1] J. C. Slater, Phys. Rev. **34**, 1293 (1929).

This form is frequently shortened to $|u(n_1/x_1)\cdots u(n_N/x_N)|$ by writing only the elements on the principal diagonal. When the subscripts are omitted, it is understood that they are in the normal order of cardinal numbers.

From this wave function, the diagonal terms of the energy matrix are then computed:

$$W_n = \int \psi_n H \psi_n^* d\tau / \int \psi_n \psi_n^* d\tau . \tag{2}$$

Here H is the energy operator neglecting spin:

$$H = \sum_i (\nabla_i^2 + 2Z/r_i) - \sum_{ij} (2/r_{ij}) . \tag{3}$$

Distances are measured in units of $a_H = 0.528$A and energies in units of Rh $\text{cm}^{-1} = 13.529$ volts $= 109678$ wave numbers. Z is the true nuclear charge in units of e.

In the development of these integrals, theorems and methods given by Slater[1] and also by Zener[2] were used. Slater shows that except where energy levels lie very close together or are degenerate the non-diagonal terms of the energy matrix are negligible. As a spherically symmetrical energy operator without spin has been assumed, the non-diagonal terms involving transitions between states with the same n and l values but different m_l and m_s values can not be neglected since these states will have the samee nergy. However, use of the principle of the constancy of diagonal sums as discussed by Slater,[1] enables one to get the correct sums of energy values without actual use of pertubation calculations. This principle is: Given an orthogonal set of wave functions: $\psi_1 \cdots \psi_N$, make an orthogonal set of linear combinations of them: $\psi_1' \cdots \psi_N'$. Let the diagonal terms of the energy matrix, referred to the original set of wave functions, be $W_1 \cdots W_N$, and the diagonal terms of the energy matrix, referred to the new wave functions be $W_1' \cdots W_N'$. Then $W_1 + \cdots + W_N = W_1' + \cdots + W_N'$, that is, to the zeroth approximation, the sum of a number of energy values is not changed by applying a pertubation even if the individual values are. If, in such a sum, each of the energy values except one is known, that one can be determined by subtracting the known values from the sum. This "method of sums" is frequently used in this paper.

If the determinants of Eq. (1) were substituted directly into the integrals of Eq. (2), $(N!)^2$ terms would appear in each integral. However, Zener[2] shows that if but one term in the expansion of the first determinant is substituted into each of the integrals, there will be no change in W. This leaves only $N!$ terms. In developing the remaining determinant, terms containing all possible transpositions of the N electrons would be found. Any of these terms which contains the electron function of a particular electron with a spin opposite to the spin of that electron in the single term of the first determinant which was retained, will also vanish. Lastly, since all the electron functions except those for $1s$ and $2s$ electrons are orthogonal and since H acts on at

[2] C. Zener, Phys. Rev. **36**, 51 (1930).

most two electron functions at a time, those terms containing three or more transpositions (except for $1s$ and $2s$) from the order of the single term will vanish. These conditions greatly reduce the number of terms involved in computing W.

Eckart[3] has shown that if arbitrary screening constants, or as has been used in this paper, arbitrary effective nuclear charges are introduced into the electron functions and then these charges varied to give maximum negative values to W, the resulting value of W is a good approximation to the corresponding term value. From what has gone before, it is evident that this is true even when W has been calculated by the method of sums. Actually it was found in the cases tried that the numerical result was essentially the same whether the maximizing process was applied before or after the method of sums was used, though this is not theoretically necessary.

Application to the Carbon Atom

It was found convenient in the actual calculations to replace the general notation $u(n_i/x_i)$ by a shorter non-systematic notation as given in Table I.

Table I.

$1s$	$u(100/x_i)$	$u=2(\alpha^3)^{1/2}e^{-\alpha r}Y_{0,0}$	$=u^+$
$2s$	$u(200/x_i)$	$v=(\beta^3/2)^{1/2}e^{-\beta r}(1-\beta r/2)Y_{0,0}$	$=v^+$
$2p(m_l=0)$	$u(210/x_i)$	$x=(\gamma^3/6)^{1/2}(\gamma r/2)e^{-\gamma r/2}Y_{1,0}$	$=x^+$
$2p(m_l=-1)$	$u(21-1/x_i)$	$w=(\gamma^3/6)^{1/2}(\gamma r/2)e^{-\gamma r/2}Y_{1,-1}$	$=y^+$
$2p(m_l=+1)$	$u(211/x_i)$	$y=(\gamma^3/6)^{1/2}(\gamma r/2)e^{-\gamma r/2}Y_{1,+1}$	$=w^+$

$$Y_{l,m_l}=\left(\frac{(2l+1)\,(l-m_l)!}{4\pi(l+m_l)!}\right)^{1/2}e^{im_l\phi}P_{l_{m_l}}(\cos\theta)$$

$$Y_{0,0}=(1/4\pi)^{1/2}$$
$$Y_{1,0}=(3/4\pi)^{1/2}\cos\theta$$
$$Y_{1,-1}=(3/8\pi)^{1/2}\sin\theta\, e^{-i\phi}$$
$$Y_{1,+1}=(3/8\pi)^{1/2}\sin\theta\, e^{+i\phi}$$
$$Y_{2,0}=(5/4\pi)^{1/2}(1/2)\,(3\cos^2\theta-1)$$
$$Y_{2,\pm1}=(15/8\pi)^{1/2}e^{\pm i\phi}\sin\theta\cos\theta$$
$$Y_{2,\pm2}=(15/32\pi)^{1/2}e^{\pm 2i\phi}\sin^2\theta$$

In this new notation the spin quantum number is not directly included but is represented by a $(+)$ or $(-)$ sign written as a superscript. The undetermined nuclear charges which are to be determined by the maximizing process described above are represented by α for $1s$ electrons, β for $2s$ and γ for $2p$ electrons. It was found desirable in making the numerical calculations to transform these quantities by $\beta=\alpha/x$ and $\gamma=\alpha/(x+y)$.

The lowest states of the carbon atom arise from the configurations $1s^22s^2 2p^2$ and $1s^22s2p^3$. The possible wave functions for the first of these configurations are given in Table II and for the second in Table III. The fourth columns in these tables give the allowed states assuming Russell-Saunders coupling and noting that in the first configuration there are two "equivalent" p-electrons outside of the closed shells while in the second configuration there are three "equivalent" p-electrons and an s-electron outside of the closed shell. These allowed states are discussed in "Structure of Line Spectra" by

[3] C. Eckart, Phys. Rev. **36**, 878 (1930).

TABLE II.

	Σm_l	Σm_s			
$\psi_a = \lvert u^+u^-v^+v^-y^+y^- \rvert$	2	0	^1D		
$\psi_b = \lvert u^+u^-v^+v^-y^+x^+ \rvert$	1	1	^3P		
$\psi_c = \lvert u^+u^-v^+v^-w^+y^+ \rvert$	0	1	^3P		
$\psi_d = \lvert u^+u^-v^+v^-y^+x^- \rvert$	1	0	^1D	^3P	
$\psi_e = \lvert u^+u^-v^+v^-x^+y^- \rvert$	1	0	^1D	^3P	
$\psi_f = \lvert u^+u^-v^+v^-y^+w^- \rvert$	0	0	^1D	^3P	^1S
$\psi_g = \lvert u^+u^-v^+v^-x^+x^- \rvert$	0	0	^1D	^3P	^1S
$\psi_h = \lvert u^+u^-v^+v^-w^+y^- \rvert$	0	0	^1D	^3P	^1S

TABLE III.

	Σm_l	Σm_s				
$\psi_1 = \lvert u^+u^-v^+w^+x^+y^+ \rvert$	0	2	^5S			
$\psi_2 = \lvert u^+u^-v^+y^+x^+y^- \rvert$	2	1	^3D			
$\psi_3 = \lvert u^+u^-v^+y^+x^+x^- \rvert$	1	1	^3D	^3P		
$\psi_4 = \lvert u^+u^-v^+y^+w^+y^- \rvert$	1	1	^3D	^3P		
$\psi_5 = \lvert u^+u^-v^+y^+x^+w^- \rvert$	0	1	^3D	^3P	^5S	^3S
$\psi_6 = \lvert u^+u^-v^+y^+w^+x^- \rvert$	0	1	^3D	^3P	^5S	^3S
$\psi_7 = \lvert u^+u^-v^+x^+w^+y^- \rvert$	0	1	^3D	^3P	^5S	^3S
$\psi_8 = \lvert u^+u^-v^-y^+x^+w^+ \rvert$	0	1	^3D	^3P	^5S	^3S
$\psi_9 = \lvert u^+u^-v^+y^+y^-x^- \rvert$	2	0	^3D	^1D		
$\psi_{10} = \lvert u^+u^-v^-y^+y^-x^+ \rvert$	2	0	^3D	^1D		
$\psi_{11} = \lvert u^+u^-v^+y^+y^-w^- \rvert$	1	0	^3D	^1D	^3P	^1P
$\psi_{12} = \lvert u^+u^-v^+x^+y^-x^- \rvert$	1	0	^3D	^1D	^3P	^1P
$\psi_{13} = \lvert u^+u^-v^-y^-y^+w^+ \rvert$	1	0	^3D	^1D	^3P	^1P
$\psi_{14} = \lvert u^+u^-v^-x^-y^+x^+ \rvert$	1	0	^3D	^1D	^3P	^1P

and six others

Pauling and Goudsmit, Chapter IX and in many other places. The wave function of a state having a given value of $M = \Sigma m_l$ and a given Russell-Saunders symbol is a linear combination of the ψ's appearing opposite these entries in Tables II and III. Thus for example:

$$\psi(^3P,\ M = 1) = a\psi_d + b\psi_e$$
$$\psi(^1D,\ M = 1) = c\psi_d + d\psi_e.$$

These linear transformations are always orthogonal and it is thus possible to apply the method of sums.

In expanding the integrals of Eq. (2), the methods of Zener[2] as discussed above were followed. For example:

$$W_1 = \int \psi_1 H \psi_1^* d\tau \Big/ \int \psi_1 \psi_1^* d\tau$$

$$\int \psi_1 H \psi_1^* d\tau = \int uuvwxy\, H\, [uuvyxw - vuuyxw - yuvuxw - xuvyuw$$
$$- wuvyxu - uuyvxw - uuxyvw - uuwyxv - uuvwxy - uuvxyw$$
$$- uuvywx + vuuwxy + vuuxyw + vuuywx + yuuvxw + xuuyvw$$
$$+ wuuyxv + vuyuxw + vuxyuw + vuwyxu]d\tau$$

$$\int \psi_1 \psi_1^* d\tau = \int uuvwxy[uuvyxw - vuuyxw]d\tau.$$

Here the conjugate complex functions have been replaced by their equivalents as given in Table I. Hence from here on, orthogonalities are computed without using the conjugate of one of the functions.

Because of orthogonalities between functions of s- and p-electrons and between those of two p-electrons, the sum of whose m_l values is not zero, $[\int(u \text{ or } v)(w \text{ or } x \text{ or } y)d\tau = \int wx\,d\tau = \int xy\,d\tau = \int ww\,d\tau = \int yy\,d\tau = 0]$ these integrals fall into two groups. In the first two integrals of the above example, there are no such orthogonalities and an integral takes the form:

$$\int uuvwxy\left[\sum_i(\nabla_i^2 + 2Z/r_i) - \sum_{ij}(2/r_{ij})\right]uuvyxwd\tau.$$

In the others, the presence of two orthogonalities causes all terms coming from the first summation to vanish and only integrals of the form:

$$\int uuvwxy\sum_{ij}(2/r_{ij})uuvyxwd\tau$$

remain. In expanding the summations, two distinct types of integrals result, those coming from the first summation and those from the second. The first of these types involves the product of two normalized spherical surface harmonics. Eckart[3] gives the following formulas (here corrected for certain typographical errors which appear in his paper) for reducing these to integrals of more familiar algebraic functions and for evaluation of the new integrals.

$$\iint\{f(r_1)[Y_1(\theta,\phi)]^2g(r_2)/r_{1,2}\}d\tau_1d\tau_2$$

$$=4\pi\int_{r_1=0}^{\infty}f(r_1)r_1\int_{r_2=0}^{r_1}g(r_2)r_2^2dr_2dr_1$$

$$+4\pi\int_{r_1=0}^{\infty}f(r_1)r_1^2\int_{r_2=r_1}^{\infty}g(r_2)r_2dr_2dr_1$$

$$\iint\{f(r_1)Y_1(\theta_1,\phi_1)g(r_2)Y_1(\theta_2,\phi_2)/r_{1,2}\}d\tau_1d\tau_2$$

$$=\left\{4\pi\int_{r_1=0}^{\infty}f(r_1)r_1^{1-l}\int_{r_2=0}^{r_1}g(r_2)r_2^{l+2}dr_2dr_1\right.$$

$$\left.+4\pi\int_{r_1=0}^{\infty}f(r_1)r_1^{2+l}\int_{r_2=r_1}^{\infty}g(r_2)r_2^{1-l}dr_2dr_1\right\}\frac{1}{(2l+1)}$$

$$\int_r^{\infty}r^ne^{-ar}dr = (n!/a^{n+1})e^{-ar}\sum_{k=0}^{n}(ar)^k/k!$$

and of course

$$\int_0^r r^ne^{-ar}dr = \frac{n!}{a^{n+1}} - \int_r^{\infty}r^ne^{-ar}dr$$

since only integral values of n are involved. The second type involves the product of four harmonics. These can be reduced to products of two only by the following relations which are easily shown to be true by substituting the actual values of the harmonics.

$$Y_{1,0}{}^2 = \frac{1}{(4\pi)^{1/2}} Y_{0,0} + \frac{1}{(5\pi)^{1/2}} Y_{2,0} \qquad Y_{1,\pm1} Y_{10} = \left(\frac{3}{20\pi}\right)^{1/2} Y_{2,\pm1}$$

$$Y_{1,-1} Y_{1,+1} = \frac{1}{(4\pi)^{1/2}} Y_{0,0} - \frac{1}{(20\pi)^{1/2}} Y_{2,0} \qquad Y_{1,\pm1}{}^2 = \left(\frac{3}{10\pi}\right)^{1/2} Y_{2,\pm2}$$

Table IV gives all the resulting integrals.

TABLE IV.

$$b = \int uv\,d\tau = (2x)^{3/2}(x-1)/(x+\tfrac{1}{2})^4$$

$$h_u{}^u = \int u[\nabla^2 u + 2Zu/r]\,d\tau = (2Z-\alpha)\alpha$$

$$h_v{}^v = \int v[\nabla^2 v + 2Zv/r]\,d\tau = (2Z-\alpha/x)\alpha/4x$$

$$h_x{}^x = \int x[\Delta^2 x + 2Zx/r]\,d\tau = \int w[\nabla^2 y + 2Zy/r]\,d\tau = -\frac{\alpha}{4(x+y)}\left[2Z - \frac{\alpha}{x+y}\right]$$

$$h_u{}^v = \int [u\nabla^2 v + v\nabla^2 u + 4uvZ/r]\,d\tau = \{2\alpha bx/(x-1)\}[Z-\alpha/4 - (Z-\alpha)/4x^2]$$

$$\alpha A = \int u_1{}^2 u_2{}^2 2d\tau/r_{12} = 1.25\alpha$$

$$\alpha B = \int u_1 v_1 u_2{}^2 2d\tau/r_{12} = \alpha 8(2x)^{1/2}\left[\frac{2x-1}{(2x+1)^3} - \frac{60x^2-8x-1}{(6x+1)^4}\right]$$

$$\alpha C = \int u_1{}^2 v_2{}^2\, 2d\tau/r_{12} = \frac{\alpha}{2x}\left[1 - \frac{2(4x+1)}{(2x+1)^3} - \frac{4(5x+1)}{(2x+1)^4} + \frac{3(6x+1)}{(2x+1)^5}\right]$$

$$\alpha D = \int u_1{}^2 x_2{}^2 2d\tau/r_{12} = \int u_1{}^2 w_2 y_2 2d\tau/r_{12} = \frac{\alpha}{2(x+y)}\left[1 - \frac{6(x+y)+1}{(2x+2y+1)^5}\right]$$

$$\alpha E = \int u_1 v_1 u_2 v_2 2d\tau/r_{12} = \alpha 32x^2\left[\frac{20x^2-30x+13}{(2x+1)^7}\right]$$

$$\alpha G = \int u_1 v_1 x_2{}^2 2d\tau/r_{12} = \int u_1 v_1 w_2 y_2 2d\tau/r_{12} = \alpha 8(2x)^{1/2}\left\{\frac{2x-1}{(2x+1)^3} - \right.$$

$$\frac{(x+y)^2}{(2x^2+2xy+3x+y)^3}\left[2x^2+2xy+x-y+\frac{6x(x^2+xy-y)}{2x^2+2xy+3x+y} + \right.$$

$$\left.\left.\frac{6x^2(2x^2+2xy-x-3y)}{(2x^2+2xy+3x+y)^2} + \frac{16x^3(x^2+xy-x-2y)}{(2x^2+2xy+3x+y)^3}\right]\right\}$$

$$\alpha H = \int u_1 w_1 u_2 y_2 2d\tau/r_{12} = \int u_1 x_1 u_2 x_2 2d\tau/r_{12} = \frac{224\alpha(x+y)^2}{3[2x+2y+1]^7}$$

$$\alpha I = \int u_1 y_1 v_2 w_2 2d\tau/r_{12} = \int u_1 x_1 v_2 x_2 2d\tau/r_{12} = (-)(256/3)\alpha(2x)^{1/2}(x+y)^2$$

$$\left[\frac{y}{(2x+2y+1)^5\,(2x+y)^3} + \frac{2x^2+2xy+x-y}{(2x+2y+1)^5\,(2x^2+2xy+3x+y)^3} + \right.$$

$$\frac{4x(x^2+xy-y)}{(2x+2y+1)^4\,(2x^2+2xy+3x+y)^4} + \frac{3x^2(2x^2+2xy-x-3y)}{(2x+2y+1)^3\,(2x^2+2xy+3x+y)^5} +$$

$$\left.\frac{6x^3(x^2+xy-x-2y)}{(2x+2y+1)^2\,(2x^2+2xy+3x+y)^6}\right]$$

$$\alpha K = \int v_1{}^2 x_2{}^2 2d\tau/r_{12} = \frac{\alpha}{2(x+y)}\left[1 - \frac{x^4(45x^3+106x^2y+86xy^2+24y^3)}{(2x+y)^7}\right]$$

$$\alpha L = \int v_1 x_1 v_2 x_2 2d\tau/r_{12} = \frac{2\alpha x^4(x+y)^2}{3(2x+y)^9}[45x^2+132xy+101y^2]$$

$$\alpha O = \int w_1 y_1 x_2{}^2 2d\tau/r_{12} = 894\alpha/2560(x+y)$$

$$\alpha P = \int w_1 x_1 y_2 x_2 2d\tau/r_{12} = 54\alpha/2560(x+y)$$

$$(O+2P)\alpha = \int x_1{}^2 x_2{}^2 2d\tau/r_{12}$$

$$(O+P)\alpha = \int w_1 y_1 w_2 y_2 2d\tau/r_{12}$$

$$2\alpha P = \int w_1{}^2 y_2{}^2 2d\tau/r_{12}$$

$$\alpha Q = \int v_1{}^2 v_2{}^2 2d\tau/r_{12} = 77\alpha/256x$$

$$\alpha T = \int v_1^2 v_2 u_2 2d\tau / r_{12} = \alpha 8(2x)^{1/2} \frac{1}{(2x+3)^5 (2x+1)^2} [32+80(2x+1)+$$
$$24(2x+1)^2+10(2x+1)^3+(2x+1)^4 - \frac{1}{(2x+1)(2x+3)} [128+384(2x+1)+$$
$$490(2x+1)^2+100(2x+1)^3+36(2x+1)^4+3(2x+1)^5]]$$

Certain useful contractions in notation.

$R_1 = 2h_u^u + h_v^v + 3h_z^z - \alpha[A+2C+6D+3K]$
$R_2 = b^2 h_u^u + 2bh_u^v + 3b^2 h_z^z - \alpha[2bB+2b^2D+E+6G]$
$R_a = 2h_u^u + 2h_v^v + 2h_z^z - \alpha[A+4C+4K+Q]$
$R_b = b^2 h_u^u + b^2 h_v^v + bh_u^v + 2b^2 h_z^z - \alpha[2bB+b^2C+2b^2D+E+4bG+2b^2K+2bT]$
$R_c = 2b^3 h_u^v + 2b^4 h_z^z - \alpha[6b^2E+8bG]$

$S_1 = -\alpha[-3H+6bI-3L]$	$0.8369\,(1-b^2)$
$S_2 = -\alpha[-(3-b^2)H+4bI-2L]$	$0.5841\,(1-b^2)$
$S_3 = -\alpha[-3(1-b^2)H]$	$0.0785\,(1-b^2)$
$S_4 = -\alpha[-(3-2b^2)H+2bI-L]$	$0.3313\,(1-b^2)$
$S_a = -\alpha[-2(1-b^2)H+4b(1-b^2)I-2(1-b^2)L]$	$0.5580\,(1-b^2)^2$
$F_1 = [S_1+R_1-R_2]/(1-b^2)$	77.8358
$F_2 = [S_2+R_1-R_2]/(1-b^2)$	77.5830
$F_3 = [S_3+R_1-R_2]/(1-b^2)$	77.0774
$F_4 = [S_4+R_1-R_2]/(1-b^2)$	77.3303
$F_a = [S_a+R_a-2R_b+R_c]/(1-b^2)^2$	75.8699
$(R_1-R_2)/(1-b^2)$	76.9989
$(R_a-2R_b+R_c)/(1-b^2)^2$	75.3119

Numerical Results and Comparison with Experimental Data

In evaluating the W's for different assumed values of α, x, and y, it was found that $\alpha=5.7$, $x=1.3$, $y=0.6$ or $\alpha=5.7$, $\beta=4.37$ and $\gamma=3.0$ gave maximum numerical values to all the W's of both configurations. The numerical values given in the different tables are all computed for these values of the effective nuclear charges. In varying α, x and y to get these values, the maximum was very flat, i.e., considerable changes in these parameters changed the value of the maximum but little. Hence this method is not at all critical for the determination of the best effective nuclear charges. However, this very flatness makes it unnecessary to vary α, x and y by excessively small steps.

The numerical values for the different W's are given in Table V.

Table V.

For the $1s^2 2s^2 2p^2$ configuration	Maximum numerical value
$W(^1D) = W_a = W_f = W_h = F_a - \alpha O - \alpha P$	74.7589
$W(^3P) = W_b = W_c = F_a - \alpha O + \alpha P$	74.8855
$W_d = W_e = F_a - \alpha O$	74.8222
$W_g = F_a - \alpha O - 2\alpha P$	74.6956
and by the method of sums,	
$W(^1S) = W_f + W_g + W_h - W(^1D) - W(^3P)$	74.5691
For the $1s^2 2s 2p^3$ configuration	
$W(^5S) = W_1 = F_1 - 3\alpha O + 3\alpha P$	74.8826
$W(^3D) = W_2 = W_5 = W_7 = F_2 - 3\alpha O$	74.4401
$W_3 = W_4 = F_2 - 3\alpha O - \alpha P$	74.3769
$W_6 = F_2 - 3\alpha O + \alpha P$	74.5034
$W_8 = F_2 - 3\alpha O + 3\alpha P$	74.1243
$W_9 = W_{10} = F_4 - 3\alpha O$	74.1837
$W_{11} = W_{12} = W_{13} = W_{14} = F_4 - 3\alpha O - \alpha P$	74.1241
and by the method of sums,	
$W(^3P) = W_4 + W_3 - W(^3D)$	74.3135
$W(^3S) = W_5 + W_6 + W_7 + W_8 - W(^3D) - W(^3P) - W(^5S)$	73.8717
$W(^1D) = W_9 + W_{10} - W(^3D)$	73.9345
$W(^1P) = 4W_{11} - W(^3D) - W_7(^1D) - W(^3P)$	73.8083

A comparison of the results of these computations with experimental[4] data is given in Table VI. In the fourth column of this table are given some experimentally[5] determined intervals for the N^+ ion. Except for the effect of the increased nuclear charge, this ion should have the same possible levels as the carbon atom. The rather high value for the $2p^3$, ^3S level of carbon is suggested by the corresponding high value for this level in N^+.

TABLE VI.

$1s^2 2s^2 2p^2$ configuration	Computed	Experimental	N^+ Experimental
$2p^2, {}^3P - 2p^2, {}^1D$	0.1266	0.0925	0.14
$2p^2, {}^3P - 2p^2, {}^1S$	0.3164	0.1970	0.298
$1s^2 2s 2p^3$ configuration			
$2p^3, {}^3D - 2p^3, {}^5S$	−0.4425		
$2p^3, {}^3D - 2p^3, {}^3P$	0.1266	0.1018	
$2p^3, {}^3D - 2p^3, {}^1D$	0.5056	0.1288	
$2p^3, {}^3D - 2p^3, {}^3S$	0.5684		
$2p^3, {}^3D - 2p^3, {}^1P$	0.6318	0.1296	
$2p^2, {}^3P - 2p^3, {}^5S$	0.0029	(0.12)	
$2p^2, {}^3P - 2p^3, {}^3D$	0.4454	0.5839	0.84
$2p^2, {}^3P - 2p^3, {}^3P$	0.5720	0.6857	1.0
$2p^2, {}^3P - 2p^3, {}^1D$	0.9510	0.7127	
$2p^2, {}^3P - 2p^3, {}^3S$	1.0138		1.42
$2p^2, {}^3P - 2p^3, {}^1P$	1.0772	0.7135	

It has been suggested from band spectra data, but the evidence is of doubtful value, that the $2p^3$, ^5S level might lie about 1.6 volts above the normal and that is the only basis for the 0.12 value given in the table.

CONCLUSIONS

One of the reasons for undertaking this set of caluclations was to determine the position or the $2p^3$, ^5S level. According to certain theories of valence as applied to the carbon atom, this level should lie near the normal.[6] While these calculations are not able to fix its exact value, they do suggest that it is the level lying nearest to the normal $2p^2$, ^3P level.

It is to be noted that except for the $2p^3$, ^1D and ^1P levels, the computed intervals between different levels, of the same configuration are all larger (24, 37 and 55 percent) than the observed intervals. On the other hand, computed intervals between levels of different configurations are smaller (17 and 23 percent) than the observed intervals. In the case of the $2p^3$, ^1D and ^1P levels, it seems uncertain whether this form of calculation gives less satisfactory results for these levels or if, as is more probable, the published data which is admitted to be questionable, is wrong.

[4] Experimental data for carbon from Paschen and Kruger, Ann. d. Pkysik **7**, 1 (1930).

[5] I. S. Bowen, Phys. Rev. **29**, 231 (1927).

[6] Molecular Binding and Low ^5S Terms of N^+ and C. L. A. Turner, Nat. Acad. Sci. Proc. **15**, 526 (1929).

The value of Slater's $F^2(1n:1n)$ comes out as $25\alpha P/3=0.5273$.

This set of calculations seems to show that while something can be learned of the location of energy levels by such approximations, still the accuracy of the results is rather worse than might have been expected from similar work on the still more simple atoms.

In conclusion I wish to express my sincere thanks to Professor Carl Eckart who suggested this problem and under whose general direction this work was done, and also my thanks to Professor R. S. Mulliken for his active interest in the work.

EMISSION AND ABSORPTION SPECTRA OF BaF

By F. A. Jenkins and A. Harvey*
Department of Physics, University of California

(Received January 25, 1932)

Abstract

Comparison of the emission and absorption spectra of BaF under high dispersion shows that all of the known band systems involve the normal state of the molecule. The following electronic terms and vibration frequencies are established: A, $0(\omega_e = 469.1)$; B, 11,646.3 and 12,280.4 (437.7); C, 14,064.5 (424.6); D, 19,998.2 and 20,197.2 (455.8); E, 24,152.3 and 26,222.3 (506.6). Terms A and B have already been recognized as $^2\Sigma$ and $^2\Pi$ states, while C is known to be an excited $^2\Sigma$ state. The term D is shown in the present work to constitute an electronic doublet, and another doublet state, E, is identified by the discovery of a new band system in the ultraviolet. Some changes are made in previous assignments of vibrational quantum numbers in the $B \rightleftarrows A$ system. Electronic terms and vibration frequencies for the analogous molecules LaO, SrF, YO, CaF, and ScO are tabulated, some of these having been re-evaluated from the original data on the basis of the new interpretation.

IN A recent article by Harvey,[1] observations of the band spectra of CaF and SrF in absorption have been used to decide the correct assignment of vibrational quantum numbers, and to obtain information about the rotational structure of the bands. We have now extended this work to the spectrum of BaF, which has been variously interpreted by different observers, all of whom studied the emission spectrum from the barium fluoride arc. The bands are closely grouped in sequences, and high dispersion is required to adequately separate the band heads. Plates were obtained in the first order of the 21-ft grating showing the spectrum in both absorption and emission for the range 3600—9000A. Four distinct band systems were found in the absorption spectrum, covering the regions $\lambda\lambda 3650-4136$, $4842-5139$, $6912-7426$ and $7862-8690$. Portions of each of these are shown in the enlargements of Fig. 1. The four band systems will be discussed separately.

1. The Ultraviolet System

There appears to be no reference in the literature to this system, and it occurs on our absorption plates only at the highest temperatures used, about 1200°C. Walters and Barratt[2] observed the absorption spectrum under low dispersion as far as $\lambda 2800$, but the only ultraviolet bands recorded by them are nine faint heads between 3311 and 3497A. We have been unable to observe the bands in emission, probably because of their intrinsic weakness. Table I contains the wave numbers of the heads of this system, which are sharp, and degraded toward the further ultraviolet. The almost constant

* Commonwealth Fund Fellow.

[1] A. Harvey, Proc. Roy Soc. **133A**, 336 (1931).

[2] O. H. Walters and S. Barratt, Proc. Roy. Soc. **118A**, 132 (1928).

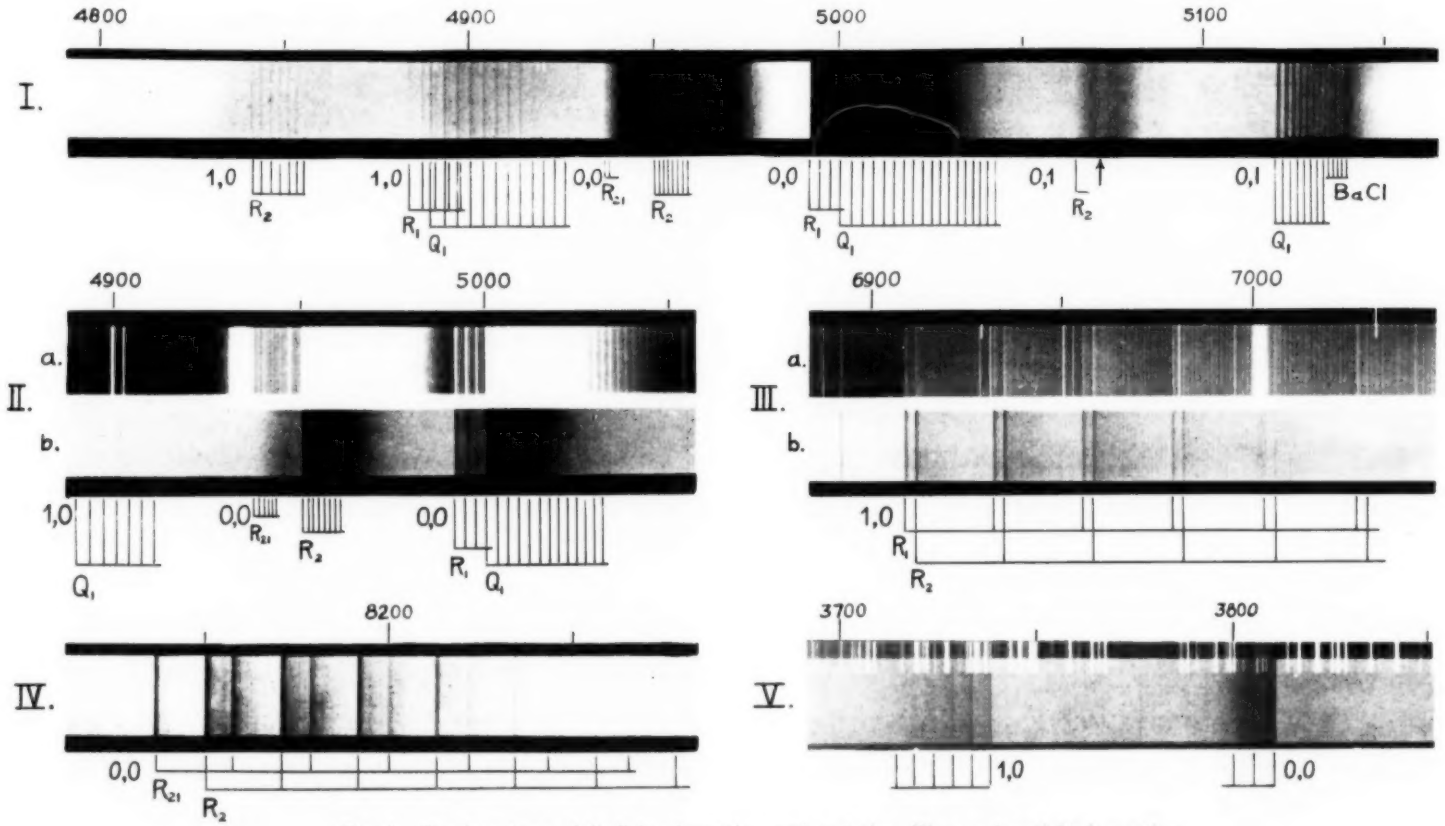

Fig. 1. *Band systems of BaF in absorption and emission.* First order of 21-ft grating.

I. The entire green system in absorption. At the temperature of the absorption tube used for this spectrogram, (about 1200°C), the R_{21} head of the 0,0 band is just visible. The sequences of heads starting with 1,0 are new, as they have not been obtained in emission. The apparent continuum marked 0,1 is due to the overlapping of a number of bands which do not form heads, but whose origins lie approximately at the position of the arrow. Higher members of the 0,1 sequence of Q_1 heads are overlapped by a sequence of BaCl bands, which appear here as an impurity.

II. Central part of the green system, *a* in emission, *b* in absorption. The temperature of the absorption tube was here slightly lower than in I, so that the R_{21} head of the 0,0 band does not appear.

III. The +1 sequence of the extreme red system, *a* in emission, *b* in absorption. The designation of the heads R_1 and R_2 is arbitrary, and could equally well be reversed.

IV. Absorption of the 0 sequence representing the higher-frequency component of the infrared system.

V. Part of the higher-frequency component of the ultraviolet system in absorption. Iron arc comparison spectrum.

separation of 2,070 cm^{-1} between bands of corresponding intensity indicates that all bands belong to one system, whose upper state is a wide electronic doublet. The appearance of the sequences $v'-v''=0$ and $+1$ of the high-

TABLE I. *Wave numbers and estimated intensities of band heads of the ultraviolet BaF system.*

v'	v'' 0	1	2	3	4	5	$\Delta G'(v+\frac{1}{2})$
0	26,240.4 (10)	25,774.8 (3)	25,313.1 (1)				501.8
	24,172.1 (4)						504.6
1	26,742.0 (6)	26,276.8 (5)	25,814.9 (2)	25,356.8 (1)			498.6
	24,676.7 (4)	24,211.4 (1)					501.7
2	27,240.9 (2)	26,775.3 (5)	(00)	25,855.1 (1)	(00)		495.6
	25,177.3 (2)	24,712.2 (3)					496.8
3		27,270.9 (2)	26,809.1 (4)		25,896.4 (0)		492.5
	(00)	25,208.9 (2)	24,747.4 (2)				493.2
4			27,301.6 (2)	26,843.4 (2)			489.5
		(00)	25,240.6 (3)	24,782.6 (1)			489.7
5				27,332.9 (1)	26,878.1 (0)		485.8
			(00)	25,272.3 (3)	24,818.0 (0)		485.9
6					27,363.9 (0)		
					25,303.9 (2)		
7						27,395.8 (0)	
						25,355.4 (2)	
$\Delta G''(v+\frac{1}{2})$	465.5	461.8	458.2	454.8			
	465.2	461.5	458.0	454.3			

frequency component is shown in Fig. 1,V. The wave numbers of the heads are well represented by the equation

$$\nu = \begin{matrix} 26,222.3+504.9(v'+\frac{1}{2})-1.54(v'+\frac{1}{2})^2 \\ 24,152.3+508.4(v'+\frac{1}{2})-1.88(v'+\frac{1}{2})^2 \end{matrix} \Big\} - 468.9(v''+\tfrac{1}{2})+1.79(v''+\tfrac{1}{2})^2.$$

There is no doubt about the assignment of vibrational quantum numbers, since the intensity distribution is of a common type (see Fig. 1, V and Table I). The differences between the vibrational constants of the two components of the upper state, though small, are probably real. If they were due entirely to the fact that we are using heads instead of origins, a correspondingly large difference might be expected in the lower state constants, but this is not found.

2. THE GREEN SYSTEM

This system has been studied in some detail by Johnson,[3] who divides it somewhat arbitrarily into two overlapping systems, $^2\Sigma \rightleftarrows {}^2\Sigma$ and $^2\Delta_{3/2} \rightleftarrows {}^2\Sigma$. By a consideration of the difference in appearance of the bands in absorption and emission, which are similar to those found in the $^2\Pi \rightleftarrows {}^2\Sigma$ systems of CaF and SrF, we conclude that only one doublet system is present, with an electronic separation of about 200 cm^{-1} in the upper state. The chief difficulty en-

[3] R. C. Johnson, Proc. Roy. Soc. **122A**, 190 (1929).

countered in previous interpretations of the green group has been the fact that only one sequence of heads besides the strong sequences with $v'-v''=0$ has been known. We have now obtained the required data by identifying the $+1$ sequence in both components, and the -1 sequence in the high-frequency component of the electronic doublet. These are extremely faint relative to the main sequences, as will be seen by reference to Fig. 1, I and II. In the -1 sequence sharp heads are not formed at the temperature of the absorption tube, but the sequence presents merely a diffuse double maximum due to a number of superimposed bands. No difficulty was found in assigning values of v, since all the other sequences begin abruptly. The correct analysis of this system is shown in Table II, in which we have used Johnson's data except in the case of the new bands, for which estimates of the relative intensity are given.

The notation used in designating the band heads in Fig. 1, I and II, assumes a rotational structure of the $^2\Pi\rightleftarrows{}^2\Sigma$ type, the R_{21} and R_2 heads representing the high-frequency component of the doublet, and the R_1 and Q_1

TABLE II. *Vibrational analysis of the green system of BaF.*

v', v''	R_{21} head	R_2	R_1	Q_1	v', v''	R_2	R_1	Q_1
0, 0	20,248.5	20,193.3	20,026.1	19,992.0	0, 1		19,592.1	19,529.4
1, 1	242.4	185.9	015.7	980.0	1, 2	Diffuse	584.2	521.2
2, 2	237.0	178.9	003.6	968.2	2, 3	edge at	577.1	513.4
3, 3	231.8	172.3	19,992.6	956.8	3, 4	19,736.4	571.0	506.3
4, 4	226.9	—	982.2	945.6	4, 5	Minimum	565.6	498.5
5, 5	222.5	160.0	—	934.9	5, 6	at		491.5
6, 6	218.3	154.3	962.1	924.3	6, 7	19,715.8		484.9
7, 7	214.5	148.9	952.4	914.1	7, 8			478.7
8, 8	211.3	144.0	943.0	904.0	8, 9			472.6
9, 9	207.6	139.2		894.4	9, 10			466.8
10, 10		134.9		884.9	10, 11			461.4
11, 11		—		875.7	11, 12			456.6
12, 12		127.1		866.7				

v', v''	R_2	R_1	Q_1	$\Delta G'(v'-\frac{1}{2})$	$\Delta G''(v''+\frac{1}{2})$
1, 0	20,647.8 (0)	20,469.3 (0)	20,444.5 (2)	452.6	464.5
2, 1	636.9 (1)	454.1 (1)	429.2 (3)	449.2	460.9
3, 2	626.3 (1)	439.2 (1)	414.1 (3)	445.9	457.2
4, 3	616.3 (0)	424.6 (0)	399.3 (3)	442.5	453.7
5, 4	606.3 (0)	410.7 (00)	384.8 (2)	439.2	450.0
6, 5	597.4 (00)		370.5 (1)	435.6	446.2
7, 6			356.7 (0)	432.4	442.6
8, 7			343.3 (0)	429.2	439.3
9, 8			329.8 (0)	425.8	435.4
10, 9			316.9 (00)	422.5	432.0

heads the low-frequency component. The justification of this assumption lies in the obvious similarity of the gross structure to that of other known $^2\Pi\rightleftarrows{}^2\Sigma$ systems. According to this interpretation, the system designated $^2\Sigma\rightarrow{}^2\Sigma$ by Johnson is the low-frequency component ($^2\Pi_{3/2}\rightleftarrows{}^2\Sigma$ if the doublet is inverted) while $^2\Delta_{3/2}\rightarrow{}^2\Sigma$ is the high-frequency component ($^2\Pi_{1/2}\rightleftarrows{}^2\Sigma$). Our data on the new sequences permit for the first time the evaluation of the vibrational term-differences for the high-frequency component, at least to the

approximation permitted by measurements of heads only. That this is not a close approximation in bands of this type, where the heads are formed at high rotational quantum numbers, has been emphasized by Harvey.[1] The best values of the vibrational differences are those listed in Table II, obtained from the Q_1 heads, which are closest to origins. There is still some divergence of the values of $\Delta G_v''$ from those obtained for the ultraviolet system, the first vibrational quantum, $\Delta G_{1/2}''$, being 465.5 and 464.5 cm^{-1} from the ultraviolet and visible systems, respectively.

The diffuse appearance of the -1 R_2 sequence is expected, since in this sequence the heads must be formed at the highest values of the rotational quantum number, K. This is invariably true in the case of bands degraded towards the red, because it is then known that the rotational constants $B_0'' > B_1'' > B_0'$. An analogous effect occurs[1] in the $+1$ sequence of the $^2\Pi \rightleftarrows {}^2\Sigma$ CaF bands, which are shaded toward the violet. Further support for our identification of this sequence is obtained by taking the wave number difference between the R_2 head of the 0,0 band and the minimum of the diffuse patch (marked by the arrow in Fig. 1, I), which should represent fairly closely the origin of the 0,1 band of the high-frequency component. This yields 477.8 cm^{-1}, a value which is expected to be slightly greater than $\Delta G_{1/2}''$ (464.5), since the R_2 head is at a considerable distance from the origin. The doublet character of this system therefore seems well established, and our analysis is in entire agreement with the modifications of the vibrational and rotational intensity distributions in passing from emission to absorption. A good example of this is shown in Fig. 1, II by the suppression of the R_{21} heads of the 0 sequence in absorption. This would be predicted because of the very high rotational quantum numbers at which these heads are formed.

3. The Extreme Red System

The correct vibrational analysis of this system has been given by Johnson,[3] but he designates the components of the close double heads R and Q, and the electronic transition $^2\Delta \rightarrow {}^2\Sigma$. It was shown in the preliminary report of the present work[4] that this system is analogous to the $^2\Sigma \rightleftarrows {}^2\Sigma$ systems of CaF and SrF, and should be given the same designation. The double character of the heads results from the splitting of the R branch into two, R_1 and R_2, which is known as spin doubling.[5] The resemblance of these bands, shown in Fig. 1, III, to the corresponding system in CaF is very striking. We also assigned the infrared system (discussed below) to a $^2\Pi \rightleftarrows {}^2\Sigma$ transition, by the same analogy. In a subsequent publication Nevin[6] has apparently independently drawn the same conclusions. He has extended the original measurements of George on the extreme red system, identifying an additional sequence, $v' - v'' = +2$. Nevin's work was exclusively with the emission spectrum.

The $^2\Sigma \rightleftarrows {}^2\Sigma$ system appears plainly on our absorption plates (Fig. 1, III), with but slight modification from the emission spectrum. The heads must

[4] A. Harvey and F. A. Jenkins, Phys. Rev. **37**, 1709 (1931).
[5] A. Harvey and F. A. Jenkins, Phys. Rev. **36**, 1413 (1930).
[6] T. E. Nevin, Proc. Phys. Soc. **43**, 554 (1931).

therefore be formed at much lower values of K than in the corresponding system in CaF and SrF, where they are almost completely suppressed in absorption. Since the correct assignment of vibrational quantum numbers, as well as very complete data for this system, are contained in the article by Nevin, we give no measurements here, but merely quote the equations deduced by Nevin for the high- and low-frequency components, respectively, of the double heads:

$$\nu = 14{,}070.6 + 424.3(v' + \tfrac{1}{2}) - 1.95(v' + \tfrac{1}{2})^2 - 468.2(v'' + \tfrac{1}{2}) + 1.82(v'' + \tfrac{1}{2})^2,$$

$$\nu = 14{,}064.4 + 424.5(v' + \tfrac{1}{2}) - 1.80(v' + \tfrac{1}{2})^2 - 468.7(v'' + \tfrac{1}{2}) + 1.80(v'' + \tfrac{1}{2})^2.$$

The vibrational constants for the lower $^2\Sigma$ state agree satisfactorily with those deduced by us from the ultraviolet system: $\omega_e'' = 468.9$ $x_e''\omega_e'' = 1.79$.

4. The Infrared System

This is the resonance system of BaF, and appears very strongly in absorption (Fig. 1, IV). The first measurements of any completeness were made by Querbach[7] on the emission spectrum from the arc. Because of the frequent confusion with atomic lines, and of the faintness of some of the leading heads of the sequences, Querbach's assignment of vibrational quantum numbers required revision in several respects.[4] Also, the conclusions drawn by Querbach concerning the electronic transitions are partly wrong, being based entirely on the approximate agreement of certain vibrational constants with those given by Johnson for the visible systems. The assignments thus reached are not consistent with the magnitudes of the electronic term-differences involved, and hence are meaningless.

The more probable designation of this system as $^2\Pi \rightleftarrows {}^2\Sigma$ was first given by the writers,[4] although overlooked in Nevin's subsequent work.[6] Nevin gives a complete remeasurement of the band heads, including a number which were not contained in the earlier work of Querbach. A new sequence, $v' - v'' = -1$ of the high-frequency component, is added. Although some of the wrong assignments of v occurring in Querbach's work are given correctly by Nevin, his analysis of the low-frequency component is incomplete, and in some respects erroneous. We therefore give, in Table III, the analysis shown to be correct by a study of the absorption spectrum. The proper assignment of v is very apparent on the absorption plates, since the bands are clear of impurities and the beginning of each sequence is definite. The data of Table III are measurements of the absorption heads made with reference to neon standards.

The principal differences between our arrangement and that given by Nevin are: (1) Lowering of the vibrational quantum numbers in the $v' - v'' = 0$ sequence of Q_1 heads by one unit. This changes the electronic separation in the $^2\Pi$ state from 602.1 to 633.8 cm^{-1}. The R_1 and Q_1 heads are closely superposed at the start of this sequence, but the low intensity of the first head shows clearly that it represents the R_1 head only. (2) Lowering of the

[7] J. Querbach, Zeits. f. Physik **60**, 117 (1930).

vibrational quantum numbers in the +1 sequence of Q_1 heads, also by one unit. Nevin did not observe the earliest members of this sequence, and assigned values of v to conform with the false assignment in the 0 sequence. (3) Addition of the −1 sequence of R_{21} heads, which was not observed by Nevin. (4) Addition of the 0 sequence of R_1 heads. These were probably over-

TABLE III. *Vibrational analysis of the infrared system.*

v'	v'' 0	1	2	3	4	5	6	7	$\Delta G'(v+\frac{1}{2})$
0	R_{21} 12,285.6 R_1 12,264.5 R_1 11,663.2 Q_1 11,630.7	11,827.7 11,800.1 — —							434.2
1	12,715.0 12,698.3 12,090.7 12,064.9	12,253.4 12,232.9 11,630.7 11,599.3	11,798.9 11,771.7 — —						430.7
2		12,678.7 12,662.7 12,055.0 12,030.0	12,220.9 12,200.9 11,599.3 11,568.1	11,769.3 11,743.4 — —					426.7
3			12,642.6 12,626.9 12,019.3 11,994.8	12,188.1 12,168.9 11,568.1 11,536.4	11,739.7 11,714.8 — —				423 2
4				12,606.2 12,591.1 11,983.2 11,959.6	12,155.3 12,136.7 11,536.4 11,504.8	11,710.2 11,686.2 — —			419.5
5					12,569.9 12,555.3 11,947.8 11,924.2	— 12,104.5 11,503.8 —	11,680.8 11,657.7 — —		
6						— — 12,912.1 11,889.2	— 12,072.2 — —		
7							12,496.9 12,483.5 — 11,853.7		
8								— 12,447.6 — —	
$\Delta G''(v+\frac{1}{2})$	465.6	461.9	458.4	454.9					—

looked by Nevin because of their approximate coincidence with the corresponding sequence of Q_1 heads. As will be seen in Table III, we have now assigned all four heads in the +1 and 0 sequences, but only those of the high-frequency component, namely R_{21} and R_2, in the −1 sequence. The R_1 and Q_1 heads of this sequence lie further in the infrared, where the sensitivity of neocyanin plates is low. The predicted position of the 0,1 Q_1 head is $\nu = 11{,}166.3$, λ8952.9. Since in this system the R_2 and Q_1 heads are closer to origins than in the green system, we expect better agreement in the vibrational term-differences derived from these heads. Thus, the value of $\Delta G_{1/2}''$ from the Q_1 heads is 465.6, as compared to 465.5 from the ultraviolet system, 464.5 from the green system, and 465.1 from the extreme red system. A revision of Nevin's equations for heads to accord with the modified values of v gives, for R_2 and Q_1 respectively:

$$\nu = 12{,}281.1 + 436.7(v' + \tfrac{1}{2}) - 1.82(v' + \tfrac{1}{2})^2 - 468.7(v'' + \tfrac{1}{2}) + 1.83(v'' + \tfrac{1}{2})^2,$$

$$\nu = 11{,}647.3 + 435.5(v' + \tfrac{1}{2}) - 1.68(v' + \tfrac{1}{2})^2 - 467.5(v'' + \tfrac{1}{2}) + 1.45(v'' + \tfrac{1}{2})^2.$$

The agreement of the constants of the lower state with those from the other systems is distinctly better with the new numbering.

Discussion

The fact that all four of the above systems are obtained in absorption shows that they have a common lower electronic state, which is the normal $^2\Sigma$ state of the molecule. This is in harmony with the agreement of the approximate vibrational term-differences for the lower state derived from these systems. Previous work on the emission spectrum alone led to the conclusion that some intercombinations between excited states are involved.[8] Such conclusions have resulted from the comparison of the vibrational constants only, but these are necessarily inexact, since they are derived from heads. The present work shows definitely that no combinations between excited states are known in this spectrum.

A close analogy exists between the spectra of BaF and of LaO, since both molecules contain the same number of extranuclear electrons. The lanthanum monoxide systems have been studied by Mecke,[9] Querbach,[10] Jevons,[11] and

Table IV. *Electronic terms and vibration frequencies for analogous molecules.*

		BaF	LaO	SrF	YO	CaF	ScO
$a^2\Sigma$	ν_e	0	0	0	0	0	0
	ω_e	469.1	818.5	500.1	857.5	587.3	—
$a^2\Pi$	ν_e	{11,647.3 {12,281.1	{12,668.1 {13,532.4	{15,068.9 {15,348.0	{16,324.2 {16,760.8	{16,482.1 {16,557.2	{16,444.7 {16,562.2
	ω_e	437.7	762.8	508.0	815.6	593.1	—
$b^2\Sigma$	ν_e	14,064.5	17,885.8	17,301.9	20,798.1	18,898.3	20,578.5
	$\Delta\nu$	6.2	8.3	22.4	3.1	6.6	1.2
	ω_e	424.6	733.2	477.0	765.0	541.5	—
$b^2\Pi$	ν_e	{19,998.2 {20,197.2	{22,639.6 {22,876.6	{26,977.8 {27,041.3	—	{29,301.5 {29,321.0	—
	ω_2	455.8	783.0	452.5	—	495.6	—
^2X	ν_e	{24,152.3 {26,222.3	~28,000	—	—	—	—
	ω_e	506.6	>818.5	—	—	—	—

[8] In reference 7, p. 120, the low-frequency component of the infrared system is assigned to an intercombination, $2^2S - 3^2D_2$, with the designation of the levels according to reference 3. To be consistent with the coefficients given in the vibrational equations, however, the designation should be $3^2D - 2^2D$, which would give a negative frequency. In his analysis of the LaO systems (reference 9), Mecke concluded that at least four systems involved excited states as their lower states. This, however, is shown to be incorrect by Johnson (reference 12), and by the analogy with BaF discussed below.

[9] R. Mecke, Naturwiss. **17**, 86 (1929).

[10] J. Querbach, Zeits. f. Physik **60**, 115 (1930).

[11] W. Jevons, Proc. Phys. Soc. **41**, 520 (1929).

Johnson.[12] Four systems are found, which are qualitatively similar to the four BaF systems discussed above. The vibrational constants show an analogous variation from one electronic state to another, with the result that corresponding band systems have the same direction of degradation and general appearance. In Table IV we have summarized the constants of these two molecules, those for LaO being taken from Jevons' work. The term symbols used are such that $a^2\Pi \rightleftarrows a^2\Sigma$ represents the infrared BaF system, $b^2\Sigma \rightleftarrows a^2\Sigma$ the extreme red system, $b^2\Pi \rightleftarrows a^2\Sigma$ the green system, and ${}^2X \rightleftarrows a\Sigma$ the ultraviolet system. We have designated the upper state of the green system $b^2\Pi$ because of its obvious similarity of structure to the infrared system, and because a $^2\Pi$ state of about the observed separation is predicted by analogy with the states of the corresponding[11] atom, Cs.

Further analogies are expected in the spectra of the isoelectronic pairs of molecules SrF, YO and CaF, ScO. The constants for these molecules are therefore also included in Table IV, as far as they are known. For SrF and CaF we have re-evaluated the constants from the data given by Johnson,[13] modifying the assignment of v in the green CaF system ($b^2\Sigma \rightleftarrows a^2\Sigma$) as indicated by Harvey.[1] It was necessary also to change the assignment given by Johnson for the SrF ${}^2\Sigma^{v+1} \rightleftarrows {}^2\Sigma^{(v)}$ sequence. Thus we have taken the first head of the A_3' sequence (ν 17,783.1) as being the high-frequency R head of the 1,0 band, and lowered the values of v in the A_3 sequence by one unit to constitute the remaining heads of this sequence. The low-frequency R heads then begin with ν 17,771.2. All of the values contained in Table IV were derived by selecting the set of band heads which is expected to be nearest to the band origins.

The transition $b^2\Pi \rightleftarrows a^2\Sigma$ is apparently represented in CaF and SrF by the known systems in the ultraviolet (the A_1, A_2 sequences of Datta).[14] These must be very weak, as we have made several unsuccessful attempts to obtain them from the CaF arc, and Johnson[3] could not observe them for SrF. Johnson has interpreted them as ${}^2\Sigma \rightleftarrows {}^2\Sigma$, but it seems more probable that the two observed heads are the R_2 and Q_1 heads of a second ${}^2\Pi \rightleftarrows {}^2\Sigma$ system. In deriving the constants for the $b^2\Pi$ state of these molecules, Johnson's assignment of v was adhered to in CaF, but in SrF his vibrational quantum numbers for the R_2 heads (sequences A_2 and A_1) have been raised by one unit throughout. Because of the fragmentary character of the data on these systems, considerable uncertainty still remains in the constants for $b^2\Pi$ given in Table IV. In the case of YO, the recent results of Johnson[12] were used, while for ScO only the frequencies of the 0,0 bands given by Meggers and Wheeler[15] were available. The quantity $\Delta\nu$ given in Table IV for the $b^2\Sigma$ state of all the molecules represents the spin doubling of the head of the 0,0 band. This depends, of course, very greatly on the rotational quantum number at which the head is formed, and hence has little theoretical meaning.

[12] R. C. Johnson, Proc. Roy. Soc. **133A**, 218 (1931).
[13] R. C. Johnson, Proc. Roy. Soc. **122A**, 161 (1929).
[14] S. Datta, Proc. Roy. Soc. **99A**, 436 (1921).
[15] W. F. Meggers and J. A. Wheeler, Phys. Rev. **37**, 106 (1931).

Concerning the atomic states of the separate atoms from which the observed molecular states are derived, little information can be obtained from the spectra. It is probable, as pointed out to us by Professor L. Pauling, that the lower states of these heavy molecules have ionic binding, and hence that the Birge-Sponer method of computing heats of dissociation is inapplicable. It appears significant, however, that the ^2X state is different from the others in having a very high vibration frequency, even higher than that of the normal state. This suggests that it may possess a different type of binding, and that possibly it is the lowest state representing binding of the electron-pair type.

THE ABSORPTION SPECTRUM OF CYANOGEN GAS IN THE ULTRAVIOLET

By Sho-Chow Woo and Richard M. Badger
Gates Chemical Laboratory, California Institute of Technology

(Received December 28, 1931)

Abstract

The absorption spectrum of cyanogen gas has been investigated in the ultraviolet down to λ1800. In the region λλ2300-1820 more than one hundred bands were found which apparently belong to one system with origin probably at 44900 cm^{-1}. The bands have a pronounced tendency to appear as doublets. The more intense ones are usually broad with edges toward the violet, but many line-like structures appear which are probably *Q* branches. Some regularities in the spectrum are pointed out and the relation of the ultraviolet spectrum to the infrared absorption and Raman spectrum is briefly discussed.

Introduction

THE work described in this paper is a part of a program of this laboratory for the investigation of the spectra of the simpler polyatomic molecules. In particular the cyanides have been chosen for study and papers by Badger and Binder[1] on the fine structure of two bands of hydrogen cyanide in the infrared, and by Badger and Woo[2] on the continuous absorption spectra of the halogen cyanides in the ultraviolet have already appeared. Cyanogen was chosen as the next subject for study since the cyanogen molecule, in its normal state at least, is undoubtedly linear and symmetrical, which permits a simple and quantitative treatment of the normal oscillations. It is further of particular interest to compare the cyanogen molecule with acetylene which is in some respects similar and has been carefully studied in infrared absorption.

Experimental Procedure

A. Middle Ultraviolet Region. The cyanogen gas used in the investigation was prepared by dropping a concentrated solution of potassium cyanide into an all glass generator containing a solution of copper sulfate. The gas generated was dried by passing through a calcium chloride tube, and then passed into the absorption tube. No further purification was made since in previous experiments it was found that cyanogen prepared by the decomposition of mercuric cyanide by heating gave the same absorption spectrum.

The absorption cell was a Pyrex tube 51.5 cm long, one end of which was provided with a plane quartz window, while the other end was separated from the hydrogen discharge tube, used as the light source, by a thin quartz film. All temporary connections were effected with picein, which proved to be least attacked by the cyanogen gas. The gas pressure used was one atmosphere at room temperature.

[1] R. M. Badger and J. L. Binder, Phys. Rev. **37**, 800 (1931).
[2] R. M. Badger and S. C. Woo, J. Am. Chem. Soc. **53**, 2572 (1931).

The hydrogen discharge tube was of a type described by Bay and Steiner,[3] but all wax joints were avoided by using a quartz window, which was very thin, attached by a quartz-to-Pyrex graded seal. Consequently, after the tube had been cleaned up by running for some time the spectrum remained very pure and continuous. The hydrogen pressure could be regulated by means of a palladium tube which was sealed to the glass.

A Bausch and Lomb quartz spectrograph was used which gives a dispersion of about 5A per mm at λ2200. Eastman D-C ortho plates were used, and were sensitized with a light transformer oil which was found to be very effective. The exposures required about two hours. As a comparison spectrum we employed the copper spark lines. Measurements of the bands were made both directly on the plates with a comparator, and on enlarged prints. Any errors will be due principally to the difficulty in deciding exactly what part of a band to measure. The error in measurement we believe to be less than 0.2A.

B. Farther Ultraviolet Region. For this region we employed a small vacuum fluorite spectrograph, with a dispersion of about 12A per mm at λ1900. The absorption cell, about 30 cm in length, had at one end no window but was sealed with picein to the spectrograph chamber and communicated with it through the slit opening. At the other end it shared a very thin quartz film window in common with the hydrogen discharge tube used as source. The total absorption path was about 75 cm.

The cyanogen gas was prepared as described above, but was condensed in a liquid air trap and then evaporated into the spectrograph and absorption cell, which had previously been thoroughly evacuated, until a pressure of about 10 mm was attained.

Eastman 40 plates, sensitized with oil, were used, and the exposures usually required two to three hours. As calibration spectrum, the zinc and aluminum spark lines were used. They covered the region λλ2100–1850 fairly well.

As before, measurements were made both on the plates and on greatly enlarged prints. The accuracy of measurement was not so great as in the middle ultraviolet region, but in the case of sharp bands the error may not be greater than 0.4A.

Experimental Results

Tables I and II give the wave-lengths and wave numbers of the absorption bands of cyanogen gas in the middle and farther ultraviolet, respectively.

The bands vary considerably in appearance and it is rather uncertain how best to describe some of them until a complete analysis is made of the spectrum. Where a sharp edge appeared this was measured, but in the case of diffuse bands and of the narrow line-like structures the center was measured. The symbols, explained at the foot of the table, indicate in each case the nature of the absorption and what was measured. The general appearance of the spectrum is probably best suggested by the diagram in Fig. 1, in which the types of bands are indicated as far as possible.

[3] Z. Bay and W. Steiner, Zeits. f. Physik **59**, 48 (1929).

The majority of the strong bands are rather broad, with edges towa violet, but a number of line-like structures are observed, which are prob Q branches. In some cases P and R branches seem to be definitely ab

TABLE I. *The cyanogen bands in the middle ultraviolet (quartz spectrograph).*

M	λ (A) (in air)	ν (cm⁻¹)	I	D	M	λ(A) (in air)	ν (cm⁻¹)	I	
VE	2252.1	44389	0		VE	2187.3	45704	00	
CL	2251.8	44395			VE	2186.9	45713		
CL	2250.6	44419	0		VE	2185.7	45738		
CL	2250.3	44425			VE	2185.3	45746	0	
RD	2242.6	44577			CL	2184.4	45765		
CL	2240.0	44629			CL	2183.3	45788	0	
VE	2239.0	44649			VE	2182.6	45803		
VE	2238.3	44663			VE	2182.0	45815	1+	
VE	2237.7	44675	3		CL	2180.5	45847		
VE	2231.2?	44805			CL	2179.9	45859	0	
VE	2230.4	44821			VE	2179.2	45874		
CL	2228.4	44861			CL	2178.6	45887	1−	
CL	2227.6	44877			CD	2177.1	45918		
CL	2227.1	44887			CD	2176.5	45931	2+	
VE	2226.7	44896			CL	2173.5	45994		
VE	2226.4	44902	5	A′	CL	2173.0	46005	00	
CL	2225.6	44918	00		CL	2167.1	46130		
CD	2223.5	44960	00		CL	2166.6	46141		
CD	2219.8	45035	0		CD	2165.5	46164		
CD	2217.5	45082	0		CL	2164.8	46179		
CD	2215.0	45133(d)	0		VE	2164.5	46186	4−	
VE	2213.0	45173			VE	2163.3	46211	00	
CL	2212.5	45184			CD	2161.3	46254	00	
VE	2212.3	45188	1		CD	2159.2	46299		
VE	2209.1	45253			VE	2158.9?	46305	0	
VE	2208.5	45265			VE	2157.9	46327		
VE	2207.2	45292			CL	2157.5	46335	0	
VE	2205.7	45322			VE	2157.3	46340		
CL	2205.2	45333			CD	2155.5	46378	00	
CL	2204.4	45350			CD	2154.1	46409	00	
CD	2203.7	45364			CD	2152.4	46445	00	
CL	2203.1?	45376			CD	2150.7	46482	00	
CL	2202.4	45391			VE	2145.6	46592	4	A″
CL	2200.6?	45428			VE	2137.7	46764	4	
CL	2200.3	45434			CD	2135.5	46813	1	
VE	2200.0	45440	5		VE	2125.0	47044(d)	7	B′
CL	2197.2	45498			CD	2124.0	47066	0	
CL	2196.7	45509			CD	2120.9	47135	0	
CL	2195.4	45536			CD	2118.9	47179	0	
CL	2194.8	45548							
VE	2188.2	45685	9	A					

EXPLANATION. Columns *M* indicate the part of a band measured, whether a violet or red edge (VE or RE), the apparent red or violet limit of a diffuse structure (RD or VD), the center of a diffuse band (CD), or the center of a narrow line-like structure, probably a *Q* branch (CL). When two parts of the same structure were measured this is indicated by brackets in these columns.

In the frequency columns brackets on the left indicate edges or maxima which apparently belong to one broad structure. Brackets on the right indicate a doublet structure, and (d) a probable doublet structure (incompletely resolved).

The columns *I* and *D* give estimated relative intensities, and designations for a few of the bands.

in others they may be relatively very weak. A pronounced tendency toward doubling will be noticed. In a band progression the doublet separation in-

creases toward the high frequency side. Some of the diffuse bands show indications of being partially resolved doublets. In some cases a number of lines or edges are observed within a broad band. We believe that these are

TABLE II. *The cyanogen bands in the farther ultraviolet (fluorite spectrograph).*

M	λ(A) (vacuum)	ν(cm⁻¹)	I	D	M	λ(A) (vacuum)	ν(cm⁻¹)	I	D
L	2110.6	47380	0		CD	1969.0	50787	2	
CL	2109.4	47407			CD	1963.5?	50930	2	
CL	2108.1	47436	7		CD	1959.6?	51031	1	
CL	2106.6	47470			CD	1958.4?	51062		
CL	2105.0	47506	1		CD	1953.5	51190		
RD	2098.4	47655			CL	1952.3	51222	5	D′
CL	2097.9	47667			CD	1949.5	51295	2	
CL	2096.3	47703			CL	1944.0	51440	4	
CL	2095.0	47733			CL	1940.4	51536	2	
VE	2094.4	47746			CL	1937.6	51610		
L or VE	2093.8	47760	10	B	CL	1936.3	51645	3	
VE	2090.4	47838	4		CD	1931.9	51763		
VD	2088.2?	47888	2		CD	1929.8	51819	10	D
VD	2086.4	47929	4		CD	1926.5	51908	7	
CL	2079.4	48091	2		RE?	1922.6	52013		
VE	2075.6	48179			CD	1918.5	52124	9	
VE	2074.5	48204	4		VE	1916.3	52184		
CD	2069.3	48326	4		VE	1915.4	52208	3	
CD	2065.0	48426	2		CD	1911.7	52310	1	
CL	2058.4	48581			CD	1909.9	52359	1	
CL	2057.6	48600			VE	1900.0(d)	52632	9	
CL	2056.8	48619			CL	1897.5	52701		
CL	2055.3	48655	7	B′	CD	1894.7	52779		
CD	2051.2	48752			VE	1893.1	52823	9	D″
CD	2049.3	48797			CD	1885.0	53050		
VE	2036.0	49116			VE	1884.6	53062	3	
CL or VE	2035.2	49135	7	C′	CL	1883.2	53101	1	
CD	2023.3	49424	3		CD	1880.6	53175	0	
CL	2021.4	49471	6		CD	1878.3	53240	2	
VE	2018.3	49547	4		CD	1875.9	53308	2	E′
CD	2015.0	49628			CL	1871.1	53427	1	
CD	2012.7	49685			CL	1867.3	53556	1	
CD	2011.1	49724			CD	1861.8	53712		
CD	2009.4	49766			CD	1859.6	53775	5	E
CD	2007.7	49808	10	C	CL	1857.2	53845	0	
CD	2003.4	49915			CL	1855.0	53908	1	
CD	2000.7	49983	8		CL	1850.3	54045	3	
CD	1999.3	50018	3		VE	1846.7	54151		
CL	1997.5	50063	3		VE	1844.1	54227	6	
CL	1995.4	50115	3		CL	1834.2	54520		
CL	1993.8	50156			VE	1827.9	54708	8	
VE	1990.8	50231	8		CD	1826.5	54750		
CL	1987.0?	50327	0		VE	1825.8	54771	4	
CL	1985.9?	50355	0		VE	1823.7	54834	8	
VE	1980.3	50497(d)	9		CD	1820.8	54921	3	
VE	1978.9?	50533	0						
CD	1975.9	50610	0						
RE	1975.1	50630							
CL	1972.7	50692							
VE	1971.2	50731	10	C″					

due to a vibrational rather than to a rotational structure in the ordinary sense of the word, since the large moment of inertia of the cyanogen molecule makes it improbable that a rotational structure would be resolved with the limited dispersion available.

Discussion of the Spectrum

The modes of oscillation of the linear symmetrical molecule of the acetylene-cyanogen type have been discussed by Mecke,[4] but his expression for the deformation frequencies does not seem to be quite right, as has been pointed out by Olson and Kramers.[5] Unfortunately cyanogen has not been investigated in the infrared with modern technique, but the old measurements of Burmeister,[6] and the Raman measurements on liquid cyanogen[7] make it fairly certain that the three longitudinal or valence vibrations have approximately the frequencies 2150 (the active vibration) and 2336 and 860 (the inactive vibrations). It is not expected that these frequencies should appear as differences in the ultraviolet absorption of the gas at room tem-

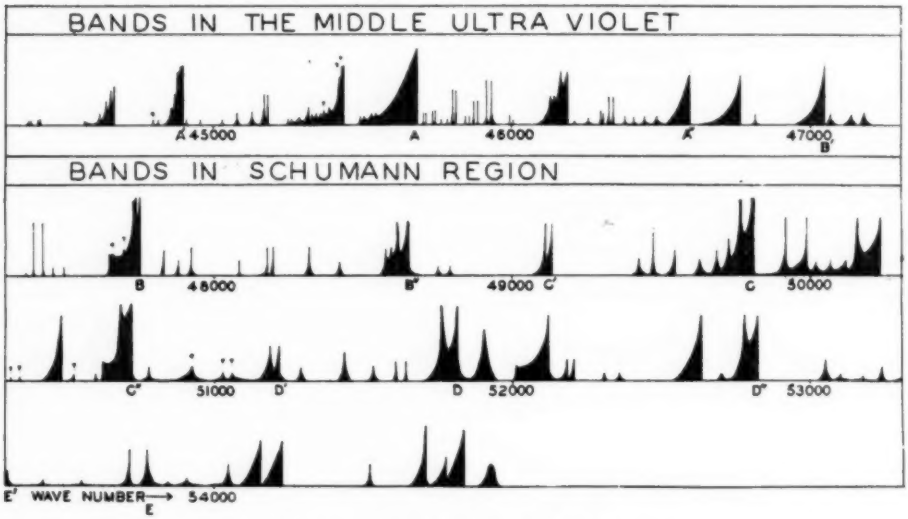

Fig. 1. The ultraviolet absorption bands of cyanogen.

perature. The small deformation frequencies which may appear are more difficult to determine from the existing data. The frequency 512 observed as a Raman shift may be due to the inactive deformation oscillation, and we believe that a weak absorption observed by Rubens[8] at 52μ indicates that the fundamental band of the active deformation oscillation is not far from this region. It will be noticed that on the red side of a number of bands in the ultraviolet absorption very much weaker bands appear with a frequency difference of about 230. We believe that these latter may be due to absorption of molecules in the first excited state with respect to the deformation oscillation.

[4] R. Mecke, Zeits. f. Physik **64,** 173 (1930).
[5] A. R. Olson and H. A. Kramers, J. Am. Chem. Soc. **54,** 136 (1932).
[6] W. Burmeister, Verh. d. D. Phys. Ges. **15,** 589 (1913).
[7] A. Petrikaln and J. Hochberg, Zeits. f. Phys. Chem. (B) **4,** 299 (1929).
[8] H. Rubens and H. von Wartenburg, Phys. Zeits. **12,** 1080 (1911).

The ultraviolet spectrum of cyanogen is on the whole extremely complex and will require some time for a complete analysis. However, we wish to point out some of the more striking regularities. In particular one notices progressions of doublet bands separated by about 2100 wave number units. Now in room temperature absorption one may expect to find only one strong progression with a given set of frequency differences, though much weaker progressions may be observed displaced to the red, corresponding to absorption from the low lying deformation oscillational levels. However, one may expect to find progressions which are rather similar. If the band system may be very approximately represented by the expression:

$$\nu = \nu_{\text{elect}} + v_1'\omega_1' + v_2'\omega_2' + v_3'\omega_3' + \cdots$$

we shall find similar progressions in any one of which one of the vibrational quantum numbers, say v_1, takes the values 0, 1, 2, etc., while the other quantum numbers v_2, v_3, etc., remain constant, but change from one progression to another. The frequency differences will not be quite the same for any two such sets of bands, due to the coupling between different kinds of vibration.

In Table III we have given some similar progressions of this sort. It will be noted that the frequency differences are nearly equal to those for the high frequency oscillations in the normal state of the molecule, indicating the persistence of a strong binding in the excited state. The moderate convergence observed shows a rather large dissociation energy for the excited molecule, which evidently must split up into highly activated products, possibly two excited cyanide radicals.

TABLE III. *Some progressions of doublet bands in the cyanogen spectrum.*

ν(cm^{-1})	$\delta\nu$	$\Delta\nu$	ν(cm^{-1})	$\delta\nu$	$\Delta\nu$	ν(cm^{-1})	$\delta\nu$	$\Delta\nu$
						(Doubtful)		
A 45685(d)		2075	*A'* 44902		2142	*A''* 46592		2063
B 47733	27	(2033)	*B'* 47044(d)			*B''* 48619	36	(2073)
47760		2048			2091	48655		2076
C 49766	42	(1997)	*C'* 49116	19	(2074)	*C''* 50692	39	(2087)
49808		2011	49135		2087	50731		2092
D 51763	56	(1949)	*D'* 51190	32	(2050)	*D''* 52779	44	
51819		1956	51222		2086	52823		
E 53712	63		*E'* 53240	68				
53775			53308					

THE PARALLEL TYPE ABSORPTION BANDS OF AMMONIA

By David M. Dennison and J. D. Hardy*
University of Michigan

(Received February 1, 1932)

Abstract

The form of the ammonia molecule is discussed together with the theory that all of the vibrational levels of the molecule should be double due to the two equivalent positions of equilibrium of the nitrogen atom. This theory serves to explain the doubling of the $\|$ band at 10.5μ and further predicts that the lines of the 3.0μ band should also appear as doublets although with a much finer separation. An experimental search is made for the doubling of the 3.0μ band using an infrared spectrometer of high resolving power. The effect is found, each fine structure line appearing as a doublet with a mean separation of about 1.6 cm^{-1}. The theoretical intensities of the $\|$ type ammonia bands are computed assuming that the hydrogen nucleus possesses a spin of $\frac{1}{2}(h/2\pi)$. When these values are compared with the observed lines of the 3.0μ and the 10.5μ bands, a very satisfactory agreement is obtained. This agreement furnishes a strong argument for the theory of the doubling of the ammonia bands. It further proves that those states of ammonia existing in nature have vibration—rotation—nuclear spin wave functions which are antisymmetrical for an interchange of two of the hydrogen atoms.

Introduction

THE infrared spectrum of ammonia, NH_3, appears to prove rather conclusively that the molecule has the form of a regular pyramid where the three hydrogen nuclei lie at the corners of an equilateral triangle with the nitrogen nucleus lying on an axis perpendicular to the plane of the hydrogens and passing through their center of gravity. The regularity of the fine structure lines of the absorption bands at 3.0μ and 10.5μ as well as the uniform spacing of the far infrared lines, guarantees that the molecule is of the symmetrical top variety where two moments of inertia are equal $A=B$, with the third moment of inertia, C, different. It is moreover clear that the atoms can not all be coplanar since then the system would possess a zero permanent electric moment, contrary to the observed datum[1] $\mu=1.5\times10^{-18}$.

These conclusions as to the form of the molecule are further strengthened by the fact that all the near infrared absorption bands of ammonia may be correlated with the aid of four fundamental frequencies, not six as would be the case if the molecule were unsymmetrical.

Symmetrical molecules of the YX_3 type which are not coplanar exhibit a feature which at first appears to be rather unusual, namely, that all the vibrational levels are double. This phenomenon depends upon the fact that there are two exactly equivalent positions of equilibrium for the Y atom, one, say, above the plane of the X atoms and the other at an equal distance below.

* National Research Fellow.

[1] For a summary of the experimental work, see P. Debye, Polar Molecules (1929) page 40.

Such a circumstance would on the basis of classical mechanics not influence the vibrational levels but a quantum mechanical treatment reveals that it causes the vibrational levels to become double.[2] The magnitude of the doublet separation is in general small compared with the spacing between the vibrational levels themselves and need not be the same for all vibrational levels. It is proposed to discuss in more detail the amount of the doublet spacing elsewhere. For the purposes of this paper it is only necessary to state that it becomes observable spectroscopically (i.e., $\delta\nu$ is at least as large as 0.1 cm^{-1}), only when the Y atom lies quite close to the plane of the X atoms.

The 10.5μ band of ammonia has been resolved into its fine structure lines by E. F. Barker[3] and consists of two similar and complete bands separated by an interval of about 33 cm^{-1}. It has been suggested that the doubling of this band is the result of the doubling of the vibrational levels which has just been described. We have attempted in the present paper to strengthen this explanation in two ways: first, by showing experimentally that the fundamental band at 3.0μ also possesses a double structure but with a much smaller doublet separation, and second, by computing the intensities of the fine structure lines of both the 10.5μ and 3.0μ bands and showing that these agree with the experimental data. This last computation will further allow us to determine the symmetry character of that part of the wave function which is independent of the coordinates and spins of the electrons.

Of the four fundamental frequencies of a symmetrical molecule YX_3, two, ν_1 and ν_3, correspond to vibrations for which the change of the electric moment lies along the symmetry axis. The fine structure of these bands, which are often called $\parallel$ type bands, is very much simpler than the fine structure of the $\perp$ type bands and consists of a strong zero branch on either side of which lies a set of lines uniformly spaced in frequency. These latter lines constitute the positive and negative branches of the band.

The fine structure of the absorption band of ammonia at 10.5μ proves that this band is of the $\parallel$ type while its great intensity shows that it must be a fundamental and we may identify it with the frequency ν_3. The band at 3.0μ has been resolved by Stinchcomb and Barker[4] who find that it also corresponds to a $\parallel$ vibration. This in itself might not with certainty serve to identify it as the second $\parallel$ frequency ν_1, since the intensity is not so great that it excludes the possibility that the band might be a strong harmonic or overtone frequency. However, in the Raman spectrum of gaseous ammonia,[5] the strongest frequency to be observed just corresponds to the 3.0μ band. This virtually proves that the band in question is a fundamental band and since its fine structure is of the $\parallel$ type we may conclude that it is the fundamental frequency ν_1.

We have represented the energy level diagram of certain of the lowest

[2] The qualitative theory which was proposed by F. Hund, Zeits. f. Physik **43**, 805 (1927) is described by D. M. Dennison, Rev. Mod. Phy. **3**, 280 (1931).

[3] E. F. Barker, Phys. Rev. **33**, 684 (1929).

[4] G. A. Stinchcomb and E. F. Barker, Phys. Rev. **33**, 305, (1929).

[5] R. G. Dickinson, R. T. Dillon and F. Rasetti, Phys. Rev. **34**, 582 (1929).

vibrational states of ammonia in Fig. 1, which for convenience is not drawn to scale. The two lowest levels form the ground state of the vibrational spectrum and are separated by an interval which we call $\delta\nu_0$. The next two levels form the first excited state of the vibration ν_3 and lie about 950 cm^{-1} above the ground state. The separation is here $(\delta\nu_3)_1$. All levels are further given the designation α or β where the states α have wave functions of which the part depending upon the vibrational coordinates alone is symmetrical for an interchange of any two of the hydrogen nuclei. The states β are antisymmetrical for this interchange. Now it may easily be shown[6] that all $\|$ type infrared bands correspond to a transition from an α state to a β state or from a β state to an α state. The transitions giving rise to the fundamental frequency ν_3 are drawn in Fig. 1, and show that this band will appear as two similar and

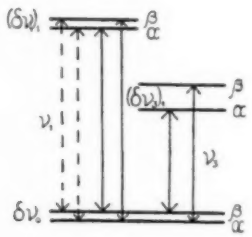

Fig. 1.

nearly superimposed bands. The doublet spacing which has been measured by Barker represents the sum of $\delta\nu_0$ and $(\delta\nu_3)_1$; thus

$$\delta\nu_0 + (\delta\nu_3)_1 = 33\,cm^{-1}.$$

Exactly the same argument may be repeated for the fundamental band ν_1. It should consist of two bands with a doublet spacing $\delta\nu_0+(\delta\nu_1)_1$. It is this quantity the experimental measurement of which will be described in the next section. It is found that $\delta\nu_0+(\delta\nu_1)_1=1.6$ cm^{-1}. Reasons may be given which make it appear very plausible why the doublet spacing should be so much smaller for the band ν_1 than for the band ν_3.

Qualitatively the magnitude of the splitting of the levels depends upon the ratio of the amplitude of the nitrogen atom (relative to the plane of the hydrogens) to the normal distance of the nitrogen atom from this plane. Now the fact that the splitting is sufficiently large to be observed spectroscopically means that the altitude of the regular pyramid in the normal state must be small and this allows us to infer the properties of the motion. In the vibration ν_3, the relative motion of the hydrogen nuclei in their plane is small and the motion consists principally of a vibration of the nitrogen atom relative to this plane. Thus we should expect that $(\delta\nu_3)_1 \gg \delta\nu_0$. It may be remarked that we should similarly expect $(\delta\nu_3)_2 \gg (\delta\nu_3)_1$ and thus if a first harmonic, $2\nu_3$,

[6] The intensity of a $\|$ type band depends upon such matrix elements as $\int_{-\infty}^{+\infty} x\psi_1\psi_2 dx$. Now x is an odd function, the ψ of an α state is an even function while the ψ of a β state is an odd function of x. The matrix element vanishes unless the integrand as a whole is an even function of x and thus we can only have transitions from states $\alpha\rightarrow\beta$ or $\beta\rightarrow\alpha$.

should ever be observed it would consist of two bands so widely separated that they would probably not be recognized as a doublet band at all.

In the limiting case of a flat pyramid, the vibration ν_1 consists principally of a motion of the hydrogen nuclei in their plane. The amplitude of the nitrogen nucleus relative to this plane would in general be small and we could infer from this that $(\delta\nu_1)_1$ would be of the same order of magnitude as $\delta\nu_0$.

These considerations are greatly strengthened by measurements of Dickinson, Dillon and Rasetti of the fine structure of the Raman band corresponding to ν_1. The arguments which showed that the $\|$ type infrared bands must be correlated with transitions from levels $\alpha\rightarrow\beta$ or $\beta\rightarrow\alpha$ also show that for a $\|$ type Raman band the transitions must be from $\alpha\rightarrow\alpha$ or from $\beta\rightarrow\beta$. These transitions for the frequency ν_1 are shown in Fig. 1 with dotted lines. Accordingly, the fine structure lines as observed in the Raman spectrum should also be doublets but with the spacing constant $(\delta\nu_1)_1-\delta\nu_0$. The measurements of Dickinson, Dillon and Rasetti show these lines to be single within the limit of observation which is probably at least as good as 1 cm^{-1}. Thus from these experimental data as well as from our theoretical conclusions (which are only presented here in qualitative form) we find $(\delta\nu_1)_1 \leqq \delta\nu_0$.

Before leaving this section we would like to remark that the far infrared rotation lines of ammonia which have been observed by Badger and Cartwright,[7] may be regarded as forming part of a $\|$ type vibration. It can easily be shown that they correspond to transitions between the two levels forming the ground state of the vibrational energy diagram. Therefore these pure rotation lines should also be double with a doublet spacing $2\delta\nu_0 \leqq 1.6$ cm^{-1}. No trace of a doubling can be noted in the experimental curves obtained by Badger and Cartwright but the dispersion of their spectrometer was certainly not sufficient to separate lines as close together as 1.6 cm^{-1}.

Experimental Procedure and Results

The spectrometer which was used in this experiment has been previously described[8] and for the region of 3μ a 7200 line echelette grating (ruled at the University of Michigan by Professor E. F. Barker) was used. The grating was so ruled as to give a very strong intensity at the 3μ region, thus permitting the use of very narrow slits. The grating spectrometer was preceded by a small prism spectrometer, the latter being used to separate the second order of 1.5μ, which is exceedingly strong, from the first order of 3μ. The separation was considered complete enough for this experiment when the prism was so adjusted that the deflections in the first order of 1.5μ were one fourth the total deflection obtained when the grating was turned to 3μ.

The thermocouple, which is of the Pfund design, was connected to a Leeds and Northrup galvanometer, the deflections of which were amplified by means of a Pfund thermoelectric amplifier. Usually an amplification of about six hundred could be used and the deflections determined to an accuracy of about one percent. The width of the slits was varied between 0.05 and 0.15

[7] R. M. Badger and C. H. Cartwright, Phys. Rev. **33**, 692 (1929).

[8] J. D. Hardy, Phys. Rev. 38, 2162, (1931).

mm depending upon the kind of work that was being done, but in the final runs both slits were set at 0.07 mm. Under these conditions deflections of 40 cm were obtained with the absorption cell out of the path and 25 cm with the cell in the path. The steadiness of the instrument was such that readings could be made in the daytime as well as at night.

When the slits were 0.15 mm in width they included a wave-length range of ten angstroms or about one frequency unit. For more careful examination of the rotation lines the slits were adjusted to include a little less than one half of one frequency unit.

The cell which was used was six centimeters in length and supplied with KBr windows. The ammonia was introduced from a tank through a liquid air trap, and the pressure of the ammonia in the cell was made to be approximately that of the atmosphere. The readings were made alternately through the cell and through the air in order to correct for water vapor absorption. No correction was applied for the absorption of the windows and the resulting curves cannot therefore be given in percent absorption. The heights of the lines give some measure of their relative intensities although not an accurate one.

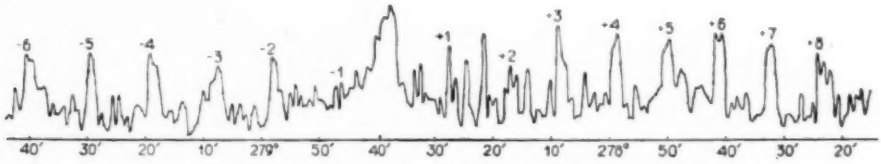

Fig. 2. 3μ ammonia band surveyed with 0.15 mm slits.

Fig. 2 shows a general survey of the 3.0μ band as made with 0.15 mm slits. There is shown the complexity of the background and an indication of the doubling of the rotation lines. The existence of this background can very probably be explained as the first harmonic of the strong ammonia band at 6.0μ. Although it is strong enough to apparently mask the simple structure of the $\|$ type band ν_1, it did not cause any very serious difficulty since after the lines belonging to ν_1 were once located they could be carefully studied individually without mapping the intervening background.

In Fig. 3a is shown the results obtained with narrowed slits. The regions between the rotation lines were not examined carefully and are therefore omitted from this diagram.

The wave-length accuracy is about one in ten thousand or three angstroms. The calibration of the grating was repeatedly checked and the position of the central image determined with each set of readings. The calibration and the position of the central image were found to remain very constant.

The observed positions of the lines in frequency units as well as the frequency intervals between lines are given in Table I. The lines are grouped in pairs by means of a bracket and the upper figure relates to a line of the $\beta \rightarrow \alpha$ band while the lower relates to a line of the $\alpha \rightarrow \beta$ band.

The doublet separation $(\delta\nu_1)_1 + \delta\nu_0$ varies from 1.4 cm^{-1} to 2.1 cm^{-1} and

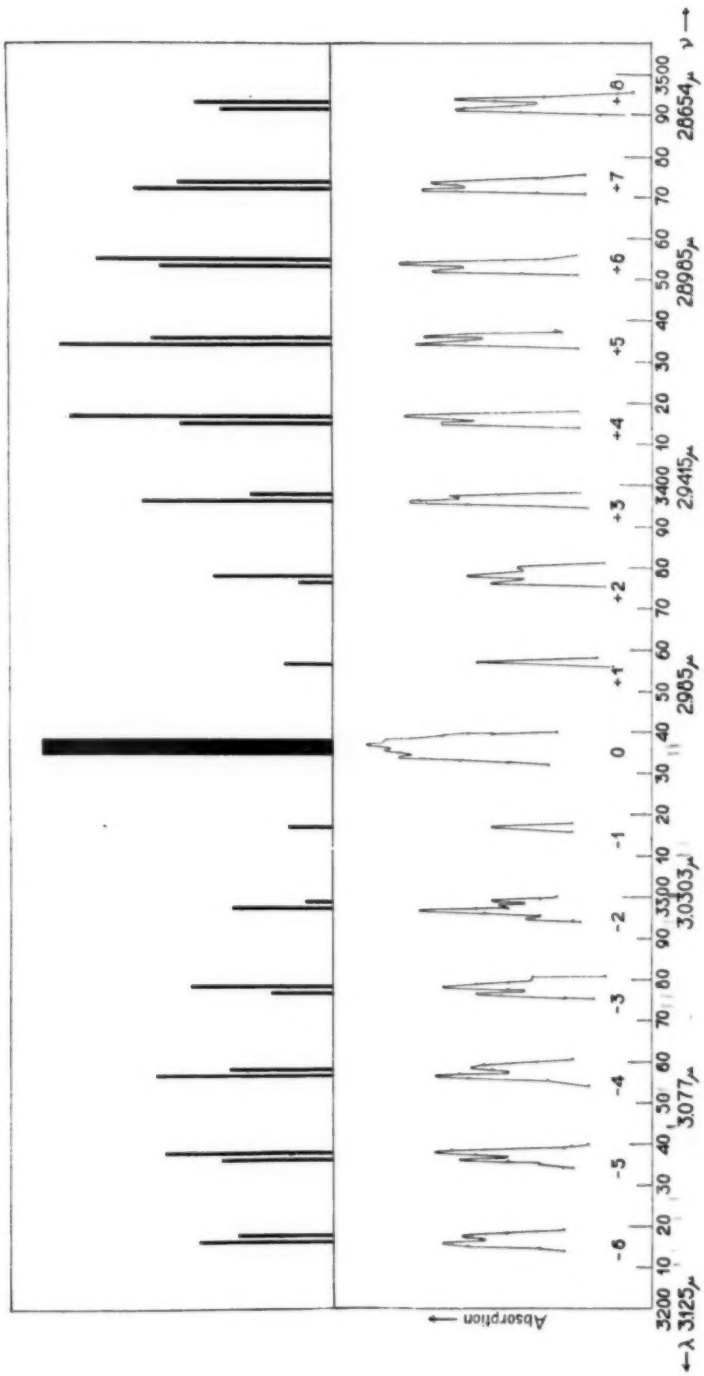

Fig. 3. Showing zero branch and rotation lines as observed under high dispersion. Slits—0.07 mm; 4A; 0.5 cm^{-1}.

has an average value of 1.6 cm^{-1}. It does not appear probable that the accuracy with which we have determined this constant can be greater than 10 to 20 percent. We feel that the considerable variation observed is very possibly due to the presence of the strong and irregularly spaced lines of the background. The average interval between lines of the $\beta \rightarrow \alpha$ band is 19.64

TABLE I.

Line No.	Positive branch	$(\delta\nu_1)_1+\delta\nu_0$	$\Delta\nu$	Negative branch	$(\delta\nu_1)_1+\delta\nu_0$	$\Delta\nu$
0	3336.8 cm^{-1}			3336.8 cm^{-1}		
1	3356.6 —	—		— 3316.8	—	-- 18.2
			19.7 —			
2	3376.3 3378.0	1.7		3297.1 3298.6	1.5	
			19.8 19.6			20.4 20.4
3	3396.1 3397.6	1.5		3276.7 3278.2	1.5	
			19.1 19.2			20.3 19.9
4	3415.2 3416.8	1.6		3256.4 3258.3	1.9	
			19.1 19.2			20.3 20.6
5	3434.3 3436.0	1.7		3236.1 3237.7	1.6	
			19.0 18.8			20.0 20.2
6	3453.3 3454.8	1.5		3216.1 3217.5	1.4	
			19.1 19.0			
7	3472.4 3473.8	1.4				
			19.2 19.9			
8	3491.6 3493.7	2.1				

cm^{-1} while the interval for the $\alpha \rightarrow \beta$ band is 19.46 cm^{-1}. These data lead to values for the moment of inertia A of 2.81 and 2.84×10^{-40} respectively in good agreement with the values of A as determined from Barker's measurements on the 10.5μ band,[9] namely, 2.79 and 2.82×10^{-40}. The observations of the Raman band corresponding to the 3.0μ vibration yield $A = 2.79 \times 10^{-40}$ while the far infrared pure rotation lines give $A = 2.78 \times 10^{-40}$. It will be noticed from Table I that while the average value of the line interval is satisfactory, there is a considerable variation in the individual values which appears to be much higher than can be accounted for as experimental error in the spectrometer itself although it might be due to the presence of the strong background lines.

[9] A slight rearrangement of the ordinal numbers given by Barker has been suggested by R. M. Badger, Phys. Rev. **35**, 1038 (1930). This identification is the one we follow here and leads to more probable values for A as well as fitting our intensity curves better.

The Intensities of the ∥ Type Lines

The theoretical intensities of the fine structure lines of ∥ type vibration bands may be computed when the moments of inertia of the molecule, A and C, are known. We shall take as an average value $A = 2.80 \times 10^{-40}$. In addition to this datum we require the constant $\beta = (A/C - 1)$. The fact that the doubling of the ∥ type bands is observable spectroscopically insures that the molecule is very flat, that is $\beta \cong -0.5$. It cannot however be exactly -0.5. From estimates based on a quantitative discussion of the doubling which will be published elsewhere we are lead to the value $\beta = -0.412$ and this will be used here in determining the intensities. Fortunately, it appears that the line intensities are relatively insensitive to small variations in β when it is in this neighborhood.

The intensity formulae have been given explicitly by Dennison[10] and need only be modified by introducing weights appropriate for the ammonia molecule. We shall take the spin of the hydrogen nucleus equal to $\frac{1}{2}(h/2\pi)$ and assume that those states which occur in nature have wave functions (the vibration—rotation—nuclear spin part) which are antisymmetrical for an interchange of any two of the hydrogens.

The weights of the states (see Table V, reference 2) may then be expressed in terms of the rotational quantum numbers J and K where the two cases of vibrational symmetry α or β occur.

	Vibrational Symmetry		
	α	β	
$g =$	0	$2(2J+1)$	for $K=0$ and J even.
$g =$	$2(2J+1)$	0	for $K=0$ and J odd.
$g =$	$(2J+1)$	$(2J+1)$	for $K \neq 0$ and not a multiple of 3.
$g =$	$2(2J+1)$	$2(2J+1)$	for $K \neq 0$ and a multiple of 3.

As an example the intensity of the lines of the negative branch of the $\alpha \rightarrow \beta$ band are given by,

$$I_{J-1}^{J} = A \sum_{K=0}^{J-1} ([x](J^2 - K^2)/J) e^{-\sigma(J^2+J)-\sigma\beta K^2}$$

where A is a proportionality constant and $\sigma = h^2/8\pi^2 A k T$. The symbol $[x]$ is 0 for $K=0$ and J even, 2 for $K=0$ and J odd, 1 for $K \neq 0$ and not a multiple of 3 and 2 for $K \neq 0$ and a multiple of 3. The intensities of the positive branch of this band as well as those of the $\beta \rightarrow \alpha$ band may be expressed by means of similar formulae. Their values have been computed (using the values of A and β given above) and are arranged in Table II according to the ordinal number of the line.

In Fig. 3b we have plotted these theoretical intensities in order that they may be compared directly with the experimental curve. The agreement appears to be very good; certainly as close as could be expected when the approximate character of the experimental intensities is taken into account.

[10] See reference 2, page 315.

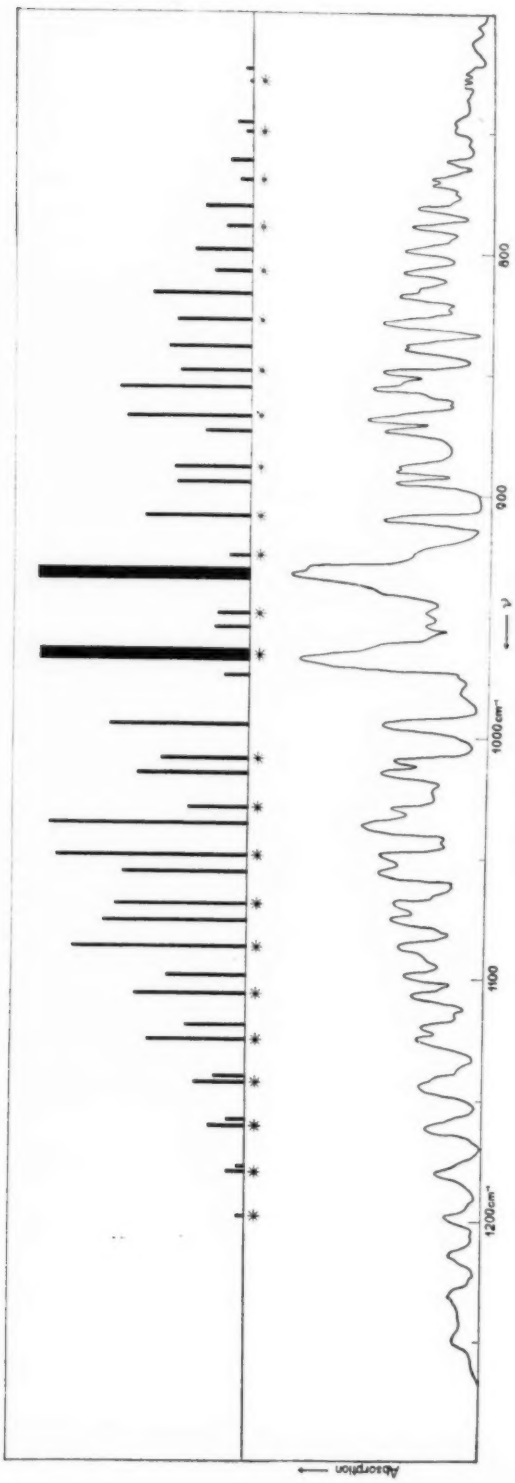

Fig. 4. The 10.5 μ band of ammonia.

TABLE II.

m	$\alpha\rightarrow\beta$ Band +	$\alpha\rightarrow\beta$ Band −	$\beta\rightarrow\alpha$ Band +	$\beta\rightarrow\alpha$ Band −
1	0.00	1.79	2.00	0.00
2	4.96	1.15	1.37	4.14
3	3.38	5.89	7.87	2.53
4	10.79	4.28	6.30	7.32
5	7.45	6.94	11.24	4.59
6	9.89	3.95	7.07	5.53
7	6.30	4.14	8.13	3.20
8	5.59	2.10	4.52	2.58
9	2.92	1.45	3.48	1.22
10	2.04	0.68	1.78	0.78
11	1.04	0.36	1.05	0.36
12	0.49	0.14	0.45	0.15

Before discussing the significance of this result we might point out that our computation is valid for any of the $\|$ type bands of ammonia and hence these theoretical intensities may be compared with the intensities of the lines of the 10.5μ band as observed by Barker. The only difference between the 3.0μ band and the 10.5μ band is that in the former the doublet separation is small compared with the distance between successive rotation lines whereas in the latter case the doublet separation is somewhat greater than the line interval. A comparison between the experimental and theoretical intensities is made in Figs. 4a and 4b and again the agreement is on the whole very good.[11]

We regard the fact that the line intensities in these two ammonia bands can be so satisfactorily accounted for as being one of considerable importance. In the first place, the peculiar intensity distribution (an alternating intensity which gradually becomes uniform for the higher band lines) depends intimately upon our interpretation of the origin of the doubling of these bands, namely, $\alpha\rightarrow\beta$ transitions and $\beta\rightarrow\alpha$ transitions. Since the observed lines show just this same unusual intensity distribution we believe that this constitutes a strong argument for the validity of the underlying theory.

The second point is that we have shown that the states of the ammonia molecule which exist in nature are those for which that part of the wave function which is independent of the electronic coordinates and spins, is totally antisymmetrical for an interchange of the hydrogen nuclei.

If this were not the case we should have found a strong line appearing in the experimental curve where a weak one was predicted and vice versa.

[11] In Fig. 4b the lines of the $\alpha\rightarrow\beta$ band are marked with a *. The heights of the lines of Fig. 4b represent theoretical intensities while the lines of Fig. 4a are given in percent absorption.

LINE REFLECTION SPECTRA OF SOLIDS

By Frank H. Spedding[1] and Richard S. Bear[2]
Department of Chemistry, University of California, Berkeley

(Received January 15, 1932)

Abstract

A new interpretation of reflection spectra in solids, particularly $SmCl_3 \cdot 6H_2O$, is offered. The appearance of new absorption lines and the strengthening of others in the spectrum of a conglomerate as compared with that of a single crystal is explained as being caused by an increased path length travelled by the light through the crystal rather than by surface atoms as heretofore considered. This increased path results from the high refractive index for the light of wave-length of the absorption lines, which makes it difficult for such a ray, once it has entered a small crystal fragment, to leave. A new phenomenon of reversal of lines from absorption in a single crystal to emission in a conglomerate is described for a multiplet of the $GdCl_3 \cdot 6H_2O$ spectrum.

THOUGH the absorption and reflection spectra of the rare earth solids have been studied by many investigators, except for a brief letter by one of us in collaboration with Dr. Freed,[3] no one to our knowledge has compared both types of spectrum from the same compound. In the letter mentioned it was stated that the reflection spectrum of $SmCl_3 \cdot 6H_20$, which was photographed by reflecting light from the surface of a conglomerate of small crystals, contained many more lines, particularly at low temperatures, than the absorption spectrum of the same salt obtained from light that had passed directly through a single crystal. It was also recorded that the lines arising from the electronic isomer which is stable at low temperatures are relatively more intense at room temperatures in the reflection spectrum than in the absorption spectrum. New photographs under high dispersion have confirmed these results, but additional experiments make it possible to offer an explanation with greater certainty.

The appearance of the new lines and the abnormal intensities of the others in the conglomerate appeared at the time of the preliminary note to be attributable to the different force fields present about the surface atoms of the crystal. These surface atoms would be of greater importance in a conglomerate because of the increased surface. This paper is a continuation of the above work and attempts to explain the anomalies of reflection spectra from a slightly different standpoint. In addition a peculiarity observed with $GdCl_3 \cdot 6H_2O$ is described.

Part I. $SmCl_3 \cdot 6H_2O$

Large single crystals of the chloride were grown, some being as large as two centimeters to an edge and eight millimeters in thickness. Photographs

[1] National Research Fellow, University of California.
[2] Du Pont Fellow in Chemistry, University of California.
[3] Freed and Spedding, Phys. Rev. **35**, 212 (1929).

of the absorption of these were obtained by the use of a three meter grating with a dispersion of about 5.6A per mm. Since the crystals are hygroscopic it was necessary to protect them at room temperatures by a glass cell, but at lower temperatures, those of liquid nitrogen and hydrogen, they could be immersed directly in the cooling liquid. The crystals were observed by means of windows in the Dewar.

The following experiments were performed and the results were as listed:

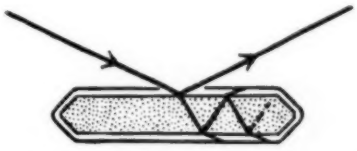

Fig. 1. Showing method used in shielding rare earth chloride crystal to eliminate all but direct reflections from a single crystal face.

1. A beam of parallel light was reflected from the surface of the crystal and the reflection observed by means of the grating at an angle equal to that of incidence. Only the continuous spectrum of the source was obtained, though various angles of incidence were tried.

2. A variation of the above with the angle of observed reflection *not* equal to the angle of incidence, i.e., scattered reflection, was tried. Though at first a faint spectrum was obtained, upon more careful shielding (see Fig. 1) the continuous spectrum of the source was again observed.

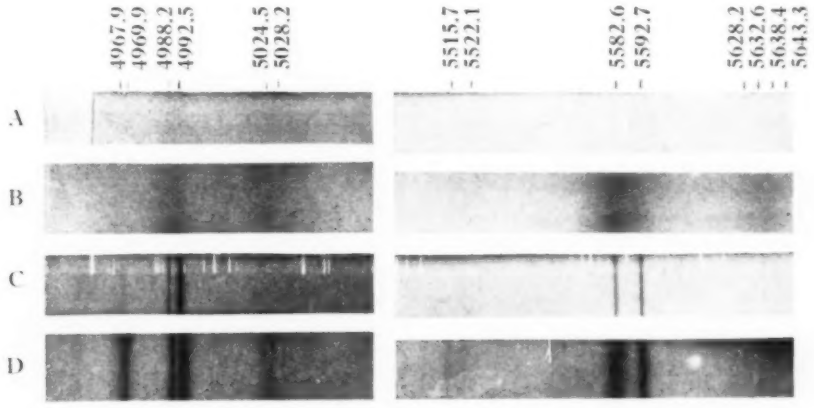

Fig. 2.

3. Light passed through or scattered from a conglomerate gave an absorption spectrum very rich in lines.

4. Photographs of light emerging from a very thick single crystal contained very faintly some of the lines that had previously been observed only with the conglomerates.

5. A large crystal was cut up into sections which were suitable for the passage of light through them in the three (monoclinic) axial directions.

Photographs of the spectra so obtained showed the same lines, though intensities varied, probably because of polarization effects. Especially noteworthy is the appearance of several new lines for the new path direction which had not been seen before in the pictures obtained with light that had traversed only the direction perpendicular to the large flat faces but had appeared in the reflection spectrum. This polarization explanation, however, can apply to only a few of the lines peculiar to the reflection spectrum.

The positions of the lines of the reflection spectrum seem to indicate slight shifts to the red as compared to the ordinary single-crystal spectrum, but this is not absolutely certain since the shifts are of the order of magnitude of our error in measurement. However, the positions of the sharpest lines measured on several plates taken at hydrogen temperatures of a single crystal and of a conglomerate gave an average displacement of 0.3 wave number to the red.

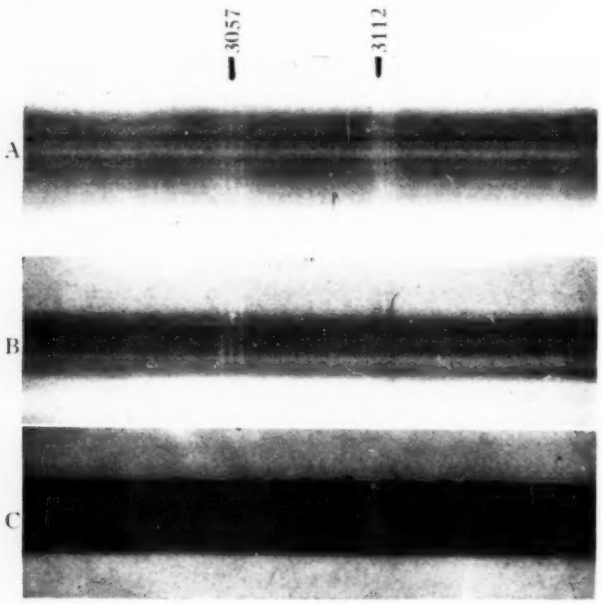

Fig. 3. A. Absorption by a single crystal of $GdCl_3 \cdot 6H_2O$. B. Absorption by a thin conglomerate of small crystals and fragments. C. Reflection from the cleavage face of a single crystal.

The observation of the greater number of lines obtained by use of thick crystals and the slight shift to the red led us to consider the following explanation as the most likely one for the increased number of lines found in the reflection spectrum, though other factors may be operating to a lesser degree. If one could examine the curve of the refractive index of the crystal plotted against the wave-length of the light, one would find in the neighborhood of the absorption lines a sudden increase in the index. After such light has entered the crystal fragment it is totally reflected many times before emerging (as with ordinary light in a diamond), resulting in a greatly increased path through what becomes effectively a very thick crystal and

giving more opportunity for absorption. On the other hand the light of wave-length slightly different from the possible absorption lines has an ordinary index of refraction and travels only a relatively short distance through the crystal. This explanation indicates why the faint lines are the ones to appear or grow relatively intense in the reflection spectrum. They are the ones that offer the most possibility of intensification, whereas the strong lines are already practically completely absorbed.

The appearance of the satellites 160 cm^{-1} to the red of the "low temperature lines" in the conglomerate spectra at "higher temperatures", instead of being attributed to the different force fields at the surface of the crystal, should be attributed to the separation of the energy levels of the electronic isomers. Lines arising from the two basic levels and ending in a common upper level would give this common interval. The lines from the "high temperatures isomer" would be relatively faint at low temperatures as the relative abundance of that isomer would be small. In addition, the transition probabilities might be very low. However, due to the relatively greater distances travelled by light of those wave-lengths in the conglomerate enough would be absorbed to make the lines visible.

PART II. $GdCl_3 \cdot 6H_2O$

The study of the reflection spectrum of $GdCl_3 \cdot 6H_2O$ brought to light a very interesting phenomenon. The usual absorption spectrum of this salt consists of some ninety sharp lines which are chiefly in the ultraviolet.[4] They occur in groups or multiplets, one of which at about 3100A is composed of four very sharp lines that exhibit the following behavior. When a light from a hydrogen discharge is passed through a single crystal these lines appear strongly in absorption and are also polarized. If the same crystal is broken up into a conglomerate the four lines appear in emission in the reflection spectrum (Fig. 3).

Further description of this peculiarity will appear in the following account of the experiments performed.

1. A quartz wedge-shaped cell varying in thickness from about 0.5 mm to 2 mm was filled with a conglomerate of crystals formed by breaking up several large ones. Light from a hydrogen source was passed through the cell and photographed with a Hilger E2 instrument. All the intense lines except the four at 3100A appeared in absorption as usual. In the pictures of the absorption by the thinnest layer of conglomerate these four lines and four, possibly five, other fainter multiplets between 4000 and 3000A appeared as emission lines. As the thickness of the absorbing section increased the fainter emission multiplets faded out and at length became absorption lines again. The four stronger emission lines were the last to reverse, requiring the whole 2 mm of conglomerate to do so.

This change from emission to absorption seems to be caused by a shift in the balance between the natural tendency to absorption and a surface

[4] Freed and Spedding, Phys. Rev. **34**, 945 (1929).

factor (see experiment 3) which causes emission or strong reflection of these lines.

2. Photographs taken with a larger E185 Hilger spectrograph with an arrangement of prisms that gave a dispersion of about 2A per mm in the region under consideration indicate that the four emission lines are shifted slightly to the red.

3. Large single crystals were prepared and a parallel beam of light was reflected from the faces of the crystal. While photographs (again with the small instrument) were made at different angles with the crystal, only those at which the angle of reflection was equal to the angle of incidence had intensity enough in the 3100A region to affect the plates. The four lines at 3100A could be observed faintly but clearly in emission against the continuous background. On the other hand the strong absorption lines at 3000 and 2700A were not even faintly visible on any of the plates examined. Careful shielding of the crystal prevented any but reflected light from being photographed.

4. Reflections from the (100) or cleavage faces of the crystals (monoclinic) seemed to be much more intense than those from the (010) or principal face. In the latter case the intensities were occasionally so faint as to be doubtful. Experiments also seemed to indicate that orientation of the crystal so that the longest axis was perpendicular to the plane of the incident and reflected rays caused the greatest intensity. However, the intensity differences were so small that it is difficult to be certain.

5. Photographs taken with a Nicol prism placed at several angles between the crystal and the spectrograph indicated that the emission lines were polarized, but because of general polarization of the background caused by the reflection further statements seem inadvisable. We hope with better experimental conditions to be able to say more about this.

It was concluded from these and other experiments that the emission lines arise from reflection from the surfaces of the crystals, particularly from the cleavage faces, and that they are not caused by fluorescence. They resemble very much the residual rays observed in the infrared with ionic crystals.

This phenomenon can not be caused by any impurity of the particular sample of $GdCl_3 \cdot 6H_2O$ used in these experiments, since with two lots having entirely different histories results agreed in every way. The conglomerate with which most of the work was done was from material of nearly atomic weight purity kindly furnished us by Professor Hopkins of the University of Illinois, and the other lot used was prepared from gadolinium salts obtained from the Wellsbach Company and containing as chief impurity about one percent of terbium.

THE TEMPERATURE SHIFT OF THE TRANSMISSION BAND OF SILVER

By J. V. Pennington
The Rice Institute, Houston, Texas

(Received February 1, 1932)

Abstract

It is shown that by Kronig's quantum theory of dispersion in metals one can account for the shift of the frequency at which maximum transmission is found for silver when the temperature is varied. The calculated rate of shift is in fair agreement with experiment.

IT HAS been known for some time that, although for wave-lengths up to 5μ the optical constants of metals show little or no temperature dependence, there is a marked temperature effect in the case of silver in the region of the minimum of reflecting power, around 3160A. Ebeling[1] first noted that raising the temperature from 15°C to 200°C produces a displacement of the reflection minimum toward the red of about 100A and an increase of reflecting power at the minimum from 4.2 to 20 or 30 percent. The reflection measurements of de Selincourt[2] at temperatures from −183 to 156°C showed that a similar effect extended throughout this range. It is to be expected that with the minimum of reflection would be associated one of absorption. Minor's experiments on silver at ordinary temperatures[3] showed minima of absorption index, reflecting power, extinction coefficient, and absorption coefficient at 3140, 3160, 3160, and 3220A respectively. Lord Rayleigh[4] first investigated the effect of temperature on the absorption minimum (transmission maximum) by passing light through silver foil at temperatures from −180 to 254°C. The transmission maximum behaved much in the same manner as the minimum in the earlier reflection experiments.

Quite recently, McLennan, Smith, and Wilhelm[5] with greatly improved methods made measurements on the transmission band of silver at temperatures from 20°C down to −269°C using liquid air, hydrogen, and helium and found the transmission maximum to vary nearly linearly with the temperature over this large range. Before the appearance of the last named paper, the author repeated Lord Rayleigh's experiments with modifications in order to determine the nature of the reported broadening of the transmission band and change in transmission intensity and found that these agreed qualitatively with the reflection experiments of de Selincourt. No quantitative explanation of the shift has been given but one should now be possible in view of

[1] Ebeling, Zeits. f. Physik **32,** 489 (1925).
[2] de Selincourt, Proc. Roy. Soc. **107,** 247 (1925).
[3] Minor, Ann. d. Physik **10,** 581 (1903).
[4] Lord Rayleigh, Proc. Roy. Soc. **128,** 131 (1930).
[5] McLennan, Smith, and Wilhelm, Phil. Mag. **12,** 833 (1931).

the work on the quantum theory of dispersion in metals by Kronig.[6] Extending Kronig's theory, Schubin[7] has shown that the quantum theory indicates the existence of an absorption minimum very near the second line of the resonance doublet of the corresponding metal vapor (for silver this line is found at 3280A). Attention had been called to this coincidence by Ebeling in the paper cited above. Schubin also shows that general qualitative considerations lead one to expect a shift of absorption minimum toward the red with increasing temperature.

In Fig. 1 are shown the experimental values of the frequency at which the absorption minimum occurs for different temperatures as found by various investigators. It is seen that the values found by McLennan and by de Selincourt fall on straight lines. In both of these cases careful photometric measurements were made. Of course, the two lines are quite distinct since one represents transmission maxima and the other minima of reflecting

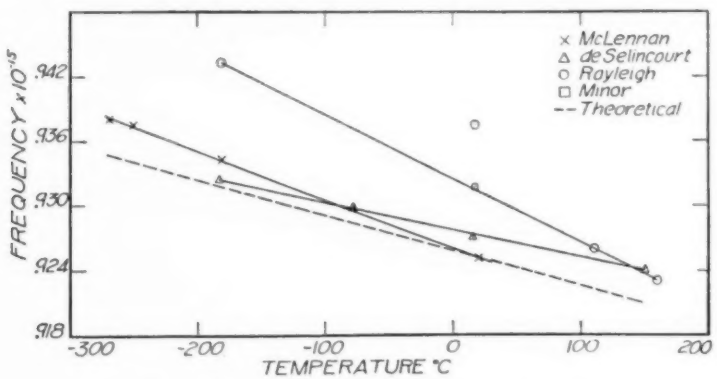

Fig. 1. Frequency of transmission maximum.

power. There is also a difference in the physical condition of the silver used. Three of Lord Rayleigh's values are on a straight line on which Minor's value at room temperature also lies.

The quantum theory of dispersion in metals as given by Kronig is based on Bloch's theory of metallic conduction.[8] The conduction electrons play the part both of free and of bound electrons. These electrons are distributed among their various quantum states according to the Fermi-Dirac statistics. Under the influence of an applied electric field and as a result of collisions with the ions of the crystal lattice, which are in temperature vibration, the conduction electrons make transitions to other states. When the applied electric field is that due to incident light of short wave-length λ, (i.e., less than about 5000A) it is shown that it is possible to neglect the collisions with the lattice.

In Kronig's ideal cubical crystal lattice the quantum states of the conduction electrons are given by three quantities ξ_1, ξ_2, ξ_3.[8] Possible transitions are those to states ξ_1', ξ_2', ξ_3' where

[6] Kronig, Proc. Roy. Soc. **124**, 409 (1929); **133**, 255 (1931).
[7] Schubin, Zeits f. Physik **73**, 273 (1931).
[8] Bloch, Zeits. f. Physik **52**, 555 (1929).

$$\xi_i' = \xi_i + 2\pi n_i \quad i = 1, 2, 3$$

and n_i is any positive or negative integer. Light of frequency ν will be absorbed by such electrons as can make such transitions under the condition

$$E(\xi_i + 2\pi n_i) = E(\xi_i) + h\nu.$$

According to Kronig, absorption is found under these conditions for $\nu = 0$ (which corresponds to absorption by free electrons under the classical theory) and also for a band $\nu_1 < \nu < \nu_2$ (corresponding to bound electrons) where ν_1 and ν_2 are of the order 10^{15}.

Now, experimentally just such an absorption band is found for silver from $\nu_1 = 0.925 \times 10^{15}$ to $\nu_2 = 1.56 \times 10^{15}$. This is best seen by comparing the conductivity calculated from Minor's experimental values of refractive index (n) and extinction coefficient (K) by Drude's expression

$$2\sigma/\nu = 2n\,\mathrm{K}$$

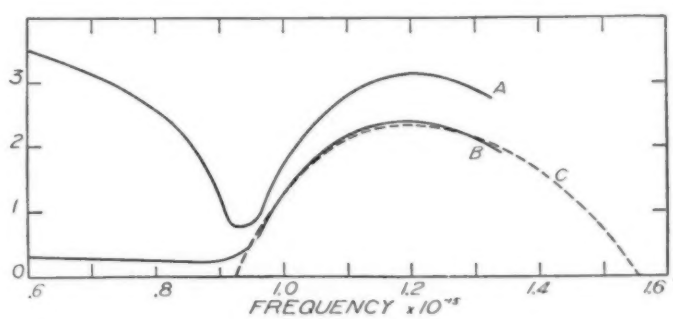

Fig. 2. A, Relative absorption coefficient ($nK\lambda_0/\lambda$) Minor; B, Conductivity $\times 10^{-15}$ calculated from Minor; C, Conductivity $\times 10^{-15}$ by quantum theory.

where σ is the conductivity, with the conductivity calculated from Kronig's formula

$$\sigma = \frac{\pi}{2}\,\frac{\Omega}{\nu}(\nu_2 - \nu)(\nu - \nu_1) \quad \nu_1 < \nu < \nu_2$$

where Ω is a constant for silver. This comparison is made in Fig. 2 where Ω is taken equal to 18. It is seen that ν_1 must have very nearly the value assigned above.

But the lower frequency limit of the absorption band will also be very nearly the upper frequency limit of the transmission band. What we propose to show is that this limit, ν_1, depends on temperature and shifts linearly toward the red with increasing temperature. If the transmission band does not widen appreciably (and the photometric measurements of de Selincourt and of McLennan do not bear out the widening reported by others for which Schubin attempts an account), the rate of shift of transmission maximum with temperature will be very nearly that of ν_1.

Kronig finds, as a theoretical value for ν_1,

$$\nu_1 = \frac{4\pi\omega}{h}(\pi - \rho_0)$$

where

$\omega = \beta(h^2/8\pi^2 ma^2)$
$\beta =$ binding constant < 1
$\rho_0 = (6\pi^2 K)^{1/3}$
$2K =$ number of conduction electrons per cell
$a =$ the lattice constant.

Thus

$$\nu_1 = \frac{\beta h(\pi - \rho_0)}{2\pi ma^2}$$

where a alone is supposed to vary with temperature according to this theory. Putting $a = a_0(1+\alpha t)$ where α is the coefficient of linear expansion for silver and t is the temperature on the Centigrade scale and putting

$$\nu_0 = \frac{\beta h(\pi - \rho_0)}{2\pi m a_0^2}$$

we get

$$\nu_1 = \frac{\nu_0}{(1+\alpha t)^2} = \nu_0(1 - 2\alpha t + \cdots)$$

$$\frac{d\nu_1}{dt} = -2\alpha\nu_0 = -2 \times 19 \times 10^{-6} \times 0.925 \times 10^{15}$$

$$= -3.5 \times 10^{10} \text{ very nearly.}$$

Based on this calculation, a theoretical curve is shown in Fig. 1 for comparison with experiment. Its slope is seen to lie between that of McLennan's curve for transmission maxima and that of de Selincourt's curve for minima of reflecting power.

In conclusion the author wishes to thank Professor H. A. Wilson for suggestions and criticisms in connection with the above work.

THE ABSORPTION BY FORMALDEHYDE VAPOR IN THE INFRARED

JOHN R. PATTY AND HARALD H. NIELSEN
MENDENHALL LABORATORY, OHIO STATE UNIVERSITY

(Received December 21, 1931)

ABSTRACT

The absorption spectrum of formaldehyde vapor in the infrared has been investigated with a prism spectrometer to 7.0μ. In addition to confirming the bands reported by Salant and West at 3.5μ, 1.8μ, 1.4μ, and 1.25μ, a fifth band at 4.8μ was located. The two regions at 3.5μ and 4.8μ have been investigated under higher dispersion using an echellette grating ruled with 3600 lines per inch, and resolved into a fine structure. Polymerization of the gas into paraformaldehyde was avoided by using a cell that could be heated.

The 3.5 region. The region at 3.5μ was found to be one of intense absorption and apparently consisting of three partially overlapping bands with centers lying near 3.4μ, 3.5μ and 3.6μ. Of these two appear to have P, Q, and R branches, where the average spacings between lines is about 3.5 cm^{-1}. The third band consists of only one branch where the spacing is about 28 cm^{-1}.

The 4.8μ region. This region is a band showing P, Q, and R branches and very similar in structure to those at 3.4μ. The average spacing between lines in the P and R branches is here found to be about 3.1 cm^{-1}.

THE infrared absorption spectra of asymmetric molecules which have heretofore been investigated have shown themselves to be of a rather complex structure. They have in fact been so complex that they have been given only somewhat qualitative interpretations. The desirability of investigating the spectra of molecules which are only slightly asymmetric, and where one might consequently expect a rather simple structure, immediately suggests itself. It seems particularly desirable since such a spectrum might perhaps be rigorously interpreted, and in so doing methods of attack on more complex spectra might suggest themselves. From chemical considerations, the formaldehyde molecule appears to be just such a one. It seems probable that all the atoms lie in one plane, the carbon and the oxygen being connected by a double bond. Such a molecule would then have one relatively small moment of inertia and two relatively large moments of inertia of about the same magnitude. With this in mind, the investigation of the absorption by formaldehyde vapor in the infrared was begun.

Salant and West[1] have investigated this spectrum with a prism spectrometer and have reported the existence of bands at 3.5μ, 1.8μ, 1.4μ and 1.25μ enumerated in the order of decreasing intensities. We have repeated these measurements and extended the explorations to 7.0μ, confirming the results of Salant and West in addition locating a band at 4.8μ.

As is well-known, formaldehyde forms polymers at room temperatures and in order to maintain it in the vapor state, an absorption cell must be used which can be heated. The vapor is made from paraformaldehyde and the reaction is a reversible one,

[1] E. O. Salant and W. West, Phys. Rev. **33**, 640A (1929).

$$(CH_2O)_x \rightleftarrows xCH_2O$$

the equilibrium of reaction being pushed toward the vapor state with increase of temperature. The temperature was maintained in the neighborhood of 200°C. The cell was of brass and surrounded by a heating coil of nichrome wire. To keep the inside windows at the same temperature as the cell, double windows made of mica were used. The cell was thermally insulated with thick coatings of asbestos. In order to assure a nearly constant concentration of gas in the cell, a continual flow was maintained through it; the vapor being generated in a large test tube which also was electrically heated, and after passing through the cell, the vapor was condensed in a cooled flask. The cell and generator were heated several hours before measurements were taken in order that thermal equilibrium might be reached. It was found that measurements were most effectively made in the regions investigated if the actual path of the cell was made about two millimeters long.

For a study of the spectrum of formaldehyde under higher dispersion, a spectrometer of the Sleator type, originally built by Lowry[2] and later rebuilt by one of the writers, was available. In the usual manner, radiant energy from a Nernst glower passing through the absorption cell is focussed upon the slit of a rock salt spectrometer which serves the purpose of a monochromator. From this, the energy is focussed upon the slit of the grating spectrometer. This slit is at the principal focus of a collimating mirror which reflects the light as a parallel beam on to a grating. After diffraction the radiation is reflected back to the collimating mirror and finally concentrated on the junctions of a thermopile. Dr. J. D. Hardy, National Research Fellow at the University of Michigan, very kindly presented us with a vacuum thermopile of his own construction to be used in this work. The collimating mirror in this case had a focal length of one meter. The thermopile was used in conjunction with a Moll thermal relay and a Leeds and Northrup high sensitivity moving coil galvanometer. The sensitivity was such that the slits could be narrowed to about 17 angstroms and maintained so throughout the experiment.

The grating used was an echellette ruled by Wood on a copper-chromium surface with a spacing of about 3600 lines per inch, and concentrating the energy at about 3.5μ in the first order. The calibration of the spectrometer was obtained from measurements made upon the positions of the 1, 2, -1, -2 lines of HCl as given by Colby, Meyer and Bronk.[3]

The region reported by Salant and West at 3.5μ and that found by us at 4.8μ were found to be regions of intense absorptions; these have been carefully examined under high dispersion and resolved at least partially into a fine structure. A preliminary run was first made over each band with widened slits and readings were taken at intervals of one minute of arc on the circle. This extended on both sides of the band until the absorption fell to zero. The slits were then narrowed and readings were taken at intervals of twenty seconds of arc on the circle. Readings were taken at each setting with the cell in

[2] E. F. Lowry, J. Opt. Soc. Am. **8**, 647 (1924).
[3] W. F. Colby, C. F. Meyer, and D. W. Bronk, Astrophys. J. **57**, 7 (1924).

and out of the beam, their ratios giving the percentage of transmission. Compensating windows were not used, since the amount absorbed by the windows of the cell could satisfactorily be accounted for by making a run with the cell empty, and moreover since no atmospheric bands occur in these regions.

TABLE I.

Line No.	Wave-length in μ	Frequency in cm^{-1}	$\Delta\nu$ cm^{-1}
0	3.3604	2975.8	
			3.5
1	3.3565	2979.3	
			3.0
2	3.3531	2982.3	
			3.4
3	3.3493	2985.7	
			2.7
4	3.3463	2988.4	
			3.4
5	3.3425	2991.8	
			3.1
6	3.3390	2994.9	
			2.5
7	3.3362	2997.4	
			3.1
8	3.3328	3000.5	
			3.2
9	3.3292	3003.7	
			3.3
10	3.3256	3007.0	
			2.8
11	3.3225	3009.8	
			3.1
12	3.3191	3012.9	
			3.6
13	3.3151	3016.5	
			4.0
14	3.3107	3020.5	
			4.4
15	3.3059	3024.0	
			3.2
16	3.3025	3028.1	
			3.3
17	3.2988	3031.4	
			5.2
18	3.2932	3036.6	
			4.6
19	3.2882	3041.2	
			4.8
20	3.2830	3046.0	
			3.9
21	3.2788	3049.9	

THE REGION AT 3.5μ

This region which was reported by Salant and West as a triplet was found to consist of what is believed to be three overlapping bands of two different kinds. The centers of these lie near 3.4μ, 3.5μ and 3.6μ. The two respectively at 3.4μ and 3.6μ appear similar in structure, showing P, Q and R branches of which the Q branch is relatively weak. The spacing between the lines in the P and R branches is about 3.4 cm^{-1} at 3.6μ and 3.5 cm^{-1} for that lying at 3.4μ.

The band whose center lies near 3.5μ is of entirely different structure. It consists of one very prominent line (much resembling a Q branch) near the center and groups of closely spaced lines nearly equally spaced on both sides

TABLE II.

Line No.	Wave-length in μ	Frequency in cm^{-1}	$\Delta\nu$ cm^{-1}
1	3.5628	2806.8	
			2.3
2	3.5598	2809.1	
			6.1
3	3.5522	2815.2	
			3.3
	3.5480	2818.5	
			4.0
	3.5430	2822.5	
			3.2
	3.5390	2825.7	
			2.0
	3.5364	2827.7	
			5.9
4	3.5291	2833.6	
			8.0
5	3.5192	2841.6	
			3.2
	3.5152	2844.8	
			3.1
	3.5113	2847.9	
			7.2
	3.5025	2855.1	
			10.1
6	3.4902	2865.2	
			30.2
7	3.4538	2895.4	
			1.6
	3.4518	2897.0	
			27.7
8	3.4191	2924.7	
			2.3
	3.4165	2927.0	
			5.6
9	3.4099	2932.6	
			2.7
	3.4068	2935.3	
			3.4
	3.4029	2938.7	
			2.5
	3.4000	2941.2	
			3.2
	3.3963	2944.4	
			1.7
	3.3943	2946.1	
			4.1
10	3.3896	2950.2	
			2.4
	3.3869	2952.6	

of it. Between these more prominent lines are other groups of rather closely spaced lines of lesser intensity. These can only imperfectly be resolved and form a more or less continuous background. On the low frequency side the overlapping with the band at 3.6μ is so bad that only the approximate loca-

tions of these more prominent lines can be distinguished, but on the high frequency side, while there too is some overlapping, one can distinguish the first three of these more intense line groups at least, as well as determine to a fair

TABLE III.

Line No.	Wave-length in μ	Frequency in cm^{-1}	$\Delta\nu$ cm^{-1}
3	3.5838	2790.3	
			3.9
2	3.5889	2786.4	
			2.8
1	3.5925	2783.6	
			4.0
0	3.5977	2779.6	
			4.3
−1	3.6032	2775.3	
			3.5
−2	3.6077	2771.8	
			3.2
−3	3.6119	2768.6	
			3.0
−4	3.6158	2765.6	
			2.9
−5	3.6198	2762.7	
			3.7
−6	3.6245	2759.0	
			2.9
−7	3.6283	2756.1	
			3.1
−8	3.6326	2752.8	
			4.6
−9	3.6388	2748.2	
			3.7
−10	3.6436	2744.5	
			3.0
−11	3.6477	2741.5	
			2.6
−12	3.6511	2738.9	
			2.5
−13	3.6545	2736.4	
			3.3
−14	3.6588	2733.1	
			3.1
−15	3.6629	2730.0	
			3.6
−16	3.6678	2726.4	
			3.8
−17	3.6730	2722.6	
			3.4
−18	3.6775	2719.2	

degree of approximation what are their intensities. The spacings between the more prominent groups are about 28 cm^{-1}. Fig. 1 shows the percentage absorption due to formaldehyde vapor in this region. It represents the points which have been repeated from several runs over this region. For convenience the original circle settings have been replaced by a wave-length scale in μ and a frequency scale in waves per centimeter. A compilation of the lines of the bands at 3.4μ, 3.5μ and 3.6μ is given in Tables I, II, and III respectively.

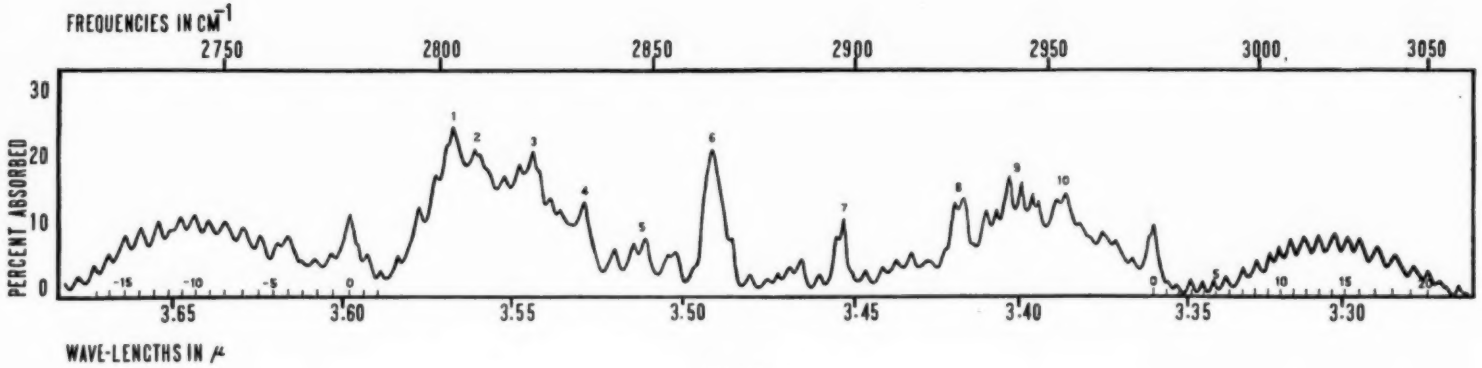
FREQUENCIES IN CM⁻¹
2750
2800
2850
2900
2950
3000
3050
PERCENT ABSORBED
30
20
10
0
3.65
3.60
3.55
3.50
3.45
3.40
3.35
3.30
WAVE-LENGTHS IN μ

Fig. 1.

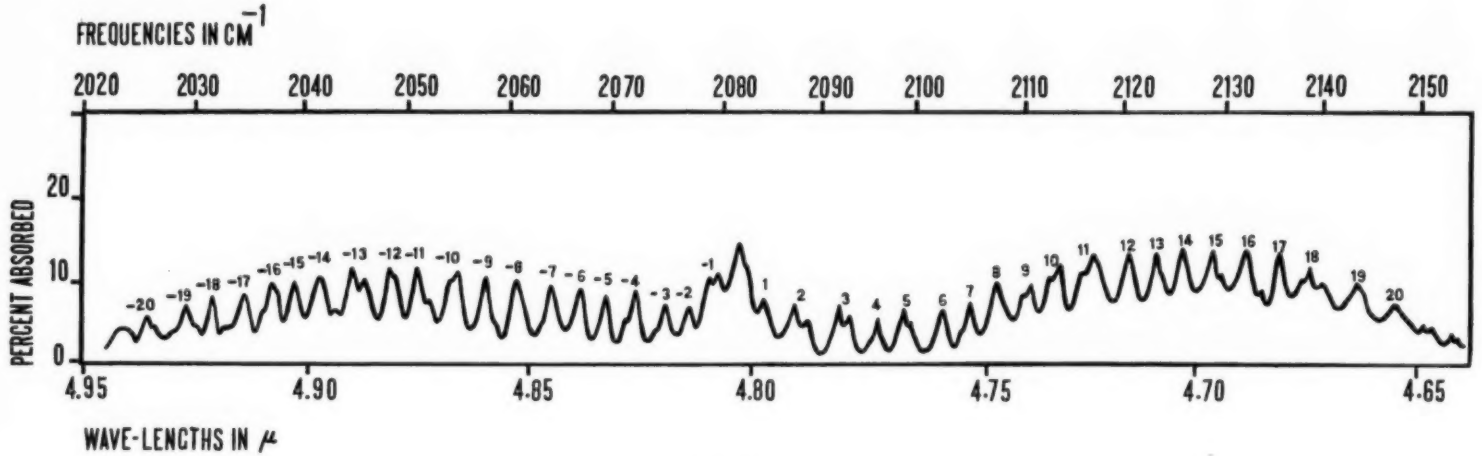
FREQUENCIES IN CM⁻¹
2020
2030
2040
2050
2060
2070
2080
2090
2100
2110
2120
2130
2140
2150
PERCENT ABSORBED
20
10
0
4.95
4.90
4.85
4.80
4.75
4.70
4.65
WAVE-LENGTHS IN μ

Fig. 2.

THE REGION AT 4.8μ

The absorption band at 4.8μ is similar to those at 3.4μ and 3.6μ, showing distinct P, Q, and R branches. As in the two earlier cases, the Q branch is relatively weak. Moreover it appears to be broadened unsymmetrically toward higher frequencies. The higher resolution in this region shows that what appeared as single lines in the P and R branches of the bands at 3.4μ and 3.6μ is actually several lines lying so close together that they cannot be resolved. In this region what appeared as single lines before occurs as quite broad lines with indications of a finer structure. The spacing between the maxima of these groups is somewhat less than in the other two bands of this kind, and is about 3.1 cm^{-1}. Fig. 2 shows the percentage absorption in the 4.8μ region. As before, it is a composite curve showing the characteristics which recur in all runs. As in Fig. 1, wave-length scales and frequency scales have been substituted for the original circle settings. In Table IV is given a compilation of the wave-lengths and frequencies of the observed lines of this band.

TABLE IV.

Line No.	Wave-length in μ	Frequency in cm^{-1}	$\Delta\nu$ cm^{-1}
−20	4.9364	2025.7	
			3.5
−19	4.9280	2029.2	
			2.4
−18	4.9222	2031.6	
			2.9
−17	4.9153	2034.5	
			2.7
−16	4.9088	2037.2	
			2.1
−15	4.9037	2039.3	
			2.4
−14	4.8980	2041.7	
			3.3
−13	4.8899	2045.0	
			3.4
−12	4.8818	2048.4	
			2.9
−11	4.8749	2051.3	
			3.2
−10	4.8674	2054.5	
			2.9
−9	4.8604	2057.4	
			3.0
−8	4.8535	2060.4	
			3.3
−7	4.8457	2063.7	
			2.8
−6	4.8392	2066.5	
			2.6
−5	4.8331	2069.1	
			2.5
−4	4.8272	2071.6	
			3.1
−3	4.8199	2074.7	
			2.2
−2	4.8149	2076.9	
			2.6
−1	4.8088	2079.5	

TABLE IV. (*Continued*).

Line No.	Wave-length in μ	Frequency in cm^{-1}	$\Delta\nu$ cm^{-1}
			2.5
0	4.8030	2082.0	
			2.4
1	4.7976	2084.4	
			3.6
2	4.7892	2088.0	
			4.0
3	4.7800	2092.0	
			3.6
4	4.7719	2095.6	
			2.8
5	4.7654	2098.4	
			3.5
6	4.7577	2101.9	
			2.9
7	4.7511	2104.8	
			2.7
8	4.7449	2107.5	
			2.9
9	4.7384	2110.4	
			3.0
10	4.7318	2113.4	
			3.0
11	4.7249	2116.4	
			4.0
12	4.7162	2120.4	
			3.0
13	4.7095	2123.4	
			2.5
14	4.7038	2125.9	
			3.3
15	4.6955	2129.2	
			3.4
16	4.6890	2132.6	
			3.2
17	4.6821	2135.8	
			3.5
18	4.6743	2139.3	
			4.6
19	4.6643	2143.9	
			4.4
20	4.6548	2148.3	

INTERPRETATION OF THE OBSERVED BANDS

While the rigorous interpretation of these bands is left for a later communication, it seems not wholly amiss here to point out some of the details of the observed bands which are characteristic of molecules of this kind.

The theory of the asymmetric rotator predicts that for a molecule like CH_2O, where the atoms are assumed to be coplanar, three different types of bands may occur.[4] These shall be designated, where the electric moment changes along the least axis of inertia, as type A, where the electric moment changes along the intermediate axis, as type B, and where the vibration is along the largest axis of inertia, as type C.[5] Types B and C will be very nearly

[4] H. A. Kramers and G. P. Ittmann, Zeits. f. Physik **53**, 553 (1929); S. C. Wang, Phys. Rev. **58**, 730 (1929); O. Klein, Zeits. f. Physik **58**, 125 (1929).

[5] H. H. Nielsen, Phys. Rev. **38**, 1432 (1931).

alike since the two larger moments of inertia are nearly equivalent, the relation being: $A_x = A_y + A_z$, where A_x, A_y, and A_z are chosen the three principal moments of inertia and where $A_x > A_y > A_z$. Of these three types, only two have been observed; namely, type A and either type B or type C. The type A bands arise when the electric moment vibrates along the least axis of inertia and consist of P, Q, and R branches. As we have seen, three such bands have been observed, namely, those at 3.4μ, 3.6μ, and 4.8μ. Whether the band occurring at 3.5μ is of type B or type C can only definitely be determined by an analysis of the normal modes of vibration or by a detailed study of the rotations of the molecule. The rather high frequency position of the band in the spectrum, however, indicates that the interatomic forces involved are relatively large. This suggests that the band observed is due to a vibration of CH_2 configuration along the intermediate axis of inertia, and hence it would be of type B. Moreover, a type C band would in our molecule arise from a vibration perpendicular to the plane of the molecule, and it seems likely that the forces that would here enter into play would be much smaller, and that consequently the band would lie at longer wave-lengths than those we were able to explore because of the increasing opacity of mica in this region.

Let us first consider the type A bands. In the case of the symmetric rotator, this type arises from transitions where $J \to J$, $K \to K$; $J \to J \pm 1$, $K \to K$, the first giving the Q branch and the other the P and R branches. In the nearly linear slightly asymmetric rotator the levels resemble those of the nearly linear symmetric rotator a great deal except that each level save one ($K = 0$) is split up into two, say K' and K''.* Complete discussions of the transition rules for the asymmetric rotator have been given by several writers,[6] but the ones of importance to us may be given as follows: The transition rule in our case corresponding to that above for the symmetric case becomes $J \to J$ and $K' \to K''$ or $K'' \to K'$. Consequently, no sharp Q branch can be expected but, as is observed, one that is somewhat broadened. The other transition rule from above becomes $J \to J \pm 1$, $K' \to K'$ or $K'' \to K''$. This gives rise moreover to a fine structure of each of the lines in P and R branches since the splitting up of the levels is different for different values of J. This fine structure is here observed as a broadening of each line in the P and R branches with occasional evidence of complex structure. It is well-known that this type of vibration in the linear molecule gives a band with a missing line at the center. It was shown by Bennett and Meyer[7] in the case of the methyl-halides that as the largest moment of inertia increased from one halide to another while the small one remained approximately the same (i.e., as this series

* It has seemed in the case of asymmetric rotators of only very slight asymmetry to retain a nomenclature analogous to that used in symmetric rotators would be an advantage. Hence the K used for the symmetric case has been replaced by K' and K'' instead of using the τ's introduced by Dennison. This may be done because the actual splitting up of the symmetric levels is small and because the transitions permitted in such rotators which may not occur in the symmetric case occur with only very small intensities.

[6] H. A. Kramers and G. P. Ittmann, Zeits. f. Physik **60**, 663 (1930); D. M. Dennison, Rev. Mod. Phys. **3**, 280 (1931).

[7] W. H. Bennett and C. F. Meyer, Phys. Rev. **32**, 888 (1928).

of molecules effectively more and more approached the linear case) the Q branch diminished in intensity. In the case of formaldehyde which does not depart radically from the linear model we might expect to find exactly this same effect, and this is just one of the details which we have observed at 3.4μ, 3.6μ and 4.8μ.

Type B bands occur in the symmetric rotator when transitions of the kind: $J\rightarrow J$, $K\rightarrow K\pm 1$; $J\rightarrow J\pm 1$, $K\rightarrow K\pm 1$ take place. An analogous set of rules may be formulated for the asymmetric rotator and in our case they may be summarized so: $J\rightarrow J$, $K'\rightarrow K'\pm 1$; $K''\rightarrow K''\pm 1$; $J\rightarrow J\pm 1$, $K'\rightarrow K''\pm 1$, $K''\rightarrow K'\pm 1$. In the symmetric top the envelope of this kind of band shows only one maximum, each line being made up of several exactly superposed lines arising from several quantum transitions. Here one would not expect them exactly to coincide and consequently a rather complex structure would result. The tendency would be to give a rather intense line group where before there occurred a single line, and now with weaker lines in between. This is precisely what one observes at 3.5μ. A further complication which is encountered is the existence of the identical hydrogen atoms in the molecule. Under these circumstances the levels must be classified as symmetric and antisymmetric, of which the latter are populated three times as densely as the others. In the case of our molecule this would lead to an unsymmetry of the appearance of the lines about the center, a detail which is not exceedingly apparent here because of the strong overlapping. It is, however, clearly evident between the extremely strong line at the center and its mate which is only roughly one third as intense. It is another observed fact that the spacing of the intense line groups of the type B band is about eight times that in the type A bands. This too is in agreement with theory, for as is well-known, as one approaches the linear model the spacings of this type of band becomes ever larger with respect to the spacing of the other type until finally in the limiting case, this type of band disappears completely—the lines being separated by infinite spacings.

Summarizing, we may say that an investigation of the formaldehyde spectrum in the infrared has shown it to consist of at least two different kinds of bands with different spacings. The one type, type A, shows P, Q, and R branches of which the Q branch is relatively weak and the spacings between lines in the P and R branches are quite fine; type B consists only of one branch with a maximum at the center and with spacings between the line groups about eight times as great as in Type A. Finally a qualitative discussion has been given accounting for the more obvious details of this spectrum on the basis of the theory of an asymmetric rotator model not departing radically from the linear type.

The writers wish to express their appreciation to Dr. J. D. Hardy who very kindly presented them with a vacuum thermopile of his own construction for use in this investigation. Also the kind cooperation of Professor Alpheus W. Smith in making available departmental funds for the purchase of gratings and other equipment is acknowledged with gratitude.

THE SURFACE-ELECTRONS

By J. E. Nyrop
Copenhagen

(Received November 19, 1931)

Abstract

The theory regarding the degenerate electronic gas inside an electron-conductor producing an electronic gas, i.e., the surface-electrons, covering the surface of the conductor is applied to the ordinary and the selective photo-effect and the evaporation from heated metals. Further, it is explained how the adsorption caused by metallic surfaces and the catalytic effect produced by them can be calculated when surface-electrons are considered and that the potential barrier which accounts for the work function also can be estimated.

ACCORDING to Sommerfeld[1] the "free" electrons of a metal can be regarded as a degenerate gas capable of expanding. Electrons will therefore escape through the surface of a metal, or other conductor able to conduct electricity wholly or partly by means of "free" electrons, but, as the conductor is surrounded by a potential barrier (which barrier is partly built up of a field produced by electrons which have crossed the surface), the electrons cannot leave the zone close to the surface. This barrier, P, is greater than a potential difference which would retard the electrons having the maximum kinetic energy, E, and the work of emergence of an electron (the "work function") is $W=P-E$. The conditions close to the surface can therefore be described in terms of the maximum kinetic energy of the "free" electrons and the height of the barrier. The electrons in the atmosphere thus produced close to the surface shall be termed the "surface-electrons". In accordance with the distribution law of Fermi the number of "free" electrons with kinetic energies between ϵ and $\epsilon+d\epsilon$ is

$$n(\epsilon)d\epsilon = \frac{4\pi(2m)^{3/2}}{h^3} \frac{\epsilon^{1/2}d\epsilon}{1+e^{(\epsilon-E)/kT}} \tag{1}$$

where h is Planck's constant, m the mass of an electron and k the Boltzmann gas constant. When $\epsilon \ll E$ we have approximately

$$n(\epsilon)d\epsilon = \frac{4\pi(2m)^{3/2}}{h^3} \epsilon^{1/2}d\epsilon$$

and when $\epsilon \gg E$

$$n(\epsilon)d\epsilon = \frac{4\pi(2m)^{3/2}}{h^3} e^{(E-\epsilon)/kT}.$$

[1] Die Naturwissenschaften **15**, 825 (1927) and Zeits. f. Physik **47**, 1 (1928).

As only few electrons have energies above E this energy is termed the "maximum" kinetic energy of the "free" electrons, and, Sommerfeld showed that

$$E = \frac{h^2}{8m}\left(\frac{3n}{\pi}\right)^{2/3}$$

or if E is in volts,

$$= 26a^{-2/3}n_i^{2/3},$$

where a is the volume occupied by a gram atom of the metal, n the number of "free" electrons per cc and n_i the number of "free" electrons per atom. If the metals are arranged in accordance with the maximum kinetic energy of their "free" electrons the following succession is obtained: Mn, W, Ni, Os, Fe, Cr, Pd, Co, Pt, Zn, Cu, C, Al, Hg, Mg, Pb, Ca, Li, Na, K. On the basis of Eq. (2) the electrons of manganese have a maximum kinetic energy of 19.7 volt-electrons, nickel 18.8, copper 14.8, aluminum 11.7 and potassium 2.1. (It must in this connection be remembered that there is a considerable uncertainty as to the proper values of n_i to be used for the different metals. The values of E mentioned have been computed on the assumption that the electronic "shell" of the ion left when electrons are set free is stable.)

If molecules of a gas or liquid in which a metal is immersed come in among surface-electrons having energy high enough to ionize them, ionization takes place. On account of the image force, ions some distance from the surface will be attracted, but quite close to the surface the space charge force will attract negative ions and repel positive. The positive ions will therefore be kept moving in a zone a certain small distance from the boundary. This zone shall be termed the "positive zone". The kinetic energy of positive ions kept in the positive zone will increase with the temperature. Some of the ions may thereby acquire energy high enough to overcome the potential barrier and thus be enabled to leave the zone as ions or, by capturing an electron, as molecules in the normal or in a higher energy state. The ions of the positive zone will alternately be neutralized, by capturing electrons, and reionized in collision with rapidly moving electrons. The distribution of velocities among the molecules (ions) kept, i.e., adsorbed, in the positive zone will be Maxwellian with regard to movements in the two dimensions parallel to the surface. In the third dimension also the distribution will tend to be Maxwellian. The distribution of velocities among the surface-electrons will also tend to be Maxwellian though the distribution among the electrons coming from the degenerate electronic gas of the metal is different, but it will approach the Maxwell distribution the further the electrons are from the surface.

The idea that the surface of a metal is covered by an electronic gas is not new. Oliphant and Moon[2] show, for instance, that the existence of the gas plays an important rôle in the neutralization of ions brought into contact with the surface of a metal and that the gas accounts for a simultaneous secondary ejection of electrons. In this paper it will be shown that the experiments on the photo-effect do not contradict the existence of the surface-electrons and

[2] Proc. Roy. Soc. **127**, 392 (1930).

that the adsorption and catalytic effect caused by metallic surfaces can be calculated when surface-electrons are taken into consideration. The following methods of treatment used in explaining the photo-electric effects, adsorption and catalysis are new.

The number of electrons inside the conductor moving with a kinetic energy near the maximum is

$$\frac{4\pi m}{h^2}\left(\frac{3n}{\pi}\right)^{1/3} d\epsilon,$$

and the number of electrons passing the surface with this energy is

$$n_0' = \frac{6\pi}{13h}\left(\frac{3n}{\pi}\right)^{2/3} d\epsilon. \tag{3}$$

Such electrons are able to move into a zone such distance from the surface that the potential energy of the electrons become equal to the mentioned maximum kinetic energy. As the electrons of the zone have altogether lost their original velocity their kinetic energy will be determined by the temperature. The number of electrons passing one square cm placed inside the zone becomes thus approximately proportional to $n_1(3kT/m)^{1/2}$ when n_1 is the number of electrons per cc of the zone, and at equilibrium

$$n_1 = \frac{\pi}{h}\left(\frac{3n}{\pi}\right)^{2/3}(3mkT)^{1/2}. \tag{4}$$

Among the electrons some will gain a velocity above the average enabling them to cross the remaining part of the barrier. The number able to do so will be

$$N = n_1\left(\frac{kT}{2m}\right)^{1/2} e^{-W/kT} = 3.8\frac{k}{h}\left(\frac{3n}{\pi}\right)^{2/3} Te^{-W/kT}. \tag{5}$$

Electrons evaporating from the surface-electrons of a hot metal (tungsten) give thus a saturation current, when the work function is 4.5 volts, of

$$J = 8.6 \times 10^6 Te^{-5.2+10^4/T} \text{ amp./cm}^2. \tag{6}$$

This equation resembles that of Richardson-Dushman. Sommerfeld and Houston and also Nordheim show that the current is proportional to T^2 when surface-electrons are not considered. Other calculations give the old $T^{1/2}$ law. In the calculations of Sommerfeld it is assumed that all electrons with a velocity larger than $(2P/m)^{1/2}$ are ejected and that the distribution of velocities is Fermi's. The measured work of emergence, W, is thus only a part of the true work of emergence of the ejected electrons. Considering the existence of surface-electrons W becomes the true work of emergence. If a field of the strength F is applied the number of electrons which can be pulled out of the metal by the field becomes, when surface-electrons are considered,

$$N' = 3.8\frac{k}{h}\left(\frac{3n}{\pi}\right)^{3/2} Te^{-(W-cF)/kT}, \tag{5'}$$

where c is a constant. Millikan has shown proportionality to $e^{-\alpha/T+\beta F}$ where α and β are constants. As in these experiments cF is small compared with W, Eq. (5′) agrees with experiment.

The number of electrons which in accordance with Eq. (1) have energies high enough to cross the total barrier is approximately

$$N_0 = \frac{3.7\pi mkT}{h^3} Pe^{-W/kT}. \tag{7}$$

At equilibrium $N = N_0$ and we get by use of (2)

$$P = 1.5E = 3W. \tag{8}$$

W can thus be calculated:

	W	W_{ex}
K	1.05	0.5–1.4
Na	1.55	1.8
Ca	2.50	2.5
Pb	3.0–4.6	3.9
Mg	3.65	3.2.

W_{ex} is the value determinated by experiments. As measurements of the work function are subject to considerable error there is good agreement between the theoretical values and the measured. Metals with a higher valency than those listed have a lower work function than that determinated by the use of Eq. (8). This is partly due to the approximate estimation of the density of the surface-electrons. Eq. (4) shows that the density increases with n_i (since n is proportional to n_i). With an increased density the outermost layers contribute a larger portion of the emission current and, since the work of emergence is lower than W for the outer electrons, metals with a high valency will therefore show a lower work function than that determined from Eq. (8).

Oxides consist of a metallic space lattice and one of oxygen. The oxygen lattice will diminish the path traversed by a free electron between two successive collisions with atoms. The low conductivity of oxides is due to such decrease in the free path of the electrons. Using Eqs. (2) and (8) W can be calculated for oxides:

	W	W_{ex}
CuO	2.08	1.8
BaO	1.93	1.7–2.0
SrO	2.24	—
CaO	2.53	2.52
MgO	3.30	3.30
Fe_2O_3	3.4	3.8
Al_2O_3	3.8	3.9
NiO	4.3	4.2.

Millikan has shown that the maximum retarding potential, W_m, for electrons emitted from a negatively charged metal when its surface is illuminated by ultraviolet light, increases linearly with the frequency, γ, of the radiation. The maximum kinetic energy of the emitted electrons is given by the Einstein equation,

$$\tfrac{1}{2}mv_m^2 = h\nu - h\nu_0 = W_{me}, \tag{9}$$

where e is the charge of an electron and v_m is the maximum velocity of the emitted electrons. ν_0 is the minimum frequency known as the "photo-electric threshold" and, if W_0 is the work function, then $h\nu_0$ is equal to $W_0 e$. For larger frequencies $h\nu_0$ becomes negligibly small compared with $h\nu$ and we get $\frac{1}{2}mv_m^2 = h\nu$ when the surface is illuminated by x-rays. The normal photo-electric current produced when the surface is illuminated by light increases with the intensity of the radiation and the number of electrons emitted per quantum absorbed increases with the frequency of the radiation. Distinct from such normal photo-effect is known the selective effect showing a maximum on the normal near frequencies corresponding with the work function.

When the surface-electrons are illuminated collisions between photons and electrons transfer energy from the radiation to the surface-electrons and the temperature of the surface-electrons will increase. In accordance with Compton, the shift in wave-length produced in the radiation on collision with an electron is

$$\Delta\lambda = \frac{h}{mc}(1 - \cos\theta),$$

where θ is the angle at which the photon is scattered. A quantum of frequency γ can therefore not transfer to an electron an energy greater than

$$\frac{2h^2\nu^2}{mc^2} = 0.95 \times 10^{-25}\lambda^{-2}, \tag{10}$$

for the use as kinetic energy. Approximately $2\mu h\nu/mc^2 = 0.48 \times 10^{-9}\alpha\lambda^{-1}$ of the initial energy of the photon is transferred to the electron, where α is a constant less than one. The average energy of an atom of a monatomic gas at the temperature T is $2 \times 10^{-16}\ T$. If therefore every electron of an electronic gas at a temperature T collides with q photons the temperature of the outermost layer of the surface-electrons will be approximately increased by

$$T_p - T = 4.7 \times 10^{-10}\alpha\lambda^{-2}q = 8 \times 10^{-5}\alpha(h\nu)\nu q. \tag{11}$$

In collision with ultraviolet light such increase in temperature is about 2°C when $q = 1$, and in collision with x-rays of the order of 10^6 degrees. Using Eq. (6) the photoelectric current becomes

$$J = 8.6 \times 10^6(8 \times 10^{-5}\alpha(h\nu)\nu q + T)e^{-5\cdot 2+10^4/8+10^{-5}\alpha h\nu^2 q+T}. \tag{12}$$

A current of 5×10^{-4} amp./cm²/cal. has been measured by Pohl and Pringsheim when the energy of radiation is of the order of 5×10^{-2} cal./sec. cm². This means that the temperature of the outer part of the surface-electrons is increased to about 2,000°C during the radiation. Variation in T is therefore of no practical importance as long as T is below the temperatures at which the surface emits visible radiation. That the photo-effect shows such independence of the temperature has been demonstrated by experiments. The photoelectric current is therefore as a first approximation

$$J = 7 \times 10^2\alpha(h\nu)\nu q e^{-6\cdot 5+10^5/\alpha(h\nu)\nu q}\ \text{Amp.}, \tag{13}$$

when $W=4.5$ volts. It must in this connection be borne in mind that the q of Eq. (11) is the number of photons with a certain frequency colliding with one electron, whereas q of Eq. (13) becomes the number of photons colliding with one electron after having collided with others, the frequency is therefore decreased so that J becomes somewhat too large.

Rayleigh has suggested that an electron may conceivably absorb wave energy from a region of the order of magnitude of the square of a wave-length of the incident light. q is hence proportional to the square of the wave-length. The photoelectric current would in this case be independent of the frequency, but as experiments show that the current per quantum absorbed increases with the frequency, q must be another function of the wave-length than the one suggested. That the general exponential, $e^{-W/f(T,\nu)}$, is part of the expression is in accordance with some experiments of Lawrence and Linford[3] which show a change of 5 percent in the lowest frequency producing a measurable photo-current when the work function is altered by an applied field equal to about 0.1 percent of that which gives rise to the work function. That experiments show a linear relation between photo-current and energy is due to a disturbance in the equilibrium which determines the density of the outermost part of the surface-electrons, since a conveyance of energy to this zone increases the photo-current but also the current in the direction of the surface. The density of the outermost part hence decreases, which will cause a diminution of the photo-current and an increase in the average work function for the ejected electrons. The calculations leading to Eq. (8) also show an increase proportional to $W=(1.5\ Tf/T-1)\ E$, where Tf is the increased temperature of the outermost zone. Eq. (13) is therefore consistent with the linear relation measured. In the above mentioned example about 2×10^{17} photons pass through one square centimeter of the surface of the surface-electrons. One electron near the surface will thus collide with $2\times10^{17}\ A$ photons, where A is the cross-section of the region from which an electron can extract wave-energy. The photoelectric current produced demands about 2,000 collisions which means that A for the wave-length in question is approximately 10^{-14} square centimeter.

The selective effect shows a resonance-maximum from which the effect falls rapidly with increasing or decreasing wave-lengths, the current being generally insignificant 100 to 150$\mu\mu$ from the maximum. Such selective effect may occur if molecules or atoms brought in among the surface-electrons are ionized by photons, since the neutralization following the ionization will, in a collision of the second kind (the neutralization takes place in a dense electronic gas), produce electrons having a kinetic energy equal to the ionization energy, and the effect will occur if the ionization energy is larger than the work of emergence at the place of neutralization. It is therefore natural to expect that the selective effect is produced in a similar manner when evaporation produces atoms of the metal moving among the surface-electrons. Atoms thus set free will alternately be neutralized and ionized by the surface-electrons as long as the atoms are close to the surface, but when they come out

[3] Phys. Rev. 36, 482 (1930).

in the outer part of the surface-electrons the electrons will not have energy high enough to ionize them. Ionization in the outer part will therefore only occur in case certain energetic photons collide with the atoms. A neutralization of ions formed in collisions with photons will, through a collision of the second kind, produce electrons with a kinetic energy equal to the ionization energy and a probability of electrons escaping through the outer part of the potential barrier is produced when the energy of ionization is larger than the work of emergence. The selective effect is thus produced. A similar effect can also be produced by adsorbed atoms or molecules. Potassium, which is ionized in the gas phase by 4.3 volt-electrons, shows a photoelectric maximum at frequencies corresponding to 3 volts. (The difference is due to a decrease in the energy of ionization produced by the field close to the surface.) Sodium is ionized by 5.1 volt-electrons, and has a maximum at 3.5. The work function measured by the evaporation of electrons from potassium is between 0.5 and 1.4 volts and for sodium 1.8 so that the maximum frequency corresponds to a potential larger than the work function. This is in accordance with the above mentioned. When the atoms set free are ionized in collision with photons, electrons with a kinetic energy $\frac{1}{2}mv^2 = h\nu - Ve$ are produced when V is the ionization potential. When the kinetic energy is larger than the work function some of the electrons produced will escape through the outer part of the potential barrier with a kinetic energy $\frac{1}{2}mv^2 - We$, where W is the work function at the place of ionization.

If a metallic surface is brought in among molecules capable of being ionized by collision with electrons having energies larger than Q, the molecules will be ionized in case the maximum kinetic energy E of the surface-electrons is larger than Q. The number of electrons crossing the surface with energies above Q will in accordance with (1) be

$$N = 1.5mh^{-3}(E^2 - Q^2). \tag{14}$$

By this equation we are able to calculate the adsorption taking place at the surface of metals or other conductors since it is the ionized molecules which are attracted and thereby adsorbed. An ion will on the average after a certain time Δt_0 be neutralized and such neutralized ion will, after the expiration of a time c'/N, have the possibility of again being ionized. A molecule will only be able to leave the zone close to the surface in case it gains—during the time c'/N—such velocity away from the surface that it is outside the zone before the expiration of the time. The molecules are thereby kept a time $y'(\Delta t' + c'/N)$ close to the surface when y' is the number of ionizations a molecule undergoes between the time when it enters the zone and leaves it. If the number of molecules per cc outside the surface zone is n, the number inside will be

$$n' = \frac{y'(\Delta t' + c'/N)}{\Delta t},$$

where Δt is the average time the molecule would stay in the zone if no ionization took place. The number of molecules colliding with a molecule kept in

the zone having a velocity and a direction such that the colliding molecule as well as the molecule in the zone can leave the surface in case the molecules are neutral is

$$knr^2vc^{-k'N^xM^y/T}$$

where T is the temperature, M the molecular weight, r the radius of the molecules and v the velocity with which they are moving into the zone. k, k', x and y are constants. The part of such collisions which take place with a neutralized ion is

$$\frac{c'/N}{c'/N + \Delta t'}$$

and we get

$$R = CA \frac{1 + \Delta t'(N/c')}{r^2} e^{k'N^xM^y/T}, \tag{16}$$

where A is the accessible area of the surface and R the adsorption.

In case the number of collisions between electrons and molecules is great compared with the number of mutual collisions amongst the molecules an electronic pressure (like the buoyancy) will try to expel the adsorbed molecules from the surface zone. In this case we get

$$R = C_0A \frac{S_ip}{S_M(MT)^{1/2}} e^{\phi(N,M,1/S_M)}, \tag{17}$$

where S_i is the area of the molecules against the electrons able to ionize them and S_M the average area against all the electrons. By combining (16) and (17) we have at constant temperature

$$R = \frac{ap}{b + p}. \tag{18}$$

(16) and (18) show that at high pressure the adsorption is independent of the pressure, viz., there is a certain saturation pressure.

Gauger and Taylor have shown that a surface of nickel is saturated with hydrogen at a pressure of 40 mm when the temperature is 298°K and that a 19-fold increase in pressure does not add to the adsorption. At 578°K the saturation pressure is 250 mm and the adsorption is 62 percent of that at 298°. The adsorption of hydrogen, carbon dioxide and carbon monoxide shows similar adsorption maxima on copper and a calculation gives $x = 0.38$. From the adsorption of ethylene, hydrogen and carbon monoxide on copper and on copper having adsorbed mercury, it can be calculated that $y = 0.6$.

The great heat evolved when molecules having electron-affinity are adsorbed can be explained by the fall of the ions through part of the potential barrier, whereby the ions gain kinetic energy which produces the heat. The first amount of oxygen adsorbed on a surface of carbon evolves an adsorption heat of 220,000 calories, on tungsten the evolved heat is 320,000 calories.

The difference in adsorption heat is equal to 4.3 volt-electrons. In accordance with Eq. (2) the difference in the maximum kinetic energy of the electrons at the two surfaces is 5.7 volts. The increase in the potential barrier of tungsten over that of carbon can thus account for the great increase in the heat of adsorption. That the heat evolved when molecules only able to produce positive ions are adsorbed is small, confirm the existence of the positive zone. Experiments of Taylor and Kistiakowsky show that carbon monoxide (ionized by 15 volts in the gas phase and presumably by 14 − 14.5 volts near the surface of a metal) adsorbed on copper (having surface-electrons with a maximum kinetic energy of 14.8 volt-electrons) evolves a heat of adsorption which at the beginning of the adsorption is 26,000 calories but decreases when the adsorption is increased until a minimum whereafter it increases to a maximum. When hydrogen (ionized in the gas phase by 15.3 volt-electrons and presumably by 14.3 − 14.8 volt-electrons near the surface) is adsorbed on copper the heat of adsorption increases from zero and passes through a maximum. This means that carbon monoxide is ionized a small distance off the positive zone, but when the adsorption is increased the oxide will have to collide with an increasing number of electrons having energy high enough to ionize it. The ionization zone will thus come closer to the positive zone and the heat of adsorption will decrease. However, as the charge of the positive zone will increase the distance between the positive zone and the ionization zone will increase by further increase in adsorption, the increase in the adsorption heat is thus produced. Hydrogen having a higher energy of ionization than carbon monoxide is first ionized in the positive zone whereby heat cannot be evolved before adsorption causes an increase in the charge of the zone.

The intermittent ionization producing the strong adsorption on metallic surfaces attempts to keep the ions in the positive zone. Ionization, however, does not influence the movements of molecules (ions) parallel to the surface. The adsorbed molecules may therefore act as a two dimensional gas. In this gas, which is partly ionized, collision between the molecules and ions may produce reactions, just like collision in ordinary gases. If two hydrogen molecules collide an energy equal to 4.4 volt-electrons must be available in case dissociation shall occur, but in case two hydrogen ions collide only 2.6 volt-electrons are required. Part of the energy used in the ionization is therefore reducing the dissociation energy, i.e., the ability of the molecules to enter into reaction is increased by ionization. If therefore a surface of an electron-conductor adsorbs hydrogen as ions the apparent activation energy of the hydrogen dissociation taking place at the surface is lowered. This is an example of the catalytic activity of metallic surfaces. The lowering of the energy of dissociation caused by ionization is due to a decrease in the energy of separation. When a molecule A with an energy of ionization I_A collides with a molecule B having an energy I_B and A is ionized, B can be ionized in case $I_A \geqq I_B$. In such collision there will be a state where it cannot be said that A nor B are ionized and, as the collision takes place in the dense electronic gas covering the surface, we have a complex of the molecules A and B and a mutual electron, a complex disposing of an energy I_A which is available for a

rearrangement of the atoms inside the complex. The apparent heat of activation of a reaction between A and B is thus lowered. A surface hence causes further chemical reactions when the surface-electrons are able to ionize those molecules most difficult to be ionized among the reacting molecules, viz., the surface acts as a catalyst. As the number of collisions increases by adsorption, the effect caused by a catalytic surface will further be due to an increase in collisions with ions.

The velocity by which the molecules come into contact with a catalyst is proportional to $p/\sqrt{(MT)^{1/2}}$, but as the number of collisions able to cause the reaction is proportional to $e^{-A'/T}$, where A' is a constant, a certain high temperature is thus demanded. To counteract the influence of the necessary increase in temperature on the velocity by which the reacting molecules come into contact with the surface the pressure will have to be above a certain value. In this way the high pressure processes employing catalysts can be explained. The synthetic ammonia process demands for this reason a high pressure. The catalyst which shall be used in the synthesis must be able to ionize nitrogen. Only catalysts of Os, Mo, Fe, Ni, Mn and W having a high maximum kinetic energy of their surface-electrons are therefore usable. Experiments have confirmed this. A nickel catalyst produces methane from carbon monoxide and hydrogen, one containing zinc produces methanol and one of copper formaldelhyde. This is due to the diminishing hydrogen adsorption in relation to carbon monoxide when the energy of the surface-electrons decreases as hydrogen has a higher ionization energy and a lower molecular weight than the monoxide. The activation energy of the para-ortho hydrogen conversion is equal to about 2.5 volt-electrons on a catalyst of platinum black. As this is the same as the energy of dissociation of hydrogen ions it indicates, as the heat of conversion is only 0.015 volt-electrons, that the conversion takes place in collision with hydrogen ions adsorbed on the platinum. The necessary possibility for a rearrangement is thus produced. All metals able to be rendered "passive" have surface-electrons with a maximum kinetic energy above 15.1 volt-electrons, or above the ionization energy of oxygen, confirming that "passivity" is due to adsorption of oxygen. The values of E determinating by Eq. (2) are also confirmed by several other processes and hence the succession of the metals mentioned above.

The experiments of Davisson and Germer have shown that for relatively high velocities of electrons the electrons show the "wave-length" which is assumed by the wave mechanics when the electrons are reflected from the surface of a nickel crystal, but only approximate agreement with the wave mechanics is observed for lower speeds. As the surface-electrons will interact with slow moving electrons reflected from the surface this approximate agreement is understandable. The conclusion from the wave mechanics that an electron may have a probability of occurring in a region in which the potential energy is greater than the total energy has been applied on the pulling out of electrons of metals by strong electric fields and the deduction arrived at seems to be in accordance with experiments. This probability of escape is explained above (Eq. (5′)) by the existence of the surface-electrons.

TABLES OF THE IONIZATION IN THE UPPER ATMOSPHERE*

By E. O. Hulburt
Naval Research Laboratory

(Received February 5, 1932)

Abstract

The present paper continues the work on the ionization of the upper atmosphere due to the ultraviolet light of the sun, developed in a series of papers in this Journal, and takes into account as far as possible the entire meteorology of the upper atmosphere and the effects of recombination, temperature diffusion and the motions of the ions and electrons in the gravitational, electric and magnetic fields of the earth. Tables are presented of the ion and electron densities over the earth. The ionization at night is worked out more completely than was done previously. After sunset as a result of temperature diffusion and electric-magnetic drift, the ionized region separates into two banks, one with a maximum of ionization at about 110 km and one with a maximum at about 140 km. Quantitative agreement is found with the skip distances and other phenomena of wireless waves and with various facts of terrestrial magnetism.

I. Introduction

THE ionization of the upper atmosphere of the earth attributable to the ultraviolet light of the sun was worked out in a series of papers,[1] and was shown to be in agreement with that inferred from various facts of terrestrial magnetism and of the propagation of radio waves. In calculating the ionization the entire physical meteorology of the high atmosphere was taken into account as far as possible as well as the laws of gaseous diffusion, ionic recombination, electronic attachment, the motions of the ions and electrons under the actions of the gravitational, magnetic and electric fields, etc. The tables of the ionization which were obtained were not published although glimpses of them were given.

During the past year the tables have been worked over completely with more rigor as to certain details and are presented in the following pages. No new physical ideas have been added to those which have already been used.[1] In one instance an improvement has been effected (the necessity for this was outlined in reference 1, section 21), namely, the combined action of temperature diffusion and electric-magnetic drift of the ionization banks at night has been worked out more carefully with the result that for the first time a fairly satisfactory quantitative agreement is found with the night-time radio wave phenomena.

The notation, definitions, assumptions, etc., of this paper are the same as those of reference 1, and to avoid continual restatement of physical ideas and equations we shall refer repeatedly to reference 1.

* Published with the permission of the Navy Department.

[1] Hulburt, Phys. Rev. **34**, 1167 (1929); **35**, 240 (1930); and references therein.

II. Temperatures and Molecular Densities in the High Atmosphere

It is assumed that the geographic and magnetic axes of the earth coincide and are perpendicular to the plane of the ecliptic. Thus our results hold approximately for equinoxial conditions but become untrustworthy for solstice conditions at high latitudes; the tables therefore cease at latitudes above 60°. It is assumed that the temperature T of the atmosphere in levels above 50 km is 400°K, at the subsolar point of the earth, is 220°K at night, and at any point of the daylight hemisphere is given by

$$T = 220 + 180 \cos c, \tag{1}$$

where c is the angular distance to the subsolar point. If θ and ψ denote, respectively, the latitude and longitude, or hour angle, measured from equinoxial high noon at the equator, then

$$\cos c = \cos\theta \cos\psi. \tag{2}$$

Values of T calculated from (1) and (2) are given in the third column of Table I. The assumption that T in the higher levels is constant with altitude is a simplifying approximation made in lack of more definite knowledge. It prob-

Table 1. *Values of various quantities for the daylight latitudes and longitudes.*

	θ	T	z_c	D	i	v	E
noon	0°	400°K	150 km	1.88×10^{16}	43.8×10^{-4}	785	232
noon	10°	397	150	1.93	41.0	680	221
noon	20°	389	149	1.87	30.5	632	265
noon	30°	376	147	1.75	20.3	566	335
noon	40°	358	145	1.60	12.8	484	416
noon	50°	336	137	1.37	7.4	349	440
noon	60°	310	127	1.02	3.7	330	628
noon	70°	282	119	0.76	1.7	250	830
noon	80°	251	111	0.45	0.5	172	1150
noon	90°	220	104	—	—	—	—
10 A.M. or 2 P.M.	0°	376	150	1.52	36.5	841	249
10 A.M. or 2 P.M.	40°	340	136	1.32	10.5	510	438
10 A.M. or 2 P.M.	60°	299	124	0.87	3.1	402	777
8 A.M. or 4 P.M.	0°	310	132	0.68	15.8	1406	413
8 A.M. or 4 P.M.	40°	285	122	0.62	5.0	910	740
8 A.M. or 4 P.M.	60°	267	115	0.45	1.9	445	855

ably is not exactly true, for on general grounds one would expect T to vary to some extent with the altitude and the variance to be a function of θ and ψ. In the present paper we have taken T to be 400° at high noon, in reference 1 we used 500°. And, although Maris' calculations[2] show that T is considerably higher during the day than in the night, there is no way of knowing at the present time which value is more nearly correct. However, none of our conclusions depend critically on the exact value assumed for T at high noon.

The molecular density n in the high atmosphere at a height z cm above sea level is given by

$$n = n_0\epsilon^{-pz},$$

[2] Maris, Terr. Mag. and Atmos. Elec. **33**, 233 (1928); **34**, 45 (1929).

where

$$p = mg/kT, \tag{3}$$

where g is the acceleration of gravity, k is the Boltzmann constant and m is the mass of the average air molecule. With $T = 360°$, 250°, 230° and 220°, respectively, (3) gives to a close approximation Maris' molecular density curves[2] for summer day, winter day, summer night and winter night conditions in temperate latitudes. From (1) and (3) the n, z curves were drawn for all points on the earth; they are not reproduced here. The curves were used throughout the ionization calculations with two insignificant exceptions, namely: for all temperatures above 360° the n, z curve for 360° was used, this being Maris' summer day curve; for tropical nights the n, z curve for 230° was used, this being Maris' summer night curve.

3. The Ions During the Day

It is probable that the ions at the greater heights are mainly atomic ions and that the proportion of molecular ions increases with decreasing height. This possible change in the mass of the average ion with height was not recognized in the present calculations, but at all heights the average ion was assumed to have a mass of 3.83×10^{-23} grams which is the average of the mass of a nitrogen atomic ion and an oxygen molecular ion. The average ion was assumed to be singly charged. The critical level z_c was calculated as in reference 1, section 7. z_c is the level where the free path of the ion is about 1/5 of the radius of magnetic gyration and is the boundary between the long and the short free path ions. Above z_c the ionized regions are diamagnetic and the ions drift under the magnetic, electric and gravitational fields. Below z_c the ions give rise to the ordinary electrical conductivity of an ionized gas. z_c is a function of θ and ψ, values of z_c are given in the fourth column of Table I for the daylight hours. At night z_c decreases from about 115 km at the equator to 100 km at the poles.

It is assumed that the earth as a whole is approximately electrically neutral so that there are no strong electric fields in the high atmosphere except the relatively small fields which arise from the motions of the ions themselves. The method underlying the ionization calculations was exactly that of reference 1, section 8, namely, to assume an ion curve, caused by the ultraviolet light of the sun, at the subsolar point $\theta = \psi = 0$ which in the long free path region is that required by Gunn's diamagnetic theory of the diurnal magnetic variation[3] and which in the short free path region agrees with the facts of wireless waves as far as they are known, i.e., the absorption of and the apparent heights reached by the waves longer than 100 meters. The curve is given in curve 1, Fig. 4, and the values of y the density of ion pairs are tabulated in column 2, Table III, for noon at latitude 0°.

From this curve the y, z curves due to the solar ultraviolet radiations were calculated at all points of the earth. The calculation fell into two interdependent parts, one dealing with the short free path ions, the S ions, and

[3] Gunn, Terr. Mag. and Atmos. Elec. **34**, 17 (1929).

one with the long free path ions, the D ions. The S ions were calculated as in reference 1, sections 11 and 34, and from these the electrical conductivity σ of a 1 cm² vertical column of the S region was calculated. The values of y for the S ions are given in Table III for z below z_c. The values of σ are in Table II, these are practically the same as those in Fig. 5, reference 1.

TABLE II. *Electrical conductivity of the upper atmosphere* $\sigma \times 10^7$ *c.g.s.e.m.u.*

Latitude	noon	10 A.M. 2 P.M.	8 A.M. 4 P.M.	6 P.M.	8 P.M.	10 P.M.	Mid-night	2 A.M.	4 A.M.	6 A.M.
0°	144	110	29	8.6	4.3	3.0	2.1	1.7	1.4	1.2
10°	139	90	26	8.3	4.1	2.8	2.0	1.6	1.3	1.1
20°	76	52	18	6.3	3.5	2.3	1.6	1.3	1.1	0.9
30°	46	34	10	4.0	2.5	1.6	1.2	1.0	0.86	0.7
40°	23	18	5.1	2.4	1.6	1.1	0.8	0.7	0.6	0.5
50°	13	8.5	2.5	1.6	1.0	0.72	0.54	0.46	0.43	0.36
60°	4.5	3.0	1.7	1.0	0.6	0.45	0.35	0.32	0.30	0.25
70°	1.5	1.0	0.8	0.6	0.3	0.27	0.25	0.21	0.18	0.15

The long free path ions in the daytime were calculated as in reference 1, sections 13 to 16, except that the present case is somewhat more complicated because a different n, z curve is used for each θ and ψ. The values of y for the D ions are given in Table III for z above z_c. There resulted from the calculation D, i, v, and E; these are given in Table I, which is similar to Table I, reference 1. D is the number of ion pairs in a 1 cm² vertical column of the D region, i and E are the current and difference of potential, respectively, in c.g.s. electromagnetic units in the horizontal direction of a 1 cm² vertical column of the D region, and v is the component in the vertical direction of the velocity of drift of the D ions due to the action of the electric field E and the earth's magnetic field. v is in the same direction for both positive and negative ions and is downward in the daylight hemisphere and upward in the night hemisphere.

The ions in the daylight hours of Table III are given a symmetrical distribution on either side of the noon meridian with the maximum at noon. Actually this cannot be exactly true, since the maximum is probably half an hour or so later than noon, as calculated in reference 1, section 34, and the distribution is only approximately symmetrical on either side of the maximum.

4. The Ions at Night

We shall first describe the case for latitude 40° and later take up the case of the equator. The y, z curves (or rather $\log_{10} y$) in the daytime for latitude 40° are plotted in Fig. 1. It is seen that during the afternoon y decreases because of the weakening sunlight and the curves sink to lower levels because of the cooling and contraction of the atmosphere. After sunset the electrical field E, which is westward during the day, reverses to become eastward and causes the D ions of both signs to rise with a velocity v. If there were no magnetic field H, or if H were vertical as at the poles, v would not exist and the ions would move downward by diffusion due to the random velocities of temperature agitation (this is the ordinary gaseous or temperature diffusion) to

attain, if possible, their equilibrium distribution in the atmosphere; the equilibrium distribution obtains when y/n is constant with z. Such equilibrium can, however, never come to pass because the ions are produced mainly in levels above 100 km and their destruction by recombination increases with decreasing z; hence the ions continually diffuse downward. If the magnetic field H were horizontal, as at the equator, there would be no downward diffusion of the D ions at night. If H is inclined to the vertical, as in temperate latitudes, the ion banks are subjected to both influences, they rise with the magnetic-electric drift velocity v and slide down along the lines of magnetic force with the diffusion velocity v' resolved along the lines. In general v' increases with z, at the greater heights it is greater than v and at the lower heights is less than v. Thus the D ions in the lower levels move up and in the higher levels move down to form a bank with the maximum value of y approximately at the level z' where $v=v'$.

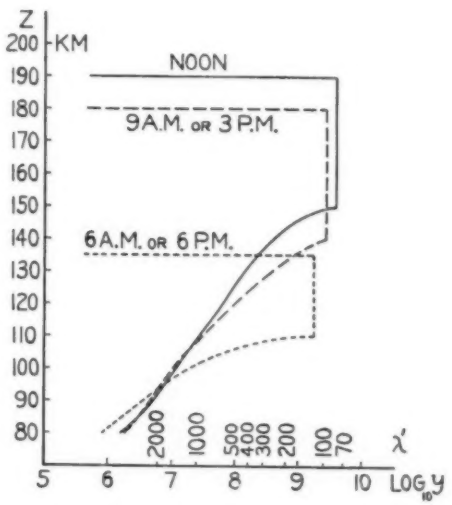

Fig. 1. Density y of ion pairs in the daytime, latitude 40°.

At a height z the number of ion pairs N which diffuse cm^{-2} sec^{-1} downward is

$$N = 0.41\gamma u(py + dy/dz)/n, \tag{4}$$

where γ is the mean free path of the ions and u their velocity of temperature agitation (reference 1, paragraph 9). Then

$$v' = (N \cos \zeta)/y, \tag{5}$$

where ζ is the angle between H and the vertical. At the level where y is a maximum $dy/dz=0$. Putting $\gamma=1/2^{1/2}\pi n\sigma^2$ where the molecular diameter σ is taken to be 3×10^{-8} cm and using $T=220°K$, (4) becomes $N=0.735\times10^{13}$ y/n. This value in (5) yields

$$v' = (0.735 \times 10^{13} \cos \zeta)/n. \tag{6}$$

To determine v during the night we turn to Table I and find that E averaged over the sunlit hemisphere is 335 e.m.u. cm^{-1}. As discussed in reference 1, section 27, the values in the table were obtained by calculating the equilibrium conditions for each slice of the atmosphere along parallels of latitude independently of the influence of adjacent slices. Such a procedure is not entirely correct because the adjacent slices influence each other, and, to make a long story short, the influence is such as to make the value 335 too large. We therefore take E to be 250 e.m.u. cm^{-1}. From this the sunset meridian of the earth is at a potential of about 5000 volts above that of the sunrise meridian. The voltage in the night D region is of course due to the eastward current flowing in the underlying S region. The values of the conductivity decrease all night, see Table II, and therefore, since the total current

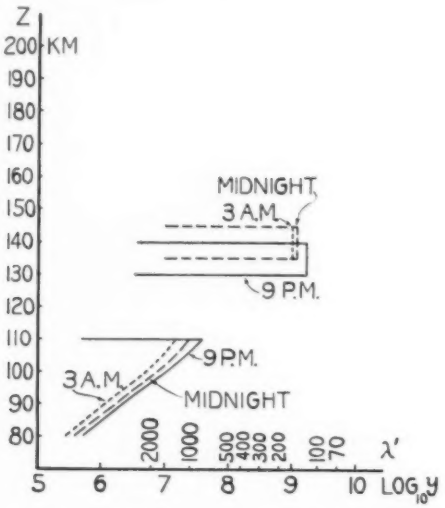

Fig. 2. Density y of ion pairs at night, latitude 40°.

in the S region is constant during the night, E increases all night, being about three times as great in the early morning hours as it is in the evening hours. Hence v, which is equal to $E \sin \zeta/H$, increases all night. As a simplifying approximation we take v to be 250 cm sec.$^{-1}$ from sunset to 10 P.M., to be 500 cm sec.$^{-1}$ from 10 P.M. until dawn, and to be constant along the meridians of longitude. Our results do not depend critically on the approximation.

To find the level where the maximum value of y of the D ion bank is between 6 and 10 P.M. we put $v' = 250$ cm sec.$^{-1}$ in (6) and get

$$n = 2.94 \times 10^{10} \cos \zeta. \tag{7}$$

At 40° latitude $\zeta = 30°\ 45'$ and $n = 2.51 \times 10^{10}$. Whence, from the night n, z curve, z' is 139 km. After 10 P.M. v' is 500 cm sec.$^{-1}$ and z' shifts up 5 km to 144 km. Therefore the D ions which at 6 P.M. are mainly in the levels from $z = 110$ to 135 km, see Fig. 1, move up to assemble in a bank around $z = 139$ km. $v = 250$ cm sec.$^{-1}$ amounts to 9 km hour^{-1}, so that the ions starting from 110 km reach the bank at about 9 P.M., although their numbers are considerably

reduced by recombination during the journey (reference 1, Eq. (17)). Calculation shows that the supply into the bank from the ascending D ions is just about sufficient to maintain $y = 1.7 \times 10^9$ in a bank 10 km thick from 130 to 140 km against the loss due to recombination of the ions. After about 9 P.M. the supply due to this source ceases. Since z_c is 110 km the ions below 110 km are S ions and are not subjected to the drift velocity v but remain where they are except for the relatively slow temperature diffusion upward and downward. Thus the ions separate into two banks. After about 10 P.M. the upper bank moves up 5 km. The degredation of y in each bank through the night due to the recombination of the ions was calculated from Sir J. J. Thomson's formula (reference 1, section 9). The night y, z curves for latitude 40° are given in Fig. 2.

The night-time ionization for latitude 60° was calculated in a manner similar to that for latitude 40°; the values of y are in Table III. A zero value in Table III merely means a small value.

TABLE III. *Ion density y in the upper atmosphere.*

		Geographic Latitude		
	z	0°	40°	60°
Noon	200 km	0	0	0
	190	4.7×10^9	4.0×10^9	0
	180	4.7×10^9	4.0×10^9	0
	170	4.7×10^9	4.0×10^9	3.1×10^9
	160	4.7×10^9	4.0×10^9	3.1×10^9
	150	4.7×10^9	4.0×10^9	3.1×10^9
	140	7.0×10^8	4.0×10^8	3.1×10^9
	130	2.3×10^8	1.4×10^8	3.1×10^9
	120	9.1×10^7	6.7×10^7	5.1×10^7
	110	3.6×10^7	2.7×10^7	2.3×10^7
	100	1.4×10^7	1.2×10^7	7.1×10^6
	90	5.8×10^6	5.4×10^6	2.7×10^6
	80	2.1×10^6	1.6×10^6	1.1×10^6
3 P.M. or 9 A.M.	200 km	0	0	0
	190	3.0×10^9	0	0
	180	3.0×10^9	2.8×10^9	0
	170	3.0×10^9	2.8×10^9	2.3×10^9
	160	3.0×10^9	2.8×10^9	2.3×10^9
	150	3.0×10^9	2.8×10^9	2.3×10^9
	140	2.8×10^8	2.8×10^9	2.3×10^9
	130	1.1×10^8	4.0×10^8	2.3×10^9
	120	4.6×10^7	1.0×10^8	1.1×10^8
	110	1.9×10^7	3.4×10^7	3.7×10^7
	100	9.1×10^6	1.2×10^7	1.1×10^7
	90	2.8×10^6	4.5×10^6	3.1×10^6
	80	1.2×10^6	1.8×10^6	1.0×10^6
6 P.M. or 6 A.M.	150 km	0	0	0
	140	1.7×10^9	0	0
	135	1.7×10^9	1.7×10^9	1.6×10^9
	130	1.7×10^9	1.7×10^9	1.6×10^9
	120	1.7×10^9	1.7×10^9	1.6×10^9
	115	1.7×10^9	1.7×10^9	1.6×10^9
	110	5.1×10^7	1.7×10^9	1.6×10^9
	100	1.3×10^7	1.9×10^7	1.4×10^7
	90	2.9×10^6	3.9×10^6	3.4×10^6
	80	8.0×10^5	8.4×10^5	8.1×10^5

TABLE III. (*Continued*).

	z	0°	40°	60°
9 P.M.	170 km	0	0	0
	160	1.7×10^{9}	0	0
	150	1.7×10^{9}	0	0
	140	0	1.7×10^{9}	1.6×10^{9}
	130	0	1.7×10^{9}	1.6×10^{9}
	120	0	0	0
	115	5.2×10^{7}	0	0
	110	2.4×10^{7}	3.8×10^{7}	3.3×10^{7}
	100	5.9×10^{6}	1.0×10^{7}	9.2×10^{6}
	90	1.3×10^{6}	2.1×10^{6}	1.9×10^{6}
	80	3.8×10^{5}	5.1×10^{5}	4.6×10^{5}
Midnight	170 km	0	0	0
	160	1.6×10^{9}	0	0
	150	1.6×10^{9}	0	0
	145	0	1.2×10^{9}	1.1×10^{9}
	135	0	1.2×10^{9}	1.1×10^{9}
	125	0	0	0
	115	3.4×10^{7}	0	0
	110	1.6×10^{7}	2.3×10^{7}	2.1×10^{7}
	100	3.6×10^{6}	2.3×10^{6}	6.5×10^{6}
	90	8.7×10^{6}	1.8×10^{6}	1.3×10^{6}
	80	4.6×10^{5}	3.7×10^{5}	3.1×10^{5}
3 A.M.	170 km	0	0	0
	160	1.5×10^{9}	0	0
	150	1.5×10^{9}	0	0
	145	0	1.0×10^{9}	9.0×10^{8}
	135	0	1.0×10^{9}	9.0×10^{8}
	125	0	0	0
	115	2.4×10^{7}	0	0
	110	1.0×10^{7}	1.5×10^{7}	1.4×10^{7}
	100	3.1×10^{6}	5.3×10^{6}	4.9×10^{6}
	90	5.5×10^{5}	1.1×10^{6}	9.4×10^{5}
	80	1.9×10^{5}	2.8×10^{5}	2.2×10^{5}

The calculation of the night-time ionization for latitude 0° presents an interesting feature. At the equator $\zeta=90°$ and from (7) $n=0$, and from the n,z curve for a summer night $z'=\infty$; which means that at the equator where H is horizontal the downward diffusion velocity v' is zero and therefore the D ions continue to rise all night with the velocity v. As a matter of fact, this does not occur because of the lateral diffusion of the ions. What happens is seen in the following way: z' was calculated for tropical latitudes from $\theta=0°$ to 20°. The z',θ curve is shown in Fig. 3, its rises sharply to ∞ at $\theta=0$, and gives the heights where the night D ion banks would be if there were no lateral diffusion to the north or south (and if the night were long enough). Such diffusion, however, occurs, for in a distance of only 0.5° or 55 km (or 30 nautical miles) from the equator z' drops from its equatorial value ∞ to 173 km. As a result the D ions rise up at night and diffuse to the north and sound along the lines of magnetic force in the tropical latitudes from, say, 20° north to 20° south to form a bank in the levels from 150 to 160 km. The tropical night values of y were then calculated just as in the case of latitude 40° and are given in the 0° latitude column of Table III.

5. Electrons

In general the electron density y_e increases with z to a maximum value y_m at a height z_m. For the daylight hours y_m was calculated from the equation

$$y_m = 3.15 \times 10^5 \cos\theta(0.126 \sin\psi + \cos\psi). \quad (8)$$

(8) is the same as (21) of reference 1 with a slight change in the numerical constants to conform with the slightly different atmospheric temperatures used in the present paper. The night values of y_m were worked out just as for the case of the ions at latitude 40° described in the preceding section; it seems unnecessary to give the details of the calculations. y_m and z_m are given in Table IV. y_e above and below y_m can not yet be calculated with certainty.

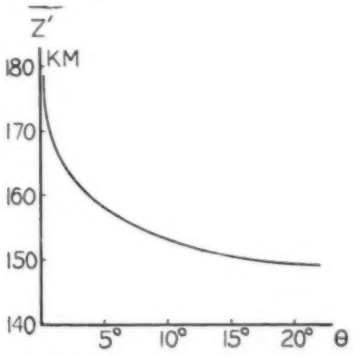

Fig. 3. z' as a function of θ.

Table IV. *Maximum electron density y_m in the upper atmosphere.*

Geographic Latitude	0°		40°		60°	
	z_m	y_m	z_m	y_m	z_m	y_m
Noon	195 km	3.2×10^5	195 km	2.4×10^5	175	1.6×10^5
3 P.M.	195	2.5×10^5	195	1.9×10^5	175	1.3×10^5
6 P.M.	144	1.2×10^5	140	0.9×10^5	140	0.6×10^5
9 P.M.	165	1.1×10^5	145	0.1×10^5	145	0
Midnight	165	1.0×10^5	145	0	145	0
3 A.M.	165	0.8×10^5	145	0	145	0
6 A.M.	144	1.0×10^5	140	0.8×10^5	140	0.5×10^5
9 A.M.	195	2.0×10^5	195	1.5×10^5	175	1.0×10^5

6. Ionization by the Ultraviolet Light of the Sun

Although explicit calculations of the ion and electron banks produced by the absorption of the ultraviolet light of the sun in the high atmosphere have been made for certain cases,[4] it is important to show that the y, z curve assumed at $\theta=\psi=0$ is the sort of curve which might be caused by the solar ultraviolet light. The curve is drawn in curve 1, Fig. 4; it is idealized of course, y being taken to be constant with z through the D region in order to simplify the problem. Without some such simplification the calculations of sections 3 and 4 could hardly even have been attempted.

[4] Hulburt, Phys. Rev. **31**, 1018 (1928).

The ions disappear only by recombination, therefore j the total rate of loss in a 1 cm² vertical column of the atmosphere is

$$j = \int_0^\infty \alpha n y^2 dz,$$

where α is the recombination coefficient. For curve 1, Fig. 4, (j) is 1.1×10^{13} pairs cm^{-2} sec.$^{-1}$ or 1.1×10^{13} W erg cm^{-2} sec.$^{-1}$, if W is the work of ionization. This is the energy necessary to maintain the ion bank and must be supplied by the sunlight. For $W=1.28\times10^{11}$ erg, corresponding to 8 volts or 1520A, the energy is 141 erg cm^{-2} sec.$^{-1}$. The energy in the solar spectrum region from 0 to 1520A is about 100 erg cm^{-2} sec.$^{-1}$ calculated on the assumption that the sun is a black body at a temperature of 6000°K and taking the solar constant to be 1.35×10^{6} erg cm^{-2} sec.$^{-1}$. In this case the solar energy is able

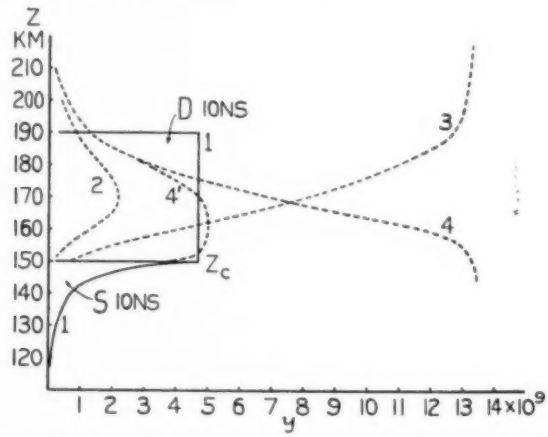

Fig. 4. Curve 1 is the assumed y, z curve for noon at the equator, the other curves are theoretical.

to maintain the ion bank. If the ionization potential is 10 volts, corresponding to 1234A the energy required to maintain the bank is 176 erg cm^{-2} sec.$^{-1}$, and the solar energy from 0 to 1234A is about 4 erg cm^{-2} sec.$^{-1}$, which is somewhat less than that required. On the whole, since the amount of the sun's energy in the far ultraviolet is entirely unknown as well as the exact processes of photo-ionization, the calculation supports the view that the solar ultraviolet energy is adequate to cause the ionization in the high atmosphere.

The form of the y, z curve will depend on the absorption coefficients of the ionizing wave-lengths of the solar ultraviolet light, on the recombination of the ions and on the manner in which the ions move about by temperature diffusion and electric-magnetic drift. If I is the energy carried by the ionizing wave-lengths outside of the atmosphere and if β is the average light absorption coefficient of these wave-lengths, the number of ion pairs v (i.e., positive and negative ions) produced per cm³ in the atmosphere at a height z is, for the sunlight incident vertically,[4]

$$q = \frac{\beta I}{W} n\epsilon^{-\beta n/p}. \tag{9}$$

With $\beta = 2.63 \times 10^{-18}$ (a reasonable value, reference 4, page 1026) and with the summer day value of $p = 0.872 \times 10^{-6}$, q was calculated from (9); the q, z curve is plotted in curve 2, Fig. 4, q being in arbitrary units.

For a static atmosphere, i.e., no diffusion or drift of the ions, $q = \alpha n y^2$. Substituting in (9) gives

$$\alpha y^2 = \frac{\beta I}{W} \epsilon^{-\beta n/p}. \tag{10}$$

From (10) with $\alpha = 0.975 \times 10^{-25}$ and $I/W = 6.83 \times 10^{12}$ y was determined, the y, z curve is plotted in curve 3, Fig. 2. In the S region the electric-magnetic drift of the ions does not exist, and calculation shows that, because of the relatively high values of the molecular density n temperature diffusion is unimportant compared to q and the recombination loss. Hence, approximately, the S region may be regarded as a static atmosphere as far as the y, z curve is concerned, and therefore curve 3, Fig. 4, is of the type which the ultraviolet light would produce in the S region. The curve is similar to curve 1 below z_c. It is seen that by a suitable choice of several values of β and of I for each β, and combining the results, the y, z curve of the S ions may be accounted for.

In the D region we take into account the electric-magnetic drift of the ions and neglect the effect of temperature diffusion; this is a justifiable approximation in the lower portion of the D region, but is not so in the upper portion and must be allowed for later. Consider an element of the D region 1 cm square and of thickness dz. The number of ion pairs produced per second in the element is $q dz$; the number which disappear per second by recombination is $\alpha n y^2 dz$; the number which leave the lower face of the element is vy, the drift velocity v being downward; and the number which enter the upper face of the element is $v(y + (dy/dz)\, dz)$. Then for a steady state

$$q = \alpha n y^2 - v dy/dz.$$

Substituting (9) we get

$$\frac{\beta I}{W} n \epsilon^{-\beta n/p} = \alpha n y^2 - v dy/dz. \tag{11}$$

We solve (11) by approximate methods. From (3) $dy/dz = -pn\, dy/dn$. Above 180 km $\beta n/p$ is small, less than 0.4, and $\epsilon^{-\beta n/p}$ is approximately unity. (11) then becomes approximately

$$\beta I/W = \alpha y^2 + pv dy/dn. \tag{12}$$

Solving (12), and putting $y = 0$ at $n = 0$, gives

$$y = (\beta I/\alpha n)^{1/2} \left(\exp \frac{2n}{pv} (I\beta\alpha/W)^{1/2} - 1 \right) \left(\exp \frac{2n}{pv} (I\beta\alpha/W)^{1/2} + 1 \right)^{-1}. \tag{13}$$

With the numerical values used for curves 1, 2 and 3, Fig. 4, the y, z curve from (13) was calculated and is given in curve 4, Fig. 4. Curve 4 is the solution of (12) approximately valid down to about 180 km. In lower levels

$\epsilon^{-\beta n/p}$ is much less than unity and curve 4 is not an approximate solution of (11) but yields values of y which are too large. Therefore the curve for (11) lies below curve 4. Its maximum, obtained by putting $dy/dz=0$, lies somewhere on curve 3. Below the maximum the curve must satisfy the requirement that the total rate of supply of the ions due to the ultraviolet light and to the drift of the ions across the maximum equal the rate of loss from recombination. Above the maximum the total rate of supply from the ultraviolet light must equal the loss from recombination and the drift of ions across the maximum. At all points on the curve y, z and dy/dz must satisfy (11). These conditions are sufficient to enable one to draw the curve with an accuracy of at least 15 percent without much trouble. Curve 4′, Fig. 4, is the curve thus obtained and is seen to be not unlike curve 1. Furthermore, the effect of temperature diffusion is to bring down ions from the levels above 190 km; these

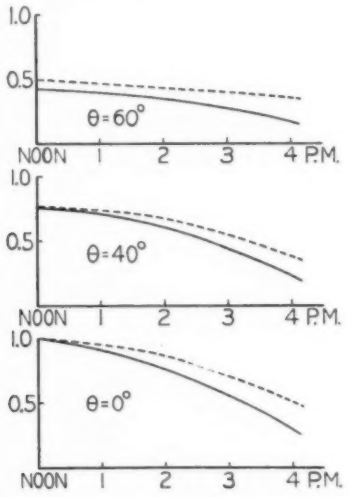

Fig. 5. The full line and dotted curves are the values of $T\,D$ and $\cos\theta\cos\psi$, respectively.

ions will bulge out curve 4′ in levels from 170 to 190 km, and make it even more like curve 1. On the whole it is concluded that curve 1 is much the sort of curve which might reasonably be expected to be produced by the ultraviolet light of the sun.

7. Agreement with the Solar Diurnal Variation of the Earth's Magnetic Field

The diamagnetic theory,[3] which accounted well for the prominent features of the solar diurnal variation of the earth's magnetism, assumed that the diamagnetism of the atmosphere due to the D ions was proportional to $\cos\theta\cos\psi$. The diamagnetism of the ions is proportional to DT. We have taken the y, z curve at $\theta=\psi=0$ such that DT is the value required by the diamagnetic theory and have calculated all the other y, z curves without reference to the theory. We must now see whether the values of Table III yield a diamagnetism in accord with the theory. The values of $T\,D$, calculated from Table

III, are plotted in the full line curves of Fig. 5; $\cos\theta\cos\psi$ is plotted in the dotted line curves. The two sets of curves agree within the tolerance of the theory; it should be remembered that they were made to fit at only one point, noon at the equator or $\theta=\psi=0$. Furthermore, the magnetic effects at the surface of the earth depend on the distance away of the diamagnetic ion bank, and the D ions are closer to the earth for the greater values of θ and ψ than they are for the lesser values. If this were taken into account the T D curves would be even closer to the dotted curves than they are in Fig. 5, and we conclude that the ionization of Table III is in close accord with the diamagnetic theory.

8. Agreement with Bauer's Analysis

From a harmonic analysis of the 1922 survey of the permanent magnetic

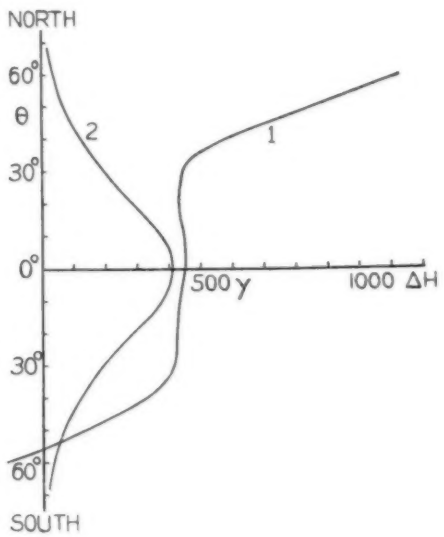

Fig. 6. Curve 1 gives the observed, curve 2 the theoretical, values of ΔH the horizontal component of the portion of the earth's magnetic field of external origin.

field of the earth Bauer[5] concluded that a portion is of external origin. His values of the horizontal component ΔH of this portion for various latitudes are plotted in curve 1, Fig. 6; the scale of abscissas is in γ or 10^{-5} gauss. From the values of i of Table I, from the values of σ of Table II and from the sunset to sunrise difference of potential of about 5000 volts (section 4) the currents from pole to pole in the D and S regions of the day and night hemispheres were calculated. They were, day D region, 21.2×10^6 amperes, day S region 15.9×10^6 amperes, night D region, 4.6×10^6 amperes and night S region, 0.7×10^6 amperes; all are eastward except the day S region current which is westward. These amount to a current of 5.3×10^6 amperes flowing eastward around the earth all the time. The distribution of the current density with latitude has the shape of curve 2, Fig. 6. The horizontal component

[5] Bauer, Terr. Mag. and Atmos. Elec. **28**, 1 (1923).

of the magnetic field due to this current sheet was calculated from the relation

$$\Delta H = 2\pi i, \tag{14}$$

and is plotted in curve 2, Fig. 6. The calculated and observed curves are most reliable in tropical latitudes and here they agree well. At high latitudes there is some disparity. However, at high latitudes (14) is a poor approximation and curve 2 is not trustworthy. The observed curve, too, is not to be trusted at high latitudes, for the data on which it was based were meagre. The program of the International Polar Year which begins this year contemplates obtaining more complete observations in polar regions which may permit a more exact magnetic analysis.

9. Agreement with Wireless Waves

From the ionization of Tables III and IV the skip distances of wireless waves were calculated taking into account the refraction of the waves in both the ion and electron banks and were found to agree well with the observed values.[4] The calculated skip distances for a 25 meter wave are given in Fig. 6.

The height z at which a wireless ray of wave-length λ is totally reflected (refracted) at normal incidence in the ionization bank is obtained by putting the refractive index μ equal to zero in the equation

$$\mu^2 = 1 - 2ye^2\lambda^2/\pi m, \tag{15}$$

solving for y and determining z from the y, z curve. For the ion bank y and m in (15) are the ionic density and mass, for the electron bank y and m are the electronic density and mass and in this case the factor 2 in (15) is omitted. In the case of electrons (15) is the dispersion formula for wave propagation polarized with the electric vector parallel to the magnetic field; for other states of polarization the appropriate dispersion formulas should be used, which are however not greatly different from (15) for wireless waves below 50 meters in length. For ions (15) is closely valid for all states of polarization of the wireless waves. The values of y for total reflection of waves of various wave-lengths are marked along the x-axis of Figs. 1 and 2. It is seen, for example, that 150 to 400 meter waves are turned down at the 100 km level during the day and that in the early part of the evening they pierce through the lower layer to be reflected (refracted) from the higher level at about 140 km. This agrees with the facts except that the observed retardation times indicated night-time heights of around 200 km or more.[6] The difference may reasonably be attributed to the group velocity retardation which is always present in the observations.

The longest wireless wave λ' which pierces vertically through the atmosphere is determined by setting $\mu = 0$ in (15), substituting the maximum value of y or y_e from Table III or IV for the time of day and the latitude in question and solving for λ. The values of λ' are given in Table V, and agree roughly

[6] Kenrick and Pickard, Proc. Inst. Rad. Eng. **18,** 649 (1930) give a summary of references; Appleton and Green, Proc. Roy. Soc. **A128,** 159 (1930); Mars, Gilliland and Kenrick, Proc. Inst. Rad. Eng. **19,** 106 (1931).

TABLE V.

Latitude	0°	40°	60°
noon	60 m	68 m	84 m
midnight	103	140	144

with the values which have been observed.[6] The agreement is to be expected because the λ' relation is a special case of the skip distance relation, namely, λ' is the wave for which the skip distance is zero. And the agreement means nothing more than that the measurements of λ' checked the predictions from the skip distances.

The limiting wave, defined as the shortest wave which can be used for reliable long distance radio communication, was observed[4] by Taylor to be about 10.5, 17, 14 and 23 meters for summer noon, summer midnight, winter noon and winter midnight, respectively, for temperate latitudes in 1925

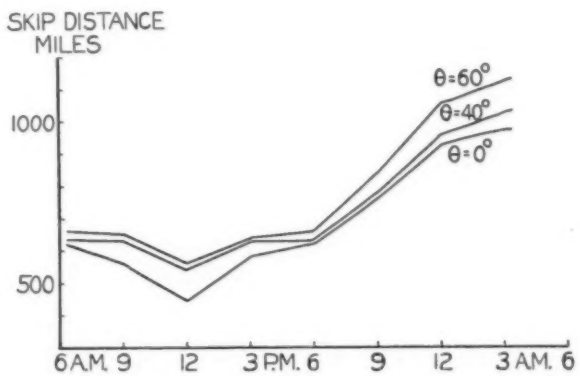

Fig. 7. Skip distances in miles for a 25 meter radio wave calculated as a function of the latitude and the time of day.

and 1926, an epoch midway between maximum and minimum solar activity. The values calculated from Tables III and IV agree within 15 percent with the observed values.

Keeping in mind that the ionization banks of Tables III and IV are necessarily somewhat idealized and are incomplete in that they do not give the electrons which exist below the maxima of the y_c, z curves, it is concluded that the ionization accounts for the main facts of the propagation of wireless waves over the earth. Further experimental facts may enable the tables to be made more complete and, if necessary, to be modified to some extent in various details. Certain modifications are possible without changing any of the present calculations. For example, the amount of ionization in the lower portion of the S region was estimated from rather uncertain experimental data, namely, the apparent heights reached by long radio waves. Future observations may indicate a greater ionization in these levels than we have put into the tables. Such changes would not change perceptibly the values of σ of Table II or any of the other calculations.

10. Summary

Each cm³ of the upper atmosphere is assumed to be approximately electrically neutral. Above 60 km the ionization is assumed to be caused by the ultraviolet light of the sun, below, by cosmic radiation. At any height z km above sea-level, denote the numbers per cm³ of singly-charged positive ions, negative ions and electrons by $y+$, $y-$ and y_e respectively. Then $y+ = y- + y_e$, and since y_e is in general small compared to $y-$, the values of $y+$ and $y-$ are nearly equal and are each denoted by y; then y also denotes the density of ion pairs. Above 60 km the values of y are given in Table III. The electron density y_e increases with z to a maximum value y_m at a height z_m; y_m and z_m are given in Table IV. Above and below the maximum y_e can not yet be estimated with certainty. The values given for y and y_m may perhaps be correct within a factor of 2, a zero value merely means a small value. The tables are for average equinoxial conditions and solar quiescence at an epoch halfway between the periods of maximum and minimum solar activity. The values should be increased, and reduced, by roughly 25 percent to refer to epochs of maximum and minimum solar activity, respectively. During magnetic storms the ionization is increased, the values being perhaps double those in the tables for a severe storm. The ionization in polar regions is probably not greatly different from that given for latitude 60°. The seasonal changes in the ionization are small at the equator. In temperate latitudes for winter and summer use the values for latitudes about 20° higher and lower, respectively, in the tables. Below 60 km the ionization due to cosmic radiation is independent of the latitude, hour of the day, solar activity, etc., and y is 8×10^2, 1.6×10^3, 1.9×10^3, 2.2×10^3, 2.9×10^3, 3.4×10^3 and 3.5×10^3 at 0, 10, 20, 30, 40, 50 and 60 km, respectively.[7]

[7] Hulburt, Phys. Rev. **37**, 1 (1931).

THE VAPOR PRESSURE CONSTANT OF AMMONIA, THE ENTROPY OF CRYSTALLINE AMMONIA, AND THE REACTION $N_2+3H_2\rightleftarrows 2NH_3$

By T. E. Sterne*

Harvard University and the Massachusetts Institute of Technology

(Received January 21, 1932)

Abstract

§1. It is shown by statistical quantum mechanics that the vapor pressure constant of an ammonia molecule whose principal moments of inertia are A, A, and C is

$$i = \log \frac{64\pi^3 m^{3/2} k^4 A C^{1/2}}{h^6} + \sum_r D_r \log \frac{G_r}{{}_r\omega_0}$$

at ordinary temperatures; where m is the mass, k is Boltzmann's constant, h is Planck's constant, and the D_r's are the gram molecular fractions of the two varieties; and where the G_r's and ${}_r\omega_0$'s are constants.

§2. The *rotational partition functions* of ammonia molecules of both varieties are evaluated, and G_1 and G_2 are found to be equal to 4/3.

§3 and §4. The spherical oscillatory motion of ammonia molecules in crystal lattices is investigated by quantum mechanics, and ${}_1\omega_0$ and ${}_2\omega_0$ are shown to be equal to 4; if the spins of the hydrogen nuclei are taken into consideration but the spin of the nitrogen nucleus neglected, which is permissible.

§5. With the values $A=2.79\times10^{-40}$ and $B=5.47\times10^{-40}$ CGS units, we find that the vapor pressure constant of ammonia, for common logarithms and atmospheres, is -1.55. This agrees with the experimental result given by Eucken, -1.50 ± 0.04.

§6 and §7. When the reaction $N_2+3H_2\rightleftarrows 2NH_3$ proceeds to the left between the crystalline phases at the absolute zero, there is an increase in entropy of $(9/4)\,R\log 3$ E.U.

§8. The value of the constant I' in the equation for the equilibrium constant in the above homogeneous gas reaction is found in accordance with the previous sections to be equal to -7.17; which agrees fairly well with Eucken's experimental value -7.04 ± 0.10.

Introduction

IN RECENT papers which appeared elsewhere,[1,2,3,4] the author has studied the vapor pressures of hydrogen, of chlorine, and of hydrogen chloride. The work was an extension of that of R. H. Fowler,[5] who first investigated, theoretically, the vapor pressure of hydrogen made up of the two non-combining varieties para-hydrogen and ortho-hydrogen.

It may be shown by using the first and second laws of thermodynamics that the vapor pressure p of a substance is given by the expression

* National Research Fellow.

[1] T. E. Sterne, Proc. Roy. Soc. **A130**, 367 (1931).

[2] T. E. Sterne, Proc. Roy. Soc. **A130**, 551 (1931).

[3] T. E. Sterne, Proc. Roy. Soc. **A131**, 339 (1931).

[4] T. E. Sterne, Proc. Roy. Soc. **A133**, 303 (1931).

[5] R. H. Fowler, Proc. Roy. Soc. **A118**, 52 (1928).

$$\log p = -\frac{\Lambda_0}{RT} + \frac{(C_p)_0}{R}\log T + \int_0^T \frac{dT'}{RT'^2}\int_0^{T'} [(C_p)_1 - (C_p)_{sol}]dT'' + i.$$

Here Λ_0 is the work which must be done to evaporate one gram molecule of the substance at the absolute zero; R is the gas constant; $(C_p)_0$ is the constant and $(C_p)_1$ is the variable part of the specific heat per gram molecule of the vapor at constant pressure; and $(C_p)_{sol}$ is the specific heat at constant pressure of the condensed phase. i is a constant called the vapor pressure constant of the substance, and since its value depends upon the choice which is made of $(C_p)_0$, the latter should be specified whenever one states the value of i. At ordinary temperatures, for monatomic gases, $(C_p)_0 = 5R/2$; for diatomic gases it is $7R/2$, and for non-linear polyatomic gases $(C_p)_0 = 4R$.

The theoretical values for the vapor pressure constants of monatomic vapors are also well understood (see, for instance, Fowler's *Statistical Mechanics*, Chap. VII) that nothing more will be said about them here. In an article which is expected to appear shortly in *The Reviews of Modern Physics* by Fowler and the author, it is shown that the vapor pressure constant at ordinary temperatures of any diatomic vapor at all should be given by the expression

$$i = \sum_r D_r i_r \tag{1}$$

where

$$i_r = \log \frac{(2\pi m_r)^{3/2} k^{7/2} 8\pi^2 I_r}{h^5} + \log \frac{G_r}{{}_r\omega_0}.$$

Here D_r is the gram molecular fraction of the molecules of the r'th species present; m_r is the mass of a molecule of the r'th species; k is Boltzmann's constant; h is Plank's constant; I_r is the moment of inertia of a molecule of the r'th species; G_r is the constant factor which appears before $8\pi^2 I_r kT/h^2$ in the rotational partition function for the r'th species; and ${}_r\omega_0$ is the number of linearly independent wave functions capable of representing a molecule of the r'th species when it is in its lowest quantum state in the crystalline phase at the absolute zero. This equation is quite general; it can be used to find the vapor pressure constant of a substance with a diatomic vapor even if the structural units in the crystalline phase are not the same molecules as those that exist in the gas, but are groups of molecules, or separate atoms, or even atomic ions and electrons. All that one needs to do is always to interpret ${}_r\omega_0$ as being equal to C^{1/P_r}, where C is the number of linearly independent wave functions which can represent the crystal of the r'th species, containing in all $2P_r$ atomic nuclei, at the absolute zero. It is shown in the article by Fowler and the author, referred to above, that there is in general a satisfactory agreement between the observed diatomic vapor pressure constants and those calculated by the use of Eq. (1).

It would be interesting to extend these methods, so as to apply them to polyatomic vapors. The simplest type of polyatomic molecule from the point of view of our methods of investigation would be the type for which the three

moments of inertia A, B, and C about the principal axes were all equal; the next simpler type would be that for which two of these moments of inertia, A and B say, were equal with C differing from A and B. The vibration-rotation spectra of both ammonia[6,7] and methane have been rather completely analysed. Since methane molecules are of the former type, while ammonia molecules are of the latter type, it might be supposed that it would be simpler to commence the study of polyatomic vapors by considering methane. The non-combining groups of terms, however, are simpler in the case of ammonia than they are in the case of methane; for there are fewer possible nuclear and vibrational arrangements in the case of ammonia; and we shall therefore proceed in this paper to discuss ammonia first in some detail, in order to make it clear in just what fashion the vapor pressure constant arises in statistical mechanics, in the case of polyatomic vapors. We shall consider the vapor pressure of methane in a subsequent paper.

§1. The Vapor Pressure of Ammonia

The ammonia molecule NH_3 very probably consists of a regular pyramid with the nitrogen nucleus at the vertex. There are two varieties of ammonia molecules, which should retain their separate identity over fairly long periods at ordinary and low temperatures. The first variety is characterized by wave functions which are completely symmetrical $S(3)$ in the spins of the three hydrogen nuclei, so that the part of a wave function depending upon the spins of those nuclei does not change its sign when any two of them are interchanged. The second variety of ammonia molecules is characterised by wave functions partly symmetrical $S(2+1)$ and by wave functions partly antisymmetrical $A(2+1)$ in the spins of the hydrogen nuclei. Following Dennison,[8] we say that there are 4 spin wave functions for the first variety with the symmetry characters α, and 2 degenerate spin wave functions for the second variety with the symmetry character (γ, δ) each. At ordinary temperatures, or after cooling from ordinary temperatures, the two varieties of molecule should exist in equal numbers, so that $D_1 = D_2 = 1/2$.

We suppose that the reader is familiar with the methods of enumerating wave functions described in chapters II, IV, V, and XXI of Fowler's *Statistical Mechanics*, and in the author's papers.[1,3] Consider an assembly containing in all X_1 molecules of the first variety, and X_2 molecules of the second variety. Let there be numbers P_1 and P_2 of the two varieties in the crystalline phase, and N_1 and N_2 in the vapor phase. Let the crystalline partition function for normal modes of oscillation of the molecules as a whole in the crystal lattice be in the form $[\kappa(z)]^{P_1+P_2}$. Then the normal modes of oscillation contribute to the total number of linearly independent wave functions capable of representing the entire assembly a factor equal to the coefficient of z^Q in $[\kappa(z)]^{P_1+P_2}$, if the total energy of these modes is Q. Let a partition function for a molecule of the r'th variety for rotations or spherical oscillations in the

[6] Barker, Phys. Rev. **33**, 684 (1929).
[7] Badger and Cartwright, Phys. Rev. **33**, 692 (1929).
[8] Dennison, Rev. of Mod. Phys. **3**, 280 (1931).

crystalline phase be $f_r(z)$. Then these motions, if their total energy is S, contribute to the total number of wave functions a factor equal to the coefficient of z^S in $f_1(z)^{P_1} f_2(z)^{P_2} (P_1+P_2)!/P_1!P_2!$. Thus the whole crystal, if its energy is U, contributes a factor equal to the coefficient of $x_1^{P_1} x_2^{P_2} z^U$ in

$$1/\{1 - \kappa(z)[x_1 f_1(z) + x_2 f_2(z)]\}.$$

We may use the classical approximation, with sufficient accuracy, to the correct Einstein-Bose statistics for the vapor. The vapor, if its total energy is F, contributes to the total number of linearly independent wave functions capable of representing the entire assembly a factor equal to the coefficient of $x_1^{N_1} x_2^{N_2} z^F$ in

$$\exp [x_1 F_1(z) + x_2 F_2(z)]$$

where $F_1(z)$ and $F_2(z)$ are the partition functions for the two varieties of gas molecules. We have of course that $N_1+P_1=X_1$, and $N_2+P_2=X_2$. Accordingly the entire assembly, if its total energy is E, and if we allow all possible partitions of the molecules between the different phases, can be represented by a total number of linearly independent wave functions equal to the coefficient of $x_1^{X_1} x_2^{X_2} z^E$ in

$$\frac{e^{x_1 F_1(z) + x_2 F_2(z)}}{1 - \kappa(z)[x_1 f_1(z) + x_2 f_2(z)]},$$

and hence this number is given by

$$W = \left(\frac{1}{2\pi i}\right)^3 \iiint \frac{dx_1 dx_2 dz e^{x_1 F_1(z) + x_2 F_2(z)}}{x_1^{X_1+1} x_2^{X_2+1} z^{E+1} \{1 - \kappa(z)[x_1 f_1(z) + x_2 f_2(z)]\}}. \tag{1.1}$$

We find by the usual methods that the mean values

$$\overline{N}_r = \xi_r F_r(\theta) \tag{1.2}$$

and

$$\overline{P}_r = \frac{\xi_r f_r(\theta) \kappa(\theta)}{1 - \kappa(\theta)[\xi_1 f_1(\theta) + \xi_2 f_2(\theta)]}. \tag{1.3}$$

Here the parameters ξ_1, ξ_2, and θ $(=e^{-1/kT})$ corresponding to the thermodynamic partial potentials and to the temperature, respectively, are determined by the unique position of the saddle point of the integrand of W, given by the vanishing of its three partial differential coefficients. If $\overline{P}_1+\overline{P}_2$ is large, then we have very nearly

$$\kappa(\theta)[\xi_1 f_1(\theta) + \xi_2 f_2(\theta)] \sim 1.$$

If, further, nearly all of the molecules are in the crystal, then we have, very nearly,

$$\overline{P}_1 : \overline{P}_2 = D_1 : D_2.$$

It follows from these equations that

$$\overline{N}_r = D_r F_r(\theta)/\kappa(\theta) f_r(\theta). \tag{1.4}$$

Making use of the relation $pV=\overline{N}kT$ where p is the pressure, it follows that the vapor pressure

$$p = \sum_{1,2} D_r p_r \tag{1.5}$$

where

$$p_r = F_r(\theta)kT/Vf_r(\theta)\kappa(\theta); \tag{1.6}$$

which is not the partial pressure of the r'th species, but is the vapor pressure of a crystal made up wholly of the r'th sort of molecule. We take as the zero of energy the state when all the molecules are in their lowest quantum states, in the lattice at the absolute zero and at zero pressure. We suppose the partition functions $f_r(\theta)$ to be of the form

$$f_r(\theta) = \sum_j {}_r\omega_j \theta^{r*j}$$

where ${}_r\omega_j$ is the number of linearly independent wave functions capable of representing the j'th eigenstate of a molecule of the r'th species in the crystal, and ${}_r\epsilon_j$ is the energy of the state. We denote by C_r the specific heat per gram molecule at constant pressure of a crystal made up wholly of the r'th sort of molecules. Then we may readily show[9] that

$$\int_0^T \frac{dT'}{RT'^2} \int_0^{T'} C_r dT'' = \log K(T) f_r(T) - \log_r \omega_0.$$

Here R is the gas constant per gram molecule. It follows from this last relation and (1.6) if we neglect all but the lowest vibrational levels of the gas molecules, that

$$\begin{aligned} \log p_r = &- \frac{\chi}{kT} + 4 \log T - \int_0^T \frac{dT'}{RT'^2} \int_0^{T'} C_r dT'' \\ &+ \log \frac{(2\pi m_r)^{3/2} k^4 16(2)^{1/2} \pi^{7/2} A C^{1/2}}{h^6} + \log \frac{G_r}{{}_r\omega_0} \end{aligned} \tag{1.7}$$

very nearly. Here G_r is a number which appears as a factor in front of $16(2)^{1/2}\pi^{7/2}AC^{1/2}(kT)^{3/2}/h^3$ in the rotational partition function for a gas molecule of the r'th sort, when nuclear spins are taken account of. We shall show how this form results for the rotational partition function, and how G_r may be found, in the next section. The quantity χ, which we have taken to be the same for all five sorts of molecules (the differences are trivial) is the work which must be done on a molecule in the crystal, in a state of zero energy defined above, in order to put it in a state of rest, in its lowest quantum state, at infinity.

We can show[9] that

$$\log p = \log (D_1 p_1 + D_2 p_2) = D_1 \log p_1 + D_2 \log p_2 \tag{1.8}$$

very nearly. Further, we can show by using the complete crystalline partition

[9] Sterne, Proc. Roy. Soc. **131**, 348 (1931).

function that if C_{sol} is the specific heat at constant pressure of the mixed crystal made up of both varieties of ammonia, then

$$C_{sol} = D_1C_1 + D_2C_2.$$

Hence, from Eqs. (1.7), (1.8), and (1.9), we obtain

$$\log p = -\frac{\chi}{kT} + 4\log T - \int_0^T \frac{dT'}{RT'^2}\int_0^{T'} C_{sol}dT'' + i \qquad (1.91)$$

where

$$i = \log \frac{64\pi^5 m^{3/2}k^4 AC^{1/2}}{h^6} + \sum_{1,2} D_r \log \frac{G_r}{{}_r\omega_0}. \qquad (1.92)$$

The quantity i is just the vapor pressure constant of ammonia; when, as should be done at ordinary temperatures, the constant part of the specific heat at constant pressure of the vapor is assigned the value $4R$ per gram molecule. We have neglected the vibrational levels other than the lowest in the gas molecules, but by adding to the right-hand member of Eq. (8) a term

$$\int_0^T \frac{dT'}{RT'^2}\int_0^{T'} (C_p)_1 dT''$$

where $(C_p)_1$ is the "vibrational", or variable, part of the specific heat at constant pressure of the vapor we may take account of the vibrations; and no change need be made in the value of i.

§2. The Rotational Partition Functions of Free Ammonia Molecules

Two of the moments of inertia of ammonia molecules, A and B, are equal; the third moment of inertia about the axis of figure, C, differs from these. The energy levels are given by[10]

$$W = \frac{h^2}{8\pi^2}\left[\frac{1}{A}j(j+1) + \left(\frac{1}{C} - \frac{1}{A}\right)K^2\right], \qquad (2.0)$$

where j and K take on positive integral values. The weights of the levels appear to be given correctly by Villars.[11] For each value of j, K can take on the values $0, 1, 2, 3, \cdots, j$. When K is 0, there are $4(2j+1)$ linearly independent wave functions for ammonia molecules of the first variety; when K is divisible by 3 there are $8(2j+1)$ linearly independent wave functions for this variety; and for all other values of K the weights for the first variety of ammonia molecules are zero. For ammonia molecules of the second variety, there are $4(2j+1)$ linearly independent wave functions when K is neither 0 nor divisible by 3. For $K=0$, or a multiple of 3, the weights for ammonia molecules of the second variety are zero. We have of course only considered those complete

[10] Dennison, reference 8.

[11] Villars, Phys. Rev. **38**, 1552 (1931); Table II.

wave functions which are antisymmetrical in the hydrogen nuclei, in accordance with the Pauli exclusion principle. Let us calculate the partition functions[12] given by the energy levels (2.0) when we use these statistical weights. Let us denote the rotational partition function for the first variety of ammonia molecule by R_1, and that for the second variety by R_2. Then we have by the definition of partition functions generally, the above rules for weights, and Eq. (2.0),

$$R_1 = 4\sum_{j=0}^{\infty}(2j+1)e^{-(\sigma/A)j(j+1)} + 8\sum_{n=1}^{\infty}e^{-\sigma(1/C-1/A)9n^2}\sum_{j=3n}^{\infty}(2j+1)e^{-(\sigma/A)j(j+1)} \tag{2.1}$$

and

$$R_2 = 4\sum_{n=0}^{\infty}e^{-\sigma(1/C-1/A)(1+3n)^2}\sum_{j=1+3n}^{\infty}(2j+1)e^{-(\sigma/A)j(j+1)} + 4\sum_{n=0}^{\infty}e^{-\sigma(1/C-1/A)(2+3n)^2}\sum_{j=2+3n}^{\infty}(2j+1)e^{-(\sigma/A)j(j+1)}, \tag{2.2}$$

where $\sigma = h^2/8\pi^2kT$. We wish to evaluate these sums for the case of ordinary and high temperatures, for which both σ/A and σ/C are small. C is of the same order of magnitude as A, but larger. To evaluate these sums approximately, and at the same time obtain some idea of the order of magnitude of the errors in the resulting approximate expressions, we proceed thus.

To evaluate the first sum, we make use of the following relations:

$$\sum_{l}^{\infty}(2j+1)e^{-(\sigma/A)j(j+1)} = \frac{A}{\sigma}e^{-(\sigma/A)l(l+1)} + O\left(\left(\frac{A}{\sigma}\right)^{1/2}\right) \quad \text{if } l < \left(\frac{A}{2\sigma}\right)^{1/2} - \tfrac{1}{2} \tag{2.3}$$

and

$$\sum_{l}^{\infty}(2j+1)e^{-(\sigma/A)j(j+1)} = \frac{A}{\sigma}e^{-(\sigma/A)l(l+1)} + O[(2l+1)e^{-(\sigma/A)l(l+1)}] \quad \text{if } l \geqq \left(\frac{A}{2\sigma}\right)^{1/2} - \tfrac{1}{2}. \tag{2.4}$$

To show this we have only to compare the series with the corresponding integral

$$\int_{l}^{\infty}(2j+1)e^{-(\sigma/A)j(j+1)}dj.$$

[12] These partition functions seem to be calculated incorrectly by Villars, reference 11. The expressions (19) and (20) in his article, which differ from those derived here by the author, do not have the correct limiting forms at high temperatures. It is for this reason that the calculations in the text above are given in considerable detail.

It is easy to show, if necessary by breaking up the sum and the integral into two parts at the maximum of the integrand which is then monotonic in each part, that they differ at most by a term of the order of the largest term occurring in the series. We have, also,

$$\sum_1^\infty e^{-\sigma(1/C-1/A)9n^2-3n(3n+1)\sigma/A} = \tfrac{1}{3}\left(\frac{C}{\sigma}\right)^{1/2} e^{\sigma C/4A^2}\int_{3(\sigma/C)^{1/2}+(\sigma C)^{1/2}/2A}^\infty e^{-x^2}dx + O(1);$$

which is true since the series is one made up of decreasing positive terms; so that the integral differs at most from the series by the first term of the series which is of the order of unity. Hence

$$\sum_1^\infty e^{-\sigma(1/C-1/A)9n^2-3n(3n+1)\sigma/A}$$

$$= \tfrac{1}{3}\left(\frac{C}{\sigma}\right)^{1/2}\left[1+O\left(\frac{\sigma C}{A^2}\right)\right]\left[\tfrac{1}{2}\pi^{1/2}+O\left(\frac{\sigma}{C}\right)^{1/2}+O\left(\frac{\sigma C}{A^2}\right)^{1/2}\right]+O(1). \qquad (2.5)$$

We have, too, that the series of increasing terms

$$\sum_1^{n_0} e^{-\sigma(1/C-1/A)9n^2} = O((AC/\sigma(C-A))^{1/2}) \qquad (2.6)$$

where

$$n_0 \sim \tfrac{1}{3}(A/2\sigma)^{1/2}$$

and that the series

$$\sum_{n_0}^\infty e^{-\sigma(1/C-1/A)9n^2}(6n+1)e^{-(\sigma/A)3n(3n+1)} = O(C/\sigma). \qquad (2.7)$$

Substituting Eqs. (2.3), (2.4), (2.5), (2.6), and (2.7) in Eq. (2.1) we find for R_1, if we remember that A and C are of the same order or magnitude.

$$R_1 = \frac{4}{3}(\pi)^{1/2}\frac{AC^{1/2}}{\sigma^{3/2}}\{1+0[(\sigma/A)^{1/2}]+\text{terms of higher order in } (\sigma/A)\}. \qquad (2.8)$$

In similar fashion we can show that

$$R_2 = \frac{4}{3}(\pi)^{1/2}\frac{AC^{1/2}}{\sigma^{3/2}}\{1+0[(\sigma/A)^{1/2}]+\text{terms of higher order in } [\sigma/A)\}. \qquad (2.9)$$

It is conceivable that methods similar to those used by Mulholland[13] and Sutherland[14] could be used instead of ours to derive these results, and to give in addition, exactly, the higher terms in the asymptotic expansions; but for the present we must be content with our results, which give what should be the correct limiting forms at high temperatures

$$R_1 \sim \frac{4}{3}\,\frac{16(2)^{1/2}\pi^{7/2}AC^{1/2}k^{3/2}T^{3/2}}{h^3} \qquad (2.91)$$

[13] Mulholland, Proc. Camb. Phil. Soc. **24,** 280 (1928).
[14] Sutherland, Proc. Camb. Phil. Soc. **26,** 402 (1930).

and

$$R_2 \sim \frac{4}{3} \frac{16(2)^{1/2}\pi^{7/2}AC^{1/2}k^{3/2}T^{3/2}}{h^3}. \tag{2.92}$$

These limiting values are in precisely the same form as the rotational partition function given by Fowler[15] when $A = B$, except for the numerical factor $4/3$ which was introduced by the symmetry properties of the wave functions. Fowler probably derived his expression from the older quantum mechanics; for the notion of a "symmetry factor" such as the σ which appears in Fowler's equation, a notion which was in use at the time when he wrote his book, has since been replaced by the notion of non-combining sets of terms obeying the Pauli exclusion principle.

From Eqs. (2.91) and (2.92) we see that G_1 and G_2 for ammonia are both $4/3$; and further, since the ratio at ordinary or high temperatures between R_1 and R_2 is unity, we see that both sorts of ammonia molecules are present in equal numbers in ammonia gas which has rested for a long time at ordinary or high temperatures.

We must now determine the values of ${}_1\omega_0$ and ${}_2\omega_0$.

§3. The Spherical Oscillatory Motion of Ammonia Molecules in Crystalline Ammonia

If we make a calculation for crystalline ammonia similar to that made for the case of chlorine by the writer,[3] it appears that at the absolute zero ammonia molecules should "oscillate", rather than "rotate", about orientations of minimum potential energy in the crystal lattice. From the low temperature thermal measurements of Eucken and Karwat[16] the specific heat of the crystalline phase appears to be 5 calories per gram molecule at a temperature of about 76°K; from which one may deduce that $h\nu_0/k$ is equal to about 230°K; and if one takes the moment of inertia in this calculation to be equal to about 3×10^{-40} CGS units, one finds V_0 to be equal to approximately 3.7×10^{-14} ergs. Taking the combined heat of transition and fusion as 1426 calories per gram molecule, we find that V_0 is equal to about 20×10^{-14} ergs. In neither case should rotation occur until temperatures of the order of 500°K have been reached. The methods of considering the motion of the molecules of ammonia, used above, were developed by Pauling[17] and the author[2] to apply to diatomic molecules, but the considerations of later portions of this section will make it obvious that the same methods may be used to investigate roughly the behavior of polyatomic molecules as well. We may therefore study the spherical oscillatory motion of a molecule of ammonia in the crystal lattice, with a fair assurance that this is the type of motion approximated to by molecules of ammonia in the crystalline lattice at very low temperatures.

We may treat the problem by a perturbation method. We take the origin,

[15] Fowler, "Statistical Mechanics", p. 146, Eq. (442).
[16] Eucken and Karwat, Zeits. f. phys. Chem. **112**, 478 (1924).
[17] L. Pauling, Phys. Rev. **36**, 430 (1930).

0, at the mass center of the molecule; and fixed orthogonal axes OX, OY, OZ such that the orientation of minimum potential energy for the ammonia molecule corresponds to the presence of a nitrogen nucleus at the point $(0, 0, a)$; and of hydrogen nuclei at the points $(-2b(3)^{1/2}/3, 0, -c)$, $(b(3)^{1/2}/3, -b, -c)$, and $(b(3)^{1/2}/3, b, -c)$. We have of course that $3c = sa$, where s is the ratio of the mass of a nitrogen nucleus to that of a hydrogen nucleus (we neglect the trivial mass of the electrons). Let us investigate the forms of the potential and kinetic energies of the molecule, regarded as rigid, for small displacements of the molecule from this orientation of minimum potential energy. We may specify the displacement by the small rotations x, y, and z of the molecule about the axes OX, OY, and OZ respectively. Let the moments of inertia of the molecule about these axes, when it is in its orientation of minimum potential energy, be A, A, and C respectively; the moments of inertia about the axes OX and OY of course being equal. Then the kinetic energy of the motion relative to the center of mass will be, very nearly, for small displacements,

$$T = \frac{A}{2}(\dot{x}^2 + \dot{y}^2) + \frac{C}{2}\dot{z}^2,$$

or in terms of the angular momenta p_x, p_y, and p_z,

$$T = \frac{1}{2A}(p_x^2 + p_y^2) + \frac{1}{2C}p_z^2.$$

We may regard the potential energy V of the molecule, for small displacements from the orientation of minimum potential energy, to be capable of expression in the form $\boldsymbol{A}(q_1^2+q_2^2+q_3^2)+\boldsymbol{B}q_4^2$ plus higher powers in the q's. Here $\boldsymbol{A}$ and $\boldsymbol{B}$ are constants; and q_1, q_2, and q_3 are the distances of the three hydrogen nuclei, and q_4 the distance of the nitrogen nucleus, from the respective positions of the nuclei when the molecule is in its position of minimum potential energy. In terms of the small rotations, this expression becomes

$$V = \boldsymbol{A}[(2b^2 + 3c^2)(x^2 + y^2) + 4b^2z^2] + a^2\boldsymbol{B}(x^2 + y^2) + \text{terms of higher order in the } x\text{'s, } y\text{'s, and } z\text{'s},$$

so that the Hamiltonian

$$H = \frac{1}{2A}(p_x^2 + p_y^2) + \frac{1}{2C}p_z^2 + [\boldsymbol{A}(2b^2 + 3c^2) + \boldsymbol{B}a^2][x^2 + y^2] + 4\boldsymbol{A}b^2z^2 + \text{terms of higher order in the } x\text{'s, } y\text{'s, and } z\text{'s}.$$

Consider now the plane passing through the vertex of the pyramidal molecule, parallel to the base, when the molecule is in its orientation of minimum potential energy. Take a set of axes $O'X'$, $O'Y'$ in this plane, with the origin at the vertex of the pyramid, and parallel to the axes OX, OY respectively. Denote the coordinates relative to these new axes of the projection P' upon the invariable plane of the vertex of the displaced pyramid by ξ and η;

so that $\xi = ay$ and $\eta = -ax$, very nearly. Imagine a lamina, of mass A/a^2, and whose center of mass is P', to move in the invariable plane; and let its moment of inertia about an axis through P' normal to the invariable plane be C. Let the angular displacement of this lamina from its orientation $\theta = O$ in the plane be denoted by θ, and let $\theta = z$. Then the position of the lamina is completely specified by the coordinates ξ, η, θ; and these coordinates also serve to specify the position of the molecule. And finally, if the lamina moves in a field of force of potential energy

$$V = \frac{A}{a^2}[(\eta^2 + \xi^2)(2b^2 + 3c^2) + 4a^2b^2\theta^2] + B[\xi^2 + \eta^2]$$

then we may regard the exact motion of the molecule as being completely specified by the motion of the lamina, when the latter is suitably perturbed. The unperturbed motion of the lamina is given by the Hamiltonian

$$H' = \frac{a^2}{2A}(p_\xi^2 + p_\eta^2) + \frac{1}{2C}\left[B + \frac{A}{a^2}(2b^2 + 3c^2)\right][\xi^2 + \eta^2] + 4Ab^2\theta^2.$$

The perturbation terms, given by $H - H'$, are all small for small displacements of the molecule from its orientation of minimum potential energy.

Let us consider the unperturbed motion of the lamina. The Hamiltonian H' is separable in the coordinates ξ, η, and θ. The wave functions of the unperturbed system can therefore be expressed in the form

$$\Psi = \psi_{n_1}(\xi)\psi_{n_2}(\eta)\psi_{n_3}(\theta)$$

where the ψ's are the usual wave functions for the linear harmonic oscillator; and the energy levels of the unperturbed system are given by the expression

$$E = h\nu_0(n_1 + \tfrac{1}{2}) + h\nu_0(n_2 + \tfrac{1}{2}) + h\nu_3(n_3 + \tfrac{1}{2}), \qquad (3.0)$$

where the n's may have any positive integral values, including zero. Here h is Planck's constant;

$$\nu_0 = (2[A(2b^2 + 3c^2) + Ba^2]/A)^{1/2}/2\pi,$$

and

$$\nu_3 = b(8A/C)^{1/2}/2\pi.$$

We thus see that the lowest energy level of the molecule, for spherical oscillations, is obtained by setting all of the n's in Eq. (3.0) equal to zero; and further that this energy level can be represented by only a single linearly independent wave function. When we take account of the perturbation terms in the Hamiltonian, the lowest energy level retains its nondegenerate character but is perhaps somewhat displaced. The higher levels corresponding to values of n_1 and n_2 greater than zero will be displaced also, but may in addition be separated; since they are degenerate. It is easy to see that these displacements and separations must be very small. For in the case of "oscillation"

the wave functions will be trivially small except for values of ξ, η, and θ very nearly equal to zero; and for these small values of the variables the perturbation terms are very small. Accordingly the energy levels when the perturbation terms are taken account of are not appreciably different in this case of oscillation from the values given by Eq. (3.0), and we shall not undertake to give here an accurate analysis of the amounts of the changes in energy caused by the perturbation terms in the Hamiltonian.

An inspection of the potential energy functions which we have used here, and a comparison of them with such expressions as $V_0(1-3\cos\theta)$ shows that the methods of Pauling and the author, employed in the beginning of this section to find out whether ammonia molecules were rotating or oscillating in the crystalline phase at very low temperatures, may be used for this purpose; although the methods were developed originally only so as to be applicable to the motions of diatomic molecules.

§4. The Values of ${}_1\omega_0$ and of ${}_2\omega_0$

Since the spin of the nitrogen nucleus contributes the same factor to both numerator and denominator of $G_r/{}_r\omega_0$, we may neglect it in these calculations. Consider now the motion of the ammonia molecule when it is in the state of spherical oscillation for which n_1, n_2, and n_3 are all equal to zero, in which all the normal modes of nuclear oscillation are in their lowest quantum states, and in which the molecule is in its lowest electronic state. We must take account of the spins of the hydrogen nuclei. The wave functions in these spins alone are eight in number; there are 4 spin wave functions of symmetry character α and 2 wave functions of symmetry character (γ, δ) each. To find the number of wave functions for the spherical and nuclear oscillations with the various symmetry characters we may consider all of the different sorts of oscillations together. In the lowest state of oscillation there are then six linearly independent wave functions when symmetry properties are neglected altogether; we may denote these six linearly independent vibrational wave functions by the following six diagrams:

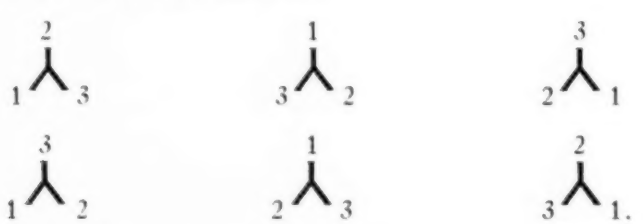

Here the numbers denote the hydrogen nuclei, and the lines indicate the directions in which the hydrogen nuclei must lie, in the base of the pyramidal molecule, if the molecule is to be in its position of minimum potential energy. Thus the upper left figure in the diagram denotes that wave function for which there is a considerable probability of finding the three atoms close to the positions indicated in the figure by the numbers, with but a very small probability of finding them in the positions indicated in the figure below it, for instance.

We have made the plausible assumption that there is only one position and not two positions for the nitrogen nucleus, when the molecule is in its orientation of minimum potential energy. When we take linear combinations of the above wave functions, we find that there are two wave functions with the symmetry character (γ, δ) each, one with the character α, and one with the character β (antisymmetrical in all three hydrogen nuclei). There are still six linearly independent wave functions, as there should be. If the molecule had been free to rotate instead of being in a field of force in a crystal, we should have found but two linearly independent wave functions instead of six, for the vibrations.

Taking account of both spins and vibrations, we wish to find the number of linearly independent complete wave functions, antisymmetrical in the hydrogen nuclei, and capable of representing the ammonia molecule in its lowest vibrational state in the crystal lattice. It follows from the above enumerations and the rules for combining the factors of the complete wave functions given by Dennison,[8] that there are eight of these linearly independent complete wave functions with the symmetry character β in the hydrogen nuclei; and of these 4 represent ammonia molecules of the first variety and 4 represent ammonia molecules of the second variety. We have thus found that ${}_1\omega_0 = {}_2\omega_0 = 4$.

§5. The Vapor Pressure Constant of Ammonia

From §2 and §4 we find that the second term in the right hand member of Eq. (1.92) is equal to log 1/3. We can now calculate i', the vapor pressure constant when pressures are expressed in atmospheres and logarithms are taken to the base 10, by the use of Eq. (1.92). With sufficient accuracy, we take the molecular weight of ammonia to be 17. Following Giauque, Blue, and Overstreet[18] we take $A = B = 2.79 \times 10^{-40}$ CGS units, and $C = 5.47 \times 10^{-40}$ CGS units. We find that the vapor pressure constant of ammonia at ordinary temperatures should be

$$i' = -1.55.$$

This is in satisfactory agreement with the experimental result given by Eucken[19], $i' = -1.50 \pm .04$.

§6. The Entropy of Crystalline Ammonia at the Absolute Zero of Temperature

Taking account of the nuclear spin ($h/2\pi$) of nitrogen, the number of linearly independent wave functions which can represent a gram molecule of crystalline ammonia at the absolute zero[20] if the molecules oscillate in the crystalline phase is

[18] Giauque, Blue, and Overstreet, Phys. Rev. **38,** 196 (1931), who take these values from the work of Badger and Cartwright, Phys. Rev. **33,** 692 (1929), and from the Raman spectral study of Dickinson, Dillon, and Rosetti, Phys. Rev. **34,** 582 (1929).

[19] Eucken, Phys. Zeits. **31,** 361 (1930).

[20] To understand the sense in which the writer uses the expression "entropy at the absolute zero" the reader is referred to the footnote in the author's paper on the vapor pressure constant

$$C = 12^{N/2}12^{N/2}N!/(N/2)!(N/2)!$$

and thus the entropy of a gram molecule of crystalline ammonia at the absolute zero, if we use Stirling's asymptotic expression for factorials and neglect trivial terms, is by the principles of statistical mechanics

$$S_0 = k \log C = R \log 24;$$

where N is the number of molecules in a gram molecule, and where R is the gas constant.

§7. The Change of Entropy Accompanying the Reaction $N_2+3H_2\rightleftarrows 2NH_3$ Between the Crystalline Phases at the Absolute Zero

The entropy of a gram molecule of crystalline ammonia at the absolute zero has just been calculated; the entropy of a gram molecule of hydrogen[1] is $R \log 4+\frac{3}{4}R \log 3$, and the entropy of a gram molecule of nitrogen calculated in the same fashion is $2R \log 3$. Accordingly, when a gram molecule of nitrogen in the crystalline phase at the absolute zero reacts with three gram molecules of hydrogen at the absolute zero in the crystalline phase and yields two gram molecules of ammonia in the crystalline phase at the absolute zero, the decrease in entropy is $(9/4)\ R \log 3$.

§8. The Constant in the Equation for the Equilibrium Constant

If K_p is the equilibrium constant in a homogeneous gas reaction, then[21]

$$\log K_p = \log \{\prod_t p_t^{q_t}\} = -\frac{(Q_p)_0}{RT} + \frac{1}{R}\sum_t q_t (C_p{}^t)_0 \log T + \int_0^T \frac{dT'}{RT'^2}\int_0^{T'} \sum_t q_t (C_p{}^t)_1 dT'' + I.$$

In this equation q_t is the number of gram molecules of the t'th species reacting, with a negative sign for those that disappear when the reaction takes place, and p_t is the partial pressure of the t'th species. $(Q_p)_0$ is the work which must be done to make the reaction go in this sense at constant pressure at the absolute zero, and $(C_p{}^t)_0$ and $(C_p{}^t)_1$ are the constant and variable parts of the specific heat at constant pressure of the t'th species. I is a constant of integration which is not to be confused in this section with the use of I, in previous sections, to denote moments of inertia. Then it is shown in the article which should appear shortly in the *Reviews of Modern Physics* by Fowler and the author that

---

of chlorine, reference 3, on page 352 of that paper; to §4 in the author's paper on the vapors of hydrogen and hydrogen chloride, reference 4; and to the article which should appear shortly in the Reviews of Modern Physics by R. H. Fowler and the author.

[21] R. H. Fowler, "Statistical Mechanics", §7.2.

$$I' = \sum_t \varrho_t i_t' + \frac{1}{R \log 10} \Delta S_0$$

if atmospheres and common logarithms are used; where ΔS_0 is the change in entropy when the reaction proceeds forwards at the absolute zero between the crystalline phases, and where the i''s are the chemical constants which we have investigated in this and other papers.

We have shown that for the reaction $N_2+3H_2-2NH_3$, ΔS_0 is equal to $9/4\ R \log 3$; and the theoretical i''s are for ammonia -1.55; for nitrogen (this will be shown in the article by Fowler and the author referred to above) -0.18; and for hydrogen[1] -3.72. Accordingly we should have for this reaction

$$I' = -7.17.$$

The value given by Eucken,[22] found experimentally, is $I' = -7.04 \pm .10$; which is in fairly satisfactory agreement with our predicted result.

The author wishes to express his appreciation for the interest taken in his work by Professors E. C. Kemble and J. C. Slater. He also wishes to thank the National Research Council for a grant which enabled these investigations to be carried out.

[22] Eucken, Phys. Zeits. **30**, 818 (1929).

SOME THERMAL PROPERTIES OF TANTALUM

By C. L. Utterback and L. A. Sanderman
University of Washington, Seattle

(Received January 29, 1932)

Abstract

Measurements have been made on the total radiation from very pure, well seasoned tantalum from 1000°K to 2220°K. A spectral temperature scale, $\lambda = 0.667\mu$, is given up to 2100°K. The variation of the resistance of tantalum has been measured up to 2600°K and the thermoelectric power of tantalum with pure platinum has been measured up to 692°K.

Total Radiation

THE total radiation from tantalum was measured by using, as a radiator, a wedge shaped piece of the metal as described by Mendenhall.[1] The V-shaped wedge was formed from a tantalum ribbon which was 0.035 cm thick. It was 3.5 cm long, 1 cm wide, and had an opening of 6 degrees. The arrangement of the apparatus used and the method of making observations on radiation have been sufficiently described by one of us[2] that further description is unnecessary. The tantalum used in the experiments here described contained less than 0.2 percent carbon.

Measurements of total radiation were made on five samples of the metal. The results are shown in Fig. 1.

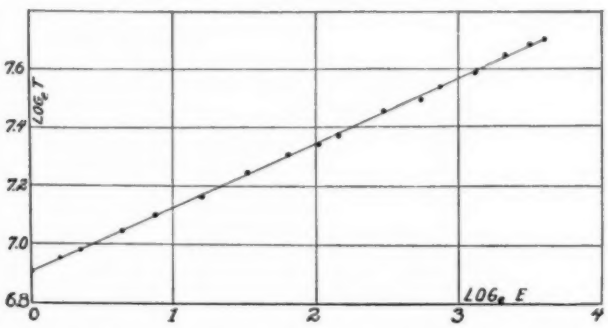

Fig. 1. Logarithmic plot of energy against temperature.

From 1000°K to 2200°K the curve is a straight line. The total emission of energy may be represented by an equation of the form

$$E = cT^n \tag{1}$$

in which the value of n is constant and equal to 4.72 over the range studied. This is not in agreement with the results of Worthing,[3] who finds the value of n to be a constant and equal to 4.80 from 1600°K to 2800°K.

[1] C. E. Mendenhall, Astrophys. J. **33**, 91 (1911).
[2] C. L. Utterback, Phys. Rev. **34**, 785 (1929).
[3] A. G. Worthing, Phys. Rev. **28**, 190 (1926).

Worthing's value of 4.80, for n, however, did not result from a direct observation of the rate of emission of energy and of the temperature. His value of n is dependent upon his value of the spectral emissivity of tantalum and that in turn is determined by the manner in which the spectral emissivity curve is located.[4] In discussing his value of $(T/E)(dE/dT)$, Worthing suggests, since it does not tend toward the theoretical value of 4, with increasing T, that some error might exist in the location of his curve. If such error exists, it will, of course, affect the value of $(T/E)(dE/dT)$, as well as the dependence of $(T/E)(dE/dT)$ on T. In our measurements of total radiation the true temperature of the radiator was directly observed by means of an optical pyrometer, calibrated against a black body held at the palladium point, sighted in the opening of the V-shaped wedge. A decrease of $(T/E)(dE/dT)$ with increasing T has not been found to exist with other metals,[2] except at transformation points where $(T/E)(dE/dT)$ changes abruptly, nor do the present authors find any change in this quantity for tantalum up to 2200°K.

Temperature Scale, $\lambda = 0.667\mu$

Wedge shaped filaments of the same dimensions as described above were used for determining the temperature scale. The apparatus for the total radiation experiments had been provided with two windows at right angles to each

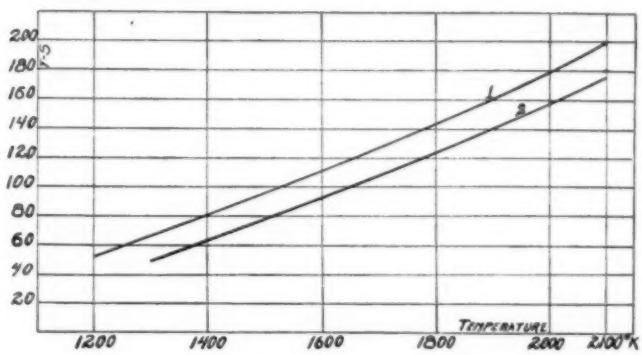

Fig. 2. Tantalum temperature scale, $\lambda = .667\mu$. Curve 1 is drawn from the results given by Worthing. Curve 2 is from those of the present authors.

other so that it could also be used for these measurements. Temperature readings were taken, simultaneously, on the outside face of the V, through one of the windows and in the opening of the wedge through the other. The surface of the metal filament was carefully polished before placing it in the vacuum chamber. It was heated very gradually to incandescence by means of storage batteries. A two stage diffusion pump backed by an oil pump was kept running during the preliminary heating and while making observations. During the observations the filaments showed no pitting. They maintained a good polish during the measurements.

In Fig. 2 the true temperature T is plotted against T-S, where S is the black body temperature of the tantalum. A comparison of curves 1 and 2

[4] A. G. Worthing, Phys. Rev. **28**, 174 (1926).

shows a small difference between our values of T-S and those obtained by Worthing.[4] This difference is slightly greater around 1300°K and 2100°K than at intermediate temperatures. The scale shown by curve 2 is in better agreement with Worthing's scale for tantalum than it is with Mendenhall and Forsythe's[5] scale or with McCauley's[6] scale. In an excellent comparison of tantalum temperature scales, determined before 1926, Worthing suggests that the scale of Mendenhall and Forsythe and the scale of McCauley might be questioned on the ground of lack of "blackness" of the V-shaped wedges used by these experimenters. However, in the present work wedges, with a slightly smaller opening than the ones used by Mendenhall and Forsythe, were used with very consistent results which are not greatly different from those of Worthing. It is our experience that open wedge shaped radiators of sufficiently small openings give considerably more consistent and reproducible results than the methods used by Worthing in the determination of the spectral emissivity.

Temperature Coefficient of Resistance

A filament in the form of a No. 24 tantalum wire, of the same purity as the metal used in the wedges, was used for the resistance measurements. The wire, 10 cm long, was mounted in a lamp by means of tungsten seals. Two

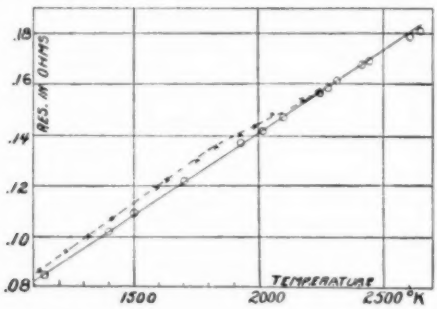

Fig. 3. Variation of the resistance of tantalum with temperature.

potential leads, of No. 36 tantalum wire, of the same purity as the filament, were welded to the filament 3 cm apart. These were connected, through tungsten seals, to a Leeds and Northrup type K potentiometer. The wire was heated by means of storage batteries. The resistance between the potential leads was computed from the current and potential readings. The lamp was evacuated by means of a two stage diffusion pump backed by an oil pump. The pressure in the lamp was maintained at a low value, never exceeding 10^{-6} mm of mercury. The filament was very free from pits and maintained an exceedingly good polish throughout the observation. The black body temperature of the wire was measured, at several points along the wire, with the optical pyrometers and the true temperature computed by means of the tantalum temperature scale previously determined. The results are given in Fig. 3.

[5] C. E. Mendenhall and W. E. Forsythe, Astrophys. J. **37**, 380 (1913).
[6] C. B. McCauley, Astrophys J. **37**, 164 (1913).

The variation in temperature with resistance is fairly well represented by the equation

$$R_T = R_{1000}[1 + \alpha(T - 1000)] \tag{2}$$

for values of T from 1000°K to 2600°K, where α has the value $81.5 \cdot 10^{-5}$. Worthing's[3] data are not sufficient to compare his result with this as his measurements do not extend to temperatures lower than 1600°K. However, if his values of resistivity be extrapolated to 1000°K, and α calculated from his data its value is about $79 \cdot 10^{-5}$. Worthing's measurements on resistivity were made up to 2800°K. He used the same type of lamp, with potential leads from the filament, as was used by the present writers. It was our experience that the lamps begin to blacken a noticeable amount at 2600°K, due to the evaporation of the tantalum and for that reason temperatures higher than this were measured with considerable uncertainty.

In Fig. 3 the dotted line shows the behavior of the resistance before the filament was well seasoned. Each sample of tantalum used in the experiments was heated to 2200°K before measurements were made. All of the filaments mounted in lamps showed an irregular change in resistance between the temperatures of 1700°K and 2200°K before heating to 2200°K. This irregular change in resistance was accompanied by mechanical changes in the wire. An irregular twisting and bending of the wire between supports occurred if the filament was mounted, as it was in some lamps, in the form of a loop or a double loop.

Thermoelectric Power

A piece of seasoned No. 30 tantalum wire was welded to a piece of No. 32 platinum wire and the thermal e.m.f.'s measured at the following temperatures: 19.2°C, 165.2°C, 232°C, 269°C and 419.4°C. The e.m.f.'s at these temperatures were 80, 230, 570, 700 and 1710 microvolts respectively. These values when plotted gave a curve which is represented well by the equation

$$\log_{10} E = A \log_{10} t + B \tag{3}$$

in which the value of A is 2.06 and that of B is -2.16 when E was expressed in microvolts and t in degrees centigrade. This gives a value for dE/dT which varies almost linearly with the temperature.

We extend our thanks for Dr. K. Newbury for aid in making observations.

LETTERS TO THE EDITOR

Prompt publication of brief reports of important discoveries in physics may be secured by addressing them to this department. Closing dates for this department are, for the first issue of the month, the twenty-eighth of the preceding month; for the second issue, the thirteenth of the month. The Board of Editors does not hold itself responsible for the opinions expressed by the correspondents.

Accurate Determination of Excitation Energy by Electron Impact

Science Abstracts 4193, 1931, calls attention to a somewhat inaccessible paper by Whiddington and Roberts[1] on the accurate determination of excitation energy by electron impacts in helium "with a degree of precision not hitherto obtained". In the table given in the abstract the observed values differ from those calculated from spectroscopic data by from two to five times the stated probable error, being always higher. This might well be interpreted as significant.

In view of this fact it is unfortunate that the agreement between observed and calculated values did not receive greater stress in a recent paper by the writer.[2] The excitation losses suffered by electrons scattered inelastically in the forward direction were measured by means of an electrostatic analyzer. Although the experiment yielded values for the energies corresponding to the first two excitation losses in helium, neon, and argon as shown in the published curves, only the values for the principal losses were discussed in the text. The second losses can be determined with almost the accuracy of the first by measuring the voltage difference between the corresponding peaks in the energy distribution curves. The results are summarized in the table.

TABLE I. *A comparison between observed and calculated values for excitation energy losses (in volts).*

Gas	Transition	Observed value	Calc. value	Difference
He	1^1S-2^1P	21.13	21.11	+0.02
He	1^1S-3^1P	23.02	22.97	+0.05
Ne	$1^1S_0-1s_4$	16.64	16.59	+0.05
			(16.6)*	+0.04
Ne	$1^1S_0-2p_8$	18.53	18.48	+0.05
			(18.5)*	+0.03
A	$1^1S_0-1s_4$	11.53	11.56	−0.03
			(11.5)*	+0.03
A		13.88	(13.9)*	−0.02

* Hertz's excitation potential values (see Franck and Jordan, "Anregung von Quantensprüngen durch Stosse", p. 162).

In the designation of the losses in neon and argon, Paschen's notation has been used for the upper terms to avoid unwarranted theoretical implications. The argon $1^1S_0-2p_8$ loss corresponding to Hertz's 13.0 volt excitation potential was not sufficiently probable to be definitely located, and the correct designation for the 13.9 volt loss is not obvious.

The agreement throughout is as good as could be expected with this type of measurement, and the conclusion is that no significant deviation from the spectroscopic values for excitation losses has been detected.

L. C. VAN ATTA

Palmer Physical Laboratory,
Princeton, New Jersey,
February 15, 1932.

[1] Whiddington and Roberts, Leeds Philosoph. and Lit. Soc. Proc. **2**, 201 (1931).

[2] Van Atta, Phys. Rev. **38**, 876 (1931).

Evaporation of Platinum in Vacuum from a Tungsten Filament

Platinum may be evaporated in vacuum at temperatures below the fusion or evaporation temperatures of tungsten. This makes possible the substitution of the evaporation technique[1] for sputtering. Previous attempts to evaporate platinum were unsuccessful be-

[1] R. S. I. **2**, 189 (1931).

cause it was not possible to heat it efficiently when a small piece was simply laid in a tungsten coiled filament. The evaporation is, however, easily effected when platinum is electro-deposited onto the tungsten filament. The citric acid platinum plating solution used near 100°C is satisfactory for this electro-deposition. Best evaporated deposits are obtained when the work is shielded from the hot tungsten filament until after the fusion temperature of platinum has been attained. For the conservation of platinum the filament may be inclosed in a box made from tungsten foil. A window in this box allows the evaporation to be restricted as desired. The platinum deposit on the walls of the box may be dissolved in hot aqua regia or if a copper box is used the platinum may be peeled off in the form of a thin foil.

Mirrors, interferometer plates, fibers, etc., may be coated with platinum by this technique with less trouble and better results than by sputtering.

JOHN STRONG
National Research Fellow,
California Institute of Technology,
Pasadena, California.
February 23, 1932.

Far Ultraviolet Eigenfrequencies of the Alkali Halides

The following preliminary experiments on the proper frequencies of absorption by the lattices of the alkali halides in the far ultraviolet have recently been carried out by the author.

A normal incidence vacuum spectrograph, having a concave speculum grating of one meter radius with a dispersion of 17 A.U. per millimeter, and a "hot spark" for a light source, was used. This apparatus, when using tungsten electrodes and oiled films, gave spectra to about 375A.U.

A. H. Phund (Phys. Rev. **32,** 39 (1928)), by a reflection method was the first to find an eigenfrequeny in the ultraviolet for NaCl and KCl. These frequencies were found to be in the 1600A.U. region, as had been predicted by Herzfeld and Wolf (Handbuch der Physik. Vol. XX).

In an extention of this work, it has been found troublesome to prepare very thin films, which besides being transparent to the region in question are at the same time mechanically strong enough to form a backing for the salt under investigation. The necessity of a thin transparent support for the distilled halide is obviated by vaporizing the salt onto the ruled surface of the grating. This is accomplished by distilling the salt from a conical platinum spiral supported in the vacuum spectrograph about ten centimeters from the grating and just far enough to one side to be out of the light path. Successive thin layers of the salt are vaporized, in this way, onto the grating, while an exposure is made for each thickness. Justification for distilling the salt on the grating is found in the observation that a very thin layer of methyl analine violet on polished speculum shows the characteristic purple transmission of the dye, while a very thick film shows the characteristic green metalic reflection.

The results show:

1. That for the very thinest salt film on the grating there is a slight general enhancement of the entire spectrum from about 1000A.U. to 2000 A.U. while the continuous absorption becomes apparent at about 400A.U.

2. That for the next thickness of salt, the sharp absorption minimum clearly reveals itself in the 1600A.U. region, while the absorption near 400A.U. broadens, extending to longer wave-lengths.

3. That with still increasing salt thickness the minimum around 1600A.U. which is due to absorption disappears, while the reflection maximum comes out rather intensely with a noticeable shift to longer wave-lengths.

4. That there is no separate absorption band at 900A.U. This band was thought to exist as a characteristic of the complete liberation of the extra electron of the negative ion from the crystal lattice.

The present work has been concerned chiefly with sodium chloride. Experiments are now in progress on the remaining alkali halides. These measurements will be checked by studying the absorption of the same salts when they are distilled onto very thin transparent supporting films, so that the true eigenfrequencies for all these substances may be determined.

At the present, the author wishes to stress the value of using this method, i.e., the distillation of the salt onto the grating, as a helpful exploratory means of investigation for similar work in the far ultraviolet. At the present early stage of the experiments, it is

not possible to say whether or not a dispersional phase change at the interface of grating and salt, increasing roughness, and other complications, may be affecting the accuracy of our results.

ALBERT SMITH

Rowland Hall,
Department of Physics,
Johns Hopkins University,
February 23, 1932.

Determination of Small Quantities of Radon and Thoron

In the measurement, by the alpha ray method, of less than 2×10^{-12} curies of radon, the limit of precision is imposed by the small statistical variations in the background of residual ionization due to cosmic and local radiation. Thus in the excellent work of Paneth and Koeck[1] a mean deviation of 3 percent in the background would introduce an uncertainty of 50 percent in the measurement of 10^{-13} curies of radon.

The laws of probability indicate that the mean deviation in the background is between 1 and 4 percent for a one hour reading on an ionization chamber of 1.5 liters volume. This is confirmed by measurements on the apparatus outlined below.

The circuit used is common in other branches of physics, but, to the writer's knowledge, has not heretofore been used for the determination of small quantities of radon or thoron, although it is well adapted to this field. It consists of two ionization chambers, identically constructed, both containing the same background gas (air, CO_2, or other), but only one containing the radon or thoron to be measured. A string electrometer is permanently connected to measure only the difference in the ionization in the two chambers. Hence, within the statistical variations of the background and the radon or thoron, the readings are proportional to the quantity of emanation present. Errors such as those due to contact potentials, stray x-radiation, variations of battery voltage, or movement of radioactive material in the vicinity of the apparatus are also eliminated.

This compensation method is used by the writer to measure the radon and thoron liberated from rocks directly heated in a special graphite furnace, without the use of a carbonate flux, as has heretofore been usual.

ROBLEY D. EVANS

California Institute of Technology
Physics Department,
February 23, 1932.

[1] Paneth and Koeck, Zeits. f. Physik. Chem. Bodenstein Festband, 1931. p. 145.

The Velocity of Sound in a Fermi-Dirac or Einstein-Bose Ideal Gas

In connection with a study of the hydrodynamics, viscosity and heat conduction of a Fermi-Dirac or Einstein-Bose gas, generalizing the methods of Lorentz, Enskog and others, we have noticed the following simple consequences of the virial theorem:

$$pv = \tfrac{2}{3}E_{\text{kin}} \qquad (1)$$

where v is the specific volume and E_{kin} is the kinetic energy per unit mass. We shall consider only gases which consist of point-molecules, so that E_{kin} is also the total energy ϵ. The results we obtain will be valid, like Eq. (1), for all statistics and in all degrees of degeneration. They are perhaps not generally known, and to our knowledge do not appear in the literature.

An immediate *thermodynamic* consequence of (1) is, that for an adiabatic change:

$$\epsilon v^{2/3} = \text{const.} \qquad (2)$$

This equation follows also from the fact that for an adiabatic change the number of molecules n_i in the different translational energy levels ϵ_i does not change, and that the ϵ_i are inversely proportional to $v^{2/3}$. Therefore $\epsilon=\Sigma\epsilon_i n_i$ is inversely proportional to $v^{2/3}$. From (1) and (2) follows that the equation of the adiabatic is always:

$$pv^{5/3} = \text{const.} \qquad (3)$$

For no degeneration, that is, when the equation of state becomes the Boyle-Gay Lussac law, this reduces to the well-known expression, because in this limiting case $c_p/c_v=5/3$ for point molecules.

A second thermodynamic consequence of Eq. (1) is that ϵ must have the form:

$$\epsilon = \frac{3}{2}\frac{RT}{M}W(Tv^{2/3}) \qquad (4)$$

where M is the molecular weight. This follows from the general equation:

$$\left(\frac{\partial\epsilon}{\partial v}\right)_T = -p + T\left(\frac{\partial p}{\partial T}\right)_v.$$

Substituting Eq. (1), and introducing W as new dependent variable, one obtains for W the partial differential equation:

$$\left(\frac{\partial W}{\partial v}\right)_T = \frac{2}{3}\,\frac{T}{v}\left(\frac{\partial W}{\partial T}\right)_v$$

of which the general solution is, that W is an arbitrary function of $Tv^{2/3}$. From (4) and (2) follows, that for an adiabatic change also:

$$Tv^{2/3} = \text{const.} \qquad (5)$$

Thus W itself is an adiabatic invariant.

Perhaps the most remarkable consequence of these equations is, that the velocity of sound (neglecting heat conduction and viscosity) in a gas of point molecules for all statistics and for all degrees of degeneration is given by:

$$C = \left(\frac{5}{3}\,\frac{p}{\rho}\right)^{1/2} \qquad (6)$$

when ρ is the density. This result follows immediately from the general formula:

$$C = \left(\frac{dp}{d\rho}\right)^{1/2}_{\text{adiab.}}$$

and Eq. (3). We were led to Eq. (6), when we observed that the derivation of the equation for the velocity of sound from the hydrodynamical equations in first approximation does not require the introduction of the equation of state. One uses only the virial theorem (1). In the case of no degeneration, that is for large values of $y = Tv^{2/3}$, W approaches unity. Then, and only then, the velocity C becomes a function of the temperature alone.

G. E. UHLENBECK
E. A. UEHLING

Department of Physics,
University of Michigan,
February 25, 1932.

Excited Electronic States of Li_2

The writer has recently made a Heitler-London calculation of those states of Li_2 which dissociate into a 2^2S atom and a 2^2P atom.[1] Of these eight states there are only two, namely $^1\Sigma A^N$ and $^1\Pi S^N$, which can make transitions to the ground state and hence are readily amenable to observation. Both are known to be attractive and their molecular constants have been accurately determined.[2] In the above calculation the $^1\Pi S^N$ state is found to be repulsive, in definite qualitative disagreement with experiment. The purpose of this note is to describe a revision of the calculations for this state.

Using the notation of the previous paper, one can choose two-electron product functions Ψ_i for the present case in such a way that the energy expressions for the states of various symmetries are of the same form as those found previously, and one then finds:

$$H_{11}' = J(pp; ss); \quad H_{21}' = J'(sp; sp);$$
$$N_{11} = 1; \qquad N_{21} = S_{ps};$$
$$H_{31}' = J'(pp; ss); \quad H_{41}' = J(sp; ps)$$
$$N_{31} = S_{pp;ss}; \qquad N_{41} = 0.$$

One would expect to obtain qualitative results by taking for the atomic p function simply the s function with a suitable surface harmonic affixed.[3] If this is done one can easily obtain the energies, since the needed integrals have already been tabulated. The $^1\Sigma A^N$, $^1\Sigma S^N$, $^3\Sigma S^N$, and $^3\Pi S^N$ curves all come out markedly attractive, and the $^1\Pi A^N$ has a slight minimum far out. The other states are repulsive, and the $^3\Sigma A^N$ shows erratic behavior similar to that shown in the case of Be_2 by $^3\Sigma S^N$. The $^1\Sigma A^N$ has heat of dissociation 1.29 volts and internuclear distance 2.55A in good agreement with the experimental values[2] of 1.25 volts and 3.13A. For the $^1\Pi S^N$ we compare calculated values with readings from a curve drawn from the experimental results, and obtain ($\alpha = \kappa R$, $\kappa = 1.26$):

$\alpha =$		3	4	5
$(E-E_0)/\kappa$	calc.	0.196	0.083	0.036
	obs.			+0.010

6	7	8	9	10
0.0186	0.0124	0.0111	0.0102	0.0097
−0.021	−0.027	−0.024	−0.017	−0.013

There is complete disagreement between the two curves.

The revision of the calculation consists in the use of a more accurate atomic $2p$ function

[1] See end of article by Furry and Bartlett, Phys. Rev. **39**, 210 (1932). This paper must be seen for notation used here. Symmetry designations for Σ states are in sense of correction at end, not of body of paper.

[2] Loomis and Nusbaum, Phys. Rev. **38**, 1447 (1931).

[3] Assumption tacitly made in previous article (reference 1). Its success here for the $^1\Sigma A^N$ state tends to justify its use for Σ states of Be_2.

obtained from the variation method. Following Guillemin and Zener,[4] we take for the 1*s* wave function $u_{1s}=c'e^{-\gamma r}$, $\gamma=z-(5/16)$, and for the 2*p* functions $c_2 r^{n^*-1}e^{-\delta r}\cos\theta$ and $c_1 r^{n^*-1}e^{-\delta r}\sin\theta\, e^{\pm i\Phi}$, where δ and n^* are parameters subject to variation. In the notation of Guillemin and Zener the energy expression is

$$E-E_k=\Delta_2{}^2-Zs_2{}^2+2k_{12}{}^{12}-k_{22}{}^{11}$$

accuracy. The remaining contribution to $j(11;ss)$ was computed from a table of A_n and B_n made up for fractional arguments. For $j'(s1;s1)^{(1)}$ a few $w_1(m, n, \alpha)$ were obtained for suitable arguments by graphical interpolation of certain functions of their logarithms. The integrals with superscript 2 are so small that we can regard them as unchanged. We then have the values given in Table I.

TABLE I

$\kappa R=\alpha=$	3	4	5	6	7	8	9	10
$S_{11}{}^{1/2}=$	0.8670	0.7720	0.6761	0.5778	0.4853	0.4014	0.3269	0.2621
$J(ll;ss)/\kappa=$	0.1702	0.0616	0.0212	0.0049	−0.0002	−0.0017	−0.0016	−0.0013
$J(sl;ls)/\kappa=$	0.0594	0.0518	0.0448	0.0368	0.0302	0.0244	0.0196	0.0157
$J'(sl;sl)/\kappa=$	0.0530	0.0434	0.0327	0.0239	0.0168	0.0110	0.0071	0.0045
$\{J'(ll;ss)$ $-j'(ll;ss)\}/\kappa$ $=$	−0.1557	−0.2123	−0.1967	−0.1572	−0.1155	−0.0796	−0.0521	−0.0329

Taking $n^*=2$, one obtains:

$\delta=$	0.51	0.52
$E-E_\kappa=$	−0.25533	−0.25547

$\delta=$	0.53	0.54
$E-E_\kappa=$	−0.25543	−0.25522

The minimum is not far from $\delta=0.525$. The adjustment of n^* is more difficult, since $k_{22}{}^{11}$ cannot be written in closed form for non-integral values of n^*. For nearly integral values a careful use of approximation methods gives ample accuracy, and for $\delta=0.525$ one obtains:

$n^*=$	1.9	2.0	2.1
$E-E_\kappa=$	−0.25536	−0.25547	−0.25422

The minimum occurs at a value of n^* quite near to, but slightly less than, 2. The result is exactly like that found by Guillemin and Zener for the 2*s* function. One must take $n^*=2$ to make the molecular calculations feasible.

The experimental value of the energy of the 2^2P state is −0.261. Thus the discrepancy is about $0.006Rh$, which is the same error as found by Guillemin and Zener for the ground state. There is good agreement of δ with $(-(E-E_K))^{1/2}$, and the values found are almost equal to the hydrogenic ones, i.e., $n^*=2$, $\delta=0.5$.

Writing $\delta=\kappa'/2$, we have $\kappa'=1.05$, which is just 5/6 of the value of κ in the *s* function. The integrals needed for the calculation of the II states are $S_{11}{}^{1/2}$, $I(11)$, $I'(11)$, $j(11;ss)$, $j(s1;1s)$, $j'(s1;s1)$, $j'(11;ss)$. Of these $S_{11}{}^{1/2}$, $I(11)$, $I'(11)$, $j(s1;1s)$, and the large contribution to $j(11;ss)$ are the same in form as in the previous work,[1] but require changes in scale to allow for the new exponential in the *p* function. Graphical interpolation gave sufficient

The values of $J(11;ss)/\kappa$, $J(s1;1s)/\kappa$, and $J'(s1;s1)/\kappa$ for the larger values of α do not differ much from those obtained with $\kappa'=\kappa$. The curve for $\{J'(11;ss)-j'(11;ss)\}/\kappa$, however, lies appreciably lower. Thus if $j'(11;ss)^{(0)}$ were smaller than its value for $\kappa'=\kappa$ we might get agreement with experiment. Being much harder to compute than the other integrels, $j'(11;ss)^{(0)}$ was calculated first at only two points. Since these show the curve for ${}^1\Pi S^N$ to be definitely repulsive, further calculation is not needed.

The integral $j'(11;ss)^{(0)}$ must be evaluated in terms of the quantities $H_0(m, n, \alpha_1, \alpha_2)$ described by Zener and Guillemin.[5] The computation of these functions for $\alpha_2\neq\alpha_1$ is quite laborious. It was found convenient to calculate $j'(11;ss)^{(0)}$ at the values $\alpha=6$ and $\alpha=9.6$.[6]

$\alpha=$	6	9.6
$j'(ll;\ ss)^{(0)}/\kappa$	0.1109	0.0259

Then at $\alpha=6$, $J'(11;ss)/\kappa=-0.0448$, and at $\alpha=10$, $J'(11;ss)/\kappa=-0.013$ approximately. One finds for the energy

$\alpha=$	6	10
${}^1\Pi S^N/\kappa=$	0.0153	0.006

These values are somewhat lower than the results of the preliminary calculation with $\kappa'=\kappa$, but the curve is still decidedly repulsive.

Thus it is shown that a straightforward application of the simple Heitler-London method

[4] Zeits. f. Physik **61,** 199 (1930).

[5] Phys. Rev. **34,** 999 (1929).

[6] I wish to thank Mr. C. E. Ireland for placing at my disposal numerical results which aided in calculating the integral at these points.

cannot give qualitatively correct results for the $^1\Pi S^N$ state of Li_2. For an adequate theory of the electronic states of molecules we must look to the development of other methods, that recently introduced by Hylleraas[7] being perhaps the most promising.

WENDELL H. FURRY

University of Illinois,
February 25, 1932.

[7] Hylleraas, Zeits. f. Physik **71,** 739 (1931).

Relative Abundance of the Isotopes of Lead in Uranium Bearing Minerals

According to Kopfermann[1] the spins of the isotopes of lead descended from uranium (206), actinium (207), and thorium (208) are respectively 0, $\frac{1}{2}$, 0. This is in agreement with the results obtained by us in the visible as well as in the ultraviolet. We have obtained Lummer[2] patterns on the same photographic plate showing the relative positions of the h.f.s. components of ordinary nonradioactive lead and of the single lines due to the 206 isotope. In this way the component which must be ascribed to this isotope in the pattern of ordinary lead can be definitely identified. Accepting Kopfermann's conclusion about the spin of 208 and Aston's[3] estimates of the relative abundances of the isotopes, the strongest component of the patterns observed by us for nonradioactive lead must be ascribed to the Thorium lead isotope.

Strong exposure to the Paschen lamp source used for uranium lead brought out also some of the components of the 207 and perhaps the 208 isotopes. The effect was particularly marked for the 4244.99A line of Pb II because this line may be brought out strongly without reversal. For it the component due to 208 does not appear on our plates even though the exposure was sufficiently strong to make the 207 components as heavy as in the comparison pattern for nonradioactive lead taken side by side on the same plate.

This shows conclusively that the ratio of the contents of the 207 to the 208 isotopes is much larger in the uranium bearing minerals (obtained from Belgian Congo) than in ordinary lead. The trace of 207 cannot be due therefore to contamination. This result is in agreement with Aston's[4] observation of the relative abundance of the isotopes of lead separated by C. S. Piggott from uranium bearing Norwegian bröggerite. The sources of the minerals as well as the methods used being different from those employed by Aston, it appears that the association of the actinium decay product with that of the uranium series may be universal and that the relative abundance of the isotopes may be estimated with ease by hyperfine structure observations.

J. L. ROSE
L. P. GRANATH

Department of Physics,
New York University,
University Heights,
New York, N. Y.,
February 26, 1932.

[1] H. Kopfermann, Naturwiss. **19,** 400 (1931); **19,** 675 (1931).

[2] Kindly loaned to us by Professor R. W Wood.

[3] F. W. Aston, Nature **120,** 224 (1927).

[4] F. W. Aston, Nature **123,** 313 (1929).
E. Rutherford, Nature **123,** 313 (1929).

Thermomagnetic e.m.f.'s in Transversely and Longitudinally Magnetized Wires

Recently C. W. Heaps[1] in referring to an article by Willaim H. Ross,[2] has pointed out that, in addition to the thermo-junctions formed by the transversely and longitudinally magnetized parts of the wire used in Ross' experiment, there will also be present junctions of magnetized and unmagnetized material where the two long ends of the wire extend from the region between the poles of the magnet into the region outside which is practically unmagnetized. He also pointed out that Ross' results were partly due to these additional junctions which would be at different temperatures due to the conduction of heat along the wires.

From experiments performed in this laboratory it has been found that the effect of these two additional junctions may be considerable. The three set-ups shown in Fig. 1 were used: (a) This is the same type of arrangement as that used by Ross. A wire, bent in a U shape, is placed in a magnetic field so that the length between the two bends is longitudinally magnetized and the leads extending away from the magnet are transversely magnetized. The

[1] C. W. Heaps, Phys. Rev. **38,** 1391, 1931).

[2] William H. Ross, Phys. Rev. **38,** 179, (1932).

bends are kept at different temperatures designated by H, hot, and C, cold, Fig. 1. (b) A single wire is placed between the poles of a magnet and at right angles to the field, so that the part of the wire lying in the field is magnetized while the ends extending away from the magnet are practically unmagnetized. A temperature difference was maintained at the junctions between the magnetized and unmagnetized parts of the wire. (c) This is similar to (b) except that the wire is longitudinally magnetized. For this set-up pole pieces with holes bored through them were used.

Referring now to (a), we can readily see that in addition to the e.m.f. due to the longitudinally and transversely magnetized junctions, there will be an e.m.f. due to the magnetized-unmagnetized junctions at A and B Fig. 1, which may be comparatively large since the length of wire from H to A and C to B is small.

In taking the data in the above experiments two readings were observed for each tabulated e.m.f. The first was taken without a magnetic field; the second with a field present. When no magnetic field is present the e.m.f.

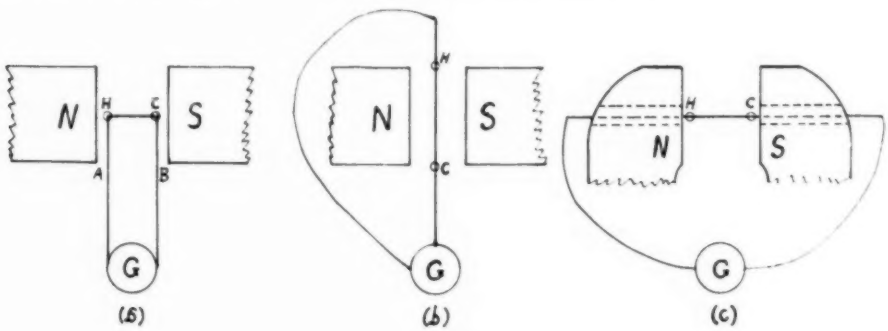

Fig. 1.

Data were taken for nickel, iron and permalloy for all three set-ups, and the curves obtained by plotting e.m.f. with field strength for each specimen were different for each arrangement.

In (b) and (c) Fig. 1 it was found that when the points which were maintained at the temperatures H and C, were moved away from the magnet the e.m.f. was decreased. This, of course, was to be expected since the temperature difference at the magnetized and unmagnetized junctions is then less. However, a considerable amount of e.m.f. is still present even when these points are moved some distance away from the magnet. For example, when the points H and C were each 20 cm away from the edges of the magnet, the e.m.f. was found to be about one-eighth as great as that produced when H and C are as shown in (b) and (c), i.e., close to the magnet.

observed is that due to the Thomson effect in the wire. The e.m.f. tabulated was taken as the difference between the first and second readings. It is to be noticed that Ross' curve for iron shows an e.m.f. of 100×10^{-7}, volts at zero field. This leads us to believe that he did not subtract the initial Thomson e.m.f. in his readings, and that his curve does not represent a purely thermomagnetic e.m.f. On the other hand his curve for nickel begins at zero e.m.f. for zero field. This leaves us at a loss as to the interpretation of his results.

Quantitative results for the above experiments will be published later.

ROLAND SCHAFFERT

Department of Physics,
University of Cincinnati,
February 26, 1932.

Solid Solutions of Lead and Tin in Bismuth

In two recent notes[1] Goetz and Fock have given some of the results and conclusions from their investigations on the magnetic properties of single crystals of bismuth and its alloys with lead and tin. In the latter communication it is stated concerning an alloy containing 3 percent tin that ". . . the x-ray

[1] Goetz and Fock, Phys. Rev. **38**, 1569, (1931); Science. **74**, 603, (1932).

analysis of such crystals does not show any difference from the normal Bi-crystal", and another statement of similar character also appears later on. The difference in the atomic radii of these metal atoms caused us to suspect that these statements were but approximations and the following measurements were made to discover if there were any discernable changes in the lattice parameters.

Materials

Bi from Merck with maximum impurities totalling 0.046 including 0.01 percent each of of Pb, Ag and S; Pb from Merck, maximum impurities of heavy metals 0.10 percent; Sn from J. T. Baker containing 0.01 percent Pb. Alloys of bismuth containing 1 percent and 10 percent Pb and 1 percent and 10 percent Sn respectively, were made by melting weighed quantities of the metals in sealed, evacuated glass tubes. The ingots were annealed for seven days at 116°C and filings from each annealed for the same period and temperature also in evacuated tubes. The filings were quenched from this temperature.

X-ray Apparatus

Seeman-Bohlin cameras of the construction devised by Phragmen.[2] These cameras are calibrated empirically against NaCl taking the lattice constant for this substance 5.628A. The measurements resulting in the values reported below were all taken in the cameras recording the most deviated reflections which in these cases give a separation of the $K\alpha$ doublet (Fe radiation) of about 1.8 mm for the outermost reflections used.

The values in Table I were obtained from measurements of the last seven $K\alpha$ doublets. The deviations are the most probable errors of our measurements and not absolute errors. They are therefore not necessarily valid criteria for comparison with the measurements of other workers. However, the agreement between the lattice dimensions of bismuth summarized by Ewald and Hermann[3] and those reported above is entirely satisfactory.

The differences observed in the dimensions of the hexagonal unit are, in our opinion, significant. The nature of the transformation to rhombohedral axes is such as to minimize these difference and hence the discussion following will refer only to the larger unit. It seems safe to say there is a slight but measurable change in the bismuth lattice when the saturated solutions of Pb or Sn in this metal are formed. The most striking fact in the above table is that the a axis decreases and the c axis increases which would therefore increase the anisotropy of the metal. This fact is possibly of importance in connection with the magnetic anisotropy discussed by Goetz and Fock. In complex structures of this sort the spacing of some planes is influenced much more than others. The effect of solid solution on the bismuth lattice could be seen very strikingly in the reflections from the 119 and 220 planes. Direct film measurements for the α-doublets for these planes are as shown in Table II. It will be seen that the two lines closest together α_2 (119) and α_1 (220) are separated by only 0.3 mm in pure Bi but by 0.7 mm in the alloy. The line width over this portion of the film is about 0.2 mm for intense lines and each of the four lines was clearly separated from its nearest neighbor. A similar behavior was noted with 10 percent Pb. On the films of

TABLE I.

		Bi	10% Pb	10% Sn
Hexagonal axes	a	4.5353 ± 0.0005	4.5331 ± 0.0003	4.5300 ± 0.0006
Hexagonal axes	c	11.836 ± 0.001	11.848 ± 0.006	11.850 ± 0.004
Hexagonal axes	a/c	2.610	2.614	2.616
Rhombohedral axes	a	4.735 ± 0.001	4.738 ± 0.002	4.737 ± 0.002
Rhombohedral axes	α	57°13.7′ ± 0.5′	57°9.6′ ± 1.6′	57°7.4′ ± 1.3′

TABLE II.

Pure Bi	(119)	α_1	35.1 mm	α_2	35.6	(220)	α_1	35.9	α_2	36.5
10% Sn	(119)	α_1	35.1 mm		35.7	(220)		36.4		37.0

[2] Phragmen, a description of these cameras is given by Westgren. Trans. American Inst. of Min. and Met. Eng'rs., Inst. Metals Div. 1931, p. 13.

[3] Ewald and Hermann, "Structurbericht 1913–1928," Acak, Verlagsges, Leipzig 1931, p. 58.

alloys containing 1 percent of the solute element apparently most or all of this shift had taken place so that the solid solution range cannot be very extensive in either case. On the other hand, these lines showed no measureable change in their relative positions compared with pure Bi on films obtained from alloys of Bi with Mg and Bi with Si.

It was somewhat surprising that both Sn and Pb which have respectively smaller and larger atomic radii than Bi should both affect the Bi lattice in the same way. The volumes of the unit hexagonal prisms are Bi $210.83 \doteq 0.07$A,[3] Bi-Pb $210.85 \doteq 0.11$ and Bi-Sn $210.58 \doteq 0.07$. The decrease in the volume in the Bi-Sn case seems significant and in the right direction. The Bi-Pb results are inconclusive.

These results are presented for their interest in connection with the problem of the magnetic properties of these substances but it is by no means even suggested that the slight variations observed in the lattice constants can account for the whole of the variations in the magnetic properties. The results given above have been obtained on alloys sufficiently high in solute concentration to insure having the solid solution phase saturated. Variations within the solid solution range cannot be measured with the means at present avilable. A new camera of considerably greater resolution and, it is hoped, greater accuracy, is in construction and it is planned to investigate this part of the problem at a later date.

ERIC R. JETTE
FRANK FOOTE

School of Mines,
Columbia University,
New York, N. Y.,
March 2, 1932.

The Infrared and Raman Spectra of CS_2

In a recent note entitled "A new long wavelength absorption band of CS_2" Dennison and Wright[1] have arrived at the conclusion that the fundamental frequencies ν_1, ν_2 and ν_3 of the CS_2 molecule are respectively given as 655.5, 396.8 and 1523. Of these three, ν_1 represents a symmetric mode of oscillation and is observed only in the Raman effect while ν_2 and ν_3 respectively arise from a transverse and a longitudinal motion of the central carbon atom and give rise to intense infrared absorption. These authors interpret the Raman line 795.0 as a harmonic of ν_2. In this connection I should like to draw attention to two earlier communications[2] by me regarding the subject. Two very faint bands were recorded in the Raman spectrum of this substance having approximate frequency shifts 412 and 1577. More reliable measurements on better photographs recently obtained show these frequencies to be 400 ± 5 and 1500 ± 20, and enable them to be identified as ν_2 and ν_3 respectively. It was also pointed out that the Raman lines 655.5 and 795.0 are both strongly polarized and to about the same extent (80 percent). More recent observations on the other hand indicate the Raman line at 400 to be practically unpolarized while the one at 1500 is partially polarized. The observed facts that 795 is inactive in infrared absorption, and strongly polarized in scattering, while ν_2 is intensely active in absorption and unpolarized in scattering do not appear easy to reconcile with the view that one is a harmonic of the other. It is evident from the facts that the two modes of oscillations of the molecule represented by the Raman lines 655.5 and 795.0 are very similar to each other. Designating the latter by the symbol ν_1', we may offer the following scheme for identifying the observed infrared absorptions.

Identification	Frequency (observed)	Frequency (calculated)
ν_2	396.8	—
ν_1	655.5	—
ν_1'	795.0	—
ν_3	1523	—
$\nu_3-\nu_1$	878	867.5
$\nu_3-\nu_1'$	746*	728
$\nu_3+\nu_1$	2179	2178.5
$\nu_3+\nu_1'$	2330	2318

* Observed only by Coblentz in the liquid state.

According to the theory recently developed by Manneback[3] ν_2 and ν_3 should not appear in the Raman effect as the corresponding oscillations would not involve any *first order* variation in either the optical polarizability or the anisotropy of the molecule. That they do appear, though with extreme feebleness, is therefore a fact of great interest.

S. BHAGAVANTAM

Calcutta, (India),
March 4, 1932.

[1] Dennison and Wright, Phys. Rev. **38**, 2077 (1931).

[2] Nature **126**, 995 (1930); Ind. Jour. Phys., **5**, 59 (1930).

[3] Manneback, Zeits. f. Physik. **62**, 224 (1930).

The Constitution of Tellurium

The isotopic constitution of tellurium has been determined by the method previously described.[1] Aston's[2] analysis was confirmed and extended. Additional isotopes of mass numbers 124, 123 and 122 were found with indications of an extremely faint isotope at 127. Fig. 1 is a positive contact print of two mass

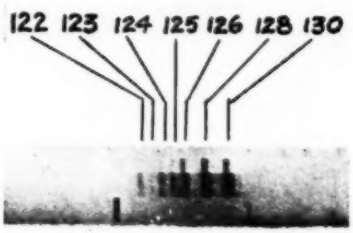

Fig. 1. Mass-spectrum of tellurium.

spectra of tellurium. The two spectra of different times of exposure overlap at the center. All of the isotopes excepting Te^{127} are clearly visible in both spectra on the original plate.

Kahlbaum tellurium was placed in "wells" in an aluminium cathode according to the method described for selenium and cadmium.[1] By controlling the current density in the discharge through neon the rate of evaporation of the tellurium was controlled and a satisfactory source of Te ions was secured.

The relative abundance of the isotopes of tellurium was determined photometrically by means of a Goos and Koch microphotometer. Aston's data for the isotopes 130, 128, 126 and 125 were used to calibrate the plate. The following results were secured.

Mass numbers of isotopes	130	128	127	126	125	124	123	122
Percentage abundance	33.1	32.8	?	19.0	6	4.5	1.6	2.9

The values give a "isotopic moment" of 1.74 and a mean mass number of 127.67. Correcting for a packing fraction of -5.0 and transposing to the chemical scale by subtracting 2.2 parts in 10,000 the atomic weight arrived at is 127.58 ± 0.15, in good agreement with the chemical value 127.5 and considerably lower than the figure 128.03 obtained by Aston.

Te^{121} forms an isobaric triplet with the heaviest isotope of tin and the lightest isotope of xenon. All of the remaining isotopes of tellurium form isobaric pairs.

The writer wishes to thank Professor E. H. Cox and the Department of Chemistry of Swarthmore College for the tellurium used in this investigation.

K. T. BAINBRIDGE
Bartol Research Foundation,
Of the Franklin Institute,
Swarthmore, Pa.,
March 4, 1932.

[1] K. T. Bainbridge, Phys. Rev. **39**, 000, (1932).

[2] F. W. Aston, Proc. Roy. Soc. **132**, 494, (1931); Phil. Mag. **49**, 1197 (1925).

BOOK REVIEWS

Traité de Pyrométrie Optique. Volume 4, Section 5 of Encyclopedie Photométrique. Gustave Ribaud. Pp. 485+xvi, figs. 163, tables 72. Revue d'Optique, Paris, 1931. Price 95 francs.

This volume is one of 27 which form L'encyclopédie Photométrique. Despite the title, the author has included in his scope the whole of radiation pyrometry. However, the greater and much the more important part relates to optical pyrometry.

In preparing this volume, the author has had in mind (1) the essentials of optical pyrometry, (2) the theory underlying its instruments and descriptions of them and (3) a complete bibliographic study of numerous results which have been obtained. With the possible exception of the omission of the mathematical development of radiation laws, which the author has thought to be outside his bounds, he has kept to his plan remarkably well, and produced an excellent book. His account of published results is especially commended as accurate and generally exhaustive, though for some reason, stellar pyrometry, other than that of the sun, has been omitted. It is unfortunate, for completeness' sake, that this volume could not include the author's most recent work on flame temperatures.

The chapter headings somewhat abridged, are, (1) High temperature pyrometry, (2) Radiation nomenclature and definitions, (3) Optical properties of bodies, (4) Laws of black body radiation, (5) Experimental verification of black body laws, (6) Monochromatic emissivities (emissive powers), (7) Color temperatures, (8) Energy radiance of non-black bodies, (9) Light emission by non-black bodies, (10) Monochromatic optical pyrometers, (11) Spectropyrometry, (12) Effective wave-lengths, (13) Choice of colored glasses for optical pyrometry, (14) Neutral absorbing glasses, (15) Realization of black bodies, (16) Realization of black bodies at melting points of metals, (17) Study of monochromatic pyrometers, (18) Disappearing filament pyrometers, (19) Standard Lamps with ribbon filaments, (20) Fixed points, (21) Total radiation pyrometers, (22) Radiation and pyrometry of some light source.

It is the most complete book of its kind which has been published. No worker in the high temperature field can afford to be without it.

A. G. WORTHING
University of Pittsburgh

The Principles and Practice of Geophysical Prospecting. Edited by A. B. Broughton Edge and T. H. Laby. Pp. 372+xiii, figs. 261. Cambridge Press, London, 1931. Price 15 s. net.

This volume contains the report of the Imperial Geophysical Experimental Survey, a project financed by the British Empire Marketing Board and the Commonwealth Government, and set up for the primary purpose of testing the practical value, under a variety of geological conditions, of the principal methods of geophysical prospecting. The Survey conducted field trials in various parts of southern and eastern Australia, as well as in Tasmania, much of the work being done in regions where existing mining and drilling records made possible a definitive test of the geophysical work.

The volume is divided into two parts. In Part I, which forms about two-thirds of the book, emphasis is given to the actual field investigations of the survey, the explanations of method being upon a sufficiently elementary level to make the exposition practical for geologists an engineers who do not have specialized training in geophysics. Part II, which forms the remaining third of the book, rehearses the same general topics covered in Part I, but forms, so to speak, a technical supplement for the specialist. Part II includes, for example, detailed explanations of field procedure, technical points relating to apparatus design, and a considerable amount of detailed theoretical development.

Part I contains an introductory chapter; Chapter II, devoted to electrical methods; Chapter III on electrical surveys in Australia; Chapter IV, on gravimetric methods; Chapter V, on magnetic methods; and Chapter VI, on seismographic methods. Part II contains four chapters

devoted, respectively, to electrical, gravimetric, magnetic, and seismographic methods. A chapter on general conclusions closes the book.

A considerable number of able English investigators took part in conducting this survey and in preparing the report. The volume reports the most considerable and most unprejudiced series of tests which geophysical methods have as yet received. The book contains, moreover, the clearest, most accurate and most able exposition of geophysical principles so far published. It has, of course, its limitations. These are perhaps most keenly felt in the sections relating to electromagnetic methods. This difficult and complex subject does not lend itself to brief or elementary exposition. The field workers, moreover, seem to have had too small experience with this method to make their conclusions authoritative. On pages 68 and 69, for example, it is recorded that, at 500 cycles per second, measurements could not be made at a greater distance than 500 feet from a large vertical loop over 100 feet long and 45 feet high. The reviewer is acquainted with successful low-frequency work, done in this country, at very much greater distances and with a very much smaller loop.

The volume is attractively printed, with a large number of figures, charts, tables, and maps. Everyone interested in this important new application of physics will wish to consult this book. It differs from most earlier reports in being, first of all, scientifically competent; and secondly, in being free from the taint of commercial secrecy.

WARREN WEAVER
Rockefeller Foundation

The Kinetics of Homogeneous Gas Reaction. Louis S. Kassel. Pp. 330, figs. 25. The Chemical Catalog Co., Inc., New York, 1932. Price $6.50.

In this monograph all of the more important contributions to the rapidly growing field of the kinetics of gas reactions are presented and analyzed. The first third of the book is devoted to a theoretical discussion of possible reaction steps, from the viewpoint of classical statistical mechanics and the newer quantum mechanics. Practically all of the available experimental material is quoted in the latter part of the book. Wherever possible, these experimental results are interpreted in terms of the methods discussed in the first section. It is worth noting, that these interpretations frequently differ from those given by the authors of the articles quoted. The treatment is definite and critical throughout.

Both because of its completeness and because of its critical analyses, this book should prove interesting and stimulating to readers interested in any phase of the subject.

ROBERT LIVINGSTON
University of Minnesota

Critique of Physics. L. L. Whyte. Pp. 196+xi. W. W. Norton and Co., Inc., New York, 1931. Price $3.00.

This is a most unusual sort of book; in it the author describes the properties which the all-inclusive physical theory that he would like to formulate would have if only he were able to formulate it. This may seem like putting the cart before the horse, or at least like forcing undesired confidences upon the reader, but the surprising thing is that it proves both suggestive and stimulating, and this even although the reader may totally disagree with some of the fundamental points of view. For example, I suppose that many would not agree that the ideal is a deductive theory, building up its edifice by logical processes from a small number of simple axioms. Disagreement on even such fundamental matters will not lessen the stimulus that the reader will find, for example, in the many shrewd observations on the general characteristics and the unsatisfactory features of physical theory as we now have it. In particular, every student of relativity should make himself familiar with the features of the theory which the author finds unsatisfactory; personally I find myself in much sympathy with the position that the inability of relativity theory to specify the structure of a clock is indicative that it cannot be an ultimate theory in the sense that many have supposed. This leads to one of the main characteristics of the theory for which the author seeks, namely that it must dispense with the four generalized coordinates at present thought so fundamental. Another important demand made of the desired theory is that it shall contain no arbitrary numbers. A consequence is that every-

thing must be reduced to a single basic length, in terms of which such constants as the velocity of light, the gravitational constant, and Planck's h can be expressed by means of completely defined mathematical functions.

The reader will doubtless find himself pausing to speculate why it is that all the keenness of observation of the author has been sterile in suggesting to him a more specific form of the desired theory. Possibly a suggestion may be found in a fundamental postulate that has to be made to justify the search at all, namely that experimental knowledge has now reached a certain finality, or at least a self-sufficiency, so that it is probable that we have in our hands all the vital fundamentals. The announcement on the front page of yesterday's paper of the experimental discovery of the "neutron" suggests the everlasting danger of any such position.

However, when all is said and done, and whether or not one agrees with either minor or major positions of the author, I believe that here is a most important contribution to what I am coming more and more to feel is the irreducible prerequisite to any real progress in understanding, namely a more vital self-consciousness and a more searching analysis of what it is that we do in dealing with the world about us.

P. W. BRIDGMAN
Harvard University

James Clerk Maxwell, A Commemoration Volume, 1831–1931. Essays by Sir J. J. Thomson, Max Planck, Albert Einstein, Sir Joseph Larmor, Sir James Jeans, William Garnett, Sir Ambrose Fleming, Sir Oliver Lodge, Sir R. T. Glazebrook, Sir Horace Lamb. The Macmillan Company, New York and Cambridge University Press, England, 1931. Price $2.50.

In his "Portraits in Miniature" by the late Lytton Strachey, we have delightful character sketches of six English historians, each by the same master-artist. In the volume here under review, we have just the converse, namely, ten differenct sketches of the same man each by a different artist of outstanding ability.

The first portrait is by one of Maxwell's successors and a fellow Trinitarian, Sir J. J. Thomson. Here is told the story of Maxwell's student days, his marriage, his several professorships, his academic friendships, the foundation of the Cavendish Laboratory, the publication of his *Matter and Motion*, the preparation of his great *Treatise*, and his work on the *Electrical Researches* of Cavendish. So much has been said about Maxwell's religious views that it is interesting to find Thomson quoting the following sentence from Maxwell; "I think the results which each man arrives at in his attempts to harmonize his science with his Christianity ought not to be regarded as having any significance except to the man himself and to him only for a time".

Speaking of Maxwell's theory of the electromagnetic field, Thomson estimates this as "his supreme contribution to physics" and adds "It got very little support outside a small group of young Cambridge men". Americans may derive some satisfaction from knowing that one of these outside supporters was Professor Rowland who during the whole of his life at Johns Hopkins was an enthusiastic expositor of the electromagnetic theory of light: so also was Helmholtz in Berlin where many American students including Magie, Brace, Keeler, Ames, Pupin, and Webster were hearing him. Science knows no national boundaries; yet it is interesting to recall that Maxwell's theory of Saturn's rings—his first serious work—was experimentally confirmed by James Keeler at the Allegheny Observatory in 1895.

The next two portraits are by eminent mathematical physicists of Berlin who, I imagine, by almost universal consent, are to be reckoned as peers of Maxwell himself, Planck and Einstein. In estimating the various parts of Maxwell's work, one is not surprised to find Planck saying that; "In the field of electrodynamics his genius stood alone"; and that his "success must be numbered among the greatest of all intellectual achievements".

A single sentence from Einstein's estimate will perhaps serve to characterize his entire sketch; " . . . before Maxwell Physical Reality, in so far as it was to represent the processes of nature, was thought of as consisting in material particles, whose variations consist only in movements governed by partial differential equations. Since Maxwell's time, Physical Reality has been thought of as represented by continuous fields, governed by partial differential equations, and not capable of any mechanical interpretation".

Sir Joseph Larmor has given us more than a picture of the great Scotsman; for, in his ad-

dress on "The Scientific Environment of Clerk Maxwell", we have almost an international portrait gallery of modern physicists. Here the reader will find Eddington, Einstein, Dirac, Bohr, Planck, de Broglie, Schrödinger, G. P. Thomson, R. H. Fowler, G. E. Hale, Michelson, the Braggs, Aston, McLennan, Richardson, Zeeman and others sketched with rare lightnes of touch, in few but accurate lines.

"Perhaps in no domain of science," says Larmor "has the neglect of history been more conspicuous than in physics". Let us hope that the volume under review and the alliance of science and history, such as was seen last summer in London, will do much to remedy this situation.

In Sir James Jean's account of Maxwell's method one is impressed by statements such as the following; "No matter how clearly he saw physical concepts in his mind's eye he never made the mistake of identifying them with ultimate physical reality. He saw too deeply into things ever to imagine that what he saw was the ultimate stratum of all—final and absolute truth."

The other five portraits are by Sir Oliver Lodge and four of Maxwell's students. On almost every page of what these students have to say, comes out the lovable character of their wonderful teacher. Sir Horace Lamb's amusing account of Maxwell's inaugural lecuture at Cambridge, of his pet toy, the dynamical top, and of the ophthalmoscope with which he employed his favorite dog as a subject, must be read in order to be appreciated. The entire volume is indeed a beautiful example of that mastery of good English style which one finds among British men of science. The book is certainly one which no serious student of physics can afford not to own.

HENRY CREW
Northwestern University

Das Kausalgesetz und seine Grenzen. Philipp Frank. Pp. 308+xv, figs. 4. Verlag von Julius Springer, Wien, Austria, 1932. Price RM. 18.60.

This book is an excellent historical and critical study of the concept of causality in the classical mechanics of particles and of continuous media, in electromagnetic theory, in classical kinetic theory, in quantum mechanics. The author, continuing the tradition of Mach, seeks to eliminate all metaphysical and theological elements from physical theory. He describes the goal of physics as the prediction of new experiences on the basis of given experiences. Scientific description begins with the assignment of symbols to immediate experience. The equations of physics express relations between symbols, so that from a set of symbols which are assignable to immediate experience, one can deduce the symbols which may be interpreted as denoting experiences at some future time. He finds that general principles tend to be transformed into definitions. Thus, the more general the form of a principle of causality, the less it asserts about the real world.

This abstract view of physics, which has also been set forth by Schlick and his group in Vienna, by Swann, by Dirac, receives one of its clearest and most forceful expositions in the present book.

Inasmuch as Professor Frank is well known as one of the editors of the new Riemenn-Weber, it is unnecessary to stress the expertness with which the fundamental concepts of physics are discussed. But the author is also a competent critic of philosophy and of the methodology of biology and sociology. He is unrelenting in his criticism of the tendency to base theological and moral speculations upon physics.

The book is non-mathematical, clearly written, very readable. It is an outstanding contribution to the methodology of physics.

V. F. LENZEN
University of California, Berkeley

AUTHOR INDEX TO VOLUME 39

References with (A) are to abstracts of papers presented at meetings of the Physical Society and references with (L) are to Letters to the Editor.

Ahlberg, J. Elston and Simon Freed. Specific heat and electronic activation in crystals—540(L)

Albertson, Walter. On the classification of certain lines of radium—385(L)

Allen, C. W. Broad lines in the arc spectrum of copper—42

——— Intensity of quartet lines in the arc spectrum of copper—55

Almy, G. M. and C. D. Hause. Band spectrum of potassium hydride—178(A)

Angus, W. Rogie. Diamagnetic susceptibility of the rare gas atoms according to Slater's method—844(L)

Ashley, Muriel (see Jenkins, F. A.)—552(A)

Babcock, Harold D. and Wendell P. Hoge. New measurements of the 1,1 band of atmospheric oxygen—550(A)

Badger, Richard M. (see Woo, Sho-Chow)—932

Bailey, C. R. and A. B. D. Cassie. Molecular configuration of N_2O—534(L)

Bainbridge, Kenneth T. Isotopic constitution of zinc—847(L)

——— Constitution of tellurium—1021(L)

Ballard, S. S. (see White, H. E.)—545(A)

Banta, H. E. The change in thermal e.m.f. produced by a magnetic field—862(A)

Bardeen, John (see Peters, Leo J.)—870(A)

Barnes, R. Bowling. Far infrared transmissions of various solids—870(A)

——— Measurements in the long wave-length infrared from 20μ to 135μ—562

Barreca, Pasquale. On the entropy of the universe—533(L)

Barrett, Charles S. and Carl E. Howe. Distribution of x-ray reflecting power in quartz crystals—177(A)

——— **and Carl E. Howe.** X-ray reflection from inhomogeneously strained quartz—889

Bartlett, J. H., Jr. (see Furry, W. H.)—186(A), 210

Barton, Donald C. Eotvos torsion balance—867(A)

Barton, H. A. (see Richtmyer, F. K.)—176(A)

Bateman, H. Book review—541

Beams, J. W. A simple ultracentrifuge—858(A)

Bear, Richard S. (see Spedding, Frank H.)—948

Bearden, J. A. Wave-length of the molybdenum and copper K series—860(A)

——— X-ray wave-lengths by the dispersion in quartz—1

Beardsley, Niel Freeborn. Approximate calculation of the lower energy levels of the carbon atom—913

Beck, Carl A. Hall effect on induced currents in circular disks of bismuth and antimony—185(A)

Bennett, R. D. (see Compton, A. H.)—873

Bennett, Willard H. Effect of the target on breakdown in cold emission—182(A)

Benz, Carl (see Poulter, Thos. C.)—190(A)

Bhagavantam, S. Infrared and Raman spectra of CS_2—1020(L)

Birge, Raymond T. Calculation of errors by the method of least squares—551(A)

——— Probable values of e, h, e/m and α—547(A)

Bitter, Francis. On the detection of inhomogeneities in the magnetization of iron—185(A)

——— On the interpretation of some ferromagnetic phenomena—337

——— On the verification of the theory of magnetization of single crystals—371

Bleakney, Walker. Additional evidence for an isotope of hydrogen of mass 2—536(L)

Boner, C. P. and Marian O. Boner. Generation of combination and harmonic frequencies by linear and non-linear vacuum tube circuits—863(A)

Boner, Marian O. (see Boner, C. P.)—863(A)

Bonner, T. W. Absorption and emission of sodium light by sodium flames—859(A)

Bourgin, D. G. The thin plate—870(A)

Bowen, I. S. Spectra of two and three-valence-electron atoms, Si II, P III, S IV, Si III, P IV and S V—8, 551(A)

Bowers, Harold E. (see Harkins, William D.)—182(A)

Bowie, R. M. (see Carr, P. H.)—858(A)

Bozorth, Richard M. Barkhausen effect: orientation of magnetization in elementary domains—353; discussion—375

——— **and F. E. Haworth.** The shot effect and electrical breakdown in insulators—845(L)

——— **and Linus Pauling.** The crystal structure of magnesium platinocyanide heptahydrate—537(L)

Bradbury, N. E. Absolute values for the mobilities of gaseous ions in pure gases—546(A)

Brady, James J. Photoelectric properties of thin films of rubidium and caesium on silver—546(A)

Bramley, Arthur. Absorption of γ rays—378(L)

——— β disintegration—188(A)

Breit, G. Dirac's equation and the spin-spin interactions of two electrons—616, 870(A)

Brennen, Herbert J. Gravitational explanation of the spectral shift of light from very distant stars—186(A)
——— Method of least squares—189(A)
Brickwedde, F. G. (see Silsbee, F. B.)—379(L)
——— (see Urey, Harold C.)—164(L), 864(A)
Bridgman, P. W. A new kind of e.m.f. and other effects thermodynamically connected with the four transverse effects—702
——— Book review—1023
Brode, Robert B. The collision cross-section of argon atoms for 300 to 2500 volt electrons—547(A)
Brown, S. Leroy. Harmonic analysis of the plate current in a vacuum tube circuit—863(A)
Brown, Weldon G. Fine structure of the visible absorption bands of bromine—190(A), 777
Bryan, A. B. (see Zirbel, N. N.)—857(A)
Byck, Harold T. and I. Esterman. Design of a high-vacuum, high-speed diffusion pump—553(A)

Cady, W. G. Low frequency vibrations in Rochelle salt and quartz plates—862(A)
Campbell, J. S. and W. V. Houston. New determination of e/m from the Zeeman effect—601
Carlson, J. F. and J. R. Oppenheimer. On the range of fast electrons and neutrons—864(A)
Carr, P. H. and R. M. Bowie. Laboratory apparatus for the determination of the acceleration of a freely falling body—858(A)
Cassie, A. B. D. (see Bailey, C. R.)—534(L)
Chambers, Leslie A. (see Gaines, Newton)—862(A)
Christensen, R. J. Soft x-ray critical potentials of beryllium—549(A)
Cioffi, P. P. Hydrogenized iron—363; discussion—376
Clark, H. T. and W. Kohlhagen. Automatic voltage control by means of a photoelectric cell—184(A)
Cohn, Willi M. Note on the origin of continuous cometary spectra—182(A)
——— Some studies of negative point discharges at low pressures—382(L)
Colby, M. Y. X-ray diffraction patterns of mixtures—861(A)
Compton, A. H. Comparison of cosmic rays in the Alps and the Rockies—190(A)
———, **R. D. Bennett and J. C. Stearns.** Ionization by penetrating radiation as a function of pressure and temperature—873
Cook, J. W. (see Silsbee, F. B.)—379(L)
Cork, J. M. Variation in the effective lattice constant of crystals with wave-lengths—177(L), 193
Crawford, F. H. Book review—751
Crew, Henry. Book review—1024
Croup, A. H. Effect of temperature on the absorption bands of benzene and some of its derivatives at low temperatures—178(A)
Dahl, O. (see Tuve, M. A.)—384(L)
Darbyshire, Orrell. Vibrational constants of the ICl molecule—162(L)
Decherd, Loraine and Arnold Romberg. Resistance bridge thermometer—858(A)
Dennison, David M. and J. D. Hardy. Parallel type absorption bands of ammonia—938
DuBridge, Lee A. Further experimental test of Fowler's theory of photoelectric emission—108, 866(A)
——— (see Roehr, W. W.)—866(A)
——— and W. W. Roehr. Photoelectric and thermionic properties of palladium—99
DuMond, Jesse W. M. Possible narrowing of Compton line-breadth by preferentially directed electron momenta in Ceylon graphite—166(L)

Eldridge, J. A. Peripheral x-ray levels of the heavy elements—177(L)
Eliashevich, M. Quantitative study of the quenching of fluorescence and of the transfer of energy in iodine vapor—532(L)
Ellett, A. (see Koenig, H. D.)—576
——— **and Lewis Larrick.** Polarization of resonance radiation and hyperfine structure, the cadmium resonance lines—181(A), 294
Esterman, I. (see Byck, Harold T.)—553(A)
———, **R. Frisch and O. Stern.** Monochromatic de Broglie waves of molecular beams—546(A)
Evans, Robley D. Determination of small quantities of radon and thoron—1014(L)
Evjen, H. M. On the stability of certain heteropolar crystals—675
Ewing, Maurice. Earth-amplitudes in seismic prospecting—868(A)
——— (see Leet, L. Don)—868(A)
Eyring, Henry. Resultant electric moment of complex molecules—746(L)

Faessler, A. (see Goetz, A.)—168(L), 553(A)
Failla, G. Comparison of 700,000-volt x-rays and gamma-rays—176(A)
Fisher, Thomas F. (see Serduke, James T.)—831
Focke, A. B (see Goetz, A.)—168(L), 553(A)
——— **and A. Goetz.** Metamagnetism in Bi single crystals—548(A)
Foote, Frank (see Jette, Eric R.)—1018(L)
Found, Clifton G. and Irving Langmuir. Study of a neon discharge by use of collectors—237
Frank, Amelia. Temperature variations of the magnetic susceptibility, gyromagnetic ratio, and heat capacity in Sm^{+++} and Eu^{+++}—119
Frank, N. H. Thermionic emission and space charge—226
Frazier, Richard H. A precision method for determining the thermal diffusivity of solids—515

Fredrickson, W. R. (see Watson, William W.)—179(A), 765
——— **and William W. Watson.** Spectrum of barium hydride—179(A), 753
Freed, Simon (see Ahlberg, J. Elston)—540(L)
Frenkel, J. On a general method of treating uncomplete systems in quantum mechanics—532(L)
———**and A. Joffé.** On the electric and photoelectric properties of contacts between a metal and a semiconductor—530(L)
Frisch, R. (see Esterman, I.)—546(A)
Fuller, H. Q. (see Loomis, F. W.)—180(A)
Furry, Wendell H. Excited electronic states of Li_2—1015(L)
——— **and J. H. Bartlett, Jr.** Beryllium molecule—186(A), 210

Gabriel, V. Gabrilovitch (see Slichter, Louis B.)—869(A)
Gaines, Newton and Leslie A. Chambers. Further study of effects of intense audio-frequency sound—862(A)
Gans, David M., William D. Harkins and D. A. Wallace. A new Wilson apparatus for the photography of alpha and beta-ray tracks—184(A)
Germond, H. H. Spatial energy decay due to absorbing boundaries—859(A)
Gibson, G. E. Variation with temperature of the continuous absorption of light by diatomic gases—550(A)
——— **and O. K. Rice.** Theory of the continuous absorption of light by diatomic molecules—551(A)
Gingrich, Newell S. Note on the new effect produced by action of x-rays on matter—748(L)
Glockler, George. Book reviews—541
Goetz, A. (see Focke, A. B.)—548(A)
———, **A. Faessler and A. B. Focke.** The magnetic anisotropy of colloidal crystals of graphite—553(A)
———, **A. B. Focke and A. Faessler.** Production of large artificial graphite crystals—168(L)
———, **and R. C. Hergenrother.** X-ray determination of the thermal expansion of Bi single crystals—548(A)
Granath, L. P. (see Rose, J. L.)—1017(L)
Green, J. B. (see Wulff, John)—181(A)
——— **and John Wulff.** Paschen-Back effect of hyperfine structure, I. Thallium II and thallium III—181(A)
Gunn, Ross. On the evolution of a rotationally unstable star—130
——— On the origin of the solar system—311, 858 (A)

Hafstad, L. R. (see Tuve, M. A.)—384(L)
Hardy, J. D. (see Dennison, David M.)—938
——— (see Van Lear, G. A., Jr.)—857(A)
Harkins, William D. (see Gans, David M.)—184(A)
——— Oriented molecules at the solid-liquid interface and its non-specific nature of ordinary adsorption—190(A)
——— **and Harold E. Bowers.** Inner vibrations in molecules from the Raman effect—182(A)
Harris, Roscoe E. New method of determining thermionic work function by photoelectric cell—182 (A)
Hartley, Kenneth. New instrument for measuring very small differences in gravity—867(A)
Harvey, A. (see Jenkins, F. A.)—922
Harvey, G. G. (see Jauncey, G. E. M.)—178(A)
Hause, C. D. (see Almy, G. M.)—178(A)
Haworth, F. E. (see Bozorth, R. M.)—845(L)
Heil, Louis M. Determination of the total electric polarization and the electric moments of certain organic molecules—666
Henry, W. F. (see Rodebush, W. H.)—386(L)
Hergenrother, R. C. (see Goetz, A.)—548(A)
Herlihy, J. (see Williams, S. E.)—802
Herzfeld, Karl F. On the equations of Laplace and Maxwell—497
Heydenburg, N. P. (see Larrick, L.)—181(A), 289
Hidnert, Peter. Thermal expansion of copper alloys—551(A)
——— Thermal expansion of electrolytic chromium—186(A)
——— Thermal expansion of heat-resisting alloys—856(A)
Hill, E. L. Note on the uncertainty principle—187 (A)
——— Book review—750
Hoge, Wendell P. (see Babcock, Harold D.)—550(A)
Holbrook, B. D. Thermal motions of atoms in crystals—177(L)
Hopfield, J. J. Supercooling liquid copper—185(A)
Houston, W. V. Momentum of a moving body in special relativity—548(A)
——— (see Campbell, J. S.)—601
Howe, Carl E. (see Barrett, Charles S.)—177(A), 889
Hughes, A. L. (see McMillen, J. H.)—865(A)
——— **and J. H. McMillen.** Inelastic and elastic electron scattering in argon—585, 865(A)
Hulburt, E. O. Tables of the ionization in the upper atmosphere—977
Hutchisson, Elmer (see Muskat, Morris)—859(A)

Ingersoll, L. R. Geothermal gradient determinations in the Lake Superior copper mines—869(A)

Jakowleva, A. and V. Kondratjew. The ultraviolet absorption spectrum of ozone—533(L)
Jauncey, G. E. M. Note on Woo's paper on the scattering of x-rays by polyatomic gases—561
——— **and G. G. Harvey.** Diffuse scattering of x-rays from sylvine at low temperature—178(A)

Jenkins, F. A. (see Martin, E. V.)—549(A)
——— **and Muriel Ashley.** Nuclear spin of phosphorus from the band spectrum—552(A)
——— **and A. Harvey.** Emission and absorption spectra of BaF—922
——— **and Andrew McKellar.** Mass ratio of the boron isotopes from the spectrum of BO—549(A)
———, **Yale K. Roots and Robert S. Mulliken.** The red CN band system—16
Jette, Eric R. and Frank Foote. Solid solutions of lead and tin in bismuth—1018(L)
Joffé, A. (see Frenkel, J.)—530(L)
Johnson, M. H., Jr. Theory of complex spectra. Part I. Energy levels—197
Johnston, Herrick L. and Margery K. Walker. Raman effect in water vapor—535(L)
Jones, M. T. (see Richtmyer, F. K.)—176(A)

Kaplan, Joseph. Active nitrogen—860(A)
——— Luminescence of solid nitrogen—870(A)
——— New criterion for predissociation—180(A)
Karrer, E. Kinetic theory of the elasticity of highly elastic gels—857(A)
Kennard, E. H. Wave mechanics of radiation and free particles—435
Kennedy, Roy J. and Edward N. Thorndike. Experimental establishment of the relativity of time—871(A)
Kleeman, R. D. On the law of force between the molecules in a liquid or gaseous mixture—871(A)
Knapp, E. J. Effect of transverse magnetic fields on the thermal conductivity of bismuth at low temperatures—550(A)
Knipp, Charles T. Duration of afterglow in nitrogen—181(A)
——— The "flash" in the afterglow of argon with a fixed vacuum—871(A)
Koenig, H. D. and A. Ellett. Direct measurement of mean lives of atomic states—576
Kohlhagen, W. (see Clark, H. T.)—184(A)
Kolthoff, I. M. Book review—850
Kondratjew, V. (see Jakowleva, A.)—533(L)
Korff, S. A. Width of the *D* lines in sodium vapor—549(A)
Kunz, Jakob. Electric oscillations in ionized gases—some remarks on their present theories—183(A)
——— New method for the study of the photoelectric effect of alkali vapors—866(A)
Kurie, F. N. D. On the use of the Wilson cloud chamber for measuring the range of alpha particles from weak sources—865(A)

LaCoste, Lucien. Ruler and chart method of interpreting x-ray oscillation photographs and an application to cerussite—861(A)
Ladenburg, R., S. Levy and G. Wolfsohn. Absolute value of transition probabilities in band spectra—180(A)
Lanczos, Cornelius. Electricity as a natural property of Riemannian geometry—188(A), 716
Lang, R. J. Note on the spectrum of Sb II—538(L)
Langer, R. M. Corpuscular description of electron diffraction phenomena—187(A)
Langmuir, Irving. (see Found, Clifton G.)—237
Laning, W. A., Jr. (see Tykociner, J. T.)—189(A)
Laporte, O., G. R. Miller and R. A. Sawyer. First spark spectrum of caesium (Cs II)—458
——— **and G. E. Uhlenbeck.** The impulse-energy tensor of the Dirac equations—187(A)
Larrick, Lewis (see Ellett, A.)—181(A), 294
——— **and N. P. Heydenburg.** Polarization of mercury resonance radiation—181(A), 289
Lawrence, Ernest O. and M. Stanley Livingston. Production of high speed protons without the use of high voltages—862(A)
Leet, L. Don and W. Maurice Ewing. Velocity of elastic waves in granite—868(A)
Lenzen, V. F. Book review—1025
Lester, O. C., Jr. (see Rosaire, E. E.)—869(A)
Levy, S. (see Ladenburg, R.)—180(A)
Lind, S. C. Book review—543
Livingston, M. Stanley (see Lawrence, Ernest O.)—862(A)
Livingston, Robert. Book review—1023
Locher, Gordon L. Compound photoelectric action of x-rays in oxygen and argon—866(A)
——— Cosmic-ray particles—883
Loeb, Leonard B. Book review—849
Loomis, F. W. Rotational analysis of the red K_2 bands—189(A)
——— (see Nusbaum, R. E.)—179(A)
——— **and H. Q. Fuller.** Enhancement of the iodine absorption spectrum by the admixture of oxygen—180(A)
——— **and R. E. Nusbaum.** Magnetic rotation spectrum and heat of dissociation of the potassium molecule—89
Lozier, W. W. (see Tate, John T.)—254
Luyten, W. J. Book reviews—387, 389

MacColl, L. A. Note on the transmission and reflection of wave packets by potential barriers—859(A)
McCollum, Burton and F. A. Snell. Asymmetry of sound velocity in stratified geologic formations—868(A)
McDermott, Eugene. Reflection seismograph—an application—869(A)
McKeehan, L. W. Magnetostrain and magnetoresistance—368
McKeller, Andrew (see Jenkins, F. A.)—549(A)

McMillen, J. H. (see Hughes, A. L.)—585, 865(A)
——— **and A. L. Hughes.** Distribution of electrons ejected in ionization of argon atoms—865(A)
Margenau, Henry. Pressure shift of spectral lines—860(A)
Maris, H. B. Seasonal variations in magnetic storms—504
Martin, E. V. and F. A. Jenkins. Predissociation in the sulfur monoxide molecule—549(A)
Marvin, H. H. Book review—851
Melvin, Eugene H. (see Wulf, Oliver R.)—180(A)
Metcalf, G. F. Increasing the charge sensitivity of vacuum tube amplifiers—745(L)
Miller, L. F. Book review—174
Miller, G. R. (see Laporte, O.)—458
Millikan, Robert A. Cosmic-ray ionization and electroscope-constants as a function of pressure—397
——— Further experiments on the uniformity of distribution of the cosmic radiation—391
Monk, George S. Book review—750
Montgomery, Carol G. Magnetic properties of nickel colloids—163(L)
Mooney, R. C. L. Crystal structure of ammonium bicarbonate—861(A)
Moorhead, John G. Near infrared absorption spectrum of methane—83
——— Near infrared absorption spectra of some halogen derivatives of methane—788
Mott-Smith, L. M. On an attempt to deflect magnetically the cosmic-ray corpuscles—403
Mullikan, Robert S. (see Jenkins, F. A.)—16
Murphy, G. M. (see Urey, Harold C.)—164(L), 864(A)
Muskat, Morris and Elmer Hutchisson. Quantum mechanics of lithium hydride—859(A)

Neledsky, Leo. The continuous radiation of slow electrons—552(A)
Nielsen, Harald H. (see Patty, John R.)—957
Noll, Waldemar. X-ray diffraction of ethyl ether at the critical temperature—175(A)
Nottingham, W. B. Spurious contact potentials and "trapped" electrons—183(A)
Nusbaum, R. E. (see Loomis, F. W.)—89
——— **and F. W. Loomis.** Heats of dissociation of Na_2 and K_2—179(A)
Nyrop, J. E. Surface-electrons—967

Oppenheimer, J. R. (see Carlson, J. F.)—864(A)

Palmer, R. Ronald. Book review—544
Patty, John R. and Harald H. Nielsen. The absorption by formaldehyde vapor in the infrared—957
Pauling, Linus (see Bozorth, Richard M.)—537(L)
Penney, W. G. Theory of the excitation of atomic mercury by electron impact—467, 859(A)
Penney, W. G. Book review—174
Pennington, J. V. Temperature shift of the transmission band of silver—953
Peters, Leo J. and John Bardeen. Electrical prospecting as applied in locating oil structures—870(A)
Pfund, A. H. and S. Silverman. Absorption of infrared radiation by small particles—64
Phillips, Melba. Photoionization probabilities of atomic potassium—552(A), 905
Pietenpol, W. B. and G. W. Presnell. Current-voltage and thermal characteristics of the copper oxide rectifier—862(A)
Pike, Eugene W. Evidence on the ionization potentials of O_2—534(L)
Plyler, E. K. Infrared absorption bands of water vapor—77
Potapenko, G. Investigations in the field of the ultra-short electromagnetic waves. I. The generator for the production of ultra-short undamped waves—625; II. The normal waves and the dwarf waves—638
——— On the dependence of the length of the ultra-short electromagnetic waves upon the heating current of the tube and upon the amplitude of the oscillations—547(A)
——— On the measurement of the energy of ultra-short electromagnetic waves—551(A)
Poulter, Thos. C. and Carl Benz. Lens effect of pressure windows—190(A)
——— **and Carter Ritchey.** The effect of pressure upon the e.m.f. of the Weston standard cell—816
Presnell, G. W. (see Pietenpol, W. B.)—862(A)

Quimby, S. L. Some new experimental methods in ferromagnetism—345

Rabi, I. I. Nuclear spin of caesium by the method of molecular beams—864(A)
Ransome, W. R. Production and recording of continuous seismic waves in the ground—858(A)
Rashevsky, N. On the physical nature of ponderomotive forces between living cells—188(A)
Reyerson, L. H. Book review—751
Rice, O. K. (see Gibson, G. E.)—551(A)
Richtmyer, F. K., H. A. Barton and M. T. Jones. A 600 kv x-ray plant—176(A)
Ritchey, Carter (see Poulter, Thos. C.)—816
Rodebush, W. H. and W. F. Henry. Molecular beams of salt vapors—386(L)
Roehr, W. W. (see DuBridge, Lee A.)—99
——— **and L. A. DuBridge.** Photoelectric and thermionic properties of palladium—866(A)
Roller, Duane and Hughes Zenor. Photoelectric emission from cadmium and mercury—866(A)
Romberg, Arnold (see Decherd, Loraine)—858(A)

Roots, Yale K. (see Jenkins, F. A.)—16
Rosaire, E. E. and O. C. Lester, Jr. Seismological discovery and partial detail of the Vermillion Bay Salt Dome—869(A)
Rose, J. L. and L. P. Granath. Relative abundance of the isotopes of lead in uranium bearing minerals —1017(L)
Rosenthal, Jenny E. (see Salant, E. O.)—161(L)
Ross, P. A. Another new x-ray non-diagram line—748(L)
——— Double crystal x-ray spectrometer and spectrograph—550(A)
——— New x-ray non-diagram line—536(L)
Roth, Herman. Slowly contracting or expanding fluid sphere and its stability—525
Rupp, E. and L. Szilard. Effect of magnetic field on reflected electron beams—864(A)
Russell, H. N. (see Shenstone, A. G.)—415
Rutherford, H. Refraction profiles as aids to the reflection method—869(A)

Salant, E. O. and Jenny E. Rosenthal. Isotope effects in polyatomic molecules—161(L)
Sanderman, L. A. (see Utterback, C. L.)—1008
Sawyer, R. A. (see Laporte, O.)—458
Schaffert, Roland. Thermomagnetic e.m.f.'s in transversely and longitudinally magnetized wires—1017(L)
Schlapp, Robert. Intensities in singlet-triplet bands of diatomic molecules—806
Schmid, R. F. Excitation of the CO_2 emission-spectrum in a Back box—539(L)
——— Zeeman effect of the third positive carbon bands—538(L)
Scott, R. B. (see Silsbee, F. B.)—379(L)
Serduke, James T. and Thomas F. Fisher. Hall effect in solid mercury—831
Shenstone, A. G. and H. N. Russell. Perturbed series in line spectra—415
Silsbee, F. B., R. B. Scott, J. W. Cook and F. G. Brickwedde. Superconductivity with respect to alternating currents—379(L)
Silverman, S. (see Pfund, A. H.)—64
——— Concerning the absorption and reflection spectra of calcite in the infrared—72
Sixtus, K. J. and L. Tonks. Further experiments on the propagation of large Barkhausen discontinuities—357. Discussion—375
Slichter, Louis B. and V. Gabrilovitch Gabriel. Some special cases of the reflection and refraction of seismic waves between similar rocks, with application to the study of crustal layers by distant quakes—869(A)
Slotnick, M. M. Charts for torsion balance readings —867(A)
Smith, Albert. Far ultraviolet eigenfrequencies of the alkali halides—1013(L)
Smith, Lee Irvin. Book review—849
Smith, P. T. (see Tate, John T.)—270
Smyth, H. D. Spectrum of carbon dioxide. II. Electron levels—380(L)
Snell, F. A. (see McCollum, Burton)—868(A)
Spedding, Frank H. and Richard S. Bear. Line reflection spectra of solids—948
Spencer, R. G. Absorption of soft x-rays in air, oxygen, and argon—178(A)
Stearns, J. C. (see Compton, A. H.)—873
Stedman, C. K. Thermionic frequency doubler—184(A)
Stern, O. (see Estermann, I.)—546(A)
Sterne, T. E. Vapor pressure constant of ammonia, the entropy of crystalline ammonia, and the reaction $N_2+3H_2 \rightleftarrows 2NH_3$—993
Stewart, G. W. X-ray diffraction with the two liquid phases of ethyl ether and nitrobenzene—176(A)
Strong, John. Evaporation of platinum in vacuum from a tungsten filament—1012(L)
Struve, O. (see Swings, P.)—142
Swann, W. F. G. Book review—387
Swings, P. and O. Struve. Bands of CH and CN in stellar spectra—142
Szilard, L. (see Rupp, E.)—864(A)

Tamm, Ig. Some remarks on the theory of photoelectric effect on metals—170(L)
Tate, John T. and W. W. Lozier. Dissociation of nitrogen and carbon monoxide by electron impact—254
——— **and P. T. Smith.** Efficiencies of ionization and ionization potentials of various gases under electron impact—270
Thatcher, E. W. and N. H. Williams. Shot effect in space charge limited currents—474
Thorndike, Edward N. (see Kennedy, Roy J.)—871 (A)
Tolman, Richard C. Possibilities in relativistic thermodynamics for irreversible processes without exhaustion of free energy—320
——— **and Morgan Ward.** On the behavior of non-static models of the universe when the cosmological term is omitted—835.
Tonks, L. (see Sixtus, K. J.)—357, 375
Tuve, M. A., L. R. Hafstad and O. Dahl. High-speed protons—384(L)
Tykocinski-Tykociner, J. Methods of detecting molecular rays—863(A)
——— **and W. A. Laning, Jr.** Oscillations in corona discharges—189(A)

Uehling, E. A. Kinetic interpretations of the Kelvin relations—187(A), 821

Uehling, E. A. (see Uhlenbeck, G. E.)—1014(L)
Uhlenbeck, G. E. (see Laporte, O.)—187(A)
——— **and E. A. Uehling.** The velocity of sound in a Fermi-Dirac or Einstein-Bose ideal gas—1014(L)
Urey, Harold C., F. G. Brickwedde and G. M. Murphy. An isotope of hydrogen of mass 2 and its concentration—164(L), 864(A)
Utterback, C. L. and L. A. Sanderman. Some thermal properties of tantalum—1008

Valasek, Joseph. Book reviews—388, 852, 853
Van Atta, L. C. Accurate determination of excitation energy by electron impact—1012(L)
Van Lear, G. A., Jr. and J. D. Hardy. The effect of Brownian motion on the useful sensitivity of the resonance radiometer—857(A)
Van Orstrand, C. E. On the correlation of isogeothermal surfaces with the rock strata—869(A)
Van Vleck, J. H. Book reviews—173, 851, 852
Vance, Charles B. Velocity of sound in tubes at audible and ultrasonic frequencies—737

Wahlin, H. B. Emission of positive ions from metals—183(A)
Walker, Margery K. (see Johnston, Herrick L.)—535(L)
Wallace, D. A. (see Gans, David M.)—184(A)
Ward, Morgan (see Tolman, Richard C.)—835
Washburn, Harold W. Operating characteristics of the electro-optical shutter—688
Watson, William W. (see Fredrickson, W. R.)—179(A), 753
——— Zeeman effect and Λ-type and spin doubling in the CaH bands—278
——— **and W. R. Fredrickson.** Spectrum of strontium hydride—179(A), 765
Weaver, Warren. Book review—1022
Wehr, M. R. Absorption and resonance of the helium infrared lines—796
Werth, Sister Magna. Relative efficiency of some of the mercury arc lines in exciting the Raman spectrum of benzol—299
White, H. E. and S. S. Ballard. The silvering of Fabry-Perot etalons by evaporation—545(A)
Whitford, Albert E. Zeeman effect of the K II spectrum 860(A), 898
Whitmer, Charles. Discrepancies in *M*-series absorption edges of heavy elements—176(L)
Williams, N. H. (see Thatcher, E. W.)—474
Williams, S. E. and J. Herlihy. Intensity measurements in the arc spectrum of thallium—802
Williams, S. R. Magnetization and thermal e.m.f.'s—368. Discussion—377
Wilson, H. A. Calculation of the motion of the ground from seismograph records—867(A)
Winans, J. Gibson. Effect of heat on mercury bands—745(L)
Wolfsohn, G. (see Ladenburg, R.)—180(A)
Woo, Sho-Chow and Richard M. Badger. Absorption spectrum of CN gas in the ultraviolet—932
Woo, Y. H. Scattering of x-rays by polyatomic gases—555
Woods, J. P. Calculation of detection performance in a vacuum tube circuit for large signals—863(A)
Worthing, A. G. Book review—1022
Wulf, Oliver R. and Eugene H. Melvin. Dissociation of nitrous oxide by light, and the electronic levels of O_3, N_2O and NO_2—180(A)
Wulff, John (see Green, J. B.)—181(A)
——— **and J. B. Green.** Paschen-Back effect of hyperfine structure, II. Bismuth II and bismuth III—181(A)

Yensen, T. D. Effect of impurities on ferromagnetism—358; Discussion—376
Young, Lloyd A. Local momentum in wave mechanics. II—455

Zachariasen, W. H. On the structure of vitreous oxides—185(A)
Zeleny, Anthony. An extension of the application and interpretation of the Faraday fluxes—857(A)
Zeleny, John. Book review—850
Zenor, Hughes (see Roller, Duane)—866(A)
Zirbel, N. N. and A. B. Bryan. Heat treatment of fine metallic suspensions—857(A)
Zisman, W. A. Effect of pressure on the electrical conductance of salt solutions in water—151

ANALYTIC SUBJECT INDEX TO VOLUME 39

References marked (A) are to abstracts of papers presented at meetings of the Physical Society, those marked with (L) are to Letters to the Editor.

Absorption coefficient (see also **X-rays, absorption, Collision diameter**)
For x-rays, A. Bramley—378(L)

Absorption of light (see also **Spectra, absorption**)
Absorption and emission of sodium light by sodium flames, T. W. Bonner—859(A)
By calcite in the infrared, S. Silverman—72
Continuous absorption by diatomic gases; temperature variation, G. E. Gibson—550(A); theory, G. E. Gibson, O. K. Rice—551(A)
In infrared by small particles, A. H. Pfund, S. Silverman—64
In infrared by various substances, R. B. Barnes—562, 870(A)
Temperature shift of the transmission band of Ag, J. V. Pennington—953

Acoustics
Effects of intense audio-frequency sounds, N. Gaines, L. A. Chambers—862(A)
Velocity of sound in a Fermi-Dirac or Einstein-Bose ideal gas, G. E. Uhlenbeck, E. A. Uehling—1014(L)
Velocity of sound in stratified formations, B. McCollum, F. A. Snell—868(A)
Velocity of sound in tubes, C. B. Vance—737

Activated gases
Active nitrogen, Joseph Kaplan—860(A)

Afterglow
Duration in nitrogen, Charles T. Knipp—181(A)
"Flash" in the afterglow of argon, Charles T. Knipp—871(A)

Alpha-particles (see also **Radioactivity**)
Range from weak sources, F. N. D. Kurie—865(A)

Astrophysics
Bands of CH and CN in stellar spectra, P. Swings, O. Struve—142
Evolution of a rotationally unstable star, Ross Gunn—130
Magnetic storms, H. B. Maris—504
Origin of cometary spectra, Willi M. Cohn—182(A)
Origin of the solar system, Ross Gunn—311, 858(A)
Spectral shift of light from distant stars, Herbert J. Brennen—186(A)
Stability of fluid sphere, Herman Roth—525

Atomic and molecular beams
Determination of nuclear spin, I. I. Rabi—864(A)
Methods of detection, J. Tykocinski-Tykociner—863(A)
Monochromatic de Broglie waves, I. Estermann, R. Frisch, O. Stern—546(A)
Of salt vapors, W. H. Rodebush, W. F. Henry—386(L)

Atomic and molecular radii (see **Collision diameter**)

Atomic structure (see also **Spectra, atomic**)
Dirac's equation and spin-spin interactions, G. Breit—616, 870(A)
Excitation energies of noble gases, L. C. Van Atta—1012(L)

Atomic structure factors
For polyatomic gases, Y. H. Woo—555
Of sylvine at low temperatures, G. E. M. Jauncey, G. G. Harvey—178(A)

Barkhausen effect (see also **Magnetic properties**)
Orientation in elementary domains, Richard M. Bozorth—353; discussion—373
Propagation of large discontinuities, K. J. Sixtus, L. Tonks—357; discussion—375

Beta-particles
β disintegration, Arthur Bramley—188(A)

Biophysics
Nature of ponderomotive forces between living cells, N. Rashevsky—188(A)

Book reviews
Brillouin, Léon. l'Atome de Bohr—851
——— Die Quantenstatistik und ihre Anwendung auf die Elektronentheorie der Metalle—852
Campbell, J. W. Numerical Tables of Hyperbolic and Other Functions—750
Casimir, H. B. G. Rotation of a Rigid Body in Quantum Mechanics—174
Edge, A. B. Broughton and T. H. Laby. The Principles and Practice of Geophysical Prospecting. Report of the Imperial Geophysical Experimental Survey—1022
Eggert, J. and E. Schiebold. Fortschritte der Roentgenforschung in Methode und Anwendung. Ergebnisse der technischen Roentgenkunde. II—388

Book reviews (continued)
Fajans, Kasimir. Radioelements and Isotopes: Chemical Forces and Optical Properties of Substances—751
Franck, Siegfrid. Messentlandungsstrecken (Ionenstrecken)—850
Frank, Philipp. Das Kausalgesetz und seine Grenżen—1025
Gamow, G. Constitution of Atomic Nuclei and Radioactivity—173
Gerlach, Walter and Eugen Schweitzer. Foundations and Methods of Chemical Analysis by the Emission Spectrum—853
Glasser, Otto. Wilhelm Conrad Roentgen und die Geschichte der Roentgenstrahlen—388
Gmelin's Handbuch der anorganischen Chemie—850
Henderson, William D. Problems in Physics—174
Hale, George Ellery. Signals from the Stars—389
Jahrbuch des Forschungs-Instituts der Allgemeinen Elektricitats-Gesellschaft. Vol. II, 1930—849
James Clerk Maxwell. A Commemoration Volume. 1831–1931—1024
Kassel, Louis S. The Kinetics of Homogeneous Gas Reactions—1023
Kepler, Johann. A Tercentenary Commemoration of His Life and His Work—387
Knopf, Adolph, E. W. Brown, Arthur Holmes, A. F. Kovarik, A. C. Lane, and Charles Schuchert. Physics of the Earth. IV. The Age of the Earth—543
Kohlrausch, K. W. F. Der Smekal-Raman Effect—541
Lenzen, Victor F. Physical Theory—387
Loeb, Leonard B. Fundamentals of Electricity and Magnetism—751
——— The Nature of a Gas—544
Milne-Thomson. Die elliptischen Funktionen von Jacobi—544
Northrop, F. S. C. Science and first Principles—849
Ribaud, Gustave. Traite de Pyrometrie Optique. Volume 4, Section 5 of Encyclopedie Photometrique—1022
Schiller, L. (ed.). Handbuch der Experimental physik. Hydre- und Aerodynamik, 1. Teil, Stromungslehre und allgemeine Versuchstechnik—541
Siegbahn, Manne. Spektroskopie der Roentgenstrahlen—388
Twyman, F. The practice of Spectrum Analysis with Hilger Instruments—852
——— and D. M. Smith. Wave-length Tables for Spectrum Analysis—750
van Arkel, A. E. and J. H. de Boer. Chemische Bindung als electrostatische Erscheinung—541
Whyte, L. L. Critique of Physics—1023
Wills, A. P. Vector and Tensor Analysis—851

Brownian movement
Effect on sensitivity of the resonance radiometer, G. A. Van Lear, Jr.—857(A)

Collision diameter
Of *A* atoms for 300 to 2500 volt electrons, Robert B. Brode—547(A)

Conductivity, electrical (see **Electrical conductivity and resistance**)

Constants, physical
Values of e, h, e/m and α, Raymond T. Birge—547(A)

Contact potentials
And "trapped" electrons, W. B. Nottingham—183(A)

Cosmic radiation
Comparison in the Alps and the Rockies, A. H. Compton—190(A)
Electroscope-constants as a function of pressure, Robert A. Millikan—397
Ionization-pressure relation, A. H. Compton, R. D. Bennett, J. C. Stearns—873
Magnetic deflection of cosmic rays, L. M. Mott-Smith—403
Range of fast electrons and neutrons, J. F. Carlson, J. R. Oppenheimer—864(A)
Specific ionization and "group" phenomenon, Gordon L. Locher—883
Uniformity of distribution, Robert A. Millikan—391

Crystals and crystal structure
Diffraction patterns of mixtures, M. Y. Colby—861(A)
Large artificial graphite crystals, Alexander Goetz, Alfred B. Focke, Alfred Faessler—168(L)
Lattice constants of solutions of Pb and Sn in Bi, Eric R. Jette, Frank Foote—1018(L)
Magnetic anisotrophy of colloidal crystals, Alexander Goetz, Alfred Faessler, A. B. Focke—553(A)
Magnetism of Bi crystals, Alfred B. Focke, Alexander Goetz—548(A)
Of NH_4HCO_3, R. C. L. Mooney—861(A)
Ruler and chart method of interpreting x-ray oscillation photographs; application to cerussite, Lucien LaCoste—861(A)
Specific heat and electronic activation in crystals, J. Elston Ahlberg, Simon Freed—540(L)
Stability of certain heteropolar crystals, H. M. Evjen—675

Crystals and crystal structure (continued)
Structure of magnesium platinocyanide heptahydrate, Richard M. Bozorth, Linus Pauling—537(L)
Thermal motions of atoms, B. D. Holbrook—177(L)
Of vitreous oxides, W. H. Zachariasen—185(A)

Critical potentials (see **Potentials, critical**)

Cybotactic state
Of ethyl ether and nitrobenzene, G. W. Stewart—176(A)
X-ray diffraction of ethyl ether, Waldemar Noll—175(A)

Diamagnetism (see **Magnetic properties**)

Dielectric constants
Polarization and moments of organic molecules, Louis M. Heil—666
Resultant moment of complex molecules, Henry Eyring—746(L)

Discharge of electricity in gases (see also **Electrons in gases**)
Negative point discharges, Willi M. Cohn—382(L)
Oscillations in corona discharges, J. T. Tykociner, W. A. Laning, Jr.—189(A)
Oscillations in ionized gases, J. Kunz—183(A)
Study with collectors of Ne discharge, Clifton G. Found, Irving Langmuir—237

Discharge of electricity in high vacua (see also **Thermionic emission; High voltage tubes and machines**)
Breakdown in cold emission, Willard H. Bennett—182(A)
High speed protons without the use of high voltages, Ernest O. Lawrence, M. Stanley Livingston—862(A)

Dissociation
Energies of products in N_2 and CO, John T. Tate, W. W. Lozier—254

Dissociation, heat of (see also **Molecular structure and constants**)
Of K_2 and Na_2, F. W. Loomis, R. E. Nusbaum—89, 179(A)

Dynamics
Momentum in special relativity, W. V. Houston—548(A)
Spatial energy decay due to absorbing boundaries, H. H. Germond—859(A)
Stability of fluid sphere, Herman Roth—525

Earth's magnetic field
Seasonal variations in magnetic storms, H. B. Maris—504

Efficiency of ionization
Of N_2CO, O_2, NO, H_2 and C_2H_2, John T. Tate, P. T. Smith—270

Elasticity
Bending of thin plate, D. G. Bourgin—870(A)
Constants for granite, L. Don Leet, W. Maurice Ewing—868(A)
A kinetic theory for highly elastic gels, E. Karrer—857(A)

Electrical conductivity and resistance
Characteristics of the copper oxide rectifier, W. B. Pietenpol, G. W. Presnell—862(A)
Of contacts, J. Frenkel, A. Joffé—530(L)
Effect of pressure on the conductance of salt solutions, W. A. Zisman—151
Electrical breakdown in insulators, R. M. Bozorth, F. E. Haworth—845(L)
Superconductivity with respect to alternating currents, F. B. Silsbee, R. B. Scott, J. W. Cook, F. G. Brickwedde—379(L)
Of Ta up to 2600°K, C. L. Utterback. L. A. Sanderman—1008

Electrical circuits
Analysis of plate current, S. Leroy Brown—863(A)
Charge sensitivity of vacuum tube amplifiers, G. F. Metcalf—745(L)
Electro-optical shutter, Harold W. Washburn—688
Generation of combination and harmonic frequencies, C. P. Boner, Marian O. Boner—863(A)

Electrical oscillations and waves
Low frequency vibrations in Rochelle salt and quartz plates, W. G. Cady—862(A)
Ultra-short undampled waves, G. Potapenko—547(A), 551(A), 625
Normal and the dwarf waves, G. Potapenko—638

Electric moment (see **Dielectric constant**)

Electrolytes
Effect of pressure on the conductance of salt solutions, W. A. Zisman—151

Electrolytic cells
Effect of pressure upon the e.m.f. of the Weston cell, Thos. C. Poulter, Carter Ritchey—816

Electromagnetic theory
Application and interpretation of the Faraday fluxes, Anthony Zeleny—857(A)
Electricity as a natural property of Riemannian geometry, Cornelius Lanczos—188(A), 716
On the equations of Laplace and Maxwell, Karl F. Herzfeld—497
Wave mechanics of radiation and free particles, E. H. Kennard—435

Electrons
Continuous radiation of slow electrons, Leo Neledsky—552(A)

Electron diffraction
Corpuscular description, R. M. Langer—187(A)
Effect of magnetic field on reflected electron beams, E. Rupp, L. Szilard—864(A)

Electrons in gases
Dissociation of N_2 and CO, John T. Tate, W. W. Lozier—254

Electrons in metals
Surface-electrons, J. E. Nyrop—967

Electrons, scattering of (see also **Electrons in gases**)
In Argon, energy distribution, A. L. Hughes, J. H. McMillen—585, 865(A)
Collision cross-section of A atoms for 300 to 2500 volt electrons, Robert B. Brode—547(A)

Electro-optical effects (see also **Photoelectric effect and properties**)
Characteristics of electro-optical shutter, Harold W. Washburn—688

E/m
Values of e, h, e/m and α, Raymond T. Birge—547(A)
From the Zeeman effect, J. S. Campbell, W. V. Houston—601

Energy states of atoms (see also **Atomic structure; Spectra, atomic**)
Excitation energies of noble gases, L. C. Van Atta—1012(L)

Entropy
Of crystalline ammonia, T. E. Sterne—993
Of the universe, Pasquale Barreca—533(L)

Eotvos balance
Charts for readings, M. M. Slotnick—867(A)
Description, Donald C. Barton—867(A)
Suspensions, N. N. Zirbel, A. B. Bryan—857(A)

Errata
Die elliptischen Funktionen von Jacobi, Milne-Thomson, book review—544

Excitation of atoms and molecules
Excitation energy by electron impact of noble gases, L. C. Van Atta—1012(L)
Mean lives of atomic states of Cd, H. D. Koenig, A. Ellett—576
Theory of excitation of atoms by electron impact, W. G. Penney—467, 859(A)

Ferromagnetism (see **Magnetic properties**)

Fluorescence
Quenching in iodine vapor, M. Eliashevich—532(L)

Galvanomagnetic effects
A new kind of e.m.f. and the four transverse effects, P. W. Bridgman—702

Gamma rays (see also **Radioactivity**)
Klein-Nishina formula for absorption, Arthur Bramley—378(L)

Geophysics
Application of reflection seismograph, Eugene McDermott—869(A)
Asymmetry of sound velocity in stratified formations, Burton McCollum, F. A. Snell—868(A)
Calculation of motion from seismograph records, H. A. Wilson—867(A)
Continuous seismic waves, W. R. Ransone—858(A)
Correlation of isogeothermal surfaces with the rock strata, C. E. Van Orstrand—869(A)
Discovery of the Vermillion Bay Salt Dome, E. E. Rosaire, O. C. Lester, Jr.—869(A)
Earth-amplitudes in seismic prospecting, Maurice Ewing—868(A)
Electrical prospecting, Leo J. Peters, John Bardeen—870(A)
Geothermal gradient determinations, L. R. Ingersoll—869(A)
Reflection method, H. Rutherford—869(A)
Study of crystal layers by seismic waves, Louis B. Slichter, V. Gabrilovitch Gabriel—869(A)
Velocity of waves in granite, L. Don Leet, W. Maurice Ewing—868(A)

Hall effect
Applications of thermodynamics to four transverse effects, P. W. Bridgman—702
In Bi and Sb, Carl A. Beck—185(A)
In solid Hg, James T. Serduke, Thomas F. Fisher—831

High voltage tubes and machines
High speed protons without the use of high voltages, Ernest O. Lawrence, M. Stanley Livingston—862(A)
In production of high-speed protons, M. A. Tuve, L. R. Hafstad, O. Dahl—384(L)

Hyperfine structure
Paschen-Back effect in Bi II and Bi III, John Wulff, J. B. Green—181(A)
Paschen-Back effect in Th I, Th II and Th III, J. B. Green, John Wulff—181(A)
Of Pb in Ur bearing minerals, J. L. Rose, L. P. Granath—1017(L)

Intensities in spectra (see also **Spectra, etc.**)
Arc lines of Th, S. E. Williams, J. Herlihy—802
Quartet lines in Cu arc, C. W. Allen—55
Relative intensities of Raman lines, Sister Magna Werth—299
In singlet-triplet bands of diatomic molecules, Robert Schlapp—806

Ionization by impact (see also **Ionization potentials**)
Efficiencies in N_2, CO, O_2, NO, H_2 and C_2H_2, John T. Tate, P. T. Smith—270
Energies of products in N_2 and CO, John T. Tate, W. W. Lozier—254

Ionization potentials
Of N_2CO, O_2, NO, H_2 and C_2H_2 by electron impact, John T. Tate, P. T. Smith—270
Of O_2, Eugene W. Pike—534(L)

Ions, high speed
High-speed protons, M. A. Tuve, L. R. Hafstad, O. Dahl—384(L)
High-speed protons without the use of high voltages, Ernest O. Lawrence, M. Stanley Livingston—862(A)
Range of fast electrons and neutrons, J. F. Carlson, J. R. Oppenheimer—864(A)

Ions, mobility
Absolute values in pure gases, N. E. Bradbury—546(A)

Isotopes
Of B from spectrum of BO, F. A. Jenkins, Andrew McKellar—549(A)
Effects in polyatomic molecules, E. O. Salant, Jenny E. Rosenthal—161(L)
Of hydrogen of mass 2, Harold C. Urey, F. G. Brickwedde, G. M. Murphy, 164(L), 864(A), Walker Bleakney—536(L)
Of Pb in Ur bearing minerals, J. L. Rose, L. P. Granath—1017(L)
Of Te, K. T. Bainbridge—1021(L)
Of Zn, K. T. Bainbridge—847(L)

Kinetic theory of gases
A law of force, D. R. Kleeman—871(A)

Liquids (see also **Hydrodynamics**)
Oriented molecules at solid-liquid interface, William D. Harkins—190(A)

Luminescence
Of solid nitrogen, Joseph Kaplan—870(A)

Magnetic properties (see also **Thermomagnetic effects**)
Barkhausen effect, Richard M. Bozorth—353; discussion—375
Of Bi alloyed with Pb and Sn, Eric R. Jette, Frank Foote—1018(L)
Of Bi crystals containing foreign atoms, A. B. Focke, A. Goetz—548(A)
Diamagnetic susceptibility of the rare gas atoms, W. Rogie Angus—844(L)
Effect of impurities on ferromagnetism, T. D. Yensen—358; discussion—376
Hydrogenized iron, P. P. Cioffi—363; discussion—376
Interpretation of ferromagnetic phenomena, Francis Bitter—337
Magnetic anisotrophy of colloidal crystals, A. Goetz, A. Faessler, A. B. Focke—553(A)
Magnetization and thermal e.m.f.'s, S. R. Williams—368; discussion—377
Magnetization of single crystals, Francis Bitter—371
Magnetostrain and magnetoresistance, L. W. McKeehan—368
New experimental methods in ferromagnetism, S. L. Quimby—345
Of nickel colloids, Carol G. Montgomery—163(L)
Propagation of Barkhausen discontinuities, K. J. Sixtus, L. Tonks—357; discussion—375
Susceptibility, gyromagnetic ratio, and heat capacity in Sm^{+++} and Em^{+++}, Amelia Frank—119

Mechanics, quantum—atomic structure and spectra
Calculation of energy levels of C, Niel Freeborn Beardsley—913
Dirac's equation and spin-spin interactions, G. Breit—616, 870(A)

Mechanics, quantum—general
Excitation by electron impact, W. G. Penney—467, 859(A)
Local momentum, Lloyd A. Young—455
Radiation and free particles, E. H. Kennard—435
Transmission and reflection of wave packets, L. A. MacColl—859(A)
Uncertainty principle, E. L. Hill—187(A)
Uncomplete systems in quantum mechanics, J. Frenkel—532(L)

Mechanics, quantum—molecular structure and spectra
Normal state of LiH, Morris Muskat, Elmer Hutchisson—859(A)

Metastable atoms and molecules
In Ne discharge, Clifton G. Found, Irving Langmuir—237

Meteorology
Ionization in the upper atmosphere, E. O. Hulburt—977
Magnetic storms, H. B. Maris—504

Methods and instruments
Absorption by films on grating, Albert Smith—1013(L)
Calculation of errors by the method of least squares, Raymond T. Birge—551(A)
Charge sensitivity of vacuum tube amplifiers, G. F. Metcalf—745(L)
Charts for torsion balance readings, M. M. Slotnick—867(A)
Detection of inhomogeneities in the magnetization, Francis Bitter—185(A)
Determination of small quantities of radon and thoron, Robley D. Evans—1014(L)
Direct measurement of mean lives of atomic states, H. D. Koenig, A. Ellett—576
Double crystal x-ray spectrometer, P. A. Ross—550(A)
Eotvos torsion balance, Donald C. Barton—867(A)

Methods and instruments (continued)
Evaporation of platinum, John Strong—1012(L), H. E. White, S. S. Ballard, 545(A)
Heat treatment of fine metallic suspensions, N. N. Zirbel, A. B. Bryan—857(A)
A high-vacuum, high-speed diffusion pump, Harold T. Byck, I. Esterman—553(A)
Infrared technique, R. Bowling Barnes—562
Intense audio-frequency sounds, Newton Gaines, Leslie A. Chambers—862(A)
A laboratory apparatus for determination of g, P. H. Carr, R. M. Bowie—858(A)
Lens effect of pressure windows, Thos. C. Poulter, Carl Benz—190(A)
Low frequency vibrations in Rochelle salt and quartz plates, W. G. Cady—862(A)
Method of least squares, Herbert J. Brennen—189(A)
Molecular beams, I. Estermann, R. Frisch, O. Stern—546(A)
A new instrument for measuring very small differences in gravity, Kenneth Hartley—867(A)
Photoelectric effect of alkali vapors, Jakob Kunz—866(A)
Photography of alpha and beta-ray tracks, David M. Gans, William D. Harkins, D. A. Wallace—184(A)
Precision determination of thermal diffusivity, Richard H. Frazier—515
In production of high-speed protons, M. A. Tuve, L. R. Hafstad, O. Dahl—384(L)
Reflection seismograph, Eugene McDermott—869(A)
Resistance bridge thermometer, Loraine Decherd, Arnold Romberg—858(A)
Ruler and chart method of interpreting x-ray oscillation photographs, Lucien LaCoste—861(A)
Sensitivity of the resonance radiometer, G. A. Van Lear, Jr.—857(A)
Silvering of etalons by evaporation, H. E. White, S. S. Ballard—545(A); John Strong—1012(L)
Supercooling liquid copper, J. J. Hopfield—185(A)
Thermal expansion measured by x-ray reflection, A. Goetz, R. C. Hergenrother—548(A)
Thermonic frequency doubler, C. K. Stedman—184(A)
Thermionic work function by photoelectric cell, Roscoe E. Harris—182(A)
An ultracentrifuge, J. W. Beams—858(A)
Ultra-short electromagnetic waves, G. Potapenko—547(A), 551(A), 625, 638
Voltage control by photoelectric cell, H. T. Clark, W. Kohlhagen—184(A)
Wilson cloud chamber for measuring range of α particles, F. N. D. Kurie—865(A)

Mobility of ions (see **Ions, mobility**)
Molecular beams (see **Atomic and molecular beams**)
Molecular structure and constants (see also **Spectra, molecular and Raman spectra**)
Configuration of N_2O, C. R. Bailey, A. B. D. Cassie—534(L)
Electronic states of Li_2, Wendell H. Furry—1015(L)
Heat of dissociation of K_2, F. W. Loomis, R. E. Nusbaum—89
Of the ICl molecule, Orrell Darbyshire—162(L)
Interaction of normal Be atoms with one in $2s2p$ state, W. H. Furry, J. H. Bartlett, Jr.—186(A), 210, 1015(L)
Moment of inertia of methane, J. G. Moorhead—83
Multiplets (see also **Spectra, atomic**)
Of P, F. A. Jenkins, Muriel Ashley—552(A)
Optical instruments (see **Methods and instruments**)
Paschen-Back effect
Of hyperfine structure in Bi II and Bi III, John Wulff, J. B. Green—181(A)
Of hyperfine structure in Th I, Th II and Th III, J. B. Green, John Wulff—181(A)
By use of molecular beam, I. I. Rabi—864(A)
Peltier effect (see **Thermoelectric effect**)
Photoelectric effect and properties (see also **Photoionization**)
Of alkali vapors; new method of study, Jakob Kunz—866(A)
Of Cd and Hg films, Duane Roller, Hughes Zenor—866(A)
Of contracts, J. Frenkel, A. Joffé—530(L)
Fowler's theory, experimental tests, Lee A. DuBridge—108, 866(A)
Of gas free Pd, Fowler's theory, Lee A. DuBridge, W. W. Roehr—99, 866(A)
Of O_2 and A; action of x-rays, Gordon L. Locher—866(A)
Surface-electrons, J. E. Nyrop—967
Theory; of metals, Ig. Tamm—170(L)
Of thin films of Rb and Cs on Ag, James J. Brady—546(A)
Photoionization (see also **Photoelectric effect and properties**)
Ionization in the upper atmosphere, E. O. Hulburt—977
Probabilities of atomic potassium, Melba Phillips—552(A), 905
Variation with pressure and temperature, A. H. Compton, R. D. Bennett, J. C. Stearns—873
Polarization of radiation
Of Cd λ2288A and λ3216A, A. Ellett, L. Larrick—181(A), 294
Of Hg λ2537A, L. Larrick, N. P. Heydenburg—181(A), 289

Potentials, critical (see also **Ionization potentials**)
Soft x-ray potentials of Be, R. J. Christensen—549(A)

Proceedings of the American Physical Society
175, 545, 854

Predissociation
A new criterion, Joseph Kaplan—180(A)
In SO, E. V. Martin, F. A. Jenkins—549(A)

Quantum mechanics (see **Mechanics, quantum**)

Radiation (see also **Thermal radiation**)
Absorption of infrared by small particles, A. H. Pfund, S. Silverman—64
Continuous radiation of slow electrons, Leo Neledsky—552(A)

Radio (see **Electric oscillations and waves**)

Radioactivity
β disintegration, Arthur Bramley—188(A)
Determination of small quantities of radon and thoron, Robley D. Evans—1014(L)
Isotopes of lead, J. L. Rose, L. P. Granath—1017(L)
New effect produced by action of x-rays on matter, Newell S. Gingrich—748(L)
Photography of alpha and beta-ray tracks, David M. Gans, William D. Harkins, D. A. Wallace—184(A)
Range of alpha particles from weak sources, F. N. D. Kurie—865(A)

Raman spectra
Of CS_2 S. Bhagavantam—1020(L)
Inner vibrations in molecules; carbon-halogen band, William D. Harkins, Harold E. Bowers—182(A)
Relative intensities of lines, Sister Magna Werth—299
Of water vapor, Herrick L. Johnston, Margery K. Walker—535(L)

Rectifiers
Characteristics of the copper oxide rectifier, W. B. Pietenpol, G. W. Presnell—862(A)

Relativity
Behavior of non-static models of the universe, Richard C. Tolman, Morgan Ward—835
Electricity as a natural element of Riemannian geometry, Cornelius Lanczos—188(A)
Experimental establishment of the relativity of time, Roy J. Kennedy, Edward M. Thorndike—871(A)
Momentum of a moving body, W. V. Houston—548(A)
Thermodynamics for irreversible processes without exhaustion of free energy, Richard C. Tolman—320

Resonance radiation
In Ne discharge, Clifton G. Found, Irving Langmuir—237

Scattering of electrons (see also **Collision diameter**; **Electrons in gases**; **Electron diffraction**)

Seismograph (see **Methods and instruments**; **Geophysics**)

Shot effect
And electrical breakdown in insulators, R. M. Bozorth, F. E. Haworth—845(L)
In space charge limited currents, E. W. Thatcher, N. H. Williams—474

Sound (see **Acoustics**)

Specific heat
Variations with temperature for Sm^{+++} and Em^{+++}, Amelia Frank—119

Spectra, absorption (see also **Absorption of light**)
Of the alkali halides; ultraviolet, Albert Smith—1013(L)
1,1 band of atmospheric O_2, Harold D. Babcock, Wendell P. Hoge—550(A)
Bands of Ch and CN in stellar spectra, P. Swings, O. Struve—142
By calcite in the infrared, S. Silverman—72
Of CN in ultraviolet, Sho-Chow Woo, Richard N. Badger—932
Effect of temperature on the bands of benzene at low temperatures, A. H. Croup—178(A)
Emission and absorption of BaF, F. A. Jenkins, A. Harvey—922
Enhancement of the iodine absorption of oxygen, F. W. Loomis, H. Q. Fuller—180(A)
Fine structure of bands of halogen derivatives of methane, John G. Moorhead—788
Fine structure of visible bands of Br_2, Weldon G. Brown—190(A), 777
Of the ICl molecule, Orrell Darbyshire—162(L)
Infrared bands of H_2O, E. K. Plyler—77
Infrared of formaldehyde vapor, John R. Patty, Harald H. Nielsen—957
Infrared lines of He, M. R. Wehr—796
Magnetic rotation spectra of K_2, F. W. Loomis, R. E. Nusbaum—89
Of M_2O and dissociation, Oliver R. Wulf, Eugene H. Melvin—180(A)
Near infrared of methane, J. G. Moorhead—83
Parallel type bands of NH_3, David M. Dennison, J. D. Hardy—938
Ultra-violet spectrum of ozone, A. Jakowleva, V. Kondratjew—533(L)

Spectra, atomic
Broadening of Cu arc lines, C. W. Allen—42
Calculation of energy levels of C, Niel Freeborn Beardsley—913

Spectra, atomic (continued)
Of Cs II, O. Laporte, G. R. Miller, R. A. Sawyer—458
Intensity of quartet Cu lines, C. W. Allen—55
Perturbed series, A. G. Shenstone, H. N. Russell—415
Of Ra, classification of lines, Walter Albertson—385(L)
Of Sb II, R. J. Lang—538(L)
Of Si II, P III, S IV, Si III, P IV and S V, I. S. Bowen—8, 551(A)
Theory of complex spectra, M. H. Johnson, Jr.—197
Width of D lines, S. A. Korff—549(A)
Zeeman effect of the K II spectrum, Albert E. Whitford—898

Spectra, continuous
Effect of heat on Hg bands, J. Gibson Winans—745(L)
Origin of cometary spectra, Willi M. Cohn—182(A)

Spectra, general
Luminescence of solid nitrogen, Joseph Kaplan—870(A)
Negative point discharges at low pressures, Willi M. Cohn—382(L)
Pressure shift of spectral lines, Henry Margenau—860(A)
Retection spectra in solids, Frank H. Spedding, Richard S. Bear—948

Spectra, molecular (see also **Molecular structure and constants**)
Absolute value of transition probabilities, R. Ladenburg, S. Levy, G. Wolfsohn—180(A)
Of BaF, emission and absorption, F. A. Jenkins, A. Harvey—922
Of BaH, W. R. Fredrickson, William W. Watson—179(A), 753
Of CO_2, electron levels, H. D. Smyth—380(L)
CO_2 emission-spectrum in a Back box, R. F. Schmid—539(L)
Criterion for predissociation, Joseph Kaplan—180(A)
Of CS_2, S. Bhagavantam—1020(L)
Isotope effects, E. O. Salant, Jenny E. Rosenthal—161(L)
Of KH, G. M. Almy, C. D. Hause—178(A)
Nuclear spin of P from band spectrum, F. A. Jenkins, Muriel Ashley—552(A)
Red CN band system, F. A. Jenkins, Yale K. Roots, Robert S. Mulliken—16
Rotational analysis of the red K_2 bands, F. W. Loomis—189(A)
Of SO, E. V. Martin, F. A. Jenkins—549(A)
Of SrH, William W. Watson, W. R. Fredrickson—179(A), 765
Structure of Br_2 bands, Weldon G. Brown—190(A)
Zeeman effect, A-type, spin doubling in CaH bands, William W. Watson—278

Spinor analysis
Impulse-energy tensor, O. Laporte, G. E. Uhlenbeck—187(A)

Sun (see **Astrophysics**)

Symposia
Ferromagnetic symposium and conference at Schenectady, September 12, 1931—337

Thermal conductivity
Effect of transverse magnetic fields in Bi, E. J. Knapp—550(A)
Precision determination of thermal diffusivity; Ni, Richard H. Frazier—515

Thermal radiation
From Ta, 1000° K to 2220° K, C. L. Utterback, L. A. Sanderman—1008

Thermal expansions
Of Bi crystals by x-rays, A. Goetz, R. C. Hergenrother—548(A)
Of Cu alloys, Peter Hidnert—551(A)
Of electrolytic chromium, Peter Hidnert—186(A)
Of heat-resisting alloys, Peter Hidnert—856(A)

Thermionic emission of electrons
Space charge effects, using Fermi-Dirac statistics, N. H. Frank—226
Surface-electrons, J. E., Nyrop—967
Thermionic work function by photoelectric cell, Roscoe E. Harris—182(A)
Work function of gas free Pd, Lee A. DuBridge, W. W. Roehr—99, 866(A)

Thermionic emission of positive ions
From metals with impurities, H. B. Wahlin—183(A)

Thermodynamics
Kinetic interpretation of the Kelvin relations, E. A. Uehling—187(A), 821
Relativistic thermodynamics for irreversible processes, Richard C. Tolman—320

Thermoelectric effect
Applications of thermodynamics to four transverse effects, P. W. Bridgman—702
Change produced by a magnetic field, H. E. Banta—862(A)
And magnetization, S. R. Williams—368; discussion—377
Of Ta with Pt, C. L. Utterback, L. A. Sanderman—1008

Thermomagnetic effects
Four transverse effects, P. W. Bridgman—702
Transversely and longitudinally magnetized wires, Roland Schaffert—1017(L)

Vacuum tubes
Analysis of plate current, S. Leroy Brown—863(A)
Calculation of detection performance, J. P. Woods—863(A)
Generation of combination and harmonic frequencies, C. P. Boner, Marian O. Boner—863(A)
Vapor pressure
Constant of ammonia, T. E. Sterne—993
X-rays, absorption
In air, O_2 and A, R. G. Spencer—178(A)
M-series absorption edges of heavy elements, Charles Whitmer—176(L)
New effect produced by action of x-rays on matter, Newell S. Gingrich—748(L)
Peripheral x-ray levels, J. A. Eldridge—177(L)
X-rays, diffraction scattering, reflection and refraction
Compton line breadth in Ceylon graphite, Jesse W. M. DuMond—166(L)
Diffraction of ethyl ether at the critical temperature, Waldemar Noll—175(A)
Diffraction with two liquid phases, G. W. Stewart—176(A)
Patterns of mixtures, M. Y. Colby—861(A)
Reflecting power of strained quartz crystals, oscillating and non oscillating, Charles S. Barrett Carl E. Howe—177(A), 889
Ruler and chart method of interpreting x-ray oscillation photographs, Lucien LaCoste—861(A)
Scattering by polyatomic gases, Y. H. Woo—555
Scattering by polyatomic gases; note on above paper, G. E. M. Jauncey—561
Scattering from sylvine at low temperature, G. E. M. Jauncey, G. G. Harvey—178(A)
Thermal motions of atoms in crystals, B. D. Holbrook—177(L)
Variation of refractive index with wave-length, J. M. Cork—177(L), 193
Wave-length measurements by dispersion, J. A. Bearden—1, 860(A)
X-rays, emission
Comparison of 700,000-volt x-rays and gamma-rays, G. Failla—176(A)
Non-diagram lines, P. A. Ross—536(L), 748(L)
X-rays, spectra and spectroscopy
Double crystal spectrometer and spectrograph, P. A. Ross—550(A)
Soft x-ray critical potentials of Be, R. J. Christensen—549(A)
X-rays, tubes, apparatus
600 kv plant, F. K. Richtmyer, H. A. Barton, M. T. Jones—176(A)
Zeeman effect
In CaH bands, William W. Watson—278
Of K II spectrum, Albert E. Whitford—860(A), 898
Of the third positive carbon bands, R. F. Schmid—538(L)

CURRENT LITERATURE OF PHYSICS

Extracts from the Tables of Contents of Some of our Contemporaries

NATURE

VOL. 129, No. 3250 — FEBRUARY 13, 1932

Letters to the Editor:

Artificial Production of Fast Protons. By **J. D. Cockcroft and E. T. S. Walton** 242

Photochemical Reaction between Hydrogen and Chlorine in the Presence of Oxygen. By **Mowbray Ritchie and R. G. W. Norrish** 243

Co-ordination of Hydrogen in Associated Liquids. By **J. C. Speakman** 244

Oxygen and Everest. By **N. E. Odell** 244

Atomic Weight of Fluorine. By **H. S. Patterson, W. Cawood, and R. Whytlaw-Gray** 245

Structure and Development of Temperature Inversions in the Atmosphere. By **C. K. M. Douglas** 245

Melde's String Vibrated by Rotating Pulley. By **Satyendra Ray** 246

NATURE

VOL. 129, No. 3251 — FEBRUARY 20, 1932

Faraday's Alloy Steels. By **F. C. T.** 259

Photo-Elasticity. By **Alfred Ewing** 264

Letters to the Editor:

Nomenclature for Lines in the β-Ray Spectra of Radioactive Bodies. By **C. D. Ellis** 276

Distribution of Electrons in the Aromatic Nucleus and the Early Stages of Aromatic Substitutions. By **A. Lapworth and R. Robinson** 278

Surface Tension of Soap Solutions. By **P. Lecomte du Noüy** 278

Zodiacal Light and the Luminosity of the Night Sky. By **K. R. Ramanathan** 280

Polish on Metals. By **J. T. Randall and H. P. Rooksby** 280

Crystal Structure of β-Zirconium. By **W. G. Burgers** 281

ZEITSCHRIFT FÜR PHYSIK

VOL. 74, Nos. 3 and 4 — FEBRUARY 11, 1932

On the Theory of Non-Adiabatic Chemical Processes. By **F. London** 143

On Some Absorption, Fluorescences, and Emission Bands of Caesium. By **R. Rompe** 175

Solar Periodicity of the Hard Cosmic Radiation. By **W. Messerschmidt** 187

On the Fine Structure of the X-ray Absorption Edges. By **D. Coster and J. Veldkamp** 191

On the Anomaly of the Constricted Glow Discharge. By **Werner Koch** 209

Wave Equation of Kepler Motion in Momentum Space. By **Egil A. Hylleraas** 216

Roentgenographic Investigation of the Solubility of Silver in Copper. By **P. Wiest** 225

On the Band Spectrum of BaH. By **A. Schaafsma** 254

On the Transformation of Metals in the Solid Phase. III. Kinetic Calculations on the Basis of Atomic Theory. By **U. Dehlinger** 267

DIE NATURWISSENSCHAFTEN

VOL. 20, No. 7 — FEBRUARY 12, 1932

Position of the Theory of Relativity with Respect to other Physical Theories. By **Cornel Lanczos** 113

Short Original Contributions

On the Effect of the Lattice Forces on the X-ray Emission Spectrum. By **R. Glocker and M. Renninger** 122

On the Structure of Extremely Thin Crystalline Layers. By **F. Kirchner** 123

Spectrum and the Catalytic Effect of Imidazol-Haemine. By **W. Langenbeck** 124

Crystal Structure of Lithium Hydroxide. By **Th. Ernst** 124

COMPTES RENDUS

VOL. 194, No. 5 — FEBRUARY 1, 1932

Study of the Solar Corona with a Spectroheliograph Outside of Eclipse. By **Bernard Lyot** 443
Newtonian Potenial. By **N. Gunther** 446
Some Properties of Vacuum Thermocouples. By **J. Jaffray** 451
Intensity Measurements in Ultraviolet Spectra by Means of Photoelectric Cells Sensitized by Sodium Salicylate. By **André Chevallier and Pierre Dubouloz** 452
Action of an Electric Field on Gelatine. Effect of the Presence of an Indicator. By **Suzanne Veil** 454
Deposition Voltage of Electrolytic Copper in the Presence of Gelatine. By **P. Jacquet** 456

PROCEEDINGS OF THE NATIONAL ACADEMY OF SCIENCES OF THE U. S. A.

VOL. 18, No. 1 — JANUARY, 1932

Quantum Dynamical Correction for the Equation of State of Real Gases. By **Henry Margenau** 56
New Lines in the *K* Series of X-rays. By **William Duane** 63

BUREAU OF STANDARDS JOURNAL OF RESEARCH

VOL. 8, No. 4 — APRIL, 1932

Optical Requirements of Airplane Mapping. By **I. C. Gardner** 427
Note on the Moving Boundary Method for Measuring Transference Numbers. A Pycnometer for Determining the Volume Change Occurring at an Electrode and its Application to a Cathode of Silver Chloride in a Solution of Potassium Chloride. By **E. R. Smith** 428
Radio Field Intensity Measurements at Frequencies from 285 to 5,400 Kilocycles per second. By **S. S. Kirby and K. A. Norton** 429
Photographic Emulsion: Silver Ion and Hydrogen Ion Concentrations and Sensitivity. By **Burt H. Carrol and Donald Hubbard** 430
Capacitance and Power Factor of a Mica Capacitor as Measured at the Bureau of Standards and the National Physical Laboratory. By **Harvey L. Curtiss, C. Mathilda Sparks, L. Hartshorn, and N. F. Astbury** 431
Isolation and Determination of Normal Heptane and of Methylcyclohexane in a Mid-continent Petroleum. Including a Determination of the Phase Equilibrium Diagram for the Condensed System Normal Heptane-methylcyclohexane. By **Mildred M. Hicks-Bruun and Johannes H. Bruun** 432
Spectral Erythemic Reaction of the Untanned Human Skin to Ultraviolet Radiation. By **W. W. Coblentz, R. Stair, and J. M. Hogue** 433

JOURNAL OF THE FRANKLIN INSTITUTE

VOL. 213, No. 3 — MARCH, 1932

Extension of Paschen's Law to Include the Electrodeless Glow Discharge. By **Otto Stuhlman, Jr.** 273
Two-Dimensional Analysis of the Discrimination of differences in the Frequency of Vibrations by Means of the Sense of Touch. By **William H. Roberts** 283
The Dielectric Constant and Power Factor of Rosin Oil and Ethyl Abietate. By **S. O. Morgan and A. H. White** 313

JOURNAL OF THE OPTICAL SOCIETY OF AMERICA

VOL. 22, No. 3 — MARCH, 1932

Brock Process of Aërial Mapping. By **Edward H. Cahill** 111
Aërial Stereo-Photographic Mapping Instruments and Methods. By **C. H. Birdseye** 137
Apparatus for Motion Photomicrography on 35 mm Film. By **R. P. Loveland** 161
On Temperature Crests in Cando-Luminescence. By **E. L. Nichols and H. L. Howes** 170

THE REVIEW OF SCIENTIFIC INSTRUMENTS

VOL. 3, NO. 3 MARCH, 1932

Wenner Potentiometer. By **Leo Behr** 109
Flexure Balance. By **Kenneth S. Cole** 121
Method of Measuring Small Capacitance. By **Roger Barton** 123
Multiple Nozzle Diffusion Pumps. By **T. L. Ho** 133
Construction of an Air Cooled Electromagnet. By **I. Walerstein and A. I. May** 136
Gas X-ray Tube for Crystal Structure Analysis. By **H. Kersten** 145

IMPORTANT NOTICE TO AUTHORS AND SUBSCRIBERS

After April 1, 1932, the American Institute of Physics will take over the editorial mechanics and business management of the Physical Review.

Please note carefully the addresses to which correspondence should be sent.

THE EDITOR OF THE PHYSICAL REVIEW
University of Minnesota
MINNEAPOLIS, MINNESOTA

will continue to receive:

Manuscripts submitted for publication

All correspondence concerning manuscripts prior to their acceptance or rejection.

THE EDITORIAL SECRETARY
American Institute of Physics
11 East 38th Street
New York City, New York

will, after April first, 1932, receive:

All correspondence concerning the details of publication of accepted articles

All proof of articles in process of publication

All correspondence concerning reprint orders

All subscriptions and renewals

All orders for back numbers

This issue marks the close of Volume 39 of the Physical Review. It contains an Author and Analytic Subject Index.

Hereafter volumes will be issued quarterly.

NEW! Chromium-Plated

STUDENT ANALYTICAL WEIGHTS

No. 719

ANALYTICAL WEIGHTS—of an accuracy within the specified tolerances of the U. S. Bureau of Standards for Class S-2 weights—with gram pieces of chromium-plated brass—for resistance to wear and protection from tarnish—with large fractionals (50 to 500 mg) of pure nickel—with small fractionals (1 to 20 mg) of pure aluminum—these excellent weights for student or routine commercial use represent a real value at their selling price. The weight box is of finished hardwood with hinged, padded lid. An ivory tipped forceps completes the set.

Tolerance for U. S. B. S. Class S-2 Weights

Weight	Tolerance	Weight	Tolerance
100 g	2.5 mg	200 mg	0.25 mg
50	1.5	100	0.25
20	1.0	50	0.15
10	0.75	20	0.15
5	0.75	10	0.10
2	0.50	5	0.10
1	0.50	2	0.05
500 mg	0.25	1	0.05

No. 719 Analytical Weights

No.	A	B
Size, 1 mg to, gms	50	100
Each	$9.00	11.00

10% discount in lots of 6.

CENTRAL SCIENTIFIC COMPANY

LABORATORY SUPPLIES

Apparatus CENCO Chemicals

NEW YORK - BOSTON - CHICAGO - TORONTO - LOS ANGELES

GEORGE BANTA PUBLISHING COMPANY, MENASHA, WISCONSIN